



Faculteit Wetenschappen  
Departement Fysica  
Theorie van Kwantumsystemen en Complexe Systemen

**Effective field theory for superfluid Fermi gases**  
**Application to polarons and solitons**

---

**Effectieve veldentheorie voor superfluïde Fermigassen**  
**Toepassing op polaronen en solitonen**

Proefschrift voorgelegd tot het behalen van de graad van  
doctor in de Wetenschappen aan de Universiteit Antwerpen  
te verdedigen door Giovanni Lombardi

Promotor: prof. dr. Jacques Tempere  
Co-promotor: dr. Sergei Klimin

Antwerpen, 28 Juni, 2017



# Abstract

When a dilute gas of neutral fermionic atoms, trapped in a magnetic or optical confining potential, is cooled down to temperatures of a few tens of nanokelvins above absolute zero, the gas undergoes a phase transition. The fermionic atoms form pairs, that can flow as in an ideal fluid, without friction. This phenomenon is briefly introduced in the first chapter.

Such “superfluid” state also occurs for bosonic atoms, that however do not need to pair. For Bose systems, Gross and Pitaevskii developed a successful description of the superfluid state based on a macroscopic wavefunction. Unlike the many-particles wavefunction, which depends on the positions of all atoms in the system, the macroscopic wavefunction depends only on one position coordinate. Yet it reliably encodes many aspects of the behaviour of the superfluid. The modulus squared of the macroscopic wavefunction is interpreted as the density of superfluid particles, while the gradient of the phase is linked to the velocity field. The superfluid properties follow from the partial differential equation that this macroscopic wavefunction must satisfy. This differential equation is known for superfluid Bose gases, but up to now there was no counterpart for fermionic system. The goal of this thesis is to develop a description of superfluidity in fermionic systems in terms of a macroscopic wavefunction and to employ it to study related phenomena such as dark solitons in Fermi superfluids.

In this thesis an effective field theory (EFT) suitable to describe the superfluid phase of an ultracold system of neutral fermionic atoms in a wide range of interaction and temperature configurations is developed in the framework of the path-integral formulation of quantum field theory [1]. At the heart of the EFT lies the hypothesis that the order parameter varies slowly in both time and space. The calculations that, from this weak assumption, lead to the final form of the EFT action are carried out in full detail.

The EFT is then applied to the study of various aspects of Fermi superfluids in the BEC-BCS crossover interaction regime. By introducing fluctuations beyond mean field the spectrum of the collective excitations and the corrections to the critical temperature are evaluated, and the results are compared to those of other theoretical approaches.

Motivated by the interest gathered in recent years by the BEC polaron problem, an analogous system where the Bose-Einstein condensate is replaced by a superfluid fermionic gas is treated, and the corrections to the polaronic coupling constant and effective mass due to the interaction of an impurity with the collective excitations of the superfluid are evaluated [2]. The interaction dependence of the dispersion relations for the collective modes enables to extend the analogy with the BEC polaron system, that in principle

would be limited to the BEC limit, to a wider region of the BEC-BCS crossover.

The EFT is then applied to the study of various aspects of dark solitons in ultracold Fermi gases. At first the stable soliton solutions in (quasi-)1D are studied and the effects of interaction, temperature, and imbalance on the density profiles and dynamics are precisely characterised [3]. The main finding in this context is the fact that the soliton core is an energetically favorable place where the unpaired particles – present in the system because of a nonzero population imbalance and/or finite temperature – can be accommodated. Next the snake instability mechanism, responsible for the decay of dark solitons in 3D, is considered. The spectrum of the unstable modes is examined and compared to the results of other theoretical approaches [4]. The minimum size that the system can have in order for the soliton to be stable is estimated and the behaviour of this quantity across the BEC-BCS crossover is compared to other data found in literature. In the BEC regime the EFT gives results in very good agreement with those of both the time-dependent Bogoliubov-de Gennes (TDBdG) simulations and of the coarse grained Bogoliubov-de Gennes theory. Moreover, it appears that the EFT is the only treatment that correctly describes the change in the relevant length scale, from the healing length in the BEC regime, to the pair coherence length in the BCS regime. The effects of imbalance on the soliton stability are also examined, finding that for a fixed interaction strength, the critical size necessary to avoid decay through the snake instability is larger for an imbalanced system than for a balanced one. In principle this provides experimentalists with a method to stabilise solitons by increasing the imbalance without being forced to reduce the dimensionality of the cloud.

The description we develop in this thesis opens the way to many applications. Where other models, such as the Bogoliubov-de Gennes theory, become computationally demanding even for a single vortex or soliton, the current description has the advantage of allowing a rapid implementation. Thus, in the future it will be possible to investigate the behaviour of the system when it contains many vortices or solitons – similar as for superconductors we can characterise vortex matter and learn to manipulate vortices and solitons. Also, the theory can be easily extended to multi-component fermionic superfluids, which allows us to investigate whether new phenomena – that do not occur in the individual superfluids – can instead occur in such mixtures.

# Nederlandstalige samenvatting

Wanneer een ijl gas van neutrale fermionische atomen, ingevangen in een magnetische of optische val, wordt afgekoeld tot een temperatuur van enkele tientallen nanokelvins boven het absolute nulpunt, ondergaat het gas een faseovergang. De fermionische atomen vormen paren, die kunnen vloeien als een ideale vloeistof, zonder dissipatie. Dit fenomeen wordt kort ingeleid in het eerste hoofdstuk.

Dergelijke “superfluïde” toestand treedt ook op voor bosonische atomen, zonder dat deze moeten opparen. Voor bosonische atomen ontwikkelden Gross en Pitaevskii een succesvolle beschrijving van de superfluïde toestand aan de hand van een “macroscopische” golffunctie. In tegenstelling tot de veeldeeltjesgolffunctie, die afhangt van de posities van alle atomen in het systeem, hangt de macroscopische golffunctie slechts af van één positiecoördinaat. Toch encodeert deze golffunctie getrouw het gedrag van het superfluïdum. De modulus kwadraat van de macroscopische golffunctie wordt als dichtheid van superfluïde deeltjes geïnterpreteerd, en de fasegradiënt is gelinkt aan het snelheidsveld. De superfluïde eigenschappen volgen uit de differentiaalvergelijking waaraan de macroscopische golffunctie moet voldoen. Deze differentiaalvergelijking is gekend voor superfluïde Bose gassen, maar er was nog geen tegenhanger voor superfluïde Fermi gassen. Het doel van deze thesis is om een beschrijving van superfluïditeit in Fermi gassen op te stellen, gebaseerd op een macroscopische golffunctie, en om aan de hand hiervan superfluïde eigenschappen (zoals solitonen) te beschrijven.

Daartoe ontwikkelen we in deze thesis een effectieve veldentheorie [1] die in staat is om de superfluïde toestand te beschrijven van een ultrakoud systeem van neutrale fermionische atomen voor een groot bereik aan temperaturen en interactiesterktes. De afleiding van de theorie is gebaseerd op de padintegraalbeschrijving, in combinatie met de aanname dat de ordeparameter die het paarcondensaat beschrijft traag varieert zowel in tijd als in ruimte. De berekeningen die, vertrekkend van deze aanname, leiden tot de veldvergelijking voor de macroscopische golffunctie van het paarcondensaat, worden in detail uitgewerkt in het tweede hoofdstuk.

De effectieve veldentheorie wordt in het derde hoofdstuk toegepast om verschillende basis-aspecten van Fermi superfluïda nader te beschrijven, in het de ganse overgangsregime tussen Bardeen-Cooper-Schrieffer (BCS) paren en een Bose-Einstein condensaat (BEC) van sterk gebonden moleculen. Door fluctuaties bovenop de gemiddeld-veld oplossing te beschouwen, berekenen we het spectrum van collectieve excitaties en de correcties op de gemiddeld-veld waarde voor de kritische temperatuur. We vergelijken deze resultaten met

de reeds gepubliceerde waarden en vinden een goede overeenkomst.

In het vierde hoofdstuk zijn we toe aan een eerste uitgebreidere toepassing: polaronische effecten in een Fermi superfluidum [2]. Deze effecten treden op wanneer we een onzuiverheidsatoom in een superfluid systeem brengen. In een Bose-Einstein condensaat zullen de excitaties van het condensaat interageren met het onzuiverheidsatoom. Daardoor wordt het atoom “aangekleed” met een wolk excitaties, en verandert bijvoorbeeld de effectieve inertiaële massa van het onzuiverheidsatoom. Hier onderzoeken we dit effect met behulp van onze theorie voor een fermionisch systeem. In de limiet van sterk gebonden moleculen van twee fermionen bekomen we opnieuw het gekende resultaat voor een onzuiverheid in een Bose-Einstein condensaat, maar onze theorie stelt ons in staat om de eigenschappen ook te onderzoeken wanneer we de fermionische paren brengen in een regime waar ze zwakker gekoppeld zijn en meer lijken op Cooperparen. We kwantificeren het effect hiervan op het polaronisch effect, zowel voor de verlaging in grondtoestandsenergie als voor de verandering van de inertiaële massa.

In het vijfde hoofdstuk komt de meest uitgebreide toepassing aan bod: de studie van donkere solitonen. Dit zijn excitaties van het superfluidum, die de vorm aannemen van een solitaire dip in de dichtheid die voortbeweegt aan een constante snelheid, zonder van vorm te veranderen. Met onze theorie vinden we een analytische uitdrukking voor de vorm van deze solitonen als functie van de parameters van het Fermi gas waaruit het superfluidum gemaakt is en als functie van de temperatuur. Solitonen blijken in Fermi gassen alleen maar stabiel voor ééndimensionale systemen, terwijl experimentatoren natuurlijk enkel quasi-ééndimensionale invangingspotentialen kunnen maken voor Fermi superfluida. We berekenen de kritische dikte die het quasi-ééndimensionaal systeem moet hebben om de instabiliteit te doen optreden, aan de hand van het spectrum van excitaties. Zowel wat de vorm van het soliton betreft, als voor de kritische dikte voor stabiliteit, kunnen we onze resultaten vergelijken met de Bogoliubov-de Gennes theorie die voor het Bardeen-Cooper-Schrieffer regime werd uitgewerkt, en vinden we een goede overeenkomst. Bovendien is onze theorie de enige die de verandering van relevante lengteschaal (van coherentielengte in het BEC regime naar correlatielengte in het BCS regime) kan beschrijven.

Als er bij het maken van fermionische paren meer van één type partner aanwezig is dan van zijn paringspartner, dan spreken we van populatie-imbalans in het Fermi gas. Zo'n populatie-imbalans zal, net zoals op een feestje waar er veel meer mannen dan vrouwen zijn, de paarvorming frustreren. We vinden dat de dip in de dichtheid die met het soliton samengaat, een goede plaats is om de overschot aan meerderheidspartner in te plaatsen [3, 4]. Dit blijkt het soliton zelf stabiel te maken, en biedt hiermee een uitweg aan experimentatoren die stabiele solitonen willen produceren.

Ten slotte vatten we de resultaten samen in het laatste hoofdstuk. De beschrijving die we in deze thesis ontwikkelen opent de weg naar heel wat toepassingen. Daar waar andere modellen, zoals de Bogoliubov-de Gennes theorie, al snel computationeel erg veeleisend worden zelfs voor een enkele vortex of soliton, heeft de huidige beschrijving het voordeel dat ze een snelle implementatie toelaat. Hiermee kan in de toekomst ook onderzocht worden wat er gebeurt wanneer er zich vele vortices of solitonen in het systeem bevinden – net zoals in supergeleiders kunnen we de toestanden van vortexmaterie gaan karakteriseren en

vortices en solitonen leren manipuleren. Ook valt de theorie uit deze thesis zonder veel moeite uit te breiden naar mengsels van fermionische superfluida, waarbij we de vraag kunnen onderzoeken of zulke mengsels toelaten om fenomenen teweeg te brengen die in de individuele superfluida niet optreden. Kortom, we hopen dat de theorie uit deze thesis voor onderzoekers van superfluïde Fermi gassen net zo nuttig kan worden als de beschrijving van Gross en Pitaevskii dat was voor onderzoekers van superfluïde Bose gassen.



# Members of the jury

## Members of the individual PhD commission

Prof. dr. Milorad Milosevic  
*Condensed Matter Theory, Universiteit Antwerpen*

Prof. dr. Jacques Tempere  
*Theory of Quantum Systems & Complex Systems, Universiteit Antwerpen*

Prof. dr. Sandra Van Aert  
*Electron Microscopy for Materials Science, Universiteit Antwerpen*

## External members

Prof. dr. Luca Salasnich  
*Theoretical Condensed Matter Physics, Università degli Studi di Padova*

Dr. Christoph Weiss  
*Joint Quantum Center, Durham University*

## Co-supervisor

Dr. Sergei Klimin  
*Theory of Quantum Systems & Complex Systems, Universiteit Antwerpen*



# Contents

|  |           |
|--|-----------|
| <b>Introduction</b>  | <b>1</b>  |
| <b>1 Ultracold quantum gases</b>   | <b>3</b>  |
| 1.1 History . . . . .  | 3         |
| 1.2 Trapping and cooling methods . . . . .   | 4         |
| 1.3 From bosons to fermions: the BEC-BCS crossover . . . . .                       | 6         |
| 1.4 Imbalanced Fermi systems . . . . .   | 9         |
| 1.5 Motivation and goal of the thesis . . . . .                                    | 11        |
| <b>2 Effective field theory</b>  | <b>13</b> |
| 2.1 Path integral approach . . . . .   | 14        |
| 2.1.1 Hubbard-Stratonovich transformation . . . . .                                | 15        |
| 2.1.2 Overview of the possible approximations . . . . .                            | 20        |
| 2.2 Saddle-point approximation . . . . .   | 21        |
| 2.3 Gradient expansion of the order parameter . . . . .                            | 23        |
| 2.4 Term without derivatives, $S_{\Phi}^{(p,0)}$ . . . . .                         | 25        |
| 2.4.1 Digression: analysis of the term $S_0$ . . . . .                             | 27        |
| 2.5 Term with spatial gradient $S_{\Phi}^{p,r}$ . . . . .                          | 28        |
| 2.5.1 Term $S_{\Phi}^{(p,r,a)}$ . . . . .  | 29        |
| 2.5.2 Term $S_{\Phi}^{(p,r,b)}$ . . . . .  | 36        |
| 2.5.3 Complete term $S_{\Phi}^{(2l,r)}$ . . . . .                                  | 41        |
| 2.6 Term with time derivatives $S_{\Phi}^{p,\tau}$ . . . . .                       | 45        |
| 2.6.1 Term with first order time derivatives . . . . .                             | 47        |
| 2.6.2 Term with second order time derivatives/1: $S_{\Phi}^{(\tau^2,a)}$ . . . . . | 52        |
| 2.6.3 Term with second order time derivatives/2: $S_{\Phi}^{(\tau^2,b)}$ . . . . . | 57        |
| 2.6.4 Complete term $S_{\Phi}^{(\tau^2)}$ . . . . .                                | 60        |
| 2.7 Complete effective field theory action . . . . .                               | 63        |
| <b>3 EFT description of Fermi superfluids</b>                                      | <b>65</b> |
| 3.1 Collective excitations . . . . .   | 66        |
| 3.2 Critical temperature . . . . .   | 71        |
| 3.2.1 Fluctuation contribution to the density . . . . .                            | 72        |

|          |  |            |
|----------|--|------------|
| 3.2.2    | Results for the critical temperature . . . . .                             | 75         |
| 3.3      | Correlation functions: condensate density and correlation length . . . . . | 76         |
| 3.3.1    | Generating functional . . . . .  | 76         |
| 3.3.2    | Condensate fraction . . . . .  | 79         |
| 3.3.3    | Pair correlation length . . . . .  | 82         |
| 3.4      | Validity range of the EFT . . . . .  | 84         |
| 3.5      | Comparison with other theoretical approaches . . . . .                     | 86         |
| 3.5.1    | BEC limit . . . . .  | 86         |
| 3.5.2    | EFT vs. time-dependent Ginzburg-Landau theory . . . . .                    | 90         |
| 3.5.3    | Bogoliubov-de Gennes theory . . . . .                                      | 91         |
| <b>4</b> | <b>EFT applied to polarons in Fermi superfluids</b>                        | <b>95</b>  |
| 4.1      | Mapping the fermionic problem on the BEC-polaron problem . . . . .         | 96         |
| 4.2      | Weak coupling limit for an impurity in a BEC condensate . . . . .          | 98         |
| 4.3      | Interaction parameter and effective mass of the polaron . . . . .          | 100        |
| 4.4      | Discussion and conclusions . . . . .                                       | 101        |
| <b>5</b> | <b>EFT applied to dark solitons in Fermi superfluids</b>                   | <b>103</b> |
| 5.1      | Introduction . . . . .   | 103        |
| 5.2      | Model . . . . .  | 105        |
| 5.3      | Results for a stable soliton . . . . .                                     | 110        |
| 5.3.1    | Shape of the soliton . . . . .   | 111        |
| 5.3.2    | Dynamical properties . . . . .   | 117        |
| 5.4      | Perturbative treatment . . . . .   | 123        |
| 5.5      | Results for the snake instability . . . . .                                | 126        |
| 5.6      | Discussion and conclusions . . . . .                                       | 129        |
| <b>6</b> | <b>Conclusions and outlook</b>   | <b>133</b> |
|          | <b>References</b>  | <b>137</b> |
|          | <b>List of publications by the author</b>                                  | <b>149</b> |
|          | <b>Acknowledgements</b>  | <b>151</b> |

# Introduction

The aim of the present thesis is to provide a detailed derivation as well as some applications of an effective field theory (EFT) suitable to describe a system of ultracold fermions across the BEC-BCS interaction regime in a wide range of temperatures below the critical one,  $T_c$ .

In Chapter 1 a brief overview about ultracold atomic gases, and in particular about Fermi superfluids, is given.

The road to superfluidity in atomic gases started in 1924 when the seminal papers by Bose and Einstein predicting Bose-Einstein condensation were published. The steps (both from a theoretical and an experimental point of view) that from there led to the realisation, in the first decade of the 2000's, of fermionic superfluidity in laboratory are summarised. Moreover some basic concepts which will play a crucial role in the remainder of the thesis, such as the BEC-BCS crossover and population imbalance, are introduced.

Chapter 2 is dedicated to the detailed derivation of an effective field theory [1] for the pairing order parameter capable of describing a fermionic superfluid across the BEC-BCS crossover in a wide range of configurations of temperature (below the transition temperature  $T_c$ ) and of taking into account an imbalance between the two spin-populations composing the system. All the calculations that lead from the basic hypothesis of a slowly varying order parameter to the final form of the EFT action are carried out in detail. The more tedious parts of the calculations are isolated in subsections named "Calculations" which can be avoided at a first read.

In Chapter 3 the first applications of the EFT are analysed. The spectrum of the collective excitations of the superfluid and the behaviour of the critical temperature as a function of the interaction are examined and the results are compared to the available literature.

Moreover a method for calculating correlation functions by using a generating functional based on the EFT action is introduced and employed to calculate the condensate fraction and the pair coherence length. The latter quantity is then used to test the hypothesis of slow variation of the order parameter which lies at the heart of the EFT, and hence to give an estimate of the range of reliability for the predictions of the theory.

The EFT is then compared in the opportune limiting situations to other widely used effective theories: the Gross-Pitaevskii equation, valid at  $T = 0$  in the BEC regime, and the

time-dependent Ginzburg-Landau treatment valid in the vicinity of the transition temperature. Also a brief introduction to the Bogoliubov-de Gennes theory is given.

Chapter 4 hosts an application of some of the results obtained in Chapter 3 about the spectra of collective excitations and correlation functions. The results presented here are collected in the manuscript [2]. In recent years much attention has been focused on one particular realisation of the widely studied polaron problem: the BEC polaron [5–14], which consists of an impurity interacting with the Bogoliubov excitations of a Bose-Einstein condensate. In the present model the Bose-Einstein condensate is replaced by a Fermi superfluid and the problem is treated in the weak coupling regime using perturbation theory. The formerly known results are strictly valid only in the BEC limit, where the fermionic system effectively becomes a BEC of tightly bound bosonic molecules. By using the information about the interaction dependence of the spectrum of collective excitations derived in Section 3.1 polaron theory is extended away from the BEC limit. The corrections to the polaronic coupling constant and effective mass are described as a function of the impurity-fermion pair and of the fermion-fermion interaction strengths.

Chapter 5 is dedicated to the application of the EFT to the description of dark solitons in Fermi superfluids. The chapter is divided in two main parts based on the publications [3] and [4] respectively. The first focuses on the study of stable soliton solutions in a quasi-1D configuration. The shape properties of the soliton are examined in different conditions of interaction, temperature, imbalance and soliton velocity. From these considerations and from the comparison between the total density profiles and the order parameter profiles, it emerges that the soliton core is a convenient place where the unpaired particles – present in the system due to finite temperature and/or imbalance – can be accommodated. Also some dynamical properties of the soliton solutions such as their effective mass and physical mass are analysed.

The second part of the chapter is instead devoted to the study of the snake instability mechanism responsible for the decay of solitons in experiment. While solitons in (quasi-)1D are stable, in real 3D configurations the depletion plane is not rigid and can oscillate, provoking the decay of the soliton into one (or more) vortex-like excitations. The maximum transverse size that the atomic cloud can have in order for the soliton to be stable is estimated and its behaviour in function of interaction across the BEC-BCS crossover is compared to the predictions of other theories found in the literature. For the imbalanced case (not yet treated in the existing literature), we find that this critical width is observed to increase as a function of population imbalance, offering in principle a direct method to stabilise solitons in experiment without being forced to reduce the system dimensionality.

Finally, in Chapter 6 we summarise the results and discuss the future prospects opened by the work reported in this thesis.

# Chapter 1

## Ultracold quantum gases

### 1.1 History

The history of research about ultracold quantum gases started in the 1920's with the seminal papers by Bose [15] and Einstein [16] that predicted the phenomenon of Bose-Einstein condensation. The key idea behind Bose-Einstein condensation is the fact that, when a bosonic gas is cooled down to extremely low temperatures (in the vicinity of absolute zero), a substantial fraction of the atoms coherently condenses into the lowest accessible quantum state.

A gas at room temperature in three dimensions is well described by Boltzmann's theory, which considers the particles as mass points moving around and colliding with each other with an average kinetic energy given by  $\langle p^2 \rangle / 2m = (3/2)k_B T$ . From basic concepts of quantum mechanics we know that atoms should not be considered as point-like mass particles precisely labeled by their position and momentum coordinates, but instead as wave(packet)s. The spread of the atoms' position can be identified with the de Broglie wavelength, defined as

$$\lambda_{dB} = \sqrt{\frac{2\pi\hbar^2}{mk_B T}}.$$

The average interparticle distance in a gas of density  $n$  can be estimated as  $d = n^{-1/3}$ . In order to have a parameter that gives a measure of the ratio between the interparticle distance and the quantum mechanical uncertainty on the position of the particles in the gas, the combination  $n\lambda_{dB}^3$  is used. The value of this parameter, often referred to as the "gas parameter", is very small in standard conditions of density and temperature, but when the temperature is decreased to values close to absolute zero it can reach unity: then the wavefunctions of different particles start overlapping and the quantum mechanical nature of the atoms emerges, making the Boltzmann's description of the system invalid. As it is schematically shown in Fig. 1.1, if the gas is made of bosonic atoms the individual wavefunctions start getting "in phase" and, when all particles share the same wavefunction, Bose-Einstein condensation is obtained. In this novel phase of matter, all atoms are in the same quantum state and can be described by a macroscopic wavefunction.

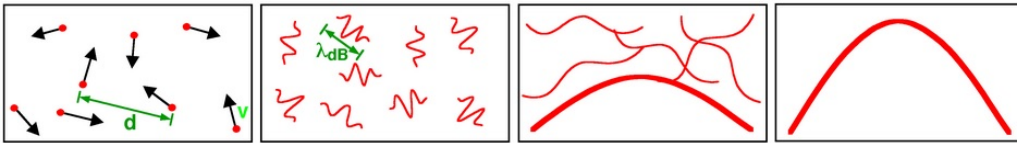


Figure 1.1: Schematic depiction of the Bose-Einstein condensation mechanism.

The experimental realisation of Bose-Einstein condensation was achieved 70 years later, in 1995, independently by E. A. Cornell and C. E. Wiemann and co-workers [17], by W. Ketterle and co-workers [18], and by Hulet and co-workers [19]. This breakthrough result earned Cornell, Wiemann, and Ketterle the 2001 Nobel Prize in physics.

## 1.2 Trapping and cooling methods

The main issues that needed to be addressed in order to obtain condensation in laboratory are the trapping of the atomic cloud and the cooling of the gas to temperatures of the order of 10 to 100 nanokelvins. In this subsection a short overview is given over the methods employed in order to achieve the desired conditions of temperature and density in experiments ultracold atomic gases. For more precise and exhaustive reviews on the topic the reader is addressed to references [20–22] (for Bose gases), and [23] (for Fermi gases).

The first method developed to confine a cloud of neutral atoms was the use of a magnetic trap [20, 21]. Due to the Zeeman effect an atom in a spatially-inhomogeneous magnetic field experiences a potential which varies in space. The energy of an atom in a state  $i$  can be written as  $E_i = c_i - \mu_i B$  where  $c_i$  is a constant term,  $\mu_i$  is the magnetic moment of the state and  $B$  is an external magnetic field. It is immediately clear that, if the magnetic moment of the atom is positive, the atom will tend to go towards spatial regions where the magnetic field  $B$  is stronger. This is the simple concept at the basis of magnetic traps: a magnetic field with a convenient spatial modulation can be used to create a trapping potential for a cloud of neutral atoms. It has to be remarked that in the case of neutral atoms, the magnetic moment  $\mu_i$  is not the intrinsic magnetic moment of the particle but the one related to its cyclotron motion: the typical magnitude of such magnetic moments is of the order of the Bohr magneton  $\mu_B = e\hbar/2m_e \sim 0.67k_B\text{K}/\text{T}$ , and the depth of the magnetic trap is  $\mu_i B$ . Hence, given that the strength of the magnetic fields commonly used in experiments is considerably less than 1T, the atoms must be cooled to temperatures substantially lower than 1K in order to feel a sizable confining potential.

The operation mechanism of optical trapping exploits instead the energy shift caused by the interaction between an atom and a laser beam due to the Stark effect. The interaction between an atom and a (time- and space-dependent) electric field  $\mathbf{E}_\omega(\mathbf{r}, t)$  with a characteristic frequency  $\omega$  is described in dipole approximation, by  $H = \mathbf{d} \cdot \mathbf{E}_\omega(\mathbf{r}, t)$ , where  $\mathbf{d}$  is the electric dipole moment of the atom. The ground state energy shift  $\Delta E_g$  due to the

Stark effect can be calculated in second order perturbation theory and results in

$$\Delta E_g = -\frac{1}{2}\alpha(\omega)\langle\mathbf{E}_\omega(\mathbf{r}, t)\rangle_t$$

where  $\langle\dots\rangle_t$  indicates a time average, and  $\alpha(\omega)$  is the real part of the dynamical polarizability, which is positive when the frequency  $\omega$  of the electric field is smaller than the atomic transition frequency (red detuning). As a consequence, a red detuned laser beam can be used to produce a minimum in the spatial distribution of the energy of an atom in the ground state and therefore obtain a trapping potential for the atomic cloud.

Up to now this introduction focused on bosonic systems: however a great advantage of optical traps over magnetic ones becomes evident when considering the typical setup of experiments with mixtures of fermionic atoms. In this case the atomic cloud is composed of two populations of fermions with different hyperfine spin which would therefore respond in different ways to a magnetic confinement. The optical trapping solves this problem since the confining potential experienced by the atoms is independent of their internal magnetic properties.

For what concerns the cooling, while a decrease in temperature increases the value of the “gas parameter”, an additional aspect concerning the density has to be considered: in the cooling process the system must be kept diluted enough that the gas does not experience a phase transition to the solid state. The solution to the problem was obtained in the late eighties when the laser cooling method was perfected. The development of this technique is due to the work of Phillips [24], Chu [25], and Cohen-Tannoudji [26], who in 1996 were awarded the Nobel Prize in physics.

The basic concept behind laser cooling is that a decrease in temperature corresponds to a decrease in the average momentum of the particles composing the gas. In practice when an atom experiences a head-on collision with a laser beam of frequency  $\omega$  corresponding to one of its absorption lines, it absorbs a photon and consequently its momentum is reduced by a quantity  $\hbar k = \hbar\omega/c$ . The now-excited atom spontaneously goes back to its initial state by emitting a photon in an arbitrary direction. A sketch of the laser cooling mechanism is shown in Fig.1.2. Still the total effect on the whole atomic cloud would not change the total kinetic energy, as some atoms would be accelerated while others would be slowed down. If however the frequency of the laser is red detuned with respect to  $\omega$ , as a consequence of the Doppler effect, the photons will be preferably absorbed by the atoms moving towards the source: a setup composed of two counterpropagating laser beams will then produce an average decrease of the momentum of the atoms along the direction of the lasers providing also a trapping effect on the atomic cloud. An additional positive effect of this technique is a decrease in the total kinetic energy of the particles, in fact due to the Doppler shift the re-emitted photons have a higher frequency than the original photons from the laser. This means that a part of the kinetic energy of the atoms has been transferred to the photons which are free to escape the system.

The temperatures reached with laser cooling (typically tens of microkelvins) are however not low enough to reach Bose-Einstein condensation in experiments: a further step is needed. This is provided by evaporative cooling: the key idea behind this method is

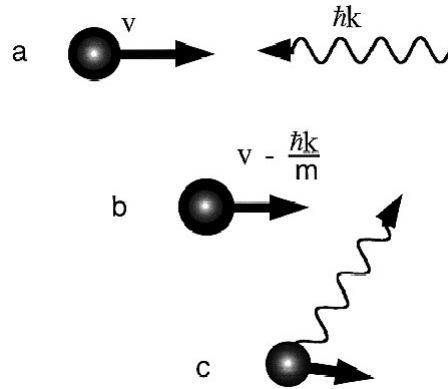


Figure 1.2: Steps of the laser cooling mechanism: (a) the atom experiences a head-on collision with the laser beam and absorbs a photon, (b) the momentum of the atom is decreased by an amount equal to the momentum of the photon, (c) the atom spontaneously re-emits a photon in an arbitrary direction. The re-emitted photon has a higher frequency than the original one because of the Doppler effect.

that, if particles with high energy are allowed to escape, the average energy of the system and, as a consequence, its temperature will be lowered. The most energetic atoms will occupy regions close to the edges of the trap. Radiofrequency (rf) radiation resonant with these atoms can be used to flip their magnetic moment from a low-field seeking one to a high-field seeking one, hence expelling them from the trap. The process can be repeated in order to eliminate atoms with lower and lower energy by adjusting the rf frequency. With a combination of laser cooling and evaporative cooling the temperature of the system can reach the values necessary to observe Bose-Einstein condensation, i.e. tens to hundreds of nanokelvins. It must be remarked that in experiments with fermionic systems another technique, named “sympathetic cooling” is used to obtain the needed conditions of temperature. The evaporative cooling mechanism works only if, after the most energetic particles have escaped the system, the remaining particles can relax back to an equilibrium state. In bosonic systems the energy is redistributed by means of elastic scattering processes, but fermions in the same quantum state cannot undergo such processes. Therefore, after evaporative cooling has been exploited on the separate populations, one spin-state component is put into contact with the other thus making the redistribution of the energy in the whole cloud possible [27].

### 1.3 From bosons to fermions: the BEC-BCS crossover

Due to the Pauli exclusion principle two identical fermions cannot share the same quantum state and therefore Bose-Einstein condensation is not accessible in a fermionic system. However, in 1911, Onnes measured that the resistivity of mercury drops to zero when the metal is cooled to temperatures below 4.7K: in this condition the material is said to be-

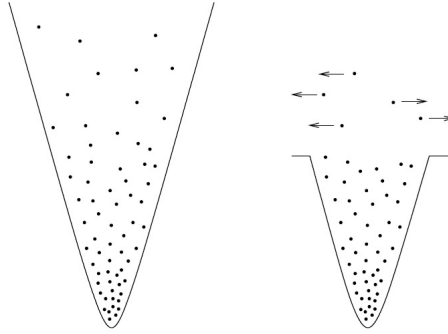


Figure 1.3: Evaporative cooling mechanism [20]: a radiofrequency radiation is employed to flip the magnetic moment of the most energetic particles in the vicinity of the edge of the trap. These particles can hence escape the trap and, as a result, the temperature of the system is decreased.

come superconducting as the conduction electrons can flow freely without experiencing resistance. This observation provided the first evidence of superfluidity of an electron gas. In an attempt to understand this phenomenon, in 1958 Bardeen, Cooper and Schrieffer proposed a theory that explains fermionic superfluidity in terms of Cooper pairs: weakly bound pairs of electrons with dimension much larger than the interparticle spacing. The explanation of the effective attractive interaction responsible for the binding of two electrons despite the Coulomb repulsion that occurs between them was provided by polaron theory. Starting with the seminal paper by Landau [28], the screening of the Coulomb potential due to the interaction between electrons and the phonons describing the lattice deformations in a polar crystal was widely studied [29–31]. At the basis of the BCS description lies the fact that the effective attractive interaction between electrons in a superconductor is due precisely to this electron-phonon interaction. Contrary to the intuitive hypothesis that fermionic superfluidity corresponds to condensation of electron pairs in real space, the work of Bardeen, Cooper, and Schrieffer proved that it can be instead interpreted as the condensation of Cooper pairs in momentum space. Despite the intrinsic difference between BCS superconductivity and Bose-Einstein condensation, at the end of the 1960’s it was proven [32–34] that the ansatz BCS ground state wavefunction provided a good description not only for a condensate of Cooper pairs, but also for a Bose-Einstein condensate of tightly bound fermionic pairs. This represented the first evidence of the existence of a bridge between BCS superfluidity and Bose-Einstein condensation. Just over ten years later, in 1980 Leggett [35] demonstrated that the regimes of Cooper pairs and of tightly bound diatomic molecules are linked through a smooth crossover: the so-called BEC-BCS crossover.

The first experimental realisation of a quantum degenerate Fermi system dates to 1999 and was achieved by the group of D. S. Jin at JILA [36]. The term “degenerate” here means that the fermionic particles in the system are at an average distance smaller than the de Broglie wavelength, and occupy (almost) all of the quantum states below a given

energy (referred to as the Fermi energy). The achievement of degeneracy was a key step towards observing superfluidity in a fermionic system. However the transition temperature  $T_c$  predicted by the BCS theory for the onset of such phase was still out of reach for experimentalists. In the conditions of temperature and density of an ultracold Fermi gas the interaction between atoms is dominated by *s-wave* scattering processes, the strength of which can be described in terms of a single parameter: the product  $k_F a_s$  of the Fermi momentum  $k_F$  and the *s-wave* scattering length  $a_s$ . Such simplification comes from the consideration that the extreme diluteness assures that the main properties of ultracold atomic systems are dominated by two-body collisions and that, at the same time, the particles are at distances much larger than the range of the Van der Waals potential. Moreover the low temperatures involved assures that also the de Broglie wavelength of the atoms is larger than this typical range and that the interaction between the atoms can be approximated by a (spherically symmetric) contact potential. The BCS transition temperature can then be expressed, in the limit of  $k_F |a_s| \ll 1$ , as  $T_c \approx 0.28 T_F e^{-\pi/(2k_F |a_s|)}$  where  $T_F$  indicates the Fermi temperature. From the previous expression it emerges that  $T_c$  becomes exponentially small for small values of  $k_F |a_s|$ . In order to bring  $T_c$  to values that are achievable in laboratory, experimentalists can in principle act on the two quantities  $k_F$  and  $a_s$ . The Fermi momentum  $k_F$  however is connected to the particle density and must remain small to assure that gas remains dilute. The tool that made the step towards Fermi superfluidity possible is the Feshbach resonance mechanism [37]. An external magnetic field is used to tune the energy of a molecular bound state and bring it close to resonance with a scattering state of two free particles. In this way the value of the *s-wave* scattering length and, as a consequence, the interaction parameter  $k_F a_s$  can be modified as shown in Fig. 1.4. By exploiting the Feshbach resonance mechanism, in 2003 three groups independently achieved the creation of a Bose-Einstein condensate of diatomic molecules. In these experiments the Feshbach mechanism was used to make the energy of the molecular bound state lower than the energy of the free-particles scattering state, reaching values of  $k_F a_s > 1$  (BEC side of the resonance), and the condensation of the bound fermion pairs was detected [38–40]. In the following years the full potential of Feshbach resonances was put to use and different values of the coupling parameter  $k_F a_s$  became accessible to experimentalists, that were hence able to produce systems in configurations all across the BEC-BCS crossover regime [41–44]. In one of these experiments, namely [42], the first direct evidence of fermionic superfluidity was observed as a lattice of quantized vortices was detected.

The BEC-BCS crossover has been the focus of major attention also from a theoretical point of view. Starting from the seminal work by Leggett [35] that gave the first description of the system at  $T = 0$  at the mean field level, a substantial amount of literature has been devoted to the study of this topic. In particular it is worth mentioning the first beyond mean-field treatment of the finite temperature case, due to Nozières and Schmitt-Rink [45] and the path integral description developed by Sá de Melo and coworkers [46]. As a result of these studies a schematic interaction-temperature phase diagram for a system of ultracold fermionic neutral atoms was obtained, an example of which can be seen in Fig. 1.5 [47]. The inclusion of fluctuations beyond-mean field enabled theorists to better analyse

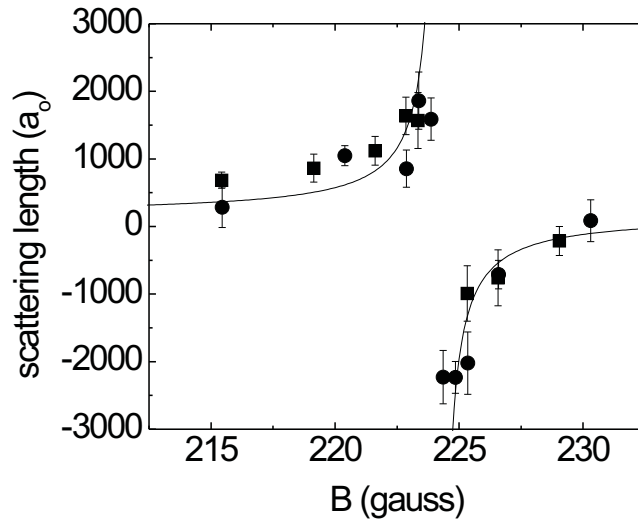


Figure 1.4: Observation of a Feshbach resonance in an untracold system of  $^{40}\text{K}$  atoms [37]. The external magnetic field  $B$  is used to tune the  $s$ -wave scattering length (here given in units of the Bohr radius  $a_0$ ). Across the resonance the sign of the scattering length changes from positive to negative.

the behaviour of the system and in particular to distinguish between two transition temperatures: the one at which pairing occurs,  $T_{pair}$ , and the one that determines the onset of the superfluid phase,  $T_c$ . The intermediate regime between the BCS and BEC limits, the so-called unitarity regime, has also drawn a lot of interest from a theoretical point of view: the fact that in this configuration the  $s$ -wave scattering length diverges implies that the only length scale of the system is given by the interparticle distance and the energy scale by the Fermi energy. In these conditions the physics of the system is said to be universal and properties such as the binding energy and the pair size are determined by universal constants times the Fermi energy and the interparticle distance respectively.

## 1.4 Imbalanced Fermi systems

One of the properties that justify the large interest drawn by ultracold atomic gases is their high degree of tunability. Experimentalists can modify a wide variety of parameters of the system, ranging from interaction to temperature, geometry, dimensionality, and population imbalance. In particular population imbalance will be the object of much attention throughout the present thesis.

As mentioned above, the typical configuration of an ultracold fermionic system consists of two populations of particles in different hyperfine states trapped in an optical potential. These two hyperfine states will be relabeled as spin-up and spin-down states, and we

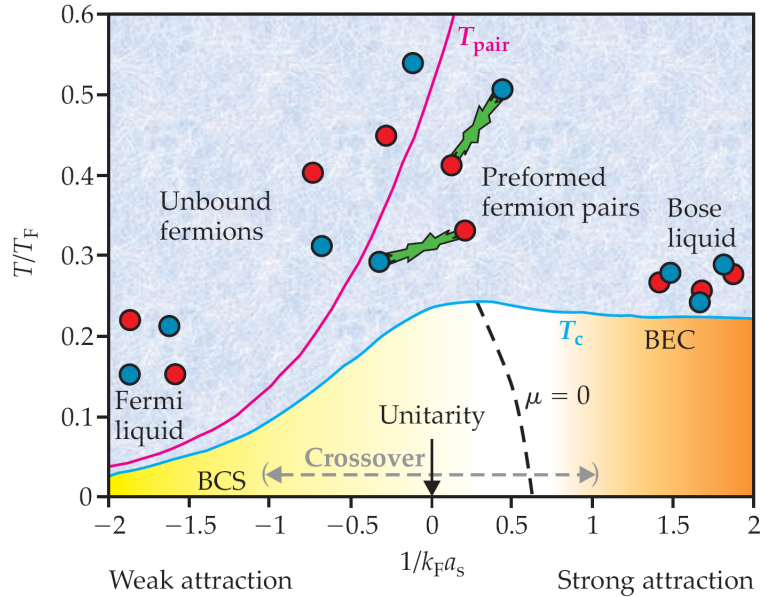


Figure 1.5: Schematic phase diagram of a system of ultracold Fermi atoms as a function of temperature and interaction (source: [47]). The BEC-BCS crossover regime is highlighted: negative values of  $(k_F a_s)^{-1}$  correspond to a BCS configuration of weakly bound Cooper pairs, while large positive values indicate the limit of a BEC of tightly bound diatomic molecules.

consider the system as a (pseudo-)spin 1/2 system. A nonzero population imbalance means that the numbers of particles in the two spin populations are different, and this has a substantial effect on the pairing mechanism, which was analysed by theorists since the early 1960's, when the seminal papers by Clogston [48] and Chandrasekhar [49] about critical magnetic fields in superconductors were published. To have a simple picture of how spin-imbalance affects the formation of fermionic pairs in an ultracold gas it is useful to resort to a toy model [50]. Figure 1.6 shows the Fermi surfaces (i.e. surfaces of constant energy  $E = E_F$ ) for the up- and down-spin particles as a function of the  $x$ - and  $y$ -components of the momentum, in a balanced (panel A) and imbalanced (panel B) situation respectively. Naming the superfluid bandgap  $\Delta$ , the BCS ansatz requires that just the particles in the interval  $[E_F - \Delta, E_F + \Delta]$  participate to the pairing, therefore in the picture a shell of width  $2\Delta$  is drawn along the Fermi surfaces. On the one hand, in a spin-balanced system the Fermi energies for the up- and down- spin particles are equal ( $E_{F\uparrow} = E_{F\downarrow}$ ) and the “pairing shells” perfectly overlap. On the other hand, in presence of a nonzero spin imbalance the Fermi energies are different (e.g.  $E_{F\uparrow} > E_{F\downarrow}$  as in the case depicted in Fig. 1.6) and the overlap between the “pairing shells” becomes smaller or ceases to exist, thus explaining the detrimental effect that imbalance has on the fermion pairs' formation mechanism.

Imbalance in ultracold Fermi systems was first experimentally engineered in 2006 [51, 52]. In these experiments it was observed that, in presence of imbalance, phase separation can occur, meaning that beyond a critical imbalance the excess component particles and

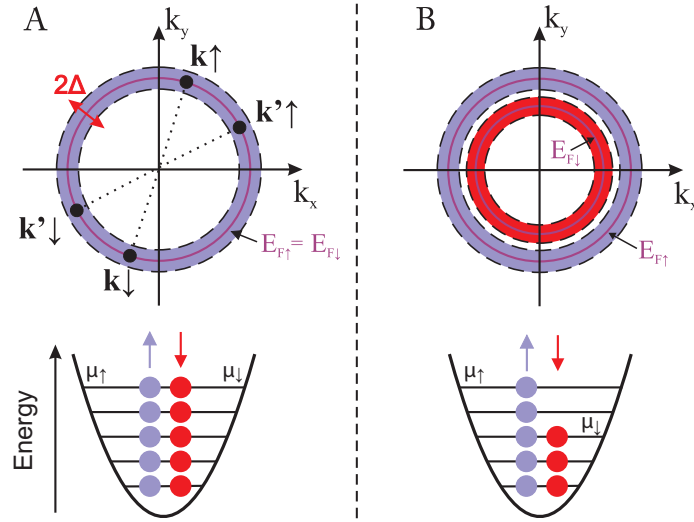


Figure 1.6: Schematic depiction of the effect of imbalance on the formation mechanism of the fermionic pairs. In a balanced system the chemical potentials of the two spin populations are equal ( $\mu_{\uparrow} = \mu_{\downarrow}$ ), while in presence of imbalance a difference arises ( $\mu_{\uparrow} \neq \mu_{\downarrow}$ ). The overlap between the “pairing shells” is maximal in the balanced situation (panel A) while it becomes smaller or even disappears in an imbalanced situation. Source: [50].

a “standard” balanced superfluid are spatially separated, with the former ones residing in the more external regions of the atomic cloud and the latter the inner core. The concept of phase separation can be clearly understood by looking at Fig. 1.7 where the densities of the two spin components (panels A and B) are shown separately and compared to the density difference (panel C). The search for possible superfluid states that can occur in an imbalanced system is still ongoing and has produced a large amount of literature: between the possible exotic superfluid phases that have been proposed as a solution to this problem, it is worth mentioning the FFLO state, theorised in the 1960’s by Fulde and Ferrel [53], and Larkin and Ovchinnikov [54], which predicts that an imbalanced superfluid can exist provided that the Cooper pairs are created with nonzero momentum in contrast with the BCS ansatz that requires the momentum of the fermion pairs to be zero.

In the remainder of the present work the effects of imbalance on various quantities will be considered: in particular the effects of imbalance on the shape and on the dynamics of dark solitons propagating in a Fermi superfluid are going to be investigated. Moreover the stability of dark solitons with respect to decay through the snake instability is going to be analysed for different levels of imbalance.

## 1.5 Motivation and goal of the thesis

As noted above, Bose-Einstein condensed gases can be described by a macroscopic wave function. This macroscopic wave function has to satisfy a differential equation known as the

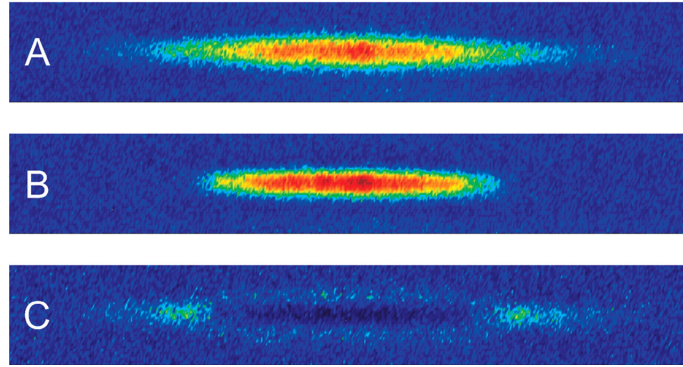


Figure 1.7: Absorption images showing the density of the majority and minority spin populations (panels A and B respectively), compared to the density difference between the two components (panel C). The slightly negative density detected at the center of the cloud in panel C is due to experimental conditions. Source: [52].

Gross-Pitaevskii equation [55,56]. The macroscopic wave function and the Gross-Pitaevskii equation allow for a useful hydrodynamic description of the system, by interpreting the modulus squared of the wave function as the density of the condensate and the phase gradients as its superfluid velocity field. In particular the link between the velocity and the phase is crucial to explain several properties of superfluidity: the quantization of circulation, singly quantized vortices, persistent currents, and the Fairbank-Hess effect [21,57] follow directly from it.

For superfluid Fermi gases, these characteristic expressions of superfluidity are also present. Therefore it makes sense to look for an analogous description of those systems in terms of a macroscopic wave function, whose modulus squared can be interpreted as a density of fermion pairs, and whose phase gradient provides the superfluid velocity field. The goal of this thesis is to provide such a description: we find the differential equation that such a “pair wavefunction” has to obey and derive several properties of the fermionic superfluid from the study of this equation and its solutions.

For superconductors, a related description based on a macroscopic wave function was developed by Ginzburg and Landau [58], and used by Abrikosov [59] to introduce the concept of a vortex. Ginzburg-Landau theory, which has proven to be extremely useful for superconductors, was lacking a counterpart for superfluid Fermi gases. In this thesis, we find this counterpart. Moreover, whereas the validity of Ginzburg-Landau theory is restricted to temperatures close to the critical temperature, the theory that we derive here will have a broader temperature range of applicability, and is valid across the BEC-BCS crossover.

# Chapter 2

## Effective field theory

The present chapter is devoted to the derivation of an effective field theory (EFT) suited for describing the BEC-BCS crossover regime in ultracold Fermi gases. The main source of inspiration for the formulation of this theory came from the well known Ginzburg-Landau (GL) treatment. This was originally developed in 1950 [58] as a phenomenological model that would allow to describe type-1 superconductors in terms of a macroscopic wavefunction (interpreted as the order parameter for the superconducting transition) rather than in terms of the microscopic degrees of freedom. Assuming a small value for the order parameter  $\Phi$  close to the transition temperature, the free energy is expanded in series as

$$F(T, V) = F_n(T, V) + V \left( a(T)|\Phi|^2 + \frac{b(T)}{2}|\Phi|^4 + \dots \right) \quad (2.1)$$

(where  $F_n(T, V)$  is the free energy for the normal state), and only the first few (typically two) lowest-order terms are retained. The coefficients  $a$  and  $b$  are fixed by the critical magnetic field and by the London penetration depth [60], and are related to the binding energy of the Cooper pairs and to the interaction amplitude between two pairs respectively. Five years later, in 1955 Lev Gor'kov managed to derive the GL theory starting from a microscopical model [61]. More recently, starting from the early 90's with the paper by Sá de Melo *et al.* [46], this treatment has been widely used to study many aspects of ultracold Fermi gases [62–66].

With respect to the GL method – which is based on the key assumption of dealing with a small order parameter – in the present study this hypothesis is substituted by the weaker requirement of having a slowly varying order parameter. This relaxation of the basic assumption leads in principle to a wider applicability range of the effective field theory. In particular, while the requirement of a small order parameter limits the validity of the Ginzburg-Landau treatment to a small range of temperatures close to the critical temperature  $T_c$ , the validity range of the EFT is found to be substantially broader. An extensive discussion about the practical range of validity of the theory including a comparison with the results of the GL treatment will take place at a later stage in this thesis. In order to have a basic picture of the system under consideration and an overview of the formalism that we are going to employ in the present treatment, we begin our discussion by writing

the Hamiltonian for an ultracold gas of fermions with spin imbalance.

$$\begin{aligned} \hat{H} &= \hat{H}_0 + \hat{H}_{INT} = \\ &= \int d\mathbf{r} \left[ \left( \hat{\psi}_\uparrow^\dagger(\mathbf{r}) \hat{\psi}_\downarrow^\dagger(\mathbf{r}) \right) \begin{pmatrix} -\frac{\hbar^2 \nabla^2}{2m} - \mu - \zeta & 0 \\ 0 & -\frac{\hbar^2 \nabla^2}{2m} - \mu + \zeta \end{pmatrix} \begin{pmatrix} \hat{\psi}_\uparrow(\mathbf{r}) \\ \hat{\psi}_\downarrow(\mathbf{r}) \end{pmatrix} + \right. \\ &\quad \left. + g \hat{\psi}_\uparrow^\dagger(\mathbf{r}) \hat{\psi}_\downarrow^\dagger(\mathbf{r}) \hat{\psi}_\downarrow(\mathbf{r}) \hat{\psi}_\uparrow(\mathbf{r}) \right] \end{aligned} \quad (2.2)$$

In the last expression  $\mu$  represents the chemical potential while  $\zeta$  can be seen as a difference in the chemical potentials between the two hyperfine states  $\uparrow$  and  $\downarrow$ . The relations between these two quantities and the chemical potentials for the spin  $\uparrow$  and spin  $\downarrow$  species are given by <sup>1</sup>

$$\mu = \frac{\mu_\uparrow + \mu_\downarrow}{2} \quad \zeta = \frac{\mu_\uparrow - \mu_\downarrow}{2}$$

The quartic term  $\hat{H}_{INT}$  describes the two body *s-wave* contact interaction between particles with opposite spin. Notice that from now on the natural system of units  $\hbar = 1$ ,  $k_F = 1$ ,  $2m = 1$ , will be adopted to simplify the notation. Here  $k_F$  is the Fermi wavevector, fixed by the total density  $n$  as  $k_F = (2\pi n)^{1/2}$  in 2D and  $k_F = (3\pi^2 n)^{1/3}$  in 3D.

The derivation of the effective field theory is quite extensive and involves lengthy algebraic manipulations; in order to enable the reader to have an overview of the derivation without being forced to go through the heavily algebraic parts, these have been isolated in subsections labeled “Calculation” which can be skipped at a first read.

The remainder of the chapter is organised in the following way: in Sections 2.1-2.2 the path integral formalism is introduced as a method to study ultracold Fermi gases, while in Section 2.3 the assumption of a slowly varying order parameter is implemented by means of a gradient expansion. Sections 2.4-2.6 host the actual calculation of the terms and coefficients of the effective field theory that are later brought together in Section 2.7 where the complete EFT action is presented.

## 2.1 Path integral approach

The path-integral formulation of quantum mechanics, introduced by Richard Feynman in 1948 [67], is based on two axioms:

- the quantum mechanical amplitude of a process is a weighted sum of the amplitudes of all possible realisations of the process.
- the weight is given by  $\exp[iS/\hbar]$  where  $S$  is the action of the system.

The fact that the different realisations are weighted by a “phase” factor ensures that the formalism can account for interference, while the presence of the factor  $S/\hbar$  at the exponent provides that, in the classical limit ( $\hbar \rightarrow 0$ ) the Lagrangian mechanics is retrieved.

---

<sup>1</sup>from now on we will always refer to the two different hyperfine (pseudospin) states as spin states

The path-integral approach has proven extremely powerful in the description of quantum many-body systems [68]: in particular a substantial fraction of the literature on ultracold quantum gases is based on this description.

The partition function of a system of ultracold fermions described by the Hamiltonian (2.2) introduced in the previous section can be written as a path integral over all possible configurations of the fermionic Grassmann fields  $\bar{\psi}_\sigma(\mathbf{r}, \tau)$  and  $\psi_\sigma(\mathbf{r}, \tau)$  as

$$\mathcal{Z} = \int \mathcal{D}\bar{\psi}_\sigma(\mathbf{r}, \tau) \mathcal{D}\psi_\sigma(\mathbf{r}, \tau) e^{-S[\bar{\psi}_\sigma(\mathbf{r}, \tau), \psi_\sigma(\mathbf{r}, \tau)]}. \quad (2.3)$$

The action  $S[\bar{\psi}_\sigma(\mathbf{r}, \tau), \psi_\sigma(\mathbf{r}, \tau)]$  is given by

$$S[\bar{\psi}_\sigma, \psi_\sigma] = \int_0^\beta d\tau \left[ \int d\mathbf{r} \sum_\sigma \bar{\psi}_\sigma(\mathbf{r}, \tau) \partial_\tau \psi_\sigma(\mathbf{r}, \tau) + H[\bar{\psi}_\sigma(\mathbf{r}, \tau), \psi_\sigma(\mathbf{r}, \tau)] \right], \quad (2.4)$$

where, with respect to (2.2), the Grassmann variables  $\bar{\psi}_\sigma(\mathbf{r}, \tau)$  and  $\psi_\sigma(\mathbf{r}, \tau)$  replace the field operators  $\hat{\psi}_\sigma^\dagger(\mathbf{r})$  and  $\hat{\psi}_\sigma(\mathbf{r})$ , and  $\beta = 1/(k_B T)$  represents the inverse temperature.

### 2.1.1 Hubbard-Stratonovich transformation

Recalling the form of the Hamiltonian of the system (2.2), it follows that the action (2.4) contains a term that is quartic in the fermionic variables. This means that the functional integral appearing in the expression of the partition function (2.3) can not be computed exactly. To overcome this problem a transformation is needed that decouples the interaction term and reduces the action to an expression that is quadratic in the fermionic fields. This goal can be achieved by means of the *Hubbard-Stratonovich transformation*. Exploiting a basic equality for Gaussian integrals,

$$\begin{aligned} & \exp \left[ -g \int_0^\beta \int d\mathbf{r} \bar{\psi}_\uparrow(\mathbf{r}, \tau) \bar{\psi}_\downarrow(\mathbf{r}, \tau) \psi_\downarrow(\mathbf{r}, \tau) \psi_\uparrow(\mathbf{r}, \tau) \right] = \\ & = \int \mathcal{D}\Phi^*(\mathbf{r}, \tau) \mathcal{D}\Phi(\mathbf{r}, \tau) \exp \left[ \int_0^\beta \int d\mathbf{r} \left( \frac{\Phi^*(\mathbf{r}, \tau) \Phi(\mathbf{r}, \tau)}{g} + \right. \right. \\ & \left. \left. + \Phi^*(\mathbf{r}, \tau) \psi_\downarrow(\mathbf{r}, \tau) \psi_\uparrow(\mathbf{r}, \tau) + \Phi(\mathbf{r}, \tau) \bar{\psi}_\uparrow(\mathbf{r}, \tau) \bar{\psi}_\downarrow(\mathbf{r}, \tau) \right) \right], \end{aligned} \quad (2.5)$$

the quartic term can be removed at the cost of introducing the complex bosonic field  $\Phi(\mathbf{r}, \tau)$  (and its conjugate  $\Phi^*(\mathbf{r}, \tau)$ ). This new bosonic field can be interpreted as the field describing the fermion pairs. A schematic depiction of the HS transformation is shown in Fig.2.1. The choice of this decomposition of the quartic term is often referred to in literature as the *Bogoliubov channel* of the *Hubbard-Stratonovich transformation*. The

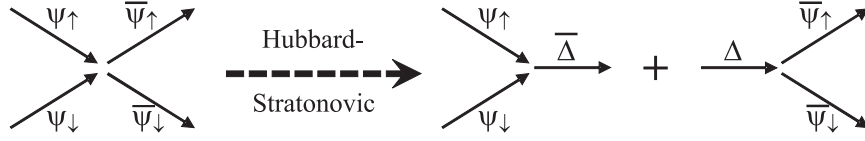


Figure 2.1: Schematic depiction of the Hubbard-Stratonovich transformation: the interaction term originally consists of a product of four fermion fields. After the HS transformation it is decomposed in a term that represents two fermions of opposite spin pairing up, a term describing the propagation of the “free” pairs (not shown) and a term for the pair breaking up into two fermions.

resulting partition function is

$$\begin{aligned} \mathcal{Z} = & \int \mathcal{D}\bar{\psi}_\sigma(\mathbf{r}, \tau) \int \mathcal{D}\psi_\sigma(\mathbf{r}, \tau) \int \mathcal{D}\Phi^*(\mathbf{r}, \tau) \int \mathcal{D}\Phi(\mathbf{r}, \tau) \\ & \exp \left[ - \int_0^\beta \int d\mathbf{r} \left( \sum_\sigma \bar{\psi}_\sigma(\mathbf{r}, \tau) (\partial_\tau - \nabla^2 - \mu_\sigma) \psi_\sigma(\mathbf{r}, \tau) + \right. \right. \\ & \left. \left. - \frac{\Phi^*(\mathbf{r}, \tau)\Phi(\mathbf{r}, \tau)}{g} - \Phi^*(\mathbf{r}, \tau)\psi_\downarrow(\mathbf{r}, \tau)\psi_\uparrow(\mathbf{r}, \tau) - \Phi(\mathbf{r}, \tau)\bar{\psi}_\uparrow(\mathbf{r}, \tau)\bar{\psi}_\downarrow(\mathbf{r}, \tau) \right) \right]. \end{aligned} \quad (2.6)$$

The action of the system is thus quadratic in the fermionic fields and can be rewritten in an even simpler form by introducing the Nambu spinor  $\Psi$  defined as

$$\Psi(\mathbf{r}, \tau) = \begin{pmatrix} \psi_\uparrow(\mathbf{r}, \tau) \\ \psi_\downarrow(\mathbf{r}, \tau) \end{pmatrix}, \quad \bar{\Psi}(\mathbf{r}, \tau) = (\bar{\psi}_\uparrow(\mathbf{r}, \tau), \bar{\psi}_\downarrow(\mathbf{r}, \tau)). \quad (2.7)$$

The action in the new notation is

$$\begin{aligned} S = & \int_0^\beta d\tau \int d\mathbf{r} \left( \bar{\Psi}(\mathbf{r}, \tau)\mathbb{A}(\mathbf{r}, \tau)\Psi(\mathbf{r}, \tau) - \frac{\Phi^*(\mathbf{r}, \tau)\Phi(\mathbf{r}, \tau)}{g} \right) = \\ = & \int_0^\beta d\tau \int d\mathbf{r} \bar{\Psi}(\mathbf{r}, \tau)\mathbb{A}(\mathbf{r}, \tau)\Psi(\mathbf{r}, \tau) + S_B, \end{aligned} \quad (2.8)$$

where in the last line  $S_B$  indicates the purely bosonic component of the action, i.e. the quadratic term in the bosonic fields.

### Inverse fermion propagator

In the last equation a compact expression for the action functional was presented in terms of the Nambu spinors  $\Psi$  and  $\bar{\Psi}$ . The matrix  $\mathbb{A}(\mathbf{r}, \tau)$  appearing in (2.8) can be identified as the inverse Green’s matrix for the interacting fermions and is defined as

$$\mathbb{A}(\mathbf{r}, \tau) = \begin{pmatrix} \partial_\tau - \nabla^2 - \mu - \zeta & -\Phi(\mathbf{r}, \tau) \\ -\Phi^*(\mathbf{r}, \tau) & \partial_\tau + \nabla^2 + \mu - \zeta \end{pmatrix} = -\mathbb{G}^{-1}(\mathbf{r}, \tau). \quad (2.9)$$

Separating the diagonal and off-diagonal components we can write

$$-\mathbb{G}^{-1}(\mathbf{r}, \tau) = -\mathbb{G}_0^{-1}(\mathbf{r}, \tau) + \mathbb{F}(\mathbf{r}, \tau),$$

where  $-\mathbb{G}_0^{-1}$  describes a free fermion and  $\mathbb{F}$  is the part proportional to the pairing field  $\Phi$ , namely

$$-\mathbb{G}_0^{-1}(\mathbf{r}, \tau) = \begin{pmatrix} \partial_\tau - \nabla^2 - \mu - \zeta & 0 \\ 0 & \partial_\tau + \nabla^2 + \mu - \zeta \end{pmatrix}, \quad (2.10)$$

$$\mathbb{F}(\mathbf{r}, \tau) = \begin{pmatrix} 0 & -\Phi(\mathbf{r}, \tau) \\ -\Phi^*(\mathbf{r}, \tau) & 0 \end{pmatrix}. \quad (2.11)$$

It is convenient to have these expressions also in momentum-frequency representation: the Fourier transform of  $-\mathbb{G}^{-1}$  is defined as

$$-\mathbb{G}^{-1}(\mathbf{k}', n' | \mathbf{k}, n) = \frac{1}{\beta V} \int_0^\beta d\tau \int d\mathbf{r} e^{i\mathbf{k}' \cdot \mathbf{r} - i\omega_{n'} \tau} (-\mathbb{G}^{-1}(\mathbf{r}, \tau)) e^{-i\mathbf{k} \cdot \mathbf{r} + i\omega_n \tau},$$

with  $V$  the volume of the system and  $\omega_n = (2n+1)\pi/\beta$  the fermionic Matsubara frequency. For the  $-\mathbb{G}_0^{-1}(\mathbf{r}, \tau)$  component we can write

$$\begin{aligned} -\mathbb{G}_0^{-1}(\mathbf{k}', n' | \mathbf{k}, n) &= -[\mathbb{G}_0(\mathbf{k}, n)]^{-1} \delta_{\mathbf{k}, \mathbf{k}'} \delta_{n, n'} \\ &= \begin{pmatrix} i\omega_n - k^2 - \mu - \zeta & 0 \\ 0 & i\omega_n + k^2 + \mu - \zeta \end{pmatrix} \delta_{\mathbf{k}, \mathbf{k}'} \delta_{n, n'}. \end{aligned} \quad (2.12)$$

The reciprocal space representation of the non-diagonal component  $\mathbb{F}$  is instead given by

$$\mathbb{F}(\mathbf{k}', n' | \mathbf{k}, n) = \begin{pmatrix} 0 & -\Phi_{\mathbf{k}+\mathbf{k}', n+n'} \\ -\Phi_{\mathbf{k}+\mathbf{k}', n+n'}^* & 0 \end{pmatrix}. \quad (2.13)$$

From the last expressions it is clear that, contrary to the free fermion component, the pairing term  $\mathbb{F}$  has non-zero contributions coming from terms with  $\mathbf{k} \neq \mathbf{k}'$ .

Finally, defining the dispersion relation  $\xi_k \equiv k^2/(2m) - \mu$ , the Green's function  $\mathbb{G}_0(\mathbf{k}, n)$  for a free fermion reads

$$\mathbb{G}_0(\mathbf{k}, n) = \begin{pmatrix} \frac{1}{i\omega_n - \xi_k + \zeta} & 0 \\ 0 & \frac{1}{i\omega_n + \xi_k + \zeta} \end{pmatrix}. \quad (2.14)$$

### Grassmann integration

Using the action (2.8), the partition function of the system in terms of the Nambu spinors  $\Psi$  and  $\bar{\Psi}$  reads

$$\mathcal{Z} = \chi \int \mathcal{D}\Phi^* \int \mathcal{D}\Phi \int \mathcal{D}\bar{\Psi} \int \mathcal{D}\Psi \exp \left[ - \int_0^\beta d\tau \int d\mathbf{r} \bar{\Psi}(\mathbf{r}, \tau) (-\mathbb{G}^{-1}(\mathbf{r}, \tau)) \Psi(\mathbf{r}, \tau) - S_B \right]. \quad (2.15)$$

The sign factor  $\chi$  in front of the integration sign is due to the rearrangement of the fermionic variables in the Nambu spinors notation: for each space-time point we have a minus sign coming from the equality

$$\begin{aligned} \int \mathcal{D}\bar{\Psi} \int \mathcal{D}\Psi &= \prod_{\mathbf{r},\tau} \left[ \int d\bar{\psi}_{\uparrow}(\mathbf{r},\tau) \int d\psi_{\uparrow}(\mathbf{r},\tau) \int d\psi_{\downarrow}(\mathbf{r},\tau) \int d\bar{\psi}_{\downarrow}(\mathbf{r},\tau) \right] = \\ &= \prod_{\mathbf{r},\tau} (-1) \int d\bar{\psi}_{\uparrow}(\mathbf{r},\tau) \int d\psi_{\uparrow}(\mathbf{r},\tau) \int d\bar{\psi}_{\downarrow}(\mathbf{r},\tau) \int d\psi_{\downarrow}(\mathbf{r},\tau). \end{aligned}$$

In order to transform the right hand side of the first line into the expression in the second line (i.e. the integration measure appearing in (2.6)), the last two Grassmann integration measures must be exchanged, thus generating a factor  $(-1)$  for each space-time point.

Since the term  $S_B$  at the exponent does not depend on the fermionic fields, the relevant integral that must be computed is just

$$\chi \int \mathcal{D}\bar{\Psi} \int \mathcal{D}\Psi \exp \left[ - \int_0^\beta d\tau \int d\mathbf{r} \bar{\Psi}(\mathbf{r},\tau) (-\mathbb{G}^{-1}(\mathbf{r},\tau)) \Psi(\mathbf{r},\tau) \right]. \quad (2.16)$$

This is the textbook Grassmann integral for a quadratic action functional and its result is simply

$$\prod_{\mathbf{r},\tau} (-1) \det_{\sigma}(-\mathbb{G}^{-1}(\mathbf{r},\tau)), \quad (2.17)$$

where the subscript  $\sigma$  indicates that the determinant is taken over the  $2 \times 2$  matrix between the Nambu spinors. With some algebraic manipulation this quantity can be rewritten as

$$\prod_{\mathbf{r},\tau} (-1) \det_{\sigma}(-\mathbb{G}^{-1}(\mathbf{r},\tau)) = \exp \left\{ \int_0^\beta d\tau \int d\mathbf{r} \ln [-\det_{\sigma}(-\mathbb{G}^{-1}(\mathbf{r},\tau))] \right\}$$

After performing the integration over the fermionic variables  $\Psi$  and  $\bar{\Psi}$  the resulting partition function is

$$\mathcal{Z} = \int \mathcal{D}\Phi^* \int \mathcal{D}\Phi \exp \left\{ - \int_0^\beta d\tau \int d\mathbf{r} \left[ -\frac{|\Phi(\mathbf{r},\tau)|^2}{g} - \ln [-\det_{\sigma}(-\mathbb{G}^{-1}(\mathbf{r},\tau))] \right] \right\}. \quad (2.18)$$

Recasting equation (2.15) in reciprocal space notation is not as straightforward: introducing the momentum-frequency representation for the pair field  $\Phi$  in (2.15) gives

$$\mathcal{Z} = \int \mathcal{D}\Phi^* \int \mathcal{D}\Phi \int \mathcal{D}\bar{\Psi} \int \mathcal{D}\Psi \exp \left[ \sum_{\mathbf{q},m} \frac{\Phi_{\mathbf{q},m}^* \Phi_{\mathbf{q},m}}{g} - \sum_{\substack{\mathbf{k},n \\ \mathbf{k}',n'}} \bar{\Psi}_{\mathbf{k},n} [-\mathbb{G}^{-1}(\mathbf{k}',n'|\mathbf{k},n)] \Psi_{\mathbf{k}',n'} \right], \quad (2.19)$$

where the following definitions for the Nambu spinors were used:

$$\Psi_{\mathbf{k},n} = \begin{pmatrix} \psi_{\mathbf{k},n,\uparrow} \\ \bar{\psi}_{\mathbf{k},n,\downarrow} \end{pmatrix} \quad \text{and} \quad (\bar{\psi}_{\mathbf{k},n,\uparrow} \quad \psi_{\mathbf{k},n,\downarrow}).$$

As remarked in the previous subsection, even in reciprocal space the inverse fermion Green's function is not diagonal due to its pairing component  $\mathbb{F}$  (2.13). The solution of this non-diagonal Grassmann integration is described in detail in reference [69] and the general result is

$$\int \mathcal{D}\bar{\psi} \int \mathcal{D}\psi \exp \left[ - \sum_{\substack{\mathbf{k},n \\ \mathbf{k}',n'}} \bar{\Psi}_{\mathbf{k},n} [-\mathbb{G}^{-1}(\mathbf{k}', n' | \mathbf{k}, n)] \Psi_{\mathbf{k}',n'} \right] = \chi \det [-\mathbb{G}^{-1}(\mathbf{k}', n' | \mathbf{k}, n)].$$

where  $\chi$  is again a sign factor that accounts for the change in the order of the integration measures and the det is taken not only on the spinor degrees of freedom, but also on the momentum and frequency ones. Through some basic matrix manipulation the previous result can be recast in the following form

$$\det(-\mathbb{G}^{-1}) = \exp [\ln (\det (-\mathbb{G}^{-1}))] = \exp [\text{Tr} (\ln (-\mathbb{G}^{-1}))].$$

As for the determinant, also the Tr in the last expression is taken over all  $\mathbf{k}, n, \sigma$  values. The partition function finally results

$$\mathcal{Z} = \chi \int \mathcal{D}\Phi^* \int \mathcal{D}\Phi \exp \left[ \sum_{\mathbf{q},m} \frac{\Phi_{\mathbf{q},m}^* \Phi_{\mathbf{q},m}}{g} + \text{Tr} [\ln (-\mathbb{G}^{-1})] \right]. \quad (2.20)$$

It is worth remarking that the presence of the sign factor  $\chi$  in front of the integrals does not affect the calculation of expectation values.

The result (2.20) can be finally rewritten in terms of an effective action depending only on the bosonic fields  $\Phi$  and  $\Phi^*$ :

$$S_{eff} = S_B - \text{Tr} [\ln (-\mathbb{G}^{-1})]. \quad (2.21)$$

From the decomposition of the matrix  $\mathbb{A}$  and from the relation (2.12) it follows that

$$\begin{aligned} S_{eff} &= S_B - \text{Tr} [\ln (-\mathbb{G}_0^{-1} + \mathbb{F})] = \\ &= S_B - \text{Tr} [\ln (-\mathbb{G}_0^{-1})] - \text{Tr} [\ln (1 - \mathbb{G}_0 \mathbb{F})] = \\ &= S_B + S_0 + \sum_{p=1}^{\infty} \frac{1}{p} \text{Tr} [(\mathbb{G}_0 \mathbb{F})^p] = \\ &= S_B + S_0 + \sum_{p=1}^{\infty} S_{\Phi}^{(p)}. \end{aligned} \quad (2.22)$$

Notice that in the second to last passage, the logarithm was expanded in a power series as  $\ln(1-x) = -\sum_{p=1}^{\infty} \frac{x^p}{p}$ .

It is important to remark that this form of the action in terms of an expansion in powers of the pairing field is a key element in many different approaches to beyond-mean field treatments of ultracold Fermi gases. For example, in the context of a Ginzburg-Landau treatment, at this point the action would be approximated by keeping just the first few lower order terms in the series, corresponding to the assumption  $\Phi \rightarrow 0$ . A brief overview of the main approximation schemes adopted to calculate (2.22) is given in Subsection 2.1.2. Instead in the following Section we will see how the entire series can be handled by imposing the weaker requirement that the bosonic field  $\Phi$  varies slowly in both time and space.

Before going ahead with the calculation we show the explicit expression for the terms  $S_{\Phi}^{(p)}$  introduced in the last line of (2.22):

$$\begin{aligned} S_{\Phi}^{(p)} &= \frac{1}{p} \text{Tr} [(\mathbb{G}_0 \mathbb{F})^p] = \\ &= \frac{1}{p} \int dx_1 \cdots \int dx_p \text{Tr} [\mathbb{G}_0(x_1 - x_2) \mathbb{F}(x_2) \mathbb{G}_0(x_2 - x_3) \mathbb{F}(x_3) \cdots \mathbb{G}_0(x_p - x_1) \mathbb{F}(x_1)] \end{aligned} \quad (2.23)$$

Notice that in the last expression a compact notation for the 4-dimensional space-"time" vectors was introduced, i.e.

$$(\mathbf{r}, \tau) \longrightarrow x.$$

This notation will be often employed in the remainder of this chapter for the sake of brevity.

## 2.1.2 Overview of the possible approximations

- Saddle-point approximation [35]

$$\sum_{p=1}^{\infty} \frac{1}{p} \text{Tr} [(\mathbb{G}_0 \mathbb{F})^p] \approx \text{Tr} [\mathbb{G}_0 \mathbb{F}_{sp}] + \frac{1}{2} \text{Tr} [\mathbb{G}_0 \mathbb{F}_{sp} \mathbb{G}_0 \mathbb{F}_{sp}] + \frac{1}{3} \text{Tr} [\mathbb{G}_0 \mathbb{F}_{sp} \mathbb{G}_0 \mathbb{F}_{sp} \mathbb{G}_0 \mathbb{F}_{sp}] + \dots$$

The pairing component  $\mathbb{F}$  is approximated by its saddle-point version  $\mathbb{F}_{sp}$  and the whole sum over  $p$  is calculated.

- Gaussian pair fluctuations [45, 46]

$$\sum_{p=1}^{\infty} \frac{1}{p} \text{Tr} [(\mathbb{G}_0 \mathbb{F})^p] \approx \text{Tr} [\mathbb{G}_0 \mathbb{F}(x_1)] + \frac{1}{2} \text{Tr} [\mathbb{G}_0 \mathbb{F}(x_1) \mathbb{G}_0 \mathbb{F}(x_2)] + \frac{1}{3} \text{Tr} [\mathbb{G}_0 \mathbb{F}_{sp} \mathbb{G}_0 \mathbb{F}_{sp} \mathbb{G}_0 \mathbb{F}_{sp}] + \dots$$

The space-time dependence of  $\mathbb{F}$  is accounted exactly but only up to  $p = 2$ .

- Gradient expansion

$$\sum_{p=1}^{\infty} \frac{1}{p} \text{Tr} [(\mathbb{G}_0 \mathbb{F})^p] \approx \text{Tr} [\mathbb{G}_0 \mathbb{F}_{grad}] + \frac{1}{2} \text{Tr} [\mathbb{G}_0 \mathbb{F}_{grad} \mathbb{G}_0 \mathbb{F}_{grad}] + \frac{1}{3} \text{Tr} [\mathbb{G}_0 \mathbb{F}_{sp} \mathbb{G}_0 \mathbb{F}_{sp} \mathbb{G}_0 \mathbb{F}_{sp}] + \dots$$

Same as for the GPF treatment only the terms up to  $p = 2$  are kept in the sum (2.23) but the full  $\mathbb{F}(x_2 - x_1)$  is approximated by

$$\mathbb{F}(x - x_1) \approx \mathbb{F}_{grad}(x - x_1) = \mathbb{F}_0 + x (\nabla \mathbb{F})_0 + \frac{1}{2} x^2 (\nabla^2 \mathbb{F})_0$$

Two possible choices of approximation are:

- ◇  $\mathbb{F}_0 \rightarrow 0$ . This assumption is valid close to  $T_c$  and the usual Ginzburg-Landau approach is retrieved.
  - ◇  $\mathbb{F}_0 \rightarrow \mathbb{F}_{sp}$  [64]. A version of the Ginzburg-Landau treatment with an extended domain of validity is obtained.
- EFT treatment

$$\sum_{p=1}^{\infty} \frac{1}{p} \text{Tr} [(\mathbb{G}_0 \mathbb{F})^p] \approx \text{Tr} [\mathbb{G}_0 \mathbb{F}_{grad}] + \frac{1}{2} \text{Tr} [\mathbb{G}_0 \mathbb{F}_{grad} \mathbb{G}_0 \mathbb{F}_{grad}] + \frac{1}{3} \text{Tr} [\mathbb{G}_0 \mathbb{F}_{sp} \mathbb{G}_0 \mathbb{F}_{grad} \mathbb{G}_0 \mathbb{F}_{grad}] + \dots$$

Up to  $p = 2$  this approach coincides with the usual gradient expansion. However in the contributions corresponding to  $p > 2$  (at most) two occurrences of  $\mathbb{F}_{sp}$  are replaced by  $\mathbb{F}_{grad}$  and the entire sum over  $p$  is computed.

## 2.2 Saddle-point approximation

In general an analytic summation of the series appearing in (2.22) is impossible: as mentioned above, in order to overcome this problem an approximation is required. The easiest way to simplify the summation in (2.22) is to consider the bosonic field  $\Phi$  to be a constant. This hypothesis corresponds to setting

$$\Phi_{\mathbf{q},m} \rightarrow \sqrt{\beta V} \delta(\mathbf{q}) \delta_{m,0} \times \Delta, \quad (2.24)$$

$$\Phi_{\mathbf{q},m}^* \rightarrow \sqrt{\beta V} \delta(\mathbf{q}) \delta_{m,0} \times \bar{\Delta}. \quad (2.25)$$

Therefore the major contribution to the bosonic integral is assumed to come from the configuration in which the Cooper pairs are condensed in the  $\mathbf{q} = 0$  state. Performing this approximation before the Grassmann integration over the fermionic fields leads to a great simplification of the calculations: the saddle-point expression for the partition function in momentum-space notation is

$$\mathcal{Z}_{sp} = \int \mathcal{D}\bar{\Psi} \int \mathcal{D}\Psi \exp \left[ \frac{|\Delta|^2}{g} - \sum_{\mathbf{k},n} \bar{\Psi}_{\mathbf{k},n} [-\mathbb{G}_{sp}^{-1}] \Psi_{\mathbf{k},n} \right],$$

where the saddle-point inverse fermion propagator is given by

$$-\mathbb{G}_{sp}^{-1}(\mathbf{k}, n) = \begin{pmatrix} i\omega_n - k^2 - \mu - \zeta & \Delta \\ \Delta & i\omega_n + k^2 + \mu - \zeta \end{pmatrix}. \quad (2.26)$$

As it is intuitively clear the approximation (2.24) has made the inverse fermion propagator diagonal in reciprocal space.

Integrating out the fermionic fields leads to

$$\begin{aligned} \mathcal{Z}_{sp} &= \exp \left\{ \frac{|\Delta|^2}{g} - \sum_{\mathbf{k},n} \ln [-\det (-\mathbb{G}_{sp}^{-1})] \right\} = \\ &= \exp \left\{ \frac{|\Delta|^2}{g} - \sum_{\mathbf{k},n} \ln [(i\omega_n - E_{\mathbf{k}} + \zeta) (-i\omega_n - E_{\mathbf{k}} - \zeta)] \right\}, \end{aligned} \quad (2.27)$$

where the single-particle excitation energy  $E_{\mathbf{k}}$  has been introduced, i.e.

$$E_{\mathbf{k}} = \sqrt{\xi_{\mathbf{k}}^2 + \Delta^2}. \quad (2.28)$$

The saddle-point partition function can be rewritten in terms of the saddle-point thermodynamic potential per unit volume  $\Omega_{sp}$  as

$$\mathcal{Z}_{sp} = \exp \{-\beta V \Omega_{sp}\}.$$

From (2.27), it follows that  $\Omega_{sp}$  is defined as

$$\Omega_{sp} = -\frac{|\Delta|^2}{g} - \frac{1}{\beta V} \sum_{\mathbf{k},n} \ln [(i\omega_n - E_{\mathbf{k}} + \zeta) (-i\omega_n - E_{\mathbf{k}} - \zeta)].$$

To obtain a more explicit expression for this quantity the fermionic Matsubara summation over the frequency  $\omega_n$  must be carried out. Doing this [68,69] leads to

$$\begin{aligned} \Omega_{sp} &= -\frac{|\Delta|^2}{g} - \frac{1}{V} \sum_{\mathbf{k}} \left\{ \frac{1}{\beta} [2 \cosh(\beta E_{\mathbf{k}}) + 2 \cosh(\beta \zeta)] - \xi_{\mathbf{k}} \right\} = \\ &= -\frac{|\Delta|^2}{8\pi k_F a_s} - \int \frac{d\mathbf{k}}{(2\pi)^3} \left\{ \frac{1}{\beta} [2 \cosh(\beta E_{\mathbf{k}}) + 2 \cosh(\beta \zeta)] - \xi_{\mathbf{k}} - \frac{|\Delta|^2}{2k^2} \right\}, \end{aligned} \quad (2.29)$$

where in the last line the regularised form of the coupling constant  $g$  [20,68]

$$\frac{1}{g} = \frac{m}{4\pi k_F a_s} - \int \frac{d^3k}{(2\pi)^3} \frac{m}{k^2}$$

has been inserted and the continuum limit has been taken for the sum over the momentum  $k$ .

From the expression for the thermodynamic potential (2.29) the explicit form for the gap and number equations can be derived. The saddle-point gap equation is given by

$$\begin{aligned} 0 &= \frac{\partial \Omega_{sp}}{\partial \Delta} \\ \iff & -\frac{1}{4\pi k_F a_s} = \int \frac{d\mathbf{k}}{(2\pi)^3} \left[ \frac{\sinh(\beta E_{\mathbf{k}})}{\cosh(\beta E_{\mathbf{k}}) + \cosh(\beta \zeta)} \frac{1}{E_{\mathbf{k}}} - \frac{1}{k^2} \right]. \end{aligned} \quad (2.30)$$

The equation for the total density is instead

$$n = - \left. \frac{\partial \Omega_{sp}}{\partial \mu} \right|_{T, \zeta, \Delta} \iff n = \int \frac{d\mathbf{k}}{(2\pi)^3} \left[ 1 - \frac{\sinh(\beta E_{\mathbf{k}})}{\cosh(\beta E_{\mathbf{k}}) + \cosh(\beta \zeta)} \frac{\xi_{\mathbf{k}}}{E_{\mathbf{k}}} \right], \quad (2.31)$$

while the equation for the excess particle density, accounting for a majority of particles in one spin component in presence of imbalance, is

$$\delta n = - \left. \frac{\partial \Omega_{sp}}{\partial \zeta} \right|_{T, \mu, \Delta} \iff \delta n = \int \frac{d\mathbf{k}}{(2\pi)^3} \frac{\sinh(\beta \zeta)}{\cosh(\beta E_{\mathbf{k}}) + \cosh(\beta \zeta)}. \quad (2.32)$$

The saddle point values for the order parameter and for the chemical potential obtained from the solution of these equations will be frequently used in the rest of this thesis: therefore the reader is addressed to the review paper [69] for a detailed discussion about the derivation of equations (2.30)-(2.32) and on their solution.

## 2.3 Gradient expansion of the order parameter

Despite giving reliable results that offer a good agreement with experiment near  $T = 0$ , the saddle point approximation proves to be unsuitable to describe the BEC-BCS crossover at finite temperature. This is mainly due to two reasons:

- it does not account for excitation modes other than the single-particle Bogoliubov mode described by the dispersion relation (2.38).
- it does not include the effect of fluctuations of the order parameter.

To overcome these limitations we propose a beyond saddle point effective field theory that can describe Fermi superfluids in the BEC-BCS crossover at finite temperatures. The main idea behind said effective field theory is to consider the order parameter  $\Phi$  to be slowly varying in both time and space. This is a weaker assumption with respect to the one at the basis of the saddle point approximation and of the normal Ginzburg-Landau treatment and is ultimately expected to lead to a larger applicability domain for the theory.

To implement the slow-variation requirement we are going to employ a gradient expansion for the field  $\Phi$ . In order to do so, as a first step we carry out in (2.23) a coordinate shift with respect to<sup>2</sup>  $x \equiv x_1$

$$x_l \longrightarrow x + x'_l \quad l \neq 1$$

---

<sup>2</sup>Notice that in the following  $x$  will be often identified with  $x_1$ : the two notations are both going to be employed. While the notation  $x_1$  is used to make more apparent the order of the indices, which will prove to be useful in the lengthy calculations of the following sections, the notation  $x$  is sometimes needed to highlight the peculiar role of said variable.

As a consequence of this shift the expression for the pairing component of the inverse propagator  $\mathbb{F}$  calculated in  $x_l$  is given by

$$\begin{aligned} \mathbb{F}(x_l) &= \mathbb{F}(x + x'_l) = \mathbb{F}(\mathbf{r} + \mathbf{r}'_l, \tau + \tau'_l) = \\ &= \mathbb{F}(\mathbf{r}, \tau) + \tau'_l \frac{\partial \mathbb{F}(\mathbf{r}, \tau)}{\partial \tau} + \mathbf{r}'_l \cdot \nabla_{\mathbf{r}} \mathbb{F}(\mathbf{r}, \tau) + \frac{1}{2} \sum_{i,j} \frac{\partial^2 \mathbb{F}(\mathbf{r}, \tau)}{\partial x_{li} \partial x_{lj}} x'_{li} x'_{lj} + \dots \end{aligned} \quad (2.33)$$

Keeping only the first few terms in this expansion corresponds precisely to the desired assumption that the field  $\Phi(\mathbf{r}, \tau)$  is slowly varying in space and time. Therefore in the following calculations only the lowest-order non vanishing terms both in the space and time derivatives will be retained. The effect of a gradient approximation on a generic function  $f(x)$  is schematically depicted in Fig.2.2 where the analytic function  $f(x)$  is compared with its gradient-approximated form  $f(x_i) + df/dx|_{x_i} \delta x$  evaluated on a grid of spacing  $\delta x$  (for two definitions of  $f$ ). It is intuitively clear that the gradient approximation becomes more accurate as the typical variation scale of the function gets larger.

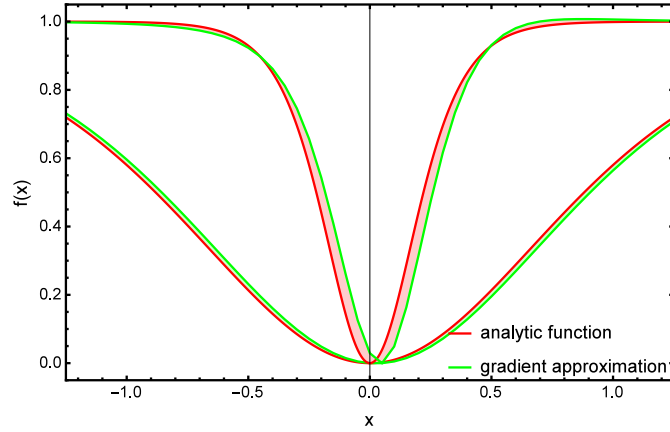


Figure 2.2: The two functions  $\tanh(2x)^2$  and  $\tanh(10x)^2$  are compared to their gradient-expanded form. It is intuitive to see that the gradient expansion is more accurate for the slower-varying function.

Before carrying out the summation over the index  $p$  in the expression for the effective action  $S_{eff}$  (2.22) we separate every single term  $S_{\Phi}^{(p)}$  depending on the pairing field into three components

$$S_{\Phi}^{(p)} = S_{\Phi}^{(p,0)} + S_{\Phi}^{(p,\tau)} + S_{\Phi}^{(p,r)},$$

where

- $S_{\Phi}^{(p,0)}$  is the component without space or time derivatives;
- $S_{\Phi}^{(p,\tau)}$  describes the contributions coming from the inclusion of time derivatives;
- $S_{\Phi}^{(p,r)}$  is the term accounting for the inclusion of spatial derivatives.

## 2.4 Term without derivatives, $S_{\Phi}^{(p,0)}$

In the calculation of  $S_{\Phi}^{(p,0)}$ , we consider just the contribution to the quantity  $S_{\Phi}^{(p)}$  coming from the first term in the gradient expansion of the order parameter (2.33), i.e.

$$\mathbb{F}(x + x'_l) \longrightarrow \mathbb{F}(x).$$

From (2.23), the explicit expression for  $S_{\Phi}^{(p,0)}$  reads

$$S_{\Phi}^{(p,0)} = \frac{1}{p} \int dx \cdots \int dx_p \text{Tr} [\mathbb{G}_0(x - x_2) \mathbb{F}(x) \mathbb{G}_0(x_2 - x_3) \mathbb{F}(x) \cdots \mathbb{G}_0(x_p - x) \mathbb{F}(x)]. \quad (2.34)$$

Inserting the Fourier series for  $\mathbb{G}_0(\mathbf{r}, \tau)$ , which is given by

$$\mathbb{G}_0(\mathbf{r}, \tau) = \frac{1}{\beta V} \sum_{\mathbf{k}, n} e^{i\mathbf{k} \cdot \mathbf{r} - i\omega_n \tau} \mathbb{G}_0(\mathbf{k}, n), \quad (2.35)$$

into (2.34) and carrying out all (but one) of the space- and time-integrals – namely integrating over  $x_2, \dots, x_p$  – we get

$$S_{\Phi}^{(p,0)} = \frac{1}{\beta V} \sum_{\mathbf{k}, n} \int d^4x \frac{1}{p} \text{Tr} [(\mathbb{G}_0(\mathbf{k}, n) \mathbb{F}(x))^p].$$

This is a strange-looking but convenient “mixed-representation”, where the Green’s functions appear in their momentum-frequency notation, while the pairing matrices  $\mathbb{F}$  appear in the time-space form. The introduction of the reciprocal space representation of the propagator  $\mathbb{G}_0$  leads to a great simplification of expression (2.34) obtained by the repeated use of the integral representation of the delta function; on the other hand the time-space representation for the matrix  $\mathbb{F}$  is a convenient choice since it enables to keep track of what elements of the gradient expansion of  $\Phi$  (2.33) are being retained. To compute the summation of the contributions  $S_{\Phi}^{(p,0)}$  to all orders in  $p$ ,

$$\sum_{p=1}^{\infty} S_{\Phi}^{(p,0)},$$

it is now convenient to treat separately the terms with even and odd powers of  $\mathbb{G}_0 \mathbb{F}$ .

**Odd powers**  $\longrightarrow \text{Tr} [(\mathbb{G}_0 \mathbb{F})^{2l+1}]$

Given the form of the matrices  $\mathbb{G}_0$  (2.14) and  $\mathbb{F}$  (2.11) it is easy to see that by multiplying them an odd number of times we always obtain a 2 by 2 matrix with elements arranged in the following way

$$\begin{pmatrix} 0 & \neq 0 \\ \neq 0 & 0 \end{pmatrix}.$$

It is then trivial to see than the trace always gives 0. Therefore we conclude that

$$\sum_{l=1}^{\infty} S_{\Phi}^{(2l+1,0)} \propto \sum_{l=1}^{\infty} \frac{1}{2l+1} \text{Tr} \left[ (\mathbb{G}_0(\mathbf{k}, n)\mathbb{F}(x))^{2l+1} \right] = 0.$$

**Even powers**  $\longrightarrow \text{Tr} \left[ (\mathbb{G}_0\mathbb{F})^{2l} \right]$

In order to study the behaviour of the elements  $S_{\Phi}^{2l,0}$  it is useful to consider the matrix  $(\mathbb{G}_0\mathbb{F})^2$  and then calculate its integer powers, thus reproducing all the even powers of  $\mathbb{G}_0\mathbb{F}$ . The product  $(\mathbb{G}_0\mathbb{F})^2$  is diagonal

$$(\mathbb{G}_0(\mathbf{k}, n)\mathbb{F}(x))^2 = \begin{pmatrix} \frac{|\Phi(x)|^2}{(i\omega_n + \zeta)^2 - \xi_{\mathbf{k}}^2} & 0 \\ 0 & \frac{|\Phi(x)|^2}{(i\omega_n + \zeta)^2 - \xi_{\mathbf{k}}^2} \end{pmatrix}. \quad (2.36)$$

Moreover from the explicit expression it emerges that the diagonal elements are equal. We can thus write a simple formula for the trace of the terms with even powers of  $(\mathbb{G}_0\mathbb{F}_0)$ , namely

$$\text{Tr} \left[ (\mathbb{G}_0(\mathbf{k}, n)\mathbb{F}(x))^{2l} \right] = 2 \left( \frac{|\Phi(x)|^2}{(i\omega_n + \zeta)^2 - \xi_{\mathbf{k}}^2} \right)^l.$$

\* \* \*

Consequently the component of the action coming from the first term in the gradient expansion (2.33) is proportional to

$$\sum_{l=1}^{\infty} \frac{1}{2l} \left( \frac{|\Phi(x)|^2}{(i\omega_n + \zeta)^2 - \xi_{\mathbf{k}}^2} \right)^l.$$

The summation over  $l$ , including the prefactor 2, can be recast into the form

$$\sum_{p=1}^{\infty} \frac{(-x)^p}{p} = -\ln(1+x).$$

Therefore it follows that

$$2 \sum_{l=1}^{\infty} \frac{1}{2l} \left( \frac{|\Phi(x)|^2}{(i\omega_n + \zeta)^2 - \xi_{\mathbf{k}}^2} \right)^l = -\ln \left[ 1 + \frac{|\Phi(x)|^2}{\xi_{\mathbf{k}}^2 - (i\omega_n + \zeta)^2} \right].$$

In conclusion we have that

$$\sum_{p=1}^{\infty} S_{\Phi}^{(p,0)} = -\frac{1}{\beta V} \int d\mathbf{r} \int_0^{\beta} d\tau \sum_{\mathbf{k}, n} \left( \ln \left[ 1 + \frac{|\Phi(x)|^2}{\xi_{\mathbf{k}}^2 - (i\omega_n + \zeta)^2} \right] \right). \quad (2.37)$$

### 2.4.1 Digression: analysis of the term $S_0$

Before going on with the calculation by tackling the sum over the fermionic Matsubara frequencies appearing in (2.37) it is convenient to examine the term  $S_0$ . As it turns out, combining the contributions of  $S_0$  and  $S_{\Phi}^{p,0}$  before exploiting the Matsubara summation makes this task easier, therefore the present derivation will follow this path. From the definition in [69]

$$S_0 = -\ln [-\det (-\mathbb{G}_0^{-1})],$$

the expression for  $S_0$  can be obtained by directly calculating the determinant of  $-\mathbb{G}_0^{-1}$  (2.35). This eventually leads to

$$S_0 = -\sum_{\mathbf{k},n} \ln [\xi_{\mathbf{k}}^2 - (i\omega + \zeta)^2].$$

\* \* \*

The expressions of  $S_0$  and  $\sum_{p=1}^{\infty} S_{\Phi}^{(p,0)}$  can be now combined to obtain

$$\begin{aligned} S_0 + \sum_{p=1}^{\infty} S_{\Phi}^{(p,0)} &= -\sum_{\mathbf{k},n} \ln [\xi_{\mathbf{k}}^2 - (i\omega + \zeta)^2] + \\ &\quad -\frac{1}{\beta V} \int d^4x \sum_{\mathbf{k},n} \left( \ln \left[ 1 + \frac{|\Phi(x)|^2}{\xi_{\mathbf{k}}^2 - (i\omega_n + \zeta)^2} \right] \right) = \\ &= -\frac{1}{\beta V} \int d^4x \sum_{\mathbf{k},n} (\ln [\xi_{\mathbf{k}}^2 - (i\omega_n + \zeta)^2 + |\Phi(x)|^2]). \end{aligned}$$

Notice that, since the terms coming from  $S_0$  do not depend on the space-time coordinates  $x$ , in order to collect everything under the integral sign, the identity  $\frac{1}{\beta V} \int d\mathbf{r} \int_0^{\beta} d\tau = 1$  was used.

The Matsubara summation over the fermionic frequencies  $\omega_n$  is performed in the standard way [68, 69] and gives

$$\sum_n \ln [\xi_{\mathbf{k}}^2 - (i\omega_n + \zeta)^2 + |\Phi(x)|^2] = [2 \cosh(\beta E_{\mathbf{k}}(x)) + 2 \cosh(\beta \zeta)] - \beta \xi_{\mathbf{k}},$$

where  $E_{\mathbf{k}}(x)$  is defined in analogy to (2.28) as

$$E_{\mathbf{k}}(x) \equiv \sqrt{\xi_{\mathbf{k}}^2 + |\Phi(x)|^2}. \quad (2.38)$$

The expression for  $S_{eff}^{(0)} = S_B + S_0 + \sum_{p=1}^{\infty} S_{\Phi}^{(p,0)}$  then reads

$$\begin{aligned} S_{eff}^{(0)} &= -\int d^4x \left\{ \frac{m |\Phi(x)|^2}{4\pi a_s} + \int \frac{d\mathbf{k}}{(2\pi)^3} \left[ \right. \right. \\ &\quad \left. \left. \frac{1}{\beta} \ln (2 \cosh(\beta E_{\mathbf{k}}(x)) + 2 \cosh(\beta \zeta)) - \xi_{\mathbf{k}} - \frac{m |\Phi(x)|^2}{k^2} \right] \right\}. \end{aligned}$$

Defining a thermodynamical potential  $\Omega_s(|\Phi|^2)$  that has the same form of the *saddle-point* thermodynamic potential but accounts for the dependence on the coordinates  $(\mathbf{r}, \tau)$  of the order parameter  $\Phi$  as

$$\Omega_s(|\Phi|) = -\frac{m|\Phi(x)|^2}{4\pi a_s} - \int \frac{d\mathbf{k}}{(2\pi)^3} \left\{ \frac{1}{\beta} \ln [2 \cosh(\beta E_{\mathbf{k}}(x)) + 2 \cosh(\beta \zeta)] - \xi_{\mathbf{k}} - \frac{m|\Phi(x)|^2}{k^2} \right\}, \quad (2.39)$$

the expression of  $S_{eff}^{(0)}$  becomes simply

$$S_{eff}^{(0)} = S_B + S_0 + S_{\Phi}^{(0)} = \int d^4x \Omega_s(|\Phi(x)|).$$

## 2.5 Term with spatial gradient $S_{\Phi}^{p,r}$

After the calculation of the contribution  $S_{EFT}^{(0)}$  coming from the first term in the expansion of the field matrix  $\mathbb{F}$ , the next lowest order terms arising from the gradient expansion must be considered in order to obtain the additional contributions to the EFT action: the form of the gradient expansion (2.33) makes it possible to treat separately the terms involving a “time”-derivative and those involving a space gradient. This section will be devoted to the study of the corrections to the action coming from the elements of the gradient expansion of the pair field matrix  $\mathbb{F}$  involving spatial gradients, namely we set

$$\mathbb{F}(x + x'_i) = \mathbb{F}(x) + \mathbf{r}'_i \cdot \nabla_{\mathbf{r}} \mathbb{F}(x) + \frac{1}{2} \sum_{\alpha, \beta} \frac{\partial^2 \mathbb{F}(x)}{\partial x_{i\alpha} \partial x_{i\beta}} x'_{i\alpha} x'_{i\beta} + \dots$$

(since the notation can lead to misunderstandings it is worth remarking that in the following the latin indices will always label the momenta relative to different Green’s functions, while the greek indices  $\alpha$  and  $\beta$  run only over the 3 spatial dimensions).

The action component  $S_{\Phi}^{(p)}$  reads

$$S_{\Phi}^{(p)} = \frac{1}{p} \int d^4x \dots \int d^4x_p \times \text{Tr} \left[ \begin{array}{l} \mathbb{F}(x) \mathbb{G}_0(x - x_2) \times \\ \times \left[ \mathbb{F}(\mathbf{r}, \tau) + \mathbf{r}'_2 \cdot \nabla_{\mathbf{r}} \mathbb{F}(x) + \frac{1}{2} \sum_{\alpha, \beta} \frac{\partial^2 \mathbb{F}(x)}{\partial x_{2\alpha} \partial x_{2\beta}} x'_{2\alpha} x'_{2\beta} + \dots \right] \mathbb{G}_0(x_2 - x_3) \times \\ \times \left[ \mathbb{F}(\mathbf{r}, \tau) + \mathbf{r}'_3 \cdot \nabla_{\mathbf{r}} \mathbb{F}(x) + \frac{1}{2} \sum_{\alpha, \beta} \frac{\partial^2 \mathbb{F}(x)}{\partial x_{3\alpha} \partial x_{3\beta}} x'_{3\alpha} x'_{3\beta} + \dots \right] \mathbb{G}_0(x_3 - x_4) \times \\ \times \dots \times \\ \times \left[ \mathbb{F}(\mathbf{r}, \tau) + \mathbf{r}'_p \cdot \nabla_{\mathbf{r}} \mathbb{F}(x) + \frac{1}{2} \sum_{\alpha, \beta} \frac{\partial^2 \mathbb{F}(x)}{\partial x_{p\alpha} \partial x_{p\beta}} x'_{p\alpha} x'_{p\beta} + \dots \right] \mathbb{G}_0(x_p - x) \end{array} \right]$$

From the last expression it can be seen that the lowest order non vanishing terms in the spatial gradients can have two possible origins:

- (a) terms linear in the second derivative  $\frac{1}{2} \sum_{\alpha,\beta} \frac{\partial^2 \mathbb{F}(x)}{\partial x_{1\alpha} \partial x_{1\beta}} x'_{1\alpha} x'_{1\beta}$ . It has to be noticed that, since our system is spherically symmetric, the only non-zero contribution to these terms comes from those in which  $\alpha = \beta$ .
- (b) terms coming from the product of two first derivatives  $(\nabla_{\mathbf{r}} \mathbb{F}(x)) \cdot (\nabla_{\mathbf{r}} \mathbb{F}(x))$ .

Again, given the form of the gradient expansion (2.33) it becomes clear that the contributions of these two kind of terms can be examined separately and then summed to obtain the total component  $S_{\Phi}^{(p,r)}$  coming from all lowest-order terms with space derivatives, namely

$$S_{\Phi}^{(r)} = \sum_p S_{\Phi}^{(p,r)} = \sum_p \left( S_{\Phi}^{(p,r,a)} + S_{\Phi}^{(p,r,b)} \right).$$

In the remainder of this section we will then proceed to the calculation of  $S_{\Phi}^{(p,r,a)}$  and  $S_{\Phi}^{(p,r,b)}$  separately.

### 2.5.1 Term $S_{\Phi}^{(p,r,a)}$

In order to calculate  $S_{\Phi}^{(p,r,a)}$ , the contribution to the action coming from terms linear in the second space-derivatives, the lowest-order non-zero contributions in

$$\frac{1}{p} \int d^4x \cdots \int d^4x_p \times \text{Tr} \left[ \begin{array}{l} \mathbb{F}(x) \mathbb{G}_0(x - x_2) \times \\ \times \left[ \mathbb{F}(x) + \frac{1}{2} \sum_{\alpha} \frac{\partial^2 \mathbb{F}(x)}{\partial x_{2\alpha}^2} (x'_{2\alpha})^2 \right] \mathbb{G}_0(x_2 - x_3) \times \\ \times \left[ \mathbb{F}(x) + \frac{1}{2} \sum_{\alpha} \frac{\partial^2 \mathbb{F}(x)}{\partial x_{3\alpha}^2} (x'_{3\alpha})^2 \right] \mathbb{G}_0(x_3 - x_4) \times \\ \times \cdots \times \\ \times \left[ \mathbb{F}(x) + \frac{1}{2} \sum_{\alpha} \frac{\partial^2 \mathbb{F}(x)}{\partial x_{p\alpha}^2} (x'_{p\alpha})^2 \right] \mathbb{G}_0(x_p - x) \end{array} \right]$$

must be isolated.

### Calculation

Selecting only the terms where the second derivative appears one single time leads to

$$S_{\Phi}^{(p,r,a)} = \frac{1}{p} \int d^4x \int d^4x_2 \cdots \int d^4x_p \times \text{Tr} \left[ \begin{array}{l} \mathbb{F}(x) \mathbb{G}_0(x - x_2) \frac{1}{2} \sum_{\alpha} \frac{\partial^2 \mathbb{F}(x)}{\partial x_{2\alpha}^2} (x'_{2\alpha})^2 \mathbb{G}_0(x_2 - x_3) \mathbb{F}(x) \mathbb{G}_0(x_3 - x_4) \cdots \mathbb{F}(x) \mathbb{G}_0(x_p - x) + \\ + \mathbb{F}(x) \mathbb{G}_0(x - x_2) \mathbb{F}(x) \mathbb{G}_0(x_2 - x_3) \frac{1}{2} \sum_{\alpha} \frac{\partial^2 \mathbb{F}(x)}{\partial x_{3\alpha}^2} (x'_{3\alpha})^2 \mathbb{G}_0(x_3 - x_4) \cdots \mathbb{F}(x) \mathbb{G}_0(x_p - x) + \\ + \cdots + \\ + \mathbb{F}(x) \mathbb{G}_0(x - x_2) \mathbb{F}(x) \mathbb{G}_0(x_2 - x_3) \mathbb{F}(x) \mathbb{G}_0(x_3 - x_4) \cdots \frac{1}{2} \sum_{\alpha} \frac{\partial^2 \mathbb{F}(x)}{\partial x_{p\alpha}^2} (x'_{p\alpha})^2 \mathbb{G}_0(x_p - x) \end{array} \right]. \quad (2.40)$$

To simplify the calculations it is now convenient to perform a coordinate shift in the following way:

$$x_i = x_{i-1} + y_i \quad i = 2, 3, \dots, p,$$

which (remembering the identification  $x_1 = x$  from the previous section) corresponds to

$$\begin{cases} x_2 = x + y_2 \\ x_3 = x_2 + y_3 = x + y_2 + y_3 \\ \dots \\ x_i = x_{i-1} + y_i = x + \sum_{j=2}^i y_j \\ \dots \\ x_p = x_{p-1} + y_p = x + y_2 + y_3 + \dots + y_p \end{cases} \quad (2.41)$$

As a result of this shift (2.40) can be rewritten as

$$S_{\Phi}^{(p,r,a)} = \frac{1}{2^p} \int d^4x \dots \int d^4x_p \times \text{Tr} \left[ \begin{aligned} & \mathbb{F}(x) \mathbb{G}_0(-y_2) \sum_{\alpha} \frac{\partial^2 \mathbb{F}(x)}{\partial x_{\alpha}^2} (y_{2\alpha})^2 \mathbb{G}_0(-y_3) \mathbb{F}(x) \dots \mathbb{F}(x) \mathbb{G}_0(y_2 + \dots + y_p) + \\ & + \mathbb{F}(x) \mathbb{G}_0(-y_2) \mathbb{F}(x) \mathbb{G}_0(-y_3) \sum_{\alpha} \frac{\partial^2 \mathbb{F}(x)}{\partial x_{\alpha}^2} (y_{2\alpha} + y_{3\alpha})^2 \dots \mathbb{F}(x) \mathbb{G}_0(y_2 + \dots + y_p) + \\ & + \dots + \\ & + \mathbb{F}(x) \mathbb{G}_0(-y_2) \mathbb{F}(x) \mathbb{G}_0(-y_3) \mathbb{F}(x) \dots \sum_{\alpha} \frac{\partial^2 \mathbb{F}(x)}{\partial x_{\alpha}^2} (y_{2\alpha} + \dots + y_{p\alpha})^2 \mathbb{G}_0(y_2 + \dots + y_p) \end{aligned} \right].$$

Inserting the Fourier expansion for  $\mathbb{G}_0$  (2.35) in the terms of the sum inside the trace sign in (2.40) we obtain

$$S_{\Phi}^{(p,r,a)} = \frac{1}{2^p} \int_0^{\beta} d\tau \int_0^{\beta} d\tau_2 \dots \int_0^{\beta} d\tau_p \int d\mathbf{r} \int d\mathbf{r}_2 \dots \int d\mathbf{r}_p \frac{1}{(\beta V)^p} \sum_{\mathbf{k}_1, \dots, \mathbf{k}_p} \sum_{n_1, \dots, n_p} \times \text{Tr} \left[ \begin{aligned} & \mathbb{F}(x) \mathbb{G}_0(\mathbf{k}_2, n_2) \sum_{\alpha} \frac{\partial^2 \mathbb{F}(x)}{\partial x_{\alpha}^2} (y_{2\alpha})^2 \mathbb{G}_0(\mathbf{k}_3, n_3) \mathbb{F}(x) \mathbb{G}_0(\mathbf{k}_4, n_4) \dots \mathbb{F}(x) \mathbb{G}_0(\mathbf{k}_1, n_1) + \\ & + \mathbb{F}(x) \mathbb{G}_0(\mathbf{k}_2, n_2) \mathbb{F}(x) \mathbb{G}_0(\mathbf{k}_3, n_3) \sum_{\alpha} \frac{\partial^2 \mathbb{F}(x)}{\partial x_{\alpha}^2} (y_{2\alpha} + y_{3\alpha})^2 \dots \mathbb{F}(x) \mathbb{G}_0(\mathbf{k}_1, n_1) + \\ & + \dots + \\ & + \mathbb{F}(x) \mathbb{G}_0(\mathbf{k}_2, n_2) \mathbb{F}(x) \mathbb{G}_0(\mathbf{k}_3, n_3) \mathbb{F}(x) \dots \sum_{\alpha} \frac{\partial^2 \mathbb{F}(x)}{\partial x_{\alpha}^2} (y_{2\alpha} + \dots + y_{p\alpha})^2 \mathbb{G}_0(\mathbf{k}_1, n_1) \end{aligned} \right] e^{-i\mathbf{k}_2 \cdot \mathbf{y}_2 - i\mathbf{k}_3 \cdot \mathbf{y}_3 - \dots + i\mathbf{k}_1 \cdot (\mathbf{y}_2 + \dots + \mathbf{y}_p)} e^{i\omega_{n_2} \tau_2' + i\omega_{n_3} \tau_3' + \dots - i\omega_{n_1} (\tau_2' + \dots + \tau_p')}.$$

The imaginary time integrations are trivial and give rise to Kronecker deltas: after summing over  $n_2, \dots, n_p$  only the single fermionic frequency  $n_1$  is left (that will be from now on renamed as  $n_1 \rightarrow n$ ), hence

$$S_{\Phi}^{(p,r,a)} = \frac{1}{2^p} \int_0^{\beta} d\tau \int d\mathbf{r} \int d\mathbf{r}_2 \dots \int d\mathbf{r}_p \frac{1}{(\beta V)^p} \sum_{\mathbf{k}_1, \dots, \mathbf{k}_p} \sum_n \times \text{Tr} \left[ \begin{aligned} & \mathbb{F}(x) \mathbb{G}_0(\mathbf{k}_2, n) \sum_{\alpha} \frac{\partial^2 \mathbb{F}(x)}{\partial x_{\alpha}^2} (y_{2\alpha})^2 \mathbb{G}_0(\mathbf{k}_3, n) \mathbb{F}(x) \mathbb{G}_0(\mathbf{k}_4, n) \dots \mathbb{F}(x) \mathbb{G}_0(\mathbf{k}_1, n) + \\ & + \mathbb{F}(x) \mathbb{G}_0(\mathbf{k}_2, n) \mathbb{F}(x) \mathbb{G}_0(\mathbf{k}_3, n) \sum_{\alpha} \frac{\partial^2 \mathbb{F}(x)}{\partial x_{\alpha}^2} (y_{2\alpha} + y_{3\alpha})^2 \dots \mathbb{F}(x) \mathbb{G}_0(\mathbf{k}_1, n) + \\ & + \dots + \\ & + \mathbb{F}(x) \mathbb{G}_0(\mathbf{k}_2, n) \mathbb{F}(x) \mathbb{G}_0(\mathbf{k}_3, n) \mathbb{F}(x) \dots \sum_{\alpha} \frac{\partial^2 \mathbb{F}(x)}{\partial x_{\alpha}^2} (y_{2\alpha} + \dots + y_{p\alpha})^2 \mathbb{G}_0(\mathbf{k}_1, n) \end{aligned} \right] e^{-i\mathbf{k}_2 \cdot \mathbf{y}_2 - i\mathbf{k}_3 \cdot \mathbf{y}_3 - \dots + i\mathbf{k}_1 \cdot (\mathbf{y}_2 + \dots + \mathbf{y}_p)}.$$

Defining the differential matrix

$$\mathbb{P}_{\alpha} = \frac{\partial^2 \mathbb{F}(x)}{\partial x_{\alpha}^2}, \quad (2.42)$$

the above expression can be rewritten in a more compact notation as

$$S_{\Phi}^{(p,r,a)} = \frac{1}{2p} \int_0^{\beta} d\tau \int d\mathbf{r} \int d\mathbf{r}_2 \cdots \int d\mathbf{r}_p \frac{1}{(\beta V)^p} \sum_{\mathbf{k}_1, \dots, \mathbf{k}_p} \sum_n \times \text{Tr} \left[ \begin{array}{l} \mathbb{F}(x) \mathbb{G}_0(\mathbf{k}_2, n) \sum_{\alpha} (y_{2\alpha})^2 \mathbb{P}_{\alpha} \mathbb{G}_0(\mathbf{k}_3, n) \mathbb{F}(x) \mathbb{G}_0(\mathbf{k}_4, n) \cdots \mathbb{F}(x) \mathbb{G}_0(\mathbf{k}_1, n) + \\ + \mathbb{F}(x) \mathbb{G}_0(\mathbf{k}_2, n) \mathbb{F}(x) \mathbb{G}_0(\mathbf{k}_3, n) \sum_{\alpha} (y_{2\alpha} + y_{3\alpha})^2 \mathbb{P}_{\alpha} \mathbb{G}_0(\mathbf{k}_4, n) \cdots \mathbb{F}(x) \mathbb{G}_0(\mathbf{k}_1, n) + \\ + \cdots + \\ + \mathbb{F}(x) \mathbb{G}_0(\mathbf{k}_2, n) \mathbb{F}(x) \mathbb{G}_0(\mathbf{k}_3, n) \mathbb{F}(x) \mathbb{G}_0(\mathbf{k}_4, n) \cdots \sum_{\alpha} (y_{2\alpha} + \cdots + y_{p\alpha})^2 \mathbb{P}_{\alpha} \mathbb{G}_0(\mathbf{k}_1, n) \end{array} \right] e^{-i\mathbf{k}_2 \cdot \mathbf{y}_2 - i\mathbf{k}_3 \cdot \mathbf{y}_3 - \cdots - i\mathbf{k}_1 \cdot (\mathbf{y}_2 + \cdots + \mathbf{y}_p)}.$$

The space-integrals over  $\mathbf{r}, \mathbf{r}_2, \dots, \mathbf{r}_p$  still need to be computed, and to do so it is convenient to use the relation

$$y_{i\alpha} e^{-i\mathbf{k}_2 \cdot \mathbf{y}_2 - i\mathbf{k}_3 \cdot \mathbf{y}_3 - \cdots - i\mathbf{k}_p \cdot \mathbf{y}_p} = i \frac{\partial}{\partial k_{i\alpha}} e^{-i\mathbf{k}_2 \cdot \mathbf{y}_2 - i\mathbf{k}_3 \cdot \mathbf{y}_3 - \cdots - i\mathbf{k}_p \cdot \mathbf{y}_p} \equiv \hat{y}_{i\alpha} e^{-i\mathbf{k}_2 \cdot \mathbf{y}_2 - i\mathbf{k}_3 \cdot \mathbf{y}_3 - \cdots - i\mathbf{k}_p \cdot \mathbf{y}_p}, \quad (2.43)$$

where the operators  $\hat{y}_{i\alpha}$ , defined as  $\hat{y}_{i\alpha} \equiv i \frac{\partial}{\partial k_{i\alpha}}$ , were introduced. Therefore

$$S_{\Phi}^{(p,r,a)} = \frac{1}{2p} \int_0^{\beta} d\tau \int d\mathbf{r} \int d\mathbf{r}_2 \cdots \int d\mathbf{r}_p \frac{1}{\beta V^p} \sum_{\mathbf{k}_1, \dots, \mathbf{k}_p} \sum_n \times \text{Tr} \left[ \begin{array}{l} \mathbb{F}(x) \mathbb{G}_0(\mathbf{k}_2, n) \sum_{\alpha} (\hat{y}_{2\alpha})^2 \mathbb{P}_{\alpha} \mathbb{G}_0(\mathbf{k}_3, n) \mathbb{F}(x) \mathbb{G}_0(\mathbf{k}_4, n) \cdots \mathbb{F}(x) \mathbb{G}_0(\mathbf{k}_1, n) + \\ + \mathbb{F}(x) \mathbb{G}_0(\mathbf{k}_2, n) \mathbb{F}(x) \mathbb{G}_0(\mathbf{k}_3, n) \sum_{\alpha} (\hat{y}_{2\alpha} + \hat{y}_{3\alpha})^2 \mathbb{P}_{\alpha} \mathbb{G}_0(\mathbf{k}_4, n) \cdots \mathbb{F}(x) \mathbb{G}_0(\mathbf{k}_1, n) + \\ + \cdots + \\ + \mathbb{F}(x) \mathbb{G}_0(\mathbf{k}_2, n) \mathbb{F}(x) \mathbb{G}_0(\mathbf{k}_3, n) \mathbb{F}(x) \mathbb{G}_0(\mathbf{k}_4, n) \cdots \sum_{\alpha} (\hat{y}_{2\alpha} + \cdots + \hat{y}_{p\alpha})^2 \mathbb{P}_{\alpha} \mathbb{G}_0(\mathbf{k}_1, n) \end{array} \right] e^{-i\mathbf{k}_2 \cdot \mathbf{y}_2 - i\mathbf{k}_3 \cdot \mathbf{y}_3 - \cdots - i\mathbf{k}_1 \cdot (\mathbf{y}_2 + \cdots + \mathbf{y}_p)}.$$

It is finally possible to carry out the integrations over  $\mathbf{r}, \mathbf{r}_2, \dots, \mathbf{r}_p$  and it is straightforward to see that the result is a series of Kronecker deltas that, together with the sum over  $\mathbf{k}_1, \mathbf{k}_2, \dots, \mathbf{k}_p$ , lead to the condition  $\mathbf{k}_1 = \mathbf{k}_2 = \cdots = \mathbf{k}_p$ , namely

$$S_{\Phi}^{(p,r,a)} = \frac{1}{2p} \int_0^{\beta} d\tau \int d\mathbf{r} \frac{1}{\beta V} \sum_{\mathbf{k}} \sum_n \times \text{Tr} \left[ \begin{array}{l} \mathbb{F}(x) \mathbb{G}_0(\mathbf{k}, n) \sum_{\alpha} (\hat{y}_{2\alpha})^2 \mathbb{P}_{\alpha} \mathbb{G}_0(\mathbf{k}, n) \mathbb{F}(x) \mathbb{G}_0(\mathbf{k}, n) \cdots \mathbb{F}(x) \mathbb{G}_0(\mathbf{k}, n) + \\ + \mathbb{F}(x) \mathbb{G}_0(\mathbf{k}, n) \mathbb{F}(x) \mathbb{G}_0(\mathbf{k}, n) \sum_{\alpha} (\hat{y}_{2\alpha} + \hat{y}_{3\alpha})^2 \mathbb{P}_{\alpha} \mathbb{G}_0(\mathbf{k}, n) \cdots \mathbb{F}(x) \mathbb{G}_0(\mathbf{k}, n) + \\ + \cdots + \\ + \mathbb{F}(x) \mathbb{G}_0(\mathbf{k}, n) \mathbb{F}(x) \mathbb{G}_0(\mathbf{k}, n) \mathbb{F}(x) \mathbb{G}_0(\mathbf{k}, n) \cdots \sum_{\alpha} (\hat{y}_{2\alpha} + \cdots + \hat{y}_{p\alpha})^2 \mathbb{P}_{\alpha} \mathbb{G}_0(\mathbf{k}, n) \end{array} \right] = \\ = \frac{1}{2p} \int_0^{\beta} d\tau \int d\mathbf{r} \frac{1}{\beta V} \sum_{\mathbf{k}, n} \sum_{\alpha} \times \text{Tr} \left[ \begin{array}{l} (\hat{y}_{2\alpha})^2 \mathbb{F}(x) \mathbb{G}_0(\mathbf{k}, n) \mathbb{P}_{\alpha} \mathbb{G}_0(\mathbf{k}, n) \mathbb{F}(x) \mathbb{G}_0(\mathbf{k}, n) \cdots \mathbb{F}(x) \mathbb{G}_0(\mathbf{k}, n) + \\ + (\hat{y}_{2\alpha} + \hat{y}_{3\alpha})^2 \mathbb{F}(x) \mathbb{G}_0(\mathbf{k}, n) \mathbb{F}(x) \mathbb{G}_0(\mathbf{k}, n) \mathbb{P}_{\alpha} \mathbb{G}_0(\mathbf{k}, n) \cdots \mathbb{F}(x) \mathbb{G}_0(\mathbf{k}, n) + \\ + \cdots + \\ + (\hat{y}_{2\alpha} + \cdots + \hat{y}_{p\alpha})^2 \mathbb{F}(x) \mathbb{G}_0(\mathbf{k}, n) \mathbb{F}(x) \mathbb{G}_0(\mathbf{k}, n) \mathbb{F}(x) \mathbb{G}_0(\mathbf{k}, n) \cdots \mathbb{P}_{\alpha} \mathbb{G}_0(\mathbf{k}, n) \end{array} \right].$$

Exploiting the cyclic permutation of the indices as

$$\begin{array}{cccccccccccc} & 2 & 3 & 4 & 5 & \cdots & p-3 & p-2 & p-1 & p & & & \\ \longrightarrow & p & p-1 & p-2 & p-3 & \cdots & 5 & 4 & 3 & 2 & & & \end{array}, \quad (2.44)$$

i.e.

$$\begin{cases} \hat{y}_2 & \longrightarrow \hat{y}_p \\ \hat{y}_3 & \longrightarrow \hat{y}_{p-1} \\ \dots & \\ \hat{y}_p & \longrightarrow \hat{y}_2 \end{cases},$$

we can rearrange the terms in the last expression in order to bring the operator  $\mathbb{P}_\alpha$  at the right side in every line and hence group all the traces together as

$$\begin{aligned} S_{\Phi}^{(p,r,a)} &= \frac{1}{2p} \int_0^\beta d\tau \int d\mathbf{r} \frac{1}{\beta V} \sum_{\mathbf{k},n} \sum_{\alpha} [(\hat{y}_{p\alpha})^2 + (\hat{y}_{p\alpha} + \hat{y}_{p-1\alpha})^2 + \dots + (\hat{y}_{p\alpha} + \dots + \hat{y}_{2\alpha})^2] \\ &\times \underbrace{\text{Tr} [\mathbb{G}_0(\mathbf{k}, n) \mathbb{F}(x) \mathbb{G}_0(\mathbf{k}, n) \mathbb{F}(x) \mathbb{G}_0(\mathbf{k}, n) \dots \mathbb{F}(x) \mathbb{G}_0(\mathbf{k}, n) \mathbb{P}_\alpha]}_{p \text{ couples of operators}}. \end{aligned} \quad (2.45)$$

Exploiting the spherical symmetry of the system, the sum over the index  $\alpha$  can be reduced in the following way

$$[\dots] \mathbb{P}_\alpha = \frac{1}{3} \sum_{\alpha=1}^3 [\dots] \mathbb{P}_\alpha = \frac{1}{3} [\dots] \nabla_{\mathbf{r}}^2 \mathbb{F}(x).$$

It can be demonstrated that the result of the integration by parts on the  $\mathbf{k}$ -space (in the continuum limit for the momenta  $\mathbf{k}$ ) consists in the change

$$[(\hat{y}_{p\alpha})^2 + (\hat{y}_{p\alpha} + \hat{y}_{p-1\alpha})^2 + \dots + (\hat{y}_{p\alpha} + \dots + \hat{y}_{2\alpha})^2] \longrightarrow - \sum_{s=1}^{p-1} \left[ s \sum_{i=1}^{p-s} \hat{y}_{i\alpha} \hat{y}_{i+s\alpha} \right]. \quad (2.46)$$

It is useful to show how this substitution comes in place in the easiest possible case, i.e. when  $p = 2$ : the integration that has to be carried out is

$$\begin{aligned} &\int d\mathbf{k} \sum_{\alpha} (\hat{y}_{2\alpha})^2 \text{Tr} [\mathbb{G}_0(\mathbf{k}_1, n) \mathbb{F}(x) \mathbb{G}_0(\mathbf{k}_2, n) \mathbb{P}_\alpha]_{\{\mathbf{k}_1=\mathbf{k}_2=\mathbf{k}\}} = \\ &= - \int d\mathbf{k} \sum_{\alpha} \frac{\partial^2}{\partial k_{2\alpha}^2} \text{Tr} [\mathbb{G}_0(\mathbf{k}_1, n) \mathbb{F}(x) \mathbb{G}_0(\mathbf{k}_2, n) \mathbb{P}_\alpha]_{\{\mathbf{k}_1=\mathbf{k}_2=\mathbf{k}\}} = \\ &= + \int d\mathbf{k} \sum_{\alpha} \frac{\partial}{\partial k_{1\alpha}} \frac{\partial}{\partial k_{2\alpha}} \text{Tr} [\mathbb{G}_0(\mathbf{k}_1, n) \mathbb{F}(x) \mathbb{G}_0(\mathbf{k}_2, n) \mathbb{P}_\alpha]_{\{\mathbf{k}_1=\mathbf{k}_2=\mathbf{k}\}} = \\ &= - \int d\mathbf{k} \sum_{\alpha} (\hat{y}_{1\alpha}) (\hat{y}_{2\alpha}) \text{Tr} [\mathbb{G}_0(\mathbf{k}_1, n) \mathbb{F}(x) \mathbb{G}_0(\mathbf{k}_2, n) \mathbb{P}_\alpha]_{\{\mathbf{k}_1=\mathbf{k}_2=\mathbf{k}\}}, \end{aligned}$$

where the subscripts for the momenta inside the trace were restored to make the notation more clear. From the left hand side of (2.46) we can also calculate the total number of terms that arise from the integration by parts; for  $p = 2l$  this is found to be

$$N_{2l} = \sum_{s=1}^{2l-1} \left[ s \sum_{i=1}^{2l-s} (1) \right] = \frac{1}{3} l (4l^2 - 1). \quad (2.47)$$

In the last expression the sum inside the square brackets describes the number of terms appearing inside each of the round brackets in (2.46), while the outer summation counts the number of separate round bracket terms.

Equation (2.45) becomes

$$S_{\Phi}^{(2l,r,a)} = -\frac{1}{3} \frac{1}{4l} \int_0^{\beta} d\tau \int d\mathbf{r} \frac{1}{\beta V} \sum_{\mathbf{k}, n} \sum_{\alpha} \sum_{s=1}^{p-1} \left[ s \sum_{i=1}^{p-s} \hat{y}_{i\alpha} \hat{y}_{i+s\alpha} \right] \times \text{Tr} \left[ \mathbb{G}_0(\mathbf{k}_1, n) \mathbb{F}(x) \mathbb{G}_0(\mathbf{k}_2, n) \mathbb{F}(x) \mathbb{G}_0(\mathbf{k}_3, n) \cdots \mathbb{F}(x) \mathbb{G}_0(\mathbf{k}_p, n) \nabla_{\mathbf{r}}^2 \mathbb{F}(x) \right] \Big|_{\mathbf{k}_i = \mathbf{k}}. \quad (2.48)$$

As in the calculation of the contribution coming from the terms without gradients, it is now necessary to make a distinction between the terms with odd  $(s-1)$  and those with even  $(s-1)$ . As it is clear from (2.48) the number  $(s-1)$  corresponds to the number of (couples of) operators  $\mathbb{G}_0 \mathbb{F}$  that lie between  $\mathbb{G}_0(\mathbf{k}_i, n) \mathbb{F}$  and  $\mathbb{G}_0(\mathbf{k}_{i+s}, n) \mathbb{F}$  with  $i$  and  $i+s$  being the indices of the momenta on which the two operators  $\hat{y}$  act in every term of the summation over the index  $i$ .

### Terms with even $(s-1)$

The term with  $s=1$  is

$$\hat{y}_{i\alpha} \hat{y}_{i+1\alpha} \mathbb{G}_0(\mathbf{k}_i, n) \mathbb{F}(x) \mathbb{G}_0(\mathbf{k}_{i+1}, n) \mathbb{F}(x) \Big|_{\mathbf{k}_i = \mathbf{k}_{i+1}} = -\frac{\partial \mathbb{G}_0(\mathbf{k}_i, n)}{\partial k_{i\alpha}} \mathbb{F}(x) \frac{\partial \mathbb{G}_0(\mathbf{k}_{i+1}, n)}{\partial k_{i+1\alpha}} \mathbb{F}(x) \Big|_{\mathbf{k}_i = \mathbf{k}_{i+1}}. \quad (2.49)$$

The momentum derivatives give

$$\hat{y}_{i\alpha} \mathbb{G}_0(\mathbf{k}_i, n) = i \frac{\partial \mathbb{G}_0(\mathbf{k}_i, n)}{\partial k_{i\alpha}} = i \frac{k_{i\alpha}}{m} \begin{pmatrix} \frac{1}{(i\omega_n - \xi_{\mathbf{k}_i} + \zeta)} & 0 \\ 0 & -\frac{1}{(i\omega_n + \xi_{\mathbf{k}_i} + \zeta)} \end{pmatrix} \equiv i \frac{k_{i\alpha}}{m} \mathbb{G}_1(\mathbf{k}_i, n) : \quad (2.50)$$

therefore (2.49) becomes

$$\begin{aligned} \hat{y}_{i\alpha} \hat{y}_{i+1\alpha} \mathbb{G}_0(\mathbf{k}_i, n) \mathbb{F}(x) \mathbb{G}_0(\mathbf{k}_{i+1}, n) \mathbb{F}(x) \Big|_{\mathbf{k}_i = \mathbf{k}_{i+1}} &= -\frac{k_{\alpha}^2}{m} [\mathbb{G}_1(\mathbf{k}, n) \mathbb{F}(x)]^2 \\ &= \frac{k_{\alpha}^2}{m} \frac{|\Phi(x)|^2}{(\xi_{\mathbf{k}}^2 - (i\omega_n + \zeta)^2)^2} \begin{pmatrix} 1 & 0 \\ 0 & 1 \end{pmatrix}. \end{aligned} \quad (2.51)$$

It must be noticed that there is a particular term appearing in the trace that needs special attention. This is the term in which one of the  $\hat{y}$  operators acts on the momentum that labels the Green's function  $\mathbb{G}_0$  immediately to the left of the space derivative  $\nabla_{\mathbf{r}}^2 \mathbb{F}(x)$  of the pairing component  $\mathbb{F}$ . Also this term can be rewritten as a diagonal matrix as

$$\hat{y}_{p-1\alpha} \hat{y}_{p\alpha} \mathbb{G}_0(\mathbf{k}_{p-1}, n) \mathbb{F}(x) \mathbb{G}_0(\mathbf{k}_p, n) \nabla_{\mathbf{r}}^2 \mathbb{F}(x) \Big|_{\mathbf{k}_{p-1} = \mathbf{k}_p} = \frac{k_{\alpha}^2}{m} \begin{pmatrix} \frac{\Phi^*(x) \nabla_{\mathbf{r}}^2 \Phi(x)}{(\xi_{\mathbf{k}}^2 - (i\omega_n + \zeta)^2)^2} & 0 \\ 0 & \frac{\Phi(x) \nabla_{\mathbf{r}}^2 \Phi^*(x)}{(\xi_{\mathbf{k}}^2 - (i\omega_n + \zeta)^2)^2} \end{pmatrix}. \quad (2.52)$$

Given the form of the elements (2.51) and (2.52) all of the even- $(s-1)$  terms can be reduced to the shape of the ones with  $s=1$ .

### Terms with odd $(s-1)$

The lowest- $s$  term with odd  $(s-1)$  is the one with  $s=2$ : to study it we calculate the quantity

$$\begin{aligned} &\hat{y}_{i\alpha} \hat{y}_{i+2\alpha} \mathbb{G}_0(\mathbf{k}_i, n) \mathbb{F}(x) \mathbb{G}_0(\mathbf{k}_{i+1}, n) \mathbb{F}(x) \mathbb{G}_0(\mathbf{k}_{i+2}, n) \mathbb{F}(x) \mathbb{G}_0(\mathbf{k}_{i+3}, n) \mathbb{F}(x) \Big|_{\mathbf{k}_i = \mathbf{k}_{i+1} = \mathbf{k}_{i+2} = \mathbf{k}_{i+3}} = \\ &= \frac{k_{\alpha}^2}{m^2} \mathbb{G}_1(\mathbf{k}, n) \mathbb{F}(x) \mathbb{G}_0(\mathbf{k}, n) \mathbb{F}(x) \mathbb{G}_1(\mathbf{k}, n) \mathbb{F}(x) \mathbb{G}_0(\mathbf{k}, n) \mathbb{F}(x) = \\ &= \frac{k_{\alpha}^2}{m^2} \frac{|\Phi(x)|^4}{(\xi_{\mathbf{k}}^2 - (i\omega_n + \zeta)^2)^2} \begin{pmatrix} \frac{1}{((i\omega_n + \zeta) - \xi_{\mathbf{k}})^2} & 0 \\ 0 & \frac{1}{((i\omega_n + \zeta) + \xi_{\mathbf{k}})^2} \end{pmatrix}. \end{aligned}$$

The term with the space derivative  $\nabla_{\mathbf{r}}^2 \mathbb{F}(x)$  becomes instead

$$\begin{aligned}
& \hat{y}_{p-2\alpha} \hat{y}_{p\alpha} \mathbb{G}_0(\mathbf{k}_{p-3}, n) \mathbb{F}(x) \mathbb{G}_0(\mathbf{k}_{p-2}, n) \mathbb{F}(x) \mathbb{G}_0(\mathbf{k}_{p-1}, n) \mathbb{F}(x) \mathbb{G}_0(\mathbf{k}_p, n) \nabla_{\mathbf{r}}^2 \mathbb{F}(x) \Big|_{\mathbf{k}_p=\mathbf{k}_{p-1}=\mathbf{k}_{p-2}=\mathbf{k}_{p-3}} = \\
& = \frac{k_{\alpha}^2}{m^2} \mathbb{G}_1(\mathbf{k}, n) \mathbb{F}(x) \mathbb{G}_0(\mathbf{k}, n) \mathbb{F}(x) \mathbb{G}_1(\mathbf{k}, n) \mathbb{F}(x) \mathbb{G}_0(\mathbf{k}, n) \nabla_{\mathbf{r}}^2 \mathbb{F}(x) = \\
& = \frac{k_{\alpha}^2}{m^2} \frac{|\Phi(x)|^2}{\left(\xi_{\mathbf{k}}^2 - (\mathrm{i}\omega_n + \zeta)^2\right)^2} \begin{pmatrix} \frac{\Phi^*(x) \nabla_{\mathbf{r}}^2 \Phi(x)}{((\mathrm{i}\omega_n + \zeta) - \xi_{\mathbf{k}})^2} & 0 \\ 0 & \frac{\Phi(x) \nabla_{\mathbf{r}}^2 \Phi^*(x)}{((\mathrm{i}\omega_n + \zeta) + \xi_{\mathbf{k}})^2} \end{pmatrix} = \\
& = \frac{k_{\alpha}^2}{m^2} |\Phi(x)|^2 \begin{pmatrix} \frac{\Phi^*(x) \nabla_{\mathbf{r}}^2 \Phi(x)}{((\mathrm{i}\omega_n + \zeta) - \xi_{\mathbf{k}})^4 ((\mathrm{i}\omega_n + \zeta) + \xi_{\mathbf{k}})^2} & 0 \\ 0 & \frac{\Phi(x) \nabla_{\mathbf{r}}^2 \Phi^*(x)}{((\mathrm{i}\omega_n + \zeta) - \xi_{\mathbf{k}})^2 ((\mathrm{i}\omega_n + \zeta) + \xi_{\mathbf{k}})^4} \end{pmatrix}.
\end{aligned}$$

We can conclude that also for odd- $(s-1)$  terms all the elements are diagonal and so we can reduce every other term to the form of the one relative to  $s=2$ . The action component  $S_{\Phi}^{(2l,r,a)}$  results then

$$\begin{aligned}
S_{\Phi}^{(2l,r,a)} = & -\frac{1}{3} \frac{1}{4l} \int_0^{\beta} d\tau \int d\mathbf{r} \frac{1}{\beta V} \sum_{\mathbf{k}, n} \sum_j \\
& \left[ N_{2l}^{(odd)} \mathrm{Tr} \left[ (\mathbb{G}_0 \mathbb{F})^{2(l-2)} \hat{y}_{p-2} \hat{y}_p \mathbb{G}_0(\mathbf{k}_{p-3}, n) \mathbb{F} \mathbb{G}_0(\mathbf{k}_{p-2}, n) \mathbb{F} \mathbb{G}_0(\mathbf{k}_{p-1}, n) \mathbb{F} \mathbb{G}_0(\mathbf{k}_p, n) \nabla_{\mathbf{r}}^2 \mathbb{F} \right] + \right. \\
& \left. + N_{2l}^{(even)} \mathrm{Tr} \left[ (\mathbb{G}_0 \mathbb{F})^{2(l-1)} \hat{y}_{p-1} \hat{y}_p \mathbb{G}_0(\mathbf{k}_{p-1}, n) \mathbb{F}(x) \mathbb{G}_0(\mathbf{k}_p, n) \nabla_{\mathbf{r}}^2 \mathbb{F}(x) \right] \right] \Big|_{\mathbf{k}_1=\dots=\mathbf{k}_p=\mathbf{k}}. \quad (2.53)
\end{aligned}$$

The numbers  $N_{2l}^{(odd)}$  and  $N_{2l}^{(even)}$  can be calculated in the same way as we have calculated  $N_{2l}$  in (2.47):

$$\begin{aligned}
N_{2l}^{(odd)} = & \sum_{s \text{ even}, s=1}^{2l} \left( s \sum_{i=1}^{2l-s} (1) \right) = \sum_{m=1}^l \left( 2m \sum_{i=1}^{2l-2m} (1) \right) = \\
& = \frac{2}{3} l (l^2 - 1), \quad (2.54)
\end{aligned}$$

$$\begin{aligned}
N_{2l}^{(even)} = & \sum_{s \text{ odd}, s=1}^{2l} \left( s \sum_{i=1}^{2l-s} (1) \right) = \sum_{m=1}^l \left( (2m-1) \sum_{i=1}^{2l-2m+1} (1) \right) = \\
& = \frac{1}{3} l (2l^2 + 1). \quad (2.55)
\end{aligned}$$

Including these explicit relations and those for the traces, the complete expression for the action component  $S_{\Phi}^{(2l,r,a)}$  (2.53) becomes

$$\begin{aligned}
S_{\Phi}^{(2l,r,a)} = & -\frac{1}{12} \int_0^{\beta} d\tau \int d\mathbf{r} \frac{1}{\beta V} \sum_{\mathbf{k},n} \frac{k^2}{m} \\
& \left[ \frac{2(l^2-1)}{3} \frac{1}{\xi_{\mathbf{k}}^2 - (i\omega_n + \zeta)^2} \left( -\frac{|\Phi|^2}{\xi_{\mathbf{k}}^2 - (i\omega_n + \zeta)^2} \right)^{l-1} \times \right. \\
& \times \text{Tr} \left( \begin{array}{cc} -\frac{\Phi^*(x) \nabla_{\mathbf{r}}^2 \Phi(x)}{((i\omega_n + \zeta) + \xi_{\mathbf{k}})^2} & 0 \\ 0 & -\frac{\Phi(x) \nabla_{\mathbf{r}}^2 \Phi^*(x)}{((i\omega_n + \zeta) - \xi_{\mathbf{k}})^2} \end{array} \right) + \\
& + \frac{2l^2+1}{3} \frac{1}{(\xi_{\mathbf{k}}^2 - (i\omega_n + \zeta)^2)^2} \left( -\frac{|\Phi|^2}{\xi_{\mathbf{k}}^2 - (i\omega_n + \zeta)^2} \right)^{l-1} \times \\
& \left. \times \text{Tr} \left( \begin{array}{cc} \Phi^*(x) \nabla_{\mathbf{r}}^2 \Phi(x) & 0 \\ 0 & \Phi(x) \nabla_{\mathbf{r}}^2 \Phi^*(x) \end{array} \right) \right].
\end{aligned}$$

We can notice that in the previous expression the Matsubara frequencies  $\omega_n$  appear always in combinations with  $\zeta$ . We can therefore define new “shifted” Matsubara frequencies  $\nu_n$  such that

$$i\nu_n = i\omega_n + \zeta. \quad (2.56)$$

With this substitution we get the following expression for  $S_{\Phi}^{(2l,r,a)}$ :

$$\begin{aligned}
S_{\Phi}^{(2l,r,a)} = & -\frac{1}{12} \int_0^{\beta} d\tau \int d\mathbf{r} \frac{1}{\beta V} \sum_{\mathbf{k},n} \frac{k^2}{m^2} \\
& \left[ \frac{2l^2+1}{3} \frac{1}{(\xi_{\mathbf{k}}^2 + \nu_n^2)^2} \left( -\frac{|\Phi|^2}{\xi_{\mathbf{k}}^2 + \nu_n^2} \right)^{l-1} \text{Tr} \left( \begin{array}{cc} \Phi^*(x) \nabla_{\mathbf{r}}^2 \Phi(x) & 0 \\ 0 & \Phi(x) \nabla_{\mathbf{r}}^2 \Phi^*(x) \end{array} \right) + \right. \\
& \left. + \frac{2(l^2-1)}{3} \left( -\frac{|\Phi|^2}{\xi_{\mathbf{k}}^2 + \nu_n^2} \right)^{l-1} \text{Tr} \left( \begin{array}{cc} -\frac{\Phi^*(x) \nabla_{\mathbf{r}}^2 \Phi(x)}{(i\nu_n - \xi_{\mathbf{k}})^4 (i\nu_n + \xi_{\mathbf{k}})^2} & 0 \\ 0 & -\frac{\Phi(x) \nabla_{\mathbf{r}}^2 \Phi^*(x)}{(i\nu_n - \xi_{\mathbf{k}})^2 (i\nu_n + \xi_{\mathbf{k}})^4} \end{array} \right) \right]
\end{aligned}$$

It can be observed that, in the first term inside the square brackets, all the factors with exception of those inside the trace are proportional to  $\frac{1}{\xi_{\mathbf{k}}^2 + \nu_n^2}$ , hence the expression can be symmetrised with the replacement  $\nu_n \rightarrow -\nu_n$  and becomes

$$\begin{aligned}
S_{\Phi}^{(2l,r,a)} = & -\frac{1}{4} \int_0^{\beta} d\tau \int d\mathbf{r} \frac{1}{\beta V} \sum_{\mathbf{k},n} \text{Tr} \left( \begin{array}{cc} \Phi^*(x) \nabla_{\mathbf{r}}^2 \Phi(x) & 0 \\ 0 & \Phi(x) \nabla_{\mathbf{r}}^2 \Phi^*(x) \end{array} \right) \times \\
& \left[ \frac{2l^2+1}{3} \frac{k^2}{3m^2} \frac{1}{(\xi_{\mathbf{k}}^2 + \nu_n^2)^2} \left( -\frac{|\Phi|^2}{\xi_{\mathbf{k}}^2 + \nu_n^2} \right)^{l-1} + \right. \\
& \left. + \frac{2(l^2-1)}{3} \frac{k^2}{3m^2} |\Phi|^2 \left( \frac{1}{(\xi_{\mathbf{k}}^2 + \nu_n^2)^3} - \frac{2\xi_{\mathbf{k}}^2}{(\xi_{\mathbf{k}}^2 + \nu_n^2)^4} \right) \left( -\frac{|\Phi|^2}{\xi_{\mathbf{k}}^2 + \nu_n^2} \right)^{l-2} \right]. \quad (2.57)
\end{aligned}$$

\* \* \*

After the necessary simplifications, the final form of the action component  $S_{\Phi}^{(2l,r,a)}$  yields

$$S_{\Phi}^{(2l,r,a)} = -\frac{1}{4} \int_0^{\beta} d\tau \int d\mathbf{r} \frac{1}{\beta V} \sum_{\mathbf{k},n} \frac{k^2}{3m^2} \text{Tr} \begin{pmatrix} \Phi^*(x) \nabla_{\mathbf{r}}^2 \Phi(x) & 0 \\ 0 & \Phi(x) \nabla_{\mathbf{r}}^2 \Phi^*(x) \end{pmatrix} \times \\ \times \left( \frac{1}{(\xi_{\mathbf{k}}^2 + \nu_n^2)^2} + \frac{4}{3} (l^2 - 1) \frac{\xi_{\mathbf{k}}^2}{(\xi_{\mathbf{k}}^2 + \nu_n^2)^3} \right) \left( -\frac{|\Phi|^2}{\xi_{\mathbf{k}}^2 + \nu_n^2} \right)^{l-1}. \quad (2.58)$$

### 2.5.2 Term $S_{\Phi}^{(p,r,b)}$

In this section we are going to discuss the calculation of the other term involving spatial derivatives:  $S_{\Phi}^{(p,r,b)}$ . Even though the calculation can be again performed following the procedure described in the previous subsection, we will now provide another method to reach the result.

From (2.54), (2.55) and (2.57) it can be seen that, once the terms are classified between even and odd, the coefficients of the traces appearing in the expression of  $S_{\Phi}^{(2l,r,a)}$  are polynomials of  $l$ . The degree of such polynomials is one unit lower than the one of  $N_{2l}^{(even)}$  and  $N_{2l}^{(odd)}$ . This is due to the presence of the factor  $p$  (here  $2l$ ) at the denominator in front of every term in the expansion (2.22) that cancels one power of  $l$  at the numerator. In the following we will use this observation to calculate the expression for  $S_{\Phi}^{(2l,r,b)}$ . The first step in the calculation of the action component is then the determination of  $N_{2l}$ . The starting expression is once again

$$\frac{1}{p} \int d^4x \cdots \int d^4x_p \\ \times \text{Tr} \left[ \begin{array}{l} \mathbb{F}(x) \mathbb{G}_0(x - x_2) \times \\ \times [\mathbb{F}(x) + \mathbf{r}'_2 \cdot \nabla_{\mathbf{r}} \mathbb{F}(x)] \mathbb{G}_0(x_2 - x_3) \times \\ \times [\mathbb{F}(x) + \mathbf{r}'_3 \cdot \nabla_{\mathbf{r}} \mathbb{F}(x)] \mathbb{G}_0(x_3 - x_4) \times \\ \times \cdots \times \\ \times [\mathbb{F}(x) + \mathbf{r}'_p \cdot \nabla_{\mathbf{r}} \mathbb{F}(x)] \mathbb{G}_0(x_p - x) \end{array} \right].$$

### Calculation

Using manipulation techniques analogous to those in the previous section – i.e. selecting the second order terms in  $\nabla_{\mathbf{r}} \mathbb{F}$ , moving to the Fourier representation and performing the necessary time- and space-

integrations – the last expression can be reduced to

$$\begin{aligned}
S_{\Phi}^{(2l,r,b)} = & \frac{1}{2l} \int_0^\beta d\tau \int d\mathbf{r} \frac{1}{\beta V} \sum_{\mathbf{k}} \sum_n \sum_{\alpha=1}^3 \\
& \left\{ \begin{array}{l}
2l-2 \text{ lines} \left\{ \begin{array}{l}
\text{Tr} \left[ \mathbb{F} \mathbb{G}_0(\mathbf{k}, n) \left( \hat{y}_{2\alpha} \frac{\partial \mathbb{F}(x)}{\partial x_\alpha} \right) \mathbb{G}_0(\mathbf{k}, n) \left( (\hat{y}_{2\alpha} + \hat{y}_{3\alpha}) \frac{\partial \mathbb{F}(x)}{\partial x_\alpha} \right) \mathbb{G}_0(\mathbf{k}, n) \mathbb{F} \times \cdots \times \right. \\
\times \cdots \times \mathbb{F} \mathbb{G}_0(\mathbf{k}, n) \mathbb{F} \mathbb{G}_0(\mathbf{k}, n) + \\
+ \cdots + \\
+ \mathbb{F} \mathbb{G}_0(\mathbf{k}, n) \left( \hat{y}_{2\alpha} \frac{\partial \mathbb{F}(x)}{\partial x_\alpha} \right) \mathbb{G}_0(\mathbf{k}, n) \mathbb{F} \mathbb{G}_0(\mathbf{k}, n) \mathbb{F} \times \cdots \times \\
\times \cdots \times \mathbb{G}_0(\mathbf{k}, n) \left( (\hat{y}_{2\alpha} + \cdots + \hat{y}_{2l\alpha}) \frac{\partial \mathbb{F}(x)}{\partial x_\alpha} \right) \mathbb{G}_0(\mathbf{k}, n) + \\
2l-3 \text{ lines} \left\{ \begin{array}{l}
+ \mathbb{F} \mathbb{G}_0(\mathbf{k}, n) \mathbb{F} \mathbb{G}_0(\mathbf{k}, n) \left( (\hat{y}_{2\alpha} + \hat{y}_{3\alpha}) \cdot \nabla_{\mathbf{r}} \mathbb{F} \right) \mathbb{G}_0(\mathbf{k}, n) \left( (\hat{y}_{2\alpha} + \hat{y}_{3\alpha} + \hat{y}_{4\alpha}) \frac{\partial \mathbb{F}(x)}{\partial x_\alpha} \right) \times \\
\times \cdots \times \mathbb{F} \mathbb{G}_0(\mathbf{k}, n) \mathbb{F} \mathbb{G}_0(\mathbf{k}, n) + \\
+ \cdots + \\
+ \mathbb{F} \mathbb{G}_0(\mathbf{k}, n) \mathbb{F} \mathbb{G}_0(\mathbf{k}, n) \left( (\hat{y}_{2\alpha} + \hat{y}_{3\alpha}) \cdot \nabla_{\mathbf{r}} \mathbb{F} \right) \mathbb{G}_0(\mathbf{k}, n) \mathbb{F} \times \cdots \times \\
\times \cdots \times \mathbb{G}_0(\mathbf{k}, n) \left( (\hat{y}_{2\alpha} + \cdots + \hat{y}_{2l\alpha}) \frac{\partial \mathbb{F}(x)}{\partial x_\alpha} \right) \mathbb{G}_0(\mathbf{k}, n) + \\
+ \cdots + \\
1 \text{ line} \left\{ \begin{array}{l}
+ \mathbb{F} \mathbb{G}_0(\mathbf{k}, n) \mathbb{F} \mathbb{G}_0(\mathbf{k}, n) \mathbb{F} \mathbb{G}_0(\mathbf{k}, n) \mathbb{F} \times \cdots \times \\
\times \left( (\hat{y}_{2\alpha} + \cdots + \hat{y}_{2l-1\alpha}) \frac{\partial \mathbb{F}(x)}{\partial x_\alpha} \right) \mathbb{G}_0(\mathbf{k}, n) \left( (\hat{y}_{2\alpha} + \cdots + \hat{y}_{2l\alpha}) \frac{\partial \mathbb{F}(x)}{\partial x_\alpha} \right) \mathbb{G}_0(\mathbf{k}, n) \right] \cdot \quad (2.59)
\end{array} \right.
\end{array} \right.
\end{aligned}$$

Notice that again, due to considerations on the diagonal or antidiagonal shape of the matrices, we have introduced the condition  $p = 2l$ . To calculate the total number of terms  $N_{2l}$  we first need to know the total number of lines in (2.59). This is easily calculated as

$$N_{2l}^{\text{lines}} = \sum_{i=2}^{2l-1} (2l-i) = (l-1)(2l-1). \quad (2.60)$$

This means that the sum in brackets in (2.59) is composed by  $(l-1)(2l-1)$  lines where the generic addend has the form

$$(\text{matrices}) \left( \cdots + \hat{y}_j \right) \frac{\partial \mathbb{F}(x)}{\partial x} (\text{matrices}) \left( \sum_{s=2}^k \hat{y}_s \right) \frac{\partial \mathbb{F}(x)}{\partial x} (\text{matrices}) \quad \text{with } k \in \{j, \dots, p\}.$$

As a first step we consider the first group of terms, those with  $j = 2$ : as shown by the green brackets in (2.59) there are  $2l - 2$  of these elements, i.e.

$$\begin{aligned}
& (\text{matrices}) \left( \hat{y}_2 \right) \frac{\partial \mathbb{F}(x)}{\partial x} (\text{matrices}) \left( \hat{y}_2 + \hat{y}_3 \right) \frac{\partial \mathbb{F}(x)}{\partial x} (\text{matrices}) + \\
& + (\text{matrices}) \left( \hat{y}_2 \right) \frac{\partial \mathbb{F}(x)}{\partial x} (\text{matrices}) \left( \hat{y}_2 + \hat{y}_3 + \hat{y}_4 \right) \frac{\partial \mathbb{F}(x)}{\partial x} (\text{matrices}) + \\
& + \cdots + \\
& + (\text{matrices}) \left( \hat{y}_2 \right) \frac{\partial \mathbb{F}(x)}{\partial x} (\text{matrices}) \left( \hat{y}_2 + \hat{y}_3 + \cdots + \hat{y}_k \right) \frac{\partial \mathbb{F}(x)}{\partial x} (\text{matrices}) + \\
& + \cdots + \\
& + (\text{matrices}) \left( \hat{y}_2 \right) \frac{\partial \mathbb{F}(x)}{\partial x} (\text{matrices}) \left( \hat{y}_2 + \hat{y}_3 + \cdots + \hat{y}_{2l} \right) \frac{\partial \mathbb{F}(x)}{\partial x} (\text{matrices}).
\end{aligned}$$

Labeling every line with the highest subscript  $k$  of the operators  $\hat{y}$  in the brackets on the right, it emerges that the  $k^{\text{th}}$  line is composed by  $k - 1$  terms. The total number of terms with  $j = 2$  is therefore

$$\sum_{k=3}^{2l} (k-1) = (l-1)(2l+1).$$

For what concerns the term with  $j = 3$  we have

$$\begin{aligned}
& (\text{matrices})(\hat{y}_2 + \hat{y}_3) \frac{\partial \mathbb{F}(x)}{\partial x} (\text{matrices})(\hat{y}_2 + \hat{y}_3 + \hat{y}_4) \frac{\partial \mathbb{F}(x)}{\partial x} (\text{matrices}) + \\
& + (\text{matrices})(\hat{y}_2 + \hat{y}_3) \frac{\partial \mathbb{F}(x)}{\partial x} (\text{matrices})(\hat{y}_2 + \hat{y}_3 + \hat{y}_4 + \hat{y}_5) \frac{\partial \mathbb{F}(x)}{\partial x} (\text{matrices}) + \\
& + \dots + \\
& + (\text{matrices})(\hat{y}_2 + \hat{y}_3) \frac{\partial \mathbb{F}(x)}{\partial x} (\text{matrices})(\hat{y}_2 + \hat{y}_3 + \hat{y}_4 + \dots + \hat{y}_k) \frac{\partial \mathbb{F}(x)}{\partial x} (\text{matrices}) \\
& + \dots + \\
& + (\text{matrices})(\hat{y}_2 + \hat{y}_3) \frac{\partial \mathbb{F}(x)}{\partial x} (\text{matrices})(\hat{y}_2 + \hat{y}_3 + \hat{y}_4 + \dots + \hat{y}_{2l}) \frac{\partial \mathbb{F}(x)}{\partial x} (\text{matrices}).
\end{aligned}$$

This time the  $k^{\text{th}}$  line is composed of  $2(k-1)$  terms that add up to a total of

$$\sum_{k=4}^{2l} 2(k-1) = 2(1+l)(2l-3).$$

From these properties a general relation can be obtained that gives the total number of terms for a given value of  $j$ : this reads

$$\sum_{k=j+1}^{2l} (j-1)(k-1).$$

The total number of terms in (2.59) is then

$$\sum_{j=2}^{2l-1} \sum_{k=j+1}^{2l} (j-1)(k-1) = \frac{1}{6} l(l-1)(2l-1)(6l-1).$$

This is not yet the final result, in fact up to now we haven't taken into account the fact that some of the previously calculated terms are of the form  $\hat{y}^2$  and have to be treated differently. As seen in the previous section the integration by parts in the  $\mathbf{k}$  space has the result of substituting

$$\mathbf{y}_s^2 \longrightarrow -\hat{y}_s \sum_{s' \neq s} \hat{y}_{s'}. \quad (2.61)$$

This means that every  $\hat{y}^2$ -term will give rise to  $2l-1$  new terms. We can observe that for a given  $j$ , on every line we have exactly  $(j-1)$   $\hat{y}^2$ -elements. So from the  $(j-1)(k-1)$  elements present on the  $k^{\text{th}}$  line for a given  $j$  we have to subtract the  $(j-1)$   $\hat{y}^2$ -elements and sum the  $(j-1)(2l-1)$  elements that originate from the integration by parts. This is not a trivial passage though: looking at the result of the integration by parts (2.61) it can be noticed that some of the terms originating from it can cancel out some of the original ones. Taking into account only the dependency on  $\hat{y}$ , the schematic form of the expression inside the trace of (2.59) for a generic value of  $l$  reads:

$$Y_0(l) \equiv \sum_{j=2}^{2l-1} \left[ \sum_{k=j+1}^{2l} \left( \sum_{i=2}^j \hat{y}_i \right) \left( \sum_{i'=2}^k \hat{y}_{i'} \right) \right].$$

For example, for  $l = 2$  this becomes

$$\begin{aligned}
Y_0(2) = & \hat{y}_2 (\hat{y}_2 + \hat{y}_3) + \\
& + \hat{y}_2 (\hat{y}_2 + \hat{y}_3 + \hat{y}_4) + \\
& + (\hat{y}_2 + \hat{y}_3) (\hat{y}_2 + \hat{y}_3 + \hat{y}_4).
\end{aligned}$$

Exploiting the substitutions (2.61) due to the integration by parts in the  $\mathbf{k}$ -space leads to

$$Y(2) = -\hat{y}_1(3\hat{y}_2 + \hat{y}_3) - \hat{y}_2\hat{y}_4.$$

In general, an expression  $Y(l)$  can be defined that accounts for the effect of the integration by parts on  $Y_0(l)$ . For a given value of  $l$  this can be written as

$$Y(l) = \sum_{i=1}^{2l} \sum_{i'=1}^{2l} \mathbb{C}(l)_{ii'} \hat{y}_i \hat{y}_{i'} = (\hat{y}_1 \quad \dots \quad \hat{y}_{2l}) \mathbb{C}(l) \begin{pmatrix} \hat{y}_1 \\ \vdots \\ \hat{y}_{2l} \end{pmatrix}.$$

From the calculation of  $\mathbb{C}(l)$  for a few values of  $l$  it becomes evident that the coefficients on every line of the matrices  $\mathbb{C}(l)$  are related to the series

$$0 \quad 1 \quad 3 \quad 6 \quad 10 \quad 15 \quad 21 \quad 28 \quad 36 \quad \dots$$

whose  $i^{\text{th}}$  element can be written in the compact expression  $\sum_{k=0}^i k$ . Given this notion we can find a general formula for  $Y(l)$ , i.e.

$$Y(l) = - \sum_{j=2}^{2l} \sum_{k=0}^{2l-j} k \hat{y}_1 \hat{y}_j - \sum_{j=2}^{2l} \sum_{i=2}^{2l} \sum_{k=0}^{i-(j+1)} k \hat{y}_i \hat{y}_j,$$

where the first term describes the first row of every matrix  $\mathbb{C}(l)$  and the second term describes all of the remaining rows. In order to find the total number of terms  $\hat{y}_i \hat{y}_{i'}$  we calculate

$$\begin{aligned} N_{2l}^{(tot)} &= \sum_{j=2}^{2l} \sum_{k=0}^{2l-j} (1) k + \sum_{j=2}^{2l} \sum_{i=2}^{2l} \sum_{k=0}^{i-(j+1)} (1) k = \\ &= \frac{1}{6} l(l-1)(2l+1)(2l-1), \end{aligned} \quad (2.62)$$

Therefore the combinatorial weights in the final expression of  $S_{\Phi}^{(2l,r,b)}$  are expected to be polynomials of (at most)  $3^{\text{rd}}$  degree. At this point the lower order terms of  $S_{\Phi}^{(2l,r,b)}$  can be straightforwardly computed, giving as a result

$$S_{\Phi}^{(2,r,b)} = 0, \quad (2.63)$$

$$\begin{aligned} S_{\Phi}^{(4,r,b)} &= \frac{1}{4} \int_0^{\beta} d\tau \int dx \frac{1}{\beta V} \sum_{\mathbf{k},n} \frac{k^2}{3m^2} \times \\ &\times \left( \begin{aligned} &8 \frac{\xi_k^2}{(\omega_n^2 + \xi_k^2)^4} \Phi^* \Phi (\nabla_{\mathbf{r}} \Phi^* \cdot \nabla_{\mathbf{r}} \Phi) \\ &+ \frac{1}{(\omega_n^2 + \xi_k^2)^3} \left[ (\Phi \nabla_{\mathbf{r}} \Phi^*)^2 + (\Phi^* \nabla_{\mathbf{r}} \Phi)^2 \right] \end{aligned} \right), \end{aligned} \quad (2.64)$$

$$\begin{aligned} S_{\Phi}^{(6,r,b)} &= \frac{1}{4} \int_0^{\beta} d\tau \int d\mathbf{r} \frac{1}{\beta V} \sum_{\mathbf{k},n} \frac{k^2}{3m^2} \left( -\frac{w}{\omega_n^2 + \xi_k^2} \right) \times \\ &\times \left( \begin{aligned} &32 \frac{\xi_k^2}{(\omega_n^2 + \xi_k^2)^4} \Phi^* \Phi (\nabla_{\mathbf{r}} \Phi^* \cdot \nabla_{\mathbf{r}} \Phi) \\ &+ \left( \frac{2}{(\omega_n^2 + \xi_k^2)^3} + \frac{16}{3} \frac{\xi_k^2}{(\omega_n^2 + \xi_k^2)^4} \right) \left[ (\Phi \nabla_{\mathbf{r}} \Phi^*)^2 + (\Phi^* \nabla_{\mathbf{r}} \Phi)^2 \right] \end{aligned} \right), \end{aligned} \quad (2.65)$$

and

$$S_{\Phi}^{(8,r,b)} = \frac{1}{4} \int_0^{\beta} d\tau \int d\mathbf{r} \frac{1}{\beta V} \sum_{\mathbf{k},n} \frac{k^2}{3m^2} \left( -\frac{w}{\omega_n^2 + \xi_k^2} \right)^2 \times \left( \begin{aligned} & \frac{80\xi_k^2}{(\omega_n^2 + \xi_k^2)^4} \Phi^* \Phi (\nabla_{\mathbf{r}} \Phi^* \cdot \nabla_{\mathbf{r}} \Phi) \\ & + \left( \frac{3}{(\omega_n^2 + \xi_k^2)^3} + \frac{20\xi_k^2}{(\omega_n^2 + \xi_k^2)^4} \right) [(\Phi \nabla_{\mathbf{r}} \Phi^*)^2 + (\Phi^* \nabla_{\mathbf{r}} \Phi)^2] \end{aligned} \right). \quad (2.66)$$

Let us seek the general  $S_{\Phi}^{(2l,r,b)}$  in the form

$$S_{\Phi}^{(2l,r,b)} = \frac{1}{4} \int_0^{\beta} d\tau \int d\mathbf{r} \frac{1}{\beta V} \sum_{\mathbf{k},n} \frac{k^2}{3m^2} \left( -\frac{w}{\omega_n^2 + \xi_k^2} \right)^{l-2} \times \left( \begin{aligned} & \alpha_l \frac{\xi_k^2}{(\omega_n^2 + \xi_k^2)^4} \Phi^* \Phi (\nabla_{\mathbf{r}} \Phi^* \cdot \nabla_{\mathbf{r}} \Phi) \\ & + \left( \beta_l \frac{1}{(\omega_n^2 + \xi_k^2)^3} + \eta_l \frac{\xi_k^2}{(\omega_n^2 + \xi_k^2)^4} \right) [(\Phi \nabla_{\mathbf{r}} \Phi^*)^2 + (\Phi^* \nabla_{\mathbf{r}} \Phi)^2] \end{aligned} \right), \quad (2.67)$$

where the coefficients

$$\alpha_l = a_1 l^3 + b_1 l^2 + c_1 l + d_1, \quad (2.68)$$

$$\beta_l = a_2 l^3 + b_2 l^2 + c_2 l + d_2, \quad (2.69)$$

$$\eta_l = a_3 l^3 + b_3 l^2 + c_3 l + d_3, \quad (2.70)$$

are to be determined. Using (2.63) to (2.66), the following systems of equations are obtained,

$$\left\{ \begin{array}{l} \alpha_1 = 0 \\ \alpha_2 = 8 \\ \alpha_3 = 32 \\ \alpha_4 = 80 \end{array} \right\}, \quad \left\{ \begin{array}{l} \beta_1 = 0 \\ \beta_2 = 1 \\ \beta_3 = 2 \\ \beta_4 = 3 \end{array} \right\}, \quad \left\{ \begin{array}{l} \eta_1 = 0 \\ \eta_2 = 0 \\ \eta_3 = \frac{16}{3} \\ \eta_4 = 20 \end{array} \right\},$$

which have to be solved for  $\{a_1, b_1, c_1, d_1\}$ ,  $\{a_2, b_2, c_2, d_2\}$ ,  $\{a_3, b_3, c_3, d_3\}$  respectively. As a result, the coefficients  $\alpha_l$ ,  $\beta_l$ , and  $\eta_l$  can be determined. By plugging the solutions in (2.68)-(2.70) we finally get

$$\begin{aligned} \alpha_l &= \frac{4}{3} l(l-1)(l+1), \\ \beta_l &= l-1, \\ \eta_l &= \frac{2}{3} (l-1)(l-2)(l+1). \end{aligned}$$

\* \* \*

The resulting contribution  $S_{\Phi}^{(2l,r,b)}$  eventually reads

$$\begin{aligned}
S_{\Phi}^{(2l,r,b)} &= \frac{1}{2} \int_0^{\beta} d\tau \int d\mathbf{r} (\nabla_{\mathbf{r}} \Phi^* \cdot \nabla_{\mathbf{r}} \Phi) \times \\
&\quad \times \frac{1}{\beta V} \sum_{\mathbf{k},n} \frac{k^2}{3m^2} \left( -\frac{2}{3} l(l-1)(l+1) \frac{\xi_{\mathbf{k}}^2}{(\xi_{\mathbf{k}}^2 + \nu^2)^3} \right) \left( -\frac{|\Phi|^2}{\xi_{\mathbf{k}}^2 + \nu^2} \right)^{l-1} + \\
&+ \frac{1}{2} \int_0^{\beta} d\tau \int d\mathbf{r} [(\Phi^* \nabla_{\mathbf{r}} \Phi)^2 + (\Phi \nabla_{\mathbf{r}} \Phi^*)^2] \times \\
&\quad \times \frac{1}{\beta V} \sum_{\mathbf{k},n} \frac{k^2}{3m^2} \left( \frac{l-1}{2(\xi_{\mathbf{k}}^2 + \nu^2)^3} + \frac{1}{3} (l^2 - 1)(l-2) \frac{\xi_{\mathbf{k}}^2}{(\xi_{\mathbf{k}}^2 + \nu^2)^4} \right) \left( -\frac{|\Phi|^2}{\xi_{\mathbf{k}}^2 + \nu^2} \right)^{l-2}.
\end{aligned} \tag{2.71}$$

### 2.5.3 Complete term $S_{\Phi}^{(2l,r)}$

The expressions of  $S_{\Phi}^{(2l,r,a)}$  and  $S_{\Phi}^{(2l,r,b)}$  can be finally rearranged in order to obtain a complete and compact expression for the component of the effective action  $S_{EFT}$  involving spatial derivatives of the order parameter,  $S_{\Phi}^{(2l,r)}$ . As a first step an integration by parts on the space-variable  $\mathbf{r}$  is performed, namely

$$\begin{aligned}
&\int d\mathbf{r} (\Phi^*(x) \nabla_{\mathbf{r}}^2 \Phi(x) + \Phi(x) \nabla_{\mathbf{r}}^2 \Phi^*(x)) |\Phi|^{2(l-1)} = \\
&= \int d\mathbf{r} \left( 2l |\Phi|^{2(l-1)} (\nabla_{\mathbf{r}} \Phi^* \cdot \nabla_{\mathbf{r}} \Phi) + (l-1) |\Phi|^{2(l-2)} [(\Phi^* \nabla_{\mathbf{r}} \Phi)^2 + (\Phi \nabla_{\mathbf{r}} \Phi^*)^2] \right).
\end{aligned}$$

Given this substitution,  $S_{\Phi}^{(2l,r,a)}$  (2.58) becomes

$$\begin{aligned}
S_{\Phi}^{(2l,r,a)} &= \frac{1}{2} \int_0^{\beta} d\tau \int d\mathbf{r} (\nabla_{\mathbf{r}} \Phi^* \cdot \nabla_{\mathbf{r}} \Phi) \times \\
&\quad \times \frac{1}{\beta V} \sum_{\mathbf{k},n} \frac{k^2}{3m^2} \left( l \frac{1}{(\xi_{\mathbf{k}}^2 + \nu_n^2)^2} + \frac{4}{3} l(l^2 - 1) \frac{\xi_{\mathbf{k}}^2}{(\xi_{\mathbf{k}}^2 + \nu_n^2)^3} \right) \left( -\frac{|\Phi|^2}{\xi_{\mathbf{k}}^2 + \nu_n^2} \right)^{l-1} + \\
&+ \frac{1}{2} \int_0^{\beta} d\tau \int d\mathbf{r} [(\Phi^* \nabla_{\mathbf{r}} \Phi)^2 + (\Phi \nabla_{\mathbf{r}} \Phi^*)^2] \times \\
&\quad \times \frac{1}{\beta V} \sum_{\mathbf{k},n} \frac{k^2}{3m^2} \left( \frac{l-1}{2(\xi_{\mathbf{k}}^2 + \nu_n^2)^3} + \frac{4}{3} \frac{l-1}{2} (l^2 - 1) \frac{\xi_{\mathbf{k}}^2}{(\xi_{\mathbf{k}}^2 + \nu_n^2)^4} \right) \left( -\frac{|\Phi|^2}{\xi_{\mathbf{k}}^2 + \nu_n^2} \right)^{l-2}.
\end{aligned}$$

By comparing the last expression with the one for  $S_{\Phi}^{(2l,r,b)}$  (2.71) it becomes clear that now the factors containing the derivatives have the same form and therefore the respective

coefficients can be easily combined. We thus obtain an expression for the total contribution  $S_{\Phi}^{(2l,r)} = S_{\Phi}^{(2l,r,a)} + S_{\Phi}^{(2l,r,b)}$  originating from the terms with spatial derivatives in the gradient expansion for  $\mathbb{F}$ , i.e.

$$\begin{aligned} S_{\Phi}^{(2l,r)} &= \frac{1}{2} \int_0^{\beta} d\tau \int d\mathbf{r} (\nabla_{\mathbf{r}} \Phi^* \cdot \nabla_{\mathbf{r}} \Phi) \times \\ &\quad \times \frac{1}{\beta V} \sum_{\mathbf{k},n} \frac{k^2}{3m^2} \left( l \frac{1}{(\xi_{\mathbf{k}}^2 + \nu_n^2)^2} + \frac{2}{3} l(l^2 - 1) \frac{\xi_{\mathbf{k}}^2}{(\xi_{\mathbf{k}}^2 + \nu_n^2)^3} \right) \left( -\frac{|\Phi|^2}{\xi_{\mathbf{k}}^2 + \nu_n^2} \right)^{l-1} + \\ &\quad + \frac{1}{2} \int_0^{\beta} d\tau \int d\mathbf{r} [(\Phi^* \nabla_{\mathbf{r}} \Phi)^2 + (\Phi \nabla_{\mathbf{r}} \Phi^*)^2] \times \\ &\quad \times \frac{1}{\beta V} \sum_{\mathbf{k},n} \frac{k^2}{3m^2} \left( \frac{1}{3} l(l^2 - 1) \frac{\xi_{\mathbf{k}}^2}{(\xi_{\mathbf{k}}^2 + \nu_n^2)^4} \right) \left( -\frac{|\Phi|^2}{\xi_{\mathbf{k}}^2 + \nu_n^2} \right)^{l-2}. \end{aligned}$$

Introducing the coefficients  $\bar{C}$  and  $\bar{E}$  the component  $S_{\Phi}^{(r)}$  of the EFT action reads

$$S_{\Phi}^{(r)} = \int d^4x \left[ \frac{\bar{C}(|\Phi|^2)}{2m} (\nabla_{\mathbf{r}} \Phi^* \cdot \nabla_{\mathbf{r}} \Phi) - \frac{\bar{E}(|\Phi|^2)}{2m|\Phi|^2} [(\Phi^* \nabla_{\mathbf{r}} \Phi)^2 + (\Phi \nabla_{\mathbf{r}} \Phi^*)^2] \right], \quad (2.72)$$

where the coefficients  $\bar{C}$  and  $\bar{E}$  are defined, in function of  $|\Phi|^2$ , as

$$\bar{C} = \sum_{l=1}^{\infty} \frac{1}{\beta V} \sum_{\mathbf{k},n} \frac{k^2}{3m} \left( l \frac{1}{(\xi_{\mathbf{k}}^2 + \nu_n^2)^2} + \frac{2}{3} l(l^2 - 1) \frac{\xi_{\mathbf{k}}^2}{(\xi_{\mathbf{k}}^2 + \nu_n^2)^3} \right) \left( -\frac{|\Phi|^2}{\nu_n^2 + \xi_{\mathbf{k}}^2} \right)^{l-1} \quad (2.73)$$

$$\begin{aligned} \bar{E} &= \sum_{l=1}^{\infty} \frac{1}{\beta V} \sum_{\mathbf{k},n} \frac{k^2}{3m} \left( \frac{1}{3} l(l^2 - 1) \frac{\xi_{\mathbf{k}}^2}{(\xi_{\mathbf{k}}^2 + \nu_n^2)^4} \right) |\Phi|^2 \left( -\frac{|\Phi|^2}{\xi_{\mathbf{k}}^2 + \nu_n^2} \right)^{l-2} \\ &= - \sum_{l=1}^{\infty} \frac{1}{\beta V} \sum_{\mathbf{k},n} \frac{k^2}{3m} \left( \frac{1}{3} l(l^2 - 1) \frac{\xi_{\mathbf{k}}^2}{(\xi_{\mathbf{k}}^2 + \nu_n^2)^3} \right) \left( -\frac{|\Phi|^2}{\xi_{\mathbf{k}}^2 + \nu_n^2} \right)^{l-1}. \end{aligned} \quad (2.74)$$

The summations over the index  $l$  can be carried out analytically and lead to

$$\begin{aligned} \bar{C} &= \frac{1}{\beta V} \sum_{\mathbf{k},n} \frac{k^2}{3m} \left[ \frac{1}{\left( \nu_n^2 + \left( \sqrt{\xi_{\mathbf{k}}^2 + |\Phi|^2} \right)^2 \right)^2} - \frac{4\xi_{\mathbf{k}}^2 |\Phi|^2}{\left( \nu_n^2 + \left( \sqrt{\xi_{\mathbf{k}}^2 + |\Phi|^2} \right)^2 \right)^4} \right] = \\ &= \frac{1}{\beta V} \sum_{\mathbf{k},n} \frac{k^2}{3m} \left[ \frac{1}{(\nu_n^2 + E_{\mathbf{k}}^2)^2} - \frac{4\xi_{\mathbf{k}}^2 |\Phi|^2}{(\nu_n^2 + E_{\mathbf{k}}^2)^4} \right], \end{aligned} \quad (2.75)$$

and

$$\begin{aligned}
\bar{E} &= - \sum_{l=1}^{\infty} \frac{1}{\beta V} \sum_{\mathbf{k},n} \frac{k^2}{3m} \left( \frac{1}{3} l(l^2 - 1) \frac{\xi_{\mathbf{k}}^2}{(\xi_{\mathbf{k}}^2 + \nu_n^2)^3} \right) \left( -\frac{|\Phi|^2}{\xi_{\mathbf{k}}^2 + \nu_n^2} \right)^{l-1} = \\
&= \frac{1}{\beta V} \sum_{\mathbf{k},n} \frac{k^2}{3m} \frac{2\xi^2 |\Phi|^2}{\left( \nu^2 + \left( \sqrt{\xi^2 + |\Phi|^2} \right)^2 \right)^4} = \\
&= \frac{1}{\beta V} \sum_{\mathbf{k},n} \frac{k^2}{3m} \frac{2\xi^2 |\Phi|^2}{(\nu^2 + E_{\mathbf{k}}^2)^4} \tag{2.76}
\end{aligned}$$

respectively.

### Summations over the “shifted” Matsubara frequencies

The last remaining passage to obtain the final form of the coefficients  $\bar{C}$  and  $\bar{E}$  is the computation of the fermionic Matsubara summations present in (2.75) and (2.76). In these expressions, the “shifted” Matsubara frequencies  $\nu_n = \omega_n - i\zeta$  always appear at the denominator and in particular in the combination  $(\nu_n^2 + \xi_{\mathbf{k}}^2)$  elevated to an integer exponent. To carry out the summations it is then convenient to define the functions  $f_s(\beta, x, \zeta)$  with  $s = 1, 2, \dots$  as

$$\frac{1}{\beta} \sum_n \frac{1}{(\nu_n^2 + x^2)^s} = \frac{1}{\beta} \sum_n \frac{1}{((\omega_n - i\zeta)^2 + x^2)^s} \equiv f_s(\beta, x, \zeta). \tag{2.77}$$

All the functions  $f_s$  with index  $s$  higher than one can be easily obtained from

$$f_1(\beta, x, \zeta) = \frac{1}{2x} \frac{\sinh(\beta x)}{\cosh(\beta x) + \cosh(\beta \zeta)}$$

thanks to the recursive relation

$$f_{s+1}(\beta, x, \zeta) = \frac{1}{2s x} \frac{\partial f_s(\beta, x, \zeta)}{\partial x}. \tag{2.78}$$

### Coefficient $\bar{C}$

The summation over  $l$  present in the definition of  $\bar{C}$  (2.75) can be performed analytically and gives

$$\begin{aligned}
\bar{C} &= \frac{1}{\beta V} \sum_{\mathbf{k},n} \frac{k^2}{3m} \left[ \frac{1}{\left( \nu_n^2 + \left( \sqrt{\xi_{\mathbf{k}}^2 + |\Phi|^2} \right)^2 \right)^2} - \frac{4\xi_{\mathbf{k}}^2 |\Phi|^2}{\left( \nu_n^2 + \left( \sqrt{\xi_{\mathbf{k}}^2 + |\Phi|^2} \right)^2 \right)^4} \right] = \\
&= \frac{1}{\beta V} \sum_{\mathbf{k},n} \frac{k^2}{3m} \left[ \frac{1}{(\nu_n^2 + E_{\mathbf{k}}^2)^2} - \frac{4\xi_{\mathbf{k}}^2 |\Phi|^2}{(\nu_n^2 + E_{\mathbf{k}}^2)^4} \right].
\end{aligned}$$

The last step needed is the computation of the two summations over the “shifted” Matsubara frequencies  $\nu_n$ . From the results of the previous section (see in particular the definition (2.77) of the functions  $f_s$ ) we obtain

$$\bar{C} = \frac{1}{V} \sum_{\mathbf{k}} \frac{k^2}{3m} [f_2(\beta, E_{\mathbf{k}}, \zeta) - 4\xi_{\mathbf{k}}^2 |\Phi|^2 f_4(\beta, E_{\mathbf{k}}, \zeta)].$$

Transforming the sum on  $\mathbf{k}$  into an integral on the  $k$ -space as

$$\frac{1}{V} \sum_{\mathbf{k}} \longrightarrow \int \frac{d^3k}{(2\pi)^3}.$$

we get to the final result for  $\bar{C}$  i.e.

$$\bar{C} = \int \frac{d^3k}{(2\pi)^3} \frac{k^2}{3m} [f_2(\beta, E_{\mathbf{k}}, \zeta) - 4\xi_{\mathbf{k}}^2 |\Phi|^2 f_4(\beta, E_{\mathbf{k}}, \zeta)].$$

### Coefficient $\bar{E}$

Again the sum over  $l$  of (2.76) is computed, obtaining as a result

$$\begin{aligned} \bar{E} &= - \sum_{l=1}^{\infty} \frac{1}{\beta V} \sum_{\mathbf{k},n} \frac{k^2}{3m} \left( \frac{1}{3} l(l^2 - 1) \frac{\xi_{\mathbf{k}}^2}{(\xi_{\mathbf{k}}^2 + \nu_n^2)^3} \right) \left( - \frac{|\Phi|^2}{\xi_{\mathbf{k}}^2 + \nu_n^2} \right)^{l-1} = \\ &= \frac{1}{\beta V} \sum_{\mathbf{k},n} \frac{k^2}{3m} \frac{2\xi_{\mathbf{k}}^2 |\Phi|^2}{\left( \nu_n^2 + \left( \sqrt{\xi_{\mathbf{k}}^2 + |\Phi|^2} \right)^2 \right)^4} = \\ &= \frac{1}{\beta V} \sum_{\mathbf{k},n} \frac{k^2}{3m} \frac{2\xi_{\mathbf{k}}^2 |\Phi|^2}{(\nu_n^2 + E_{\mathbf{k}}^2)^4}. \end{aligned}$$

The calculation of the Matsubara sum leads then to

$$\bar{E} = \frac{1}{V} 2|\Phi|^2 \sum_{\mathbf{k}} \frac{k^2}{3m} [\xi_{\mathbf{k}}^2 f_4(\beta, E_{\mathbf{k}}, \zeta)].$$

This can be rewritten as

$$\bar{E} = 2|\Phi|^2 \int \frac{d^3k}{(2\pi)^3} \frac{k^2}{3m} \xi_{\mathbf{k}}^2 f_4(\beta, E_{\mathbf{k}}, \zeta).$$

\* \* \*

Using the equality

$$(\nabla_{\mathbf{r}} |\Phi|^2)^2 = (\Phi^* \nabla_{\mathbf{r}} \Phi)^2 + (\Phi \nabla_{\mathbf{r}} \Phi^*)^2 + 2|\Phi|^2 |\nabla_{\mathbf{r}} \Phi|^2,$$

the action component  $S_{\Phi}^{(r)}$  (2.72) can be recast into the form

$$S_{\Phi}^{(r)} = \int d^4x \left[ \frac{(\bar{C}(|\Phi|^2) - 2\bar{E}(|\Phi|^2)/|\Phi|^2)}{2m} (\nabla_{\mathbf{r}}\Phi^* \cdot \nabla_{\mathbf{r}}\Phi) - \frac{\bar{E}(|\Phi|^2)}{2m|\Phi|^2} (\nabla_{\mathbf{r}}|\Phi|^2)^2 \right]$$

Defining the EFT coefficients  $C$  and  $E$  as

$$C(|\Phi|^2) = \int \frac{d\mathbf{k}}{(2\pi)^3} \frac{k^2}{3m} f_2(\beta, E_k, \zeta) = \bar{C}(|\Phi|^2) - 2\bar{E}(|\Phi|^2)/|\Phi|^2, \quad (2.79)$$

$$E(|\Phi|^2) = 2 \int \frac{d\mathbf{k}}{(2\pi)^3} \frac{k^2}{3m} \xi_k^2 f_4(\beta, E_k, \zeta) = \bar{E}(|\Phi|^2)/|\Phi|^2, \quad (2.80)$$

the final form of the component  $S_{\Phi}^{(r)}$  results

$$S_{\Phi}^{(r)} = \int d^4x \left[ \frac{C(|\Phi|^2)}{2m} |\nabla_{\mathbf{r}}\Phi|^2 - \frac{E(|\Phi|^2)}{2m} (\nabla_{\mathbf{r}}|\Phi|^2)^2 \right].$$

It is worth remarking that the notation and definition for the coefficients  $C$  and  $E$  used in this section (and in the remainder of the present thesis) coincides with the one used in refs. [3, 70], but slightly differs from the one used in the article [1]<sup>3</sup>.

## 2.6 Term with time derivatives $S_{\Phi}^{p,\tau}$

This section is devoted to the calculation of the terms of the expansion (2.22) arising from the terms of the gradient expansion of  $\Phi$  with imaginary-time derivatives. The derivation will be carried out separately for the terms involving first and higher order derivatives. Again the starting point is the usual gradient expansion in which this time just the components including time derivatives are kept, i.e.

$$\mathbb{F}(x + x'_l) = \mathbb{F}(x) + \tau'_l \frac{\partial \mathbb{F}(x)}{\partial \tau} + \frac{1}{2} \frac{\partial^2 \mathbb{F}(x)}{\partial \tau^2} (\tau'_l)^2 + \dots \quad (2.81)$$

with the notation  $\tau'_l \equiv \tau_l - \tau$ . Substituting this expansion into the  $p$ -th term of the series in powers of  $\Phi$  in the EFT action, leads to

$$\tilde{S}_{\Phi}^{(p)} = \frac{1}{p} \int d^4x_1 \int d^4x_2 \dots \int d^4x_p \times \text{Tr} \left\{ \begin{array}{l} \mathbb{F}(x_1) \mathbb{G}_0(x_1 - x_2) \\ \times \left[ \mathbb{F}(x_1) + \tau'_2 \frac{\partial}{\partial \tau} \mathbb{F}(x_1) + \frac{1}{2} \frac{\partial^2 \mathbb{F}(x_1)}{\partial \tau^2} (\tau'_2)^2 \right] \mathbb{G}_0(x_2 - x_3) \\ \times \left[ \mathbb{F}(x_1) + \tau'_3 \frac{\partial}{\partial \tau} \mathbb{F}(x_1) + \frac{1}{2} \frac{\partial^2 \mathbb{F}(x_1)}{\partial \tau^2} (\tau'_3)^2 \right] \mathbb{G}_0(x_3 - x_4) \\ \times \dots \\ \times \left[ \mathbb{F}(x_1) + \tau'_p \frac{\partial}{\partial \tau} \mathbb{F}(x_1) + \frac{1}{2} \frac{\partial^2 \mathbb{F}(x_1)}{\partial \tau^2} (\tau'_p)^2 \right] \mathbb{G}_0(x_p - x_1) \end{array} \right\} + \dots \quad (2.82)$$

The lowest order non-vanishing contributions to the action comes from two sources:

<sup>3</sup>The coefficients  $C$  and  $E$  are related to  $\bar{C}$  and  $\bar{E}$  in [1] by the relations  $C = \bar{C} = C + 2\mathcal{E}$ ,  $E = \bar{E}/|\Phi|^2$

- terms with a single first order time derivative;
- terms with second order time derivatives.

The second kind of terms can be in turn divided in two categories: (a) the terms linear in  $\frac{\partial^2 \mathbb{F}(x)}{\partial \tau^2}$ , (b) terms constituted by the products of two first-order time derivatives i.e.  $\text{Tr} \left( \frac{\partial}{\partial \tau} \mathbb{F} \dots \frac{\partial}{\partial \tau_j} \mathbb{F} \dots \right)$ . Correspondingly, the aforesaid action term is a sum of two different gradient terms. Using the notations of Section 2.5 we can write:

$$S_{\Phi}^{(p,\tau^2)} = S_{\Phi}^{(p,\tau^2,a)} + S_{\Phi}^{(p,\tau^2,b)}. \quad (2.83)$$

The total sum over  $p$  is subdivided in the same way:

$$S_{\Phi}^{(\tau)} \equiv \sum_p \left[ S_{\Phi}^{(p,\tau)} + S_{\Phi}^{(p,\tau^2)} \right] = \sum_p S_{\Phi}^{(p,\tau)} + \sum_p \left[ \tilde{S}_{\Phi}^{(p,\tau^2,a)} + \tilde{S}_{\Phi}^{(p,\tau^2,b)} \right]. \quad (2.84)$$

The terms  $S_{\Phi}^{(p,\tau)}$ ,  $S_{\Phi}^{(p,\tau^2,a)}$ , and  $S_{\Phi}^{(p,\tau^2,b)}$  can be calculated separately, because up to the second order, they enter the expression for the complete action in an additive way. In order to keep the notation as clear as possible we introduce, in analogy with (2.42), the differential matrices

$$\mathbb{Q}_1 \equiv \frac{\partial \mathbb{F}}{\partial \tau}, \quad \text{and} \quad \mathbb{Q}_2 \equiv \frac{\partial^2 \mathbb{F}}{\partial \tau^2}.$$

Adopting again the coordinate transformation (2.41), the relevant terms of the gradient expansion involving first and second order imaginary time derivatives can be written in the form

$$\begin{aligned} \mathbb{F}(x_2) &= \mathbb{F}(x_1 + y_2) = \mathbb{F}(x_1) + \tau'_2 \frac{\partial \mathbb{F}(x_1)}{\partial \tau} + \dots \\ \mathbb{F}(x_3) &= \mathbb{F}(x_1 + y_2 + y_3) = \mathbb{F}(x_1) + (\tau'_2 + \tau'_3) \frac{\partial \mathbb{F}(x_1)}{\partial \tau} + \dots \\ &\dots \\ \mathbb{F}(x_p) &= \mathbb{F}(x_1 + y_2 + y_3 + \dots + y_p) = \mathbb{F}(x_1) + (\tau'_2 + \tau'_3 + \dots + \tau'_p) \frac{\partial \mathbb{F}(x_1)}{\partial \tau} + \dots \end{aligned}$$

Inserting this explicit form for the pairing field and employing the usual Fourier expansion for  $\mathbb{G}_0$  (2.35), the component of the action involving time derivatives can be recast into the mixed (normal-and-reciprocal space) representation form already used in the previous

sections as

$$\begin{aligned}
S_{\Phi}^{(p)} &= \frac{1}{p} \int_0^{\beta} d\tau_1 \int d\mathbf{r}_1 \int_0^{\beta} d\tau_2' \cdots \int_0^{\beta} d\tau_p' \frac{1}{\beta^p V} \sum_{\mathbf{k}_1} \sum_{n_1, \dots, n_{p-1}} \\
&\times \text{Tr} \left( \begin{aligned}
&\mathbb{G}_0(\mathbf{k}_1, n_1) \mathbb{F} \\
&\times \mathbb{G}_0(\mathbf{k}_1, n_2) \left( \mathbb{F} + \tau_2' \mathbb{Q}_1 + \frac{1}{2} (\tau_2')^2 \mathbb{Q} \right) \\
&\times \mathbb{G}_0(\mathbf{k}_1, n_3) \left( \mathbb{F} + (\tau_2' + \tau_3') \mathbb{Q}_1 + \frac{1}{2} (\tau_2' + \tau_3')^2 \mathbb{Q}_2 \right) \\
&\times \mathbb{G}_0(\mathbf{k}_1, n_4) \left( \mathbb{F} + (\tau_2' + \tau_3' + \tau_4') \mathbb{Q}_1 + \frac{1}{2} (\tau_2' + \tau_3' + \tau_4')^2 \mathbb{Q}_2 \right) \\
&\times \cdots \times \\
&\times \mathbb{G}_0(\mathbf{k}_1, n_p) \left( \mathbb{F} + (\tau_2' + \tau_3' + \dots + \tau_p') \mathbb{Q}_1 + \frac{1}{2} (\tau_2' + \dots + \tau_p')^2 \mathbb{Q}_2 \right)
\end{aligned} \right) \\
&\times e^{-i\omega_{n_1} \cdot (\tau_2' + \dots + \tau_p') + i\omega_{n_2} \cdot \tau_2' + i\omega_{n_3} \cdot \tau_3' + \dots + i\omega_{n_p} \cdot \tau_p' + \dots}, \tag{2.85}
\end{aligned}$$

where the trivial integrations over the space-variables  $\mathbf{r}_2, \dots, \mathbf{r}_p$  have been already carried out.

### 2.6.1 Term with first order time derivatives

The contribution to the complete effective field theory action coming from terms involving a single first order imaginary-time derivative can be obtained by selecting the terms in (2.85) in which the differential operator  $\mathbb{Q}_1$  occurs just once. The relevant contribution is easily found to be

$$\begin{aligned}
S_{\Phi}^{(p,\tau,1)} &= \frac{1}{p} \int_0^{\beta} d\tau_1 \int_0^{\beta} d\tau_2' \cdots \int_0^{\beta} d\tau_p' \int d\mathbf{r}_1 \frac{1}{\beta^p V} \sum_{n_1 \cdots n_p} \sum_{\mathbf{k}_1} e^{i\omega_2 \tau_2' + i\omega_3 \tau_3' + \dots - i\omega_1 (\tau_2' + \dots + \tau_p')} \\
&\text{Tr} \left[ \begin{aligned}
&\mathbb{G}_0(\mathbf{k}_1, n_2) \tau_2' \mathbb{Q}_1 \mathbb{G}_0(\mathbf{k}_1, n_3) \mathbb{F}(x_1) \cdots \mathbb{F}(x_1) \mathbb{G}_0(\mathbf{k}_1, n_1) \mathbb{F}(x_1) + \\
&+ \mathbb{G}_0(\mathbf{k}_1, n_2) \mathbb{F}(x_1) \mathbb{G}_0(\mathbf{k}_1, n_3) (\tau_2' + \tau_3') \mathbb{Q}_1 \cdots \mathbb{F}(x_1) \mathbb{G}_0(\mathbf{k}_1, n_1) \mathbb{F}(x_1) + \\
&+ \cdots + \\
&+ \mathbb{G}_0(\mathbf{k}_1, n_2) \mathbb{F}(x_1) \mathbb{G}_0(\mathbf{k}_1, n_3) \mathbb{F}(x_1) \cdots (\tau_2' + \dots + \tau_p') \mathbb{Q}_1 \mathbb{G}_0(\mathbf{k}_1, n_1) \mathbb{F}(x_1)
\end{aligned} \right]
\end{aligned}$$

### Calculation

Contrary to the integration on the space variables  $\mathbf{r}_2, \dots, \mathbf{r}_p$  the integrals on the imaginary time variables  $\tau_2', \dots, \tau_p'$  are not trivial and need to be handled with care. Using the same procedure employed in Section 2.5, the variables  $\tau_2', \dots, \tau_p'$  can be replaced, in analogy with (2.43), by the corresponding operators  $\hat{\tau}_2', \dots, \hat{\tau}_p'$  which act as

$$\hat{\tau}_j' \equiv -i \frac{\partial}{\partial \omega_{n_j}}. \tag{2.86}$$

With respect to the situation of Section 2.5, here a problem becomes manifest: the fermionic Matsubara frequencies  $\omega_n$  are discrete, therefore the derivative in (2.86) is ill-defined. To overcome this problem the

derivative can be thought as a finite difference, i.e.

$$\hat{\tau}'_j f(\omega_{n_j}) = -i \frac{\partial f(\omega_{n_j})}{\partial \omega_{n_j}} \rightarrow \frac{f(\omega_{n_j} + \Omega_m) - f(\omega_{n_j})}{i\Omega_m}, \quad (2.87)$$

where  $\Omega_m$  is a bosonic Matsubara frequency of the form  $\frac{2\pi m}{\beta}$  with  $m \in \mathbb{Z}$ . To put this strategy into practice we calculate the auxiliary quantity  $\tilde{S}_{\Phi}^{(p,\tau,1)}$  in which the substitution

$$\tau'_j \longrightarrow e^{i\Omega_m \tau'_j} \quad (2.88)$$

is performed. Later on, after carrying out the fermionic Matsubara sum, we will retrieve the desired result by exploiting the substitution

$$i\Omega_m \longrightarrow \omega + i\delta, \quad \delta \longrightarrow 0^+,$$

and next the limit

$$\lim_{\omega \rightarrow 0} \frac{\tilde{S}_{\Phi}^{(p,\tau,1)}(\omega) - \tilde{S}_{\Phi}^{(p,\tau,1)}(0)}{\omega}. \quad (2.89)$$

The explicit expression for  $\tilde{S}_{\Phi}^{(p,\tau,1)}$  after the substitution (2.88) is

$$\begin{aligned} \tilde{S}_{\Phi}^{(p,\tau,1)} &= \frac{1}{p} \int_0^\beta d\tau_1 \int_0^\beta d\tau'_2 \cdots \int_0^\beta d\tau'_p \int d\mathbf{r}_1 \frac{1}{\beta^p V} \sum_{n_1 \cdots n_p} \sum_{\mathbf{k}_1} e^{i\omega_2 \tau'_2 + i\omega_3 \tau'_3 + \cdots - i\omega_1 (\tau'_2 + \cdots + \tau'_p)} \\ &\quad \text{1}^{st} \text{ line } \left\{ \text{Tr} \left[ \mathbb{G}_0(\mathbf{k}_1, n_2) e^{i\Omega_m \tau'_2} \mathbb{Q}_1 \mathbb{G}_0(\mathbf{k}_1, n_3) \mathbb{F}(x_1) \cdots \mathbb{F}(x_1) \mathbb{G}_0(\mathbf{k}_1, n_1) \mathbb{F}(x_1) + \right. \right. \\ &\quad \text{2}^{nd} \text{ line } \left\{ \begin{aligned} &+ \mathbb{G}_0(\mathbf{k}_1, n_2) \mathbb{F}(x_1) \mathbb{G}_0(\mathbf{k}_1, n_3) e^{i\Omega_m (\tau'_2 + \tau'_3)} \mathbb{Q}_1 \cdots \mathbb{F}(x_1) \mathbb{G}_0(\mathbf{k}_1, n_1) \mathbb{F}(x_1) + \\ &+ \cdots + \end{aligned} \right. \\ &\quad \text{j}^{th} \text{ line } \left\{ \begin{aligned} &+ \mathbb{G}_0(\mathbf{k}_1, n_2) \mathbb{F}(x_1) \cdots \mathbb{G}_0(\mathbf{k}_1, n_j) e^{i\Omega_m (\tau'_2 + \cdots + \tau'_j)} \mathbb{Q}_1 \cdots \mathbb{F}(x_1) \mathbb{G}_0(\mathbf{k}_1, n_1) \mathbb{F}(x_1) + \\ &+ \cdots + \end{aligned} \right. \\ &\quad \text{p} - 1^{th} \text{ line } \left\{ \begin{aligned} &+ \mathbb{G}_0(\mathbf{k}_1, n_2) \mathbb{F}(x_1) \mathbb{G}_0(\mathbf{k}_1, n_3) \mathbb{F}(x_1) \cdots e^{i\Omega_m (\tau'_2 + \cdots + \tau'_p)} \mathbb{Q}_1 \mathbb{G}_0(\mathbf{k}_1, n_1) \mathbb{F}(x_1) \right\}. \end{aligned} \quad (2.90) \end{aligned}$$

In the last equation the different terms have been highlighted and labeled with the number of the line on which they appear in order to keep track of them when the integrations over the variables  $\tau_2, \cdots, \tau_p$  is carried out. The basic integral over the imaginary time variable that needs to be calculated is of the form

$$\int d\tau'_j e^{i\omega_j \tau'_j - i\omega_1 \tau'_j + i\Omega_m \tau'_j} = \delta_{n_j, n_1 - m}.$$

Carrying out the integrals, performing the sums over the indices  $n_2, \dots, n_p$ , and renaming  $n_1 \rightarrow n$  leads to

$$\tilde{S}_{\Phi}^{(p,\tau,1)} = \frac{1}{p} \int_0^\beta d\tau \int d\mathbf{r} \frac{1}{\beta V} \sum_n \sum_{\mathbf{k}} \left[ \begin{array}{l} \text{1}^{st} \text{ line } \{ \\ \text{2}^{nd} \text{ line } \{ \\ \vdots \\ \text{j}^{th} \text{ line } \{ \\ \vdots \\ \text{p} - 1^{th} \text{ line } \{ \end{array} \right. \text{Tr} \left[ \begin{array}{l} \mathbb{G}_0(\mathbf{k}, n - m) \mathbb{Q}_1 \mathbb{G}_0(\mathbf{k}, n) \mathbb{F}(x) \cdots \mathbb{F}(x) \mathbb{G}_0(\mathbf{k}, n) \mathbb{F}(x) + \\ + \mathbb{G}_0(\mathbf{k}, n - m) \mathbb{F}(x) \mathbb{G}_0(\mathbf{k}, n) \mathbb{Q}_1 \cdots \mathbb{F}(x) \mathbb{G}_0(\mathbf{k}, n) \mathbb{F}(x) + \\ + \mathbb{G}_0(\mathbf{k}, n) \mathbb{F}(x) \mathbb{G}_0(\mathbf{k}, n - m) \mathbb{Q}_1 \cdots \mathbb{F}(x) \mathbb{G}_0(\mathbf{k}, n) \mathbb{F}(x) + \\ + \cdots + \\ + \mathbb{G}_0(\mathbf{k}, n - m) \mathbb{F}(x) \cdots \mathbb{G}_0(\mathbf{k}, n) \mathbb{Q}_1 \cdots \mathbb{F}(x) \mathbb{G}_0(\mathbf{k}, n) \mathbb{F}(x) + \\ + \cdots + \\ + \mathbb{G}_0(\mathbf{k}, n) \mathbb{F}(x) \cdots \mathbb{G}_0(\mathbf{k}, n - m) \mathbb{Q}_1 \cdots \mathbb{F}(x) \mathbb{G}_0(\mathbf{k}, n) \mathbb{F}(x) + \\ + \cdots + \\ + \mathbb{G}_0(\mathbf{k}, n - m) \mathbb{F}(x) \mathbb{G}_0(\mathbf{k}, n) \mathbb{F}(x) \cdots \mathbb{G}_0(\mathbf{k}, n) \mathbb{Q}_1 \mathbb{G}_0(\mathbf{k}, n) \mathbb{F}(x) + \\ + \mathbb{G}_0(\mathbf{k}, n) \mathbb{F}(x) \mathbb{G}_0(\mathbf{k}, n - m) \mathbb{F}(x) \cdots \mathbb{G}_0(\mathbf{k}, n) \mathbb{Q}_1 \mathbb{G}_0(\mathbf{k}, n) \mathbb{F}(x) + \\ + \cdots + \\ + \mathbb{G}_0(\mathbf{k}, n) \mathbb{F}(x) \mathbb{G}_0(\mathbf{k}, n) \mathbb{F}(x) \cdots \mathbb{G}_0(\mathbf{k}, n - m) \mathbb{Q}_1 \mathbb{G}_0(\mathbf{k}, n) \mathbb{F}(x) \end{array} \right]. \quad (2.91)$$

Here two kind of terms can be recognised:

1. terms in which  $\mathbb{G}_0(\mathbf{k}, n - m)$  and  $\mathbb{Q}_1$  are separated by an even number of couples  $\mathbb{F}(x) \mathbb{G}_0(\mathbf{k}, n)$ .
2. terms in which  $\mathbb{G}_0(\mathbf{k}, n - m)$  and  $\mathbb{Q}_1$  are separated by an odd number of couples  $\mathbb{F}(x) \mathbb{G}_0(\mathbf{k}, n)$ .

As already remarked in the previous sections, given the shape of  $\mathbb{G}_0$  (2.14) and  $\mathbb{F}$  (2.13) we can see that the odd powers of  $\mathbb{G}_0 \mathbb{F}$  give off-diagonal matrices, while the even powers of  $\mathbb{G}_0 \mathbb{F}$  give diagonal matrices. Therefore all of the even powers of  $\mathbb{G}_0 \mathbb{F}$  commute with all the matrices appearing in (2.91). Moreover this consideration on the composition of the matrices tells us that again only the even- $p$  terms contribute to the action. Hence from now on we can safely set  $p = 2l$ .

It is now necessary to count how many (1)-type ("even") terms and (2)-type ("odd") terms are there in  $S_{\Phi}^{(2l,\tau,1)}$  (i.e. in (2.91) after setting  $p = 2l$ ). The first observation is that expression (2.90) is composed by  $2l - 1$  terms: it can be noticed that in the passage from (2.90) to (2.91) the  $j^{th}$  line in (2.90) gives rise to  $j$  lines in (2.91), therefore the total number of terms in (2.91) reads

$$N_l = \sum_{j=1}^{2l-1} j.$$

In particular the number of (1)-type ("even") terms in the  $i^{th}$  term of (2.91) is equal to the number of odd numbers between 1 and  $i$  and viceversa for the (2)-type ("odd") terms. For example the odd and even numbers in the interval between the integers 1 and  $i$  can be counted using respectively

$$n_{odd}(i) = \frac{1}{2} \left( i + \sin^2 \left( \frac{i}{2} \pi \right) \right) \quad n_{even}(i) = i - n_{odd}(i)$$

Hence the numbers of even and odd terms result:

$$N_l^{(even)} = \sum_{i=1}^{2l-1} n_{odd}(i) = l^2, \quad N_l^{(odd)} = \sum_{i=1}^{2l-1} n_{even}(i) = l(l-1).$$

We can thus rewrite the terms in (2.91) by dividing them in two groups:

- the (1)-type (“even”) terms assume the form

$$\mathbb{G}_0(\mathbf{k}, n-m)\mathbb{Q}_1 [\mathbb{G}_0(\mathbf{k}, n)\mathbb{F}(x)]^{2l-1}. \quad (2.92)$$

- the (2)-type (“odd”) terms assume the form

$$\mathbb{G}_0(\mathbf{k}, n-m)\mathbb{F}(x)\mathbb{G}_0(\mathbf{k}, n)\mathbb{Q}_1 [\mathbb{G}_0(\mathbf{k}, n)\mathbb{F}(x)]^{2l-2}.$$

The action term becomes then

$$\begin{aligned} \tilde{S}_{\Phi}^{(2l,\tau,1)} &= \frac{1}{2l} \int_0^\beta d\tau \int d\mathbf{r} \frac{1}{\beta V} \sum_n \sum_{\mathbf{k}} \\ &\quad \times \left[ l^2 \text{Tr} \left( \mathbb{G}_0(\mathbf{k}, n-m)\mathbb{Q}_1 [\mathbb{G}_0(\mathbf{k}, n)\mathbb{F}(x)]^{2l-1} \right) + \right. \\ &\quad \left. + l(l-1) \text{Tr} \left( \mathbb{G}_0(\mathbf{k}, n-m)\mathbb{F}(x)\mathbb{G}_0(\mathbf{k}, n)\mathbb{Q}_1 [\mathbb{G}_0(\mathbf{k}, n)\mathbb{F}(x)]^{2l-2} \right) \right] = \\ &= \frac{1}{2} \int_0^\beta d\tau \int d\mathbf{r} \frac{1}{\beta V} \sum_n \sum_{\mathbf{k}} \\ &\quad \times \left[ l \text{Tr} \left( \mathbb{G}_0(\mathbf{k}, n-m)\mathbb{Q}_1 \mathbb{G}_0(\mathbf{k}, n)\mathbb{F}(x) [\mathbb{G}_0(\mathbf{k}, n)\mathbb{F}(x)]^{2l-2} \right) + \right. \\ &\quad \left. + (l-1) \text{Tr} \left( \mathbb{G}_0(\mathbf{k}, n-m)\mathbb{F}(x)\mathbb{G}_0(\mathbf{k}, n)\mathbb{Q}_1 [\mathbb{G}_0(\mathbf{k}, n)\mathbb{F}(x)]^{2l-2} \right) \right]. \quad (2.93) \end{aligned}$$

### “Even” terms

From (2.36) we deduce that the expression for the diagonal elements of  $(\mathbb{G}_0\mathbb{F})^{2l}$  is

$$\left( \frac{|\Phi(x)|^2}{(i\omega_n + \zeta)^2 - \xi_{\mathbf{k}}^2} \right)^l :$$

this contribution can be therefore factored out of the trace and the relevant quantity that needs to be calculated becomes the simplified trace

$$\text{Tr} \left[ \mathbb{G}_0(\mathbf{k}, n-m) \frac{\partial \mathbb{F}(x)}{\partial \tau} \mathbb{G}_0 \mathbb{F} \right].$$

The result is

$$\frac{\Phi(x) \frac{\partial \Phi^*(x)}{\partial \tau}}{(\zeta + \xi_{\mathbf{k}} + i\omega_n)(-\zeta + \xi_{\mathbf{k}} - i(\omega_n - \Omega_m))} + \frac{\frac{\partial \Phi(x)}{\partial \tau} \Phi^*(x)}{(-\zeta + \xi_{\mathbf{k}} - i\omega_n)(\zeta + \xi_{\mathbf{k}} + i(\omega_n - \Omega_m))}.$$

The numerators can now be rewritten in terms of the linear combinations of  $\Phi$  and its derivative, i.e.  $\phi_- = \Phi(x) \frac{\partial \Phi^*(x)}{\partial \tau} - \frac{\partial \Phi(x)}{\partial \tau} \Phi^*(x)$ , and  $\phi_+ = \Phi(x) \frac{\partial \Phi^*(x)}{\partial \tau} + \frac{\partial \Phi(x)}{\partial \tau} \Phi^*(x)$ . It is easy to show that, when integrating over  $\tau$ , the contribution proportional to  $\phi_+$  gives zero, in fact

$$\phi_+ = \Phi(x) \frac{\partial \Phi^*(x)}{\partial \tau} + \frac{\partial \Phi(x)}{\partial \tau} \Phi^*(x) = \frac{\partial}{\partial \tau} |\Phi(x)|^2,$$

and

$$\int_0^\beta d\tau \frac{\partial}{\partial \tau} |\Phi(x)|^2 = |\Phi(\tau = \beta)|^2 - |\Phi(\tau = 0)|^2 = 0,$$

where the last equality is motivated by the boundary conditions that the bosonic field  $\Phi$  satisfies in the interval  $[0, \beta]$ . Therefore just the contribution proportional to  $\Phi(x) \frac{\partial \Phi^*(x)}{\partial \tau} - \frac{\partial \Phi(x)}{\partial \tau} \Phi^*(x)$  is non-zero, and it reads

$$\frac{i\xi_{\mathbf{k}}\Omega_m \left( \Phi(x) \frac{\partial \Phi^*(x)}{\partial \tau} - \frac{\partial \Phi(x)}{\partial \tau} \Phi^*(x) \right)}{(\zeta - \xi_{\mathbf{k}} + i\omega_n)(\zeta + \xi_{\mathbf{k}} + i\omega_n)(\zeta - \xi_{\mathbf{k}} + i(\omega_n - \Omega_m))(\zeta + \xi_{\mathbf{k}} + i(\omega_n - \Omega_m))}.$$

### “Odd” terms

The same discussion valid for the “even” terms holds also here: the standard term has the form

$$\text{Tr} \left[ \mathbb{G}_0(\mathbf{k}, n - m) \mathbb{G}_0 \mathbb{F} \frac{\partial \mathbb{F}(x)}{\partial \tau} \right].$$

After selecting the contribution proportional to  $\Phi(x) \frac{\partial \Phi^*(x)}{\partial \tau} - \frac{\partial \Phi(x)}{\partial \tau} \Phi^*(x)$  we find

$$\frac{i\xi_{\mathbf{k}}\Omega_m \left( \Phi(x) \frac{\partial \Phi^*(x)}{\partial \tau} - \frac{\partial \Phi(x)}{\partial \tau} \Phi^*(x) \right)}{(\zeta - \xi_{\mathbf{k}} + i\omega_n)(\zeta + \xi_{\mathbf{k}} + i\omega_n)(\zeta - \xi_{\mathbf{k}} + i(\omega_n - \Omega_m))(\zeta + \xi_{\mathbf{k}} + i(\omega_n - \Omega_m))}.$$

\* \* \*

Now, in order to calculate the quantity inside the square brackets in the expression for  $\tilde{S}_{\Phi}^{(2l,\tau,1)}$  (2.93), it is necessary to sum  $l$  times the contribution from the “even” terms plus  $(l - 1)$  times the contribution from the “odd terms” and then multiply everything by the factor coming from the even powers of  $\mathbb{G}_0 \mathbb{F}$  that had been factored out at an earlier stage. The resulting expression reads

$$\frac{i\xi_{\mathbf{k}}\Omega_m \left( \Phi(x) \frac{\partial \Phi^*(x)}{\partial \tau} - \frac{\partial \Phi(x)}{\partial \tau} \Phi^*(x) \right)}{(\zeta - \xi_{\mathbf{k}} + i\omega_n)(\zeta + \xi_{\mathbf{k}} + i\omega_n)(\zeta - \xi_{\mathbf{k}} + i(\omega_n - \Omega_m))(\zeta + \xi_{\mathbf{k}} + i(\omega_n - \Omega_m))} \left( \frac{|\Phi(x)|^2}{(i\omega_n + \zeta)^2 - \xi_{\mathbf{k}}^2} \right)^{l-1}.$$

Exploiting the summation over the index  $l$  present in (2.93) leads to

$$\begin{aligned} & \frac{i\xi_{\mathbf{k}}\Omega_m \left( \Phi(x) \frac{\partial \Phi^*(x)}{\partial \tau} - \frac{\partial \Phi(x)}{\partial \tau} \Phi^*(x) \right)}{(-\zeta + \xi_{\mathbf{k}} - i(\omega_n - \Omega_m))(\zeta + \xi_{\mathbf{k}} + i(\omega_n - \Omega_m)) \left( |\Phi(x)|^2 - (\zeta + i\omega_n)^2 + \xi_{\mathbf{k}}^2 \right)} \\ &= \frac{i\xi_{\mathbf{k}}\Omega_m \left( \Phi(x) \frac{\partial \Phi^*(x)}{\partial \tau} - \frac{\partial \Phi(x)}{\partial \tau} \Phi^*(x) \right)}{\left( (\nu_n - \Omega_m)^2 + \xi_{\mathbf{k}}^2 \right) \left( \nu_n^2 + \xi_{\mathbf{k}}^2 + |\Phi(x)|^2 \right)} \\ &= \frac{i\xi_{\mathbf{k}}\Omega_m \left( \Phi(x) \frac{\partial \Phi^*(x)}{\partial \tau} - \frac{\partial \Phi(x)}{\partial \tau} \Phi^*(x) \right)}{\left( (\nu_n - \Omega_m)^2 + \xi_{\mathbf{k}}^2 \right) (\nu_n^2 + E_{\mathbf{k}}^2)}, \end{aligned}$$

where in the last line the dispersion for the single particle excitations  $E_{\mathbf{k}}$  (2.38) was used. Even if it is not transparent from the notation,  $E_{\mathbf{k}}$  still carries the dependence on  $x$  given by the presence of the term  $|\Phi(x)|^2$  in its explicit expression.

The next step is to calculate the sum over the fermionic Matsubara frequencies. To do this we momentarily isolate from the integrand the terms depending on  $\nu_n$  and define the auxiliary quantity

$$\tilde{s}(i\Omega_m, E_{\mathbf{k}}) = \frac{1}{\beta} \sum_n \frac{i\xi_{\mathbf{k}}\Omega_m}{\left( (\nu_n - \Omega_m)^2 + \xi_{\mathbf{k}}^2 \right) (\nu_n^2 + E_{\mathbf{k}}^2)}.$$

The calculation of the sum over the shifted fermionic Matsubara frequencies  $\nu_n$  gives

$$\tilde{s}(i\Omega_m, E_{\mathbf{k}}) = i\xi_{\mathbf{k}}\Omega_m \frac{\Omega_m^2 (f_1(\beta, \xi_{\mathbf{k}}, \zeta) - f_1(\beta, E_{\mathbf{k}}, \zeta)) + (E_{\mathbf{k}}^2 - \xi_{\mathbf{k}}^2) (f_1(\beta, \xi_{\mathbf{k}}, \zeta) - f_1(\beta, E_{\mathbf{k}}, \zeta))}{\Omega_m^4 + 2\Omega_m(E_{\mathbf{k}}^2 + \xi_{\mathbf{k}}^2) + (E_{\mathbf{k}}^2 - \xi_{\mathbf{k}}^2)^2}.$$

Now, as anticipated at the start of the present section the formal substitution  $i\Omega_m \rightarrow \omega + i\delta$  (with  $\delta \rightarrow 0^+$ ) is performed and, in order to exploit the limiting operation (2.89) it is convenient to use the quantity

$$s(E_{\mathbf{k}}) = \lim_{\omega \rightarrow 0} \frac{\tilde{s}(\omega + i\delta, E_{\mathbf{k}}) - \tilde{s}(0, E_{\mathbf{k}})}{\omega}.$$

The explicit expression for  $s(E_{\mathbf{k}})$  is immediately found to be given by

$$s(E_{\mathbf{k}}) = \frac{\xi_{\mathbf{k}}}{|\Phi(x)|^2} [f_1(\beta, \xi_{\mathbf{k}}, \zeta) - f_1(\beta, E_{\mathbf{k}}, \zeta)],$$

and can be reintroduced into the full expression for the action component including first order time derivatives.

\* \* \*

The final result for  $S_{\Phi}^{(\tau)}$  is

$$\begin{aligned} S_{\Phi}^{(\tau)} &= \frac{1}{2} \int d\mathbf{r} \int_0^{\beta} d\tau \left( \Phi(x) \frac{\partial \Phi^*(x)}{\partial \tau} - \frac{\partial \Phi(x)}{\partial \tau} \Phi^*(x) \right) \times \\ &\times \int \frac{d\mathbf{k}}{(2\pi)^3} \frac{\xi_{\mathbf{k}}}{|\Phi(x)|^2} [f_1(\beta, \xi_{\mathbf{k}}, \zeta) - f_1(\beta, E_{\mathbf{k}}, \zeta)]. \end{aligned}$$

In order to make the analogy with the usual Ginzburg-Landau action functional [46] more apparent, the component involving the first order imaginary-time derivative of the order parameter can be finally rewritten as

$$S_{\Phi}^{(\tau)} = \int d^4x \frac{1}{2} D (|\Phi(x)|^2) \left( \Phi(x) \frac{\partial \Phi^*(x)}{\partial \tau} - \frac{\partial \Phi(x)}{\partial \tau} \Phi^*(x) \right), \quad (2.94)$$

where the coefficient  $D$  is defined as

$$D (|\Phi(x)|^2) \equiv \int \frac{d\mathbf{k}}{(2\pi)^3} \frac{\xi_{\mathbf{k}}}{|\Phi(x)|^2} [f_1(\beta, \xi_{\mathbf{k}}, \zeta) - f_1(\beta, E_{\mathbf{k}}, \zeta)]. \quad (2.95)$$

### 2.6.2 Term with second order time derivatives/1: $S_{\Phi}^{(\tau^2, a)}$

As mentioned in Section 2.6 the calculation of the component of the action involving imaginary-time derivatives of order higher than one is split in two parts that will be examined in the present and in the following subsection separately. Given the length and intricacy of the algebra involved, in order to make the notation clearer, the derivation is going to be performed in the situation without imbalance, i.e. for  $\zeta = 0$ . Only at the end of the calculation the imbalance parameter is reintroduced by substituting the normal fermionic Matsubara frequencies  $\omega_n$  with the “shifted” frequencies  $\nu_n$  defined in (2.56).

The contribution  $S_{\Phi}^{(\tau^2,a)}$  can be obtained from (2.85) by selecting the terms that are linear in the second order imaginary time derivative of the pairing matrix  $\mathbb{F}$ . Similarly to the case of the components of the action with space gradients, in order to exploit the integration over the imaginary time variables it is convenient to introduce again the operators  $\hat{\tau}'_j$  defined in (2.86), which act on a generic function  $f$  of  $\omega_{n_j}$  as in (2.87). The relevant terms contributing to  $S_{\Phi}^{(\tau^2,a)}$  can be then rewritten as

$$\begin{aligned}
S_{\Phi}^{(p)} &= \frac{1}{p} \int_0^{\beta} d\tau \int d\mathbf{r} \int_0^{\beta} d\tau'_2 \dots \int_0^{\beta} d\tau'_p \frac{1}{\beta^p V} \sum_{\mathbf{k}} \sum_{n_1, \dots, n_p} \\
&\times \text{Tr} \left( \begin{array}{c} \mathbb{G}_0(\mathbf{k}, n_1) \mathbb{F} \\ \times \mathbb{G}_0(\mathbf{k}, n_2) \left( \mathbb{F} + \frac{1}{2} (\hat{\tau}'_2)^2 \mathbb{Q}_2 \right) \\ \times \mathbb{G}_0(\mathbf{k}, n_3) \left( \mathbb{F} + \frac{1}{2} (\hat{\tau}'_2 + \hat{\tau}'_3)^2 \mathbb{Q}_2 \right) \\ \times \mathbb{G}_0(\mathbf{k}, n_4) \left( \mathbb{F} + \frac{1}{2} (\hat{\tau}'_2 + \hat{\tau}'_3 + \hat{\tau}'_4)^2 \mathbb{Q}_2 \right) \\ \times \dots \\ \times \mathbb{G}_0(\mathbf{k}, n_{p-1}) \left( \mathbb{F} + \frac{1}{2} (\hat{\tau}'_2 + \hat{\tau}'_3 + \dots + \hat{\tau}'_p)^2 \mathbb{Q}_2 \right) \end{array} \right) \\
&\times e^{i\omega_2 \tau'_2 + i\omega_3 \tau'_3 + \dots - i\omega_1 (\tau'_2 + \dots + \tau'_p)}. \tag{2.96}
\end{aligned}$$

As was the case in the previous sections, the introduction of the differential matrices enables us to calculate the integrals over the imaginary time variables  $\tau'_2, \dots, \tau'_p$ . Again these integrals give rise to Kronecker deltas that produce a nonzero contribution only when the Matsubara frequencies  $n_1, n_2, \dots, n_p$  are all equal to each other. Hence

$$\begin{aligned}
S_{\Phi}^{(p)} &= \frac{1}{p} \int_0^{\beta} d\tau \int d\mathbf{r} \frac{1}{\beta V} \sum_{\mathbf{k}} \sum_{n_1} \\
&\times \text{Tr} \left( \begin{array}{c} \mathbb{G}_0(\mathbf{k}, n_1) \mathbb{F} \\ \times \mathbb{G}_0(\mathbf{k}, n_2) \left( \mathbb{F} + \frac{1}{2} (\hat{\tau}'_2)^2 \mathbb{Q}_2 \right) \\ \times \mathbb{G}_0(\mathbf{k}, n_3) \left( \mathbb{F} + \frac{1}{2} (\hat{\tau}'_2 + \hat{\tau}'_3)^2 \mathbb{Q}_2 \right) \\ \times \mathbb{G}_0(\mathbf{k}, n_4) \left( \mathbb{F} + \frac{1}{2} (\hat{\tau}'_2 + \hat{\tau}'_3 + \hat{\tau}'_4)^2 \mathbb{Q}_2 \right) \\ \times \dots \\ \times \mathbb{G}_0(\mathbf{k}, n_{p-1}) \left( \mathbb{F} + \frac{1}{2} (\hat{\tau}'_2 + \hat{\tau}'_3 + \dots + \hat{\tau}'_p)^2 \mathbb{Q}_2 \right) \end{array} \right) \Bigg|_{\{n_j=n_1\}}. \tag{2.97}
\end{aligned}$$

## Calculation

Selecting the contributions proportional to  $\mathbb{Q}_2$  in (2.97) leads to

$$\begin{aligned}
S_{\Phi}^{(p,\tau^2,a)} &= \frac{1}{2p} \int_0^{\beta} d\tau \int d\mathbf{r} \frac{1}{\beta V} \sum_{\mathbf{k}, n} \\
&\left( \begin{array}{l} (\hat{\tau}'_2)^2 \text{Tr}(\mathbb{G}_0(\mathbf{k}, n_1) \mathbb{Q}_2 \mathbb{G}_0(\mathbf{k}, n_2) \mathbb{F} \times \dots \times \mathbb{F} \mathbb{G}_0(\mathbf{k}, n_p) \mathbb{F}) \\ + (\hat{\tau}'_2 + \hat{\tau}'_3)^2 \text{Tr}(\mathbb{G}_0(\mathbf{k}, n_1) \mathbb{F} \mathbb{G}_0(\mathbf{k}, n_2) \mathbb{Q}_2 \times \dots \times \mathbb{F} \mathbb{G}_0(\mathbf{k}, n_p) \mathbb{F}) \\ + \dots \\ + (\hat{\tau}'_2 + \hat{\tau}'_3 + \dots + \hat{\tau}'_p)^2 \text{Tr}(\mathbb{G}_0(\mathbf{k}, n_1) \mathbb{F} \mathbb{G}_0(\mathbf{k}, n_2) \mathbb{F} \times \dots \times \mathbb{Q}_2 \mathbb{G}_0(\mathbf{k}, n_p) \mathbb{F}) \end{array} \right) \Bigg|_{\{n_j=n_1\}}.
\end{aligned}$$

Using the invariance property of the trace for cyclic permutations, in all the terms the operator  $\mathbb{Q}_2$  can be brought to the last position, i.e.

$$S_{\Phi}^{(p,\tau^2,a)} = \frac{1}{2p} \int_0^\beta d\tau \int d\mathbf{r} \frac{1}{\beta V} \sum_{\mathbf{k},n} \left( \begin{array}{l} (\hat{\tau}'_2)^2 \text{Tr}(\mathbb{G}_0(\mathbf{k}, n_2) \mathbb{F} \times \dots \times \mathbb{F} \mathbb{G}_0(\mathbf{k}, n_p) \mathbb{F} \mathbb{G}_0(\mathbf{k}, n_1) \mathbb{Q}_2) \\ + (\hat{\tau}'_2 + \hat{\tau}'_3)^2 \text{Tr}(\mathbb{G}_0(\mathbf{k}, n_3) \mathbb{F} \times \dots \times \mathbb{F} \mathbb{G}_0(\mathbf{k}, n_p) \mathbb{F} \mathbb{G}_0(\mathbf{k}, n_1) \mathbb{F} \mathbb{G}_0(\mathbf{k}, n_2) \mathbb{Q}_2) \\ + \dots \\ + (\hat{\tau}'_2 + \hat{\tau}'_3 + \dots + \hat{\tau}'_p)^2 \text{Tr}(\mathbb{G}_0(\mathbf{k}, n_p) \mathbb{F} \mathbb{G}_0(\mathbf{k}, n_1) \mathbb{F} \mathbb{G}_0(\mathbf{k}, n_2) \mathbb{F} \times \dots \times \mathbb{Q}_2) \end{array} \right) \Big|_{\{n_j=n_1\}}$$

A cyclic permutation of the indices labelling the fermionic Matsubara frequencies analogous to (2.44) leads to the following compact expression for  $S_{\Phi}^{(p,\tau^2,a)}$ :

$$S_{\Phi}^{(p,\tau^2,a)} = \frac{1}{2p} \int_0^\beta d\tau \int d\mathbf{r} \frac{1}{\beta V} \sum_{\mathbf{k},n} \left( \begin{array}{l} \left[ (\hat{\tau}'_p)^2 + (\hat{\tau}'_{p-1} + \hat{\tau}'_p)^2 + \dots + (\hat{\tau}'_2 + \hat{\tau}'_3 + \dots + \hat{\tau}'_p)^2 \right] \\ \times \text{Tr}(\mathbb{G}_0(\mathbf{k}, n_1) \mathbb{F} \mathbb{G}_0(\mathbf{k}, n_2) \mathbb{F} \times \dots \times \mathbb{G}_0(\mathbf{k}, n_{p-1}) \mathbb{F} \mathbb{G}_0(\mathbf{k}, n_p) \mathbb{Q}_2) \end{array} \right) \Big|_{\{n_j=n_1\}}. \quad (2.98)$$

It is now necessary to calculate the total number of terms inside the round brackets in the previous expression: the sum inside the square brackets can be rewritten as

$$\left( \sum_{j=2}^p \hat{\tau}'_j \right)^2 = \sum_{j=2}^p (\hat{\tau}'_j)^2 + 2 \sum_{j>j'} \hat{\tau}'_j \hat{\tau}'_{j'}$$

and the number of elements arising from this summation can be evaluated by solving

$$N_p = \sum_{j=2}^p (p-j+1)^2$$

The same consideration on the shape of the matrices inside the trace made in all of the previous sections leads to the conclusion that again only the contributions  $S_{\Phi}^{(p,\tau^2,a)}$  with even  $p$  are non-zero. Therefore we can set  $p = 2l$ , and as a consequence the action component becomes

$$S_{\Phi}^{(2l,\tau^2,a)} = \frac{1}{4l} \int_0^\beta d\tau \int d\mathbf{r} \frac{1}{\beta V} \sum_{\mathbf{k},n} \left( \begin{array}{l} \left[ \hat{\tau}'_{2l}^2 + (\hat{\tau}'_{2l-1} + \hat{\tau}'_{2l})^2 + \dots + (\hat{\tau}'_2 + \hat{\tau}'_3 + \dots + \hat{\tau}'_{2l})^2 \right] \\ \times \text{Tr}(\mathbb{G}_0(\mathbf{k}, n_1) \mathbb{F} \mathbb{G}_0(\mathbf{k}, n_2) \mathbb{F} \times \dots \times \mathbb{G}_0(\mathbf{k}, n_{2l-1}) \mathbb{F} \mathbb{G}_0(\mathbf{k}, n_{2l}) \mathbb{Q}_2) \end{array} \right) \Big|_{\{n_j=n_1\}}, \quad (2.99)$$

and the total number of terms in (2.99) finally reads

$$N_{2l} = \sum_{j=2}^{2l} (2l-j+1)^2 = \frac{1}{3} l(4l-1)(2l-1) \quad (2.100)$$

The elements in (2.99) can be further classified in three categories based on a consideration on the indices of the pair of operators  $\hat{\tau}'_j \hat{\tau}'_{j+s}$  acting on the trace:

- terms with  $s = 0$ , i.e. terms of the kind  $(\hat{\tau}'_j)^2 \text{Tr}[\dots]$ ;

- terms with even  $s$ ;
- terms with odd  $s$ .

The expression  $\hat{\tau}'_j \hat{\tau}'_{j+s} \text{Tr}[\dots]$  gives, in the three different situations

$$\begin{aligned} |\Phi|^{2(l-1)} \left( \Phi^* \frac{\partial^2 \Phi}{\partial \tau^2} + \Phi \frac{\partial^2 \Phi^*}{\partial \tau^2} \right) \lambda_0, & \quad \text{for } s = 0, \\ |\Phi|^{2(l-1)} \left( \Phi^* \frac{\partial^2 \Phi}{\partial \tau^2} + \Phi \frac{\partial^2 \Phi^*}{\partial \tau^2} \right) \lambda_e, & \quad \text{for } s \text{ even}, \\ |\Phi|^{2(l-1)} \left( \Phi^* \frac{\partial^2 \Phi}{\partial \tau^2} + \Phi \frac{\partial^2 \Phi^*}{\partial \tau^2} \right) \lambda_o, & \quad \text{for } s \text{ odd}. \end{aligned}$$

where the factors  $\lambda_0, \lambda_e$  and  $\lambda_o$  are obtained by letting the operators  $\hat{\tau}_j$  (2.87) act on the corresponding Green's functions inside the trace sign, and are defined as

$$\lambda_0 = \frac{1}{(i(\omega_n + \Omega_m) - \xi)(i(\omega_n + \Omega_m) - \xi)(i\omega_n + \xi)^2}, \quad (2.101)$$

$$\lambda_e = \frac{1}{(i(\omega_n + \Omega_m) - \xi)(i(\omega_n + \Omega_k) - \xi)(i\omega_n + \xi)^2}, \quad (2.102)$$

$$\lambda_o = -\frac{1}{(i(\omega_n + \Omega_m) - \xi)(i(\omega_n + \Omega_k) + \xi)(\omega_n^2 + \xi^2)}. \quad (2.103)$$

The bosonic Matsubara frequencies  $\Omega_m$  and  $\Omega_k$  appear as a consequence of the use of the finite difference form (2.87) of the two operators  $\hat{\tau}'_j$  and  $\hat{\tau}'_{j+s}$  acting on the trace. To calculate the complete contribution  $S_{\Phi}^{(2l, \tau^2, a)}$  we will further proceed as done in Subsection 2.5.2: the combinatorial weights of the terms proportional to  $\lambda_0, \lambda_e$ , and  $\lambda_o$  are derived from the explicit evaluation of  $S_{\Phi}^{(2l, \tau^2, a)}$  for a few small values of  $l$ :

$$S_{\Phi}^{(2, \tau^2, a)} = \frac{1}{4} \int_0^\beta d\tau \int d\mathbf{r} \frac{1}{\beta V} \sum_{\mathbf{k}, n} \left( \Phi^* \frac{\partial^2 \Phi}{\partial \tau^2} + \Phi \frac{\partial^2 \Phi^*}{\partial \tau^2} \right) [\lambda_0] \left( -\frac{1}{\omega_n^2 + \xi^2} \right)^{-1},$$

$$\begin{aligned} S_{\Phi}^{(4, \tau^2, a)} &= \frac{1}{8} \int_0^\beta d\tau \int d\mathbf{r} \frac{1}{\beta V} \sum_{\mathbf{k}, n} |\Phi|^2 \left( \Phi^* \frac{\partial^2 \Phi}{\partial \tau^2} + \Phi \frac{\partial^2 \Phi^*}{\partial \tau^2} \right) \times \\ &\quad \times [6\lambda_0 + 2\lambda_e + 6\lambda_o], \end{aligned}$$

$$\begin{aligned} S_{\Phi}^{(6, \tau^2, a)} &= \frac{1}{12} \int_0^\beta d\tau \int d\mathbf{r} \frac{1}{\beta V} \sum_{\mathbf{k}, n} |\Phi|^4 \left( \Phi^* \frac{\partial^2 \Phi}{\partial \tau^2} + \Phi \frac{\partial^2 \Phi^*}{\partial \tau^2} \right) \times \\ &\quad \times [15\lambda_0 + 14\lambda_e + 26\lambda_o] \left( -\frac{1}{\omega_n^2 + \xi^2} \right). \end{aligned}$$

Since the total number of terms  $N_{2l}$  depends on  $l$  to the 4<sup>th</sup> power, the combinatorial weights for  $\lambda_0, \lambda_e$ , and  $\lambda_o$  are expected to be polynomials of (at most) order 3 in  $l$ . Defining the general expression

$$\begin{aligned} S_{\Phi}^{(2l, \tau^2, a)} &= \frac{1}{4} \int_0^\beta d\tau \int d\mathbf{r} \frac{1}{\beta V} \sum_{\mathbf{k}, n} |\Phi|^{2l-1} \left( \Phi^* \frac{\partial^2 \Phi}{\partial \tau^2} + \Phi \frac{\partial^2 \Phi^*}{\partial \tau^2} \right) \times \\ &\quad \times \left( -\frac{1}{\omega_n^2 + \xi_k^2} \right)^{l-2} [\alpha_l \lambda_0 + \beta_l \lambda_e + \eta_l \lambda_o], \end{aligned} \quad (2.104)$$

(where the prefactor  $1/l$  is included into the combinatorial weights), the generic polynomials

$$\alpha_l = a_1 l^3 + b_1 l^2 + c_1 l + d_1, \quad (2.105)$$

$$\beta_l = a_2 l^3 + b_2 l^2 + c_2 l + d_2, \quad (2.106)$$

$$\eta_l = a_3 l^3 + b_3 l^2 + c_3 l + d_3, \quad (2.107)$$

can be determined by solving the following systems of equations:

$$\begin{cases} \alpha_1 = 1 \\ \alpha_2 = 3 \\ \alpha_3 = 5 \end{cases}, \quad \begin{cases} \beta_1 = 0 \\ \beta_2 = 1 \\ \beta_3 = 14/3 \end{cases}, \quad \begin{cases} \eta_1 = 0 \\ \eta_2 = 2 \\ \eta_3 = 26/3 \end{cases}.$$

The resulting combinatorial weights are

$$\begin{aligned} \alpha_l &= 2l - 1, \\ \beta_l &= \frac{1}{3}(l-1)(4l-5), \\ \eta_l &= \frac{1}{3}(l-1)(4l+1). \end{aligned}$$

It is easy to verify that the sum  $\alpha_l + \beta_l + \eta_l$  multiplied by  $l$  correctly reproduces the value of  $N_{2l}$  (2.100).

The last step towards the final form of  $S_{\Phi}^{(2l,\tau^2,a)}$  is to reshape the factor depending on the pairing field  $\Phi$  in the first line of (2.104). This can be done by using the equality

$$\begin{aligned} &\int_0^\beta d\tau |\Phi|^{2(l-1)} \left( \Phi^* \frac{\partial^2 \Phi}{\partial \tau^2} + \Phi \frac{\partial^2 \Phi^*}{\partial \tau^2} \right) = \\ &= - \int_0^\beta d\tau \left[ 2 |\Phi|^{2(l-1)} \frac{\partial \Phi^*}{\partial \tau} \frac{\partial \Phi}{\partial \tau} + (l-1) |\Phi|^{2(l-2)} \left( \frac{\partial |\Phi|^2}{\partial \tau} \right)^2 \right]. \end{aligned}$$

Hence

$$\begin{aligned} S_{\Phi}^{(2l,\tau^2,a)} &= \frac{1}{4} \int_0^\beta d\tau \int d\mathbf{r} \frac{1}{\beta V} \sum_{\mathbf{k},n} \left[ 2 \frac{\partial \Phi^*}{\partial \tau} \frac{\partial \Phi}{\partial \tau} + \frac{l-1}{|\Phi|^2} \left( \frac{\partial |\Phi|^2}{\partial \tau} \right)^2 \right] \times \\ &\times \left( -\frac{|\Phi|}{\omega_n^2 + \xi_{\mathbf{k}}^2} \right)^{2(l-1)} [\alpha_l \lambda_0 + \beta_l \lambda_e + \eta_l \lambda_o]. \end{aligned}$$

The fermionic Matsubara summations will be performed after combining the total contribution to the action coming from terms with second order imaginary time derivatives and summing the corrections to all orders in the fluctuations by computing the sum over  $l$ .

\* \* \*

The explicit expression for  $S_{\Phi}^{(2l,\tau^2,a)}$  is given by

$$\begin{aligned} S_{\Phi}^{(2l,\tau^2,a)} &= \int_0^\beta d\tau \int d\mathbf{r} \frac{1}{\beta V} \sum_{\mathbf{k},n} \left[ |\Phi|^2 \frac{\partial \Phi^*}{\partial \tau} \frac{\partial \Phi}{\partial \tau} + \frac{l-1}{2} \left( \frac{\partial |\Phi|^2}{\partial \tau} \right)^2 \right] \left( -\frac{|\Phi|^2}{\omega_n^2 + \xi_{\mathbf{k}}^2} \right)^{l-2} \times \\ &\times \left[ \frac{2l-1}{2} \lambda_0 + \frac{(l-1)(4l-5)}{6} \lambda_e + \frac{(l-1)(4l+1)}{6} \lambda_o \right]. \end{aligned} \quad (2.108)$$

### 2.6.3 Term with second order time derivatives/2: $S_{\Phi}^{(\tau^2,b)}$

Following the same path as in the previous subsection, the contribution  $S_{\Phi}^{(\tau^2,b)}$  can be obtained from (2.85) by selecting the terms that contain two first order imaginary time derivatives of the pairing matrix  $\mathbb{F}$ . The relevant terms contributing to  $S_{\Phi}^{(\tau^2,b)}$  can be obtained from (2.85)

$$\begin{aligned}
S_{\Phi}^{(p)} &= \frac{1}{p} \int_0^{\beta} d\tau_1 \int d\mathbf{r}_1 \int_0^{\beta} d\tau'_2 \cdots \int_0^{\beta} d\tau'_p \frac{1}{\beta^p V} \sum_{\mathbf{k}_1} \sum_{n_1, \dots, n_{p-1}} \\
&\times \text{Tr} \left( \begin{array}{l} \mathbb{G}_0(\mathbf{k}_1, n_1) \mathbb{F} \\ \times \mathbb{G}_0(\mathbf{k}_1, n_2) (\mathbb{F} + \hat{\tau}'_2 \mathbb{Q}_1 + \cdots) \\ \times \mathbb{G}_0(\mathbf{k}_1, n_3) (\mathbb{F} + (\hat{\tau}'_2 + \hat{\tau}'_3) \mathbb{Q}_1 + \cdots) \\ \times \mathbb{G}_0(\mathbf{k}_1, n_4) (\mathbb{F} + (\hat{\tau}'_2 + \hat{\tau}'_3 + \hat{\tau}'_4) \mathbb{Q}_1 + \cdots) \\ \\ \times \cdots \times \\ \times \mathbb{G}_0(\mathbf{k}_1, n_p) (\mathbb{F} + (\hat{\tau}'_2 + \hat{\tau}'_3 + \cdots + \hat{\tau}'_p) \mathbb{Q}_1 + \cdots) \end{array} \right) \\
&\times e^{-i\omega_{n_1} \cdot (\tau'_2 + \cdots + \tau'_p) + i\omega_{n_2} \cdot \tau'_2 + i\omega_{n_3} \cdot \tau'_3 + \cdots + i\omega_{n_p} \cdot \tau'_p} + \dots
\end{aligned}$$

by selecting the contributions that include the operator  $\mathbb{Q}_1$  squared. In the last expression the imaginary time variables  $\tau'_2, \dots, \tau'_p$  have been replaced by the corresponding operators  $\hat{\tau}'_2, \dots, \hat{\tau}'_p$  defined in the previous section. This substitution enables us to carry out the integrations over imaginary time: the resulting Kronecker deltas determine the condition on the fermionic Matsubara frequencies  $\omega_{n_1} = \omega_{n_2} = \dots = \omega_{n_p}$ , leading to

$$\begin{aligned}
S_{\Phi}^{(p)} &= \frac{1}{p} \int_0^{\beta} d\tau_1 \int d\mathbf{r}_1 \frac{1}{\beta V} \sum_{\mathbf{k}_1} \sum_{n_1} \\
&\times \text{Tr} \left( \begin{array}{l} \mathbb{G}_0(\mathbf{k}_1, n_1) \mathbb{F} \\ \times \mathbb{G}_0(\mathbf{k}_1, n_2) (\mathbb{F} + \hat{\tau}'_2 \mathbb{Q}_1 + \cdots) \\ \times \mathbb{G}_0(\mathbf{k}_1, n_3) (\mathbb{F} + (\hat{\tau}'_2 + \hat{\tau}'_3) \mathbb{Q}_1 + \cdots) \\ \times \mathbb{G}_0(\mathbf{k}_1, n_4) (\mathbb{F} + (\hat{\tau}'_2 + \hat{\tau}'_3 + \hat{\tau}'_4) \mathbb{Q}_1 + \cdots) \\ \\ \times \cdots \times \\ \times \mathbb{G}_0(\mathbf{k}_1, n_p) (\mathbb{F} + (\hat{\tau}'_2 + \hat{\tau}'_3 + \cdots + \hat{\tau}'_p) \mathbb{Q}_1 + \cdots) \end{array} \right) \Bigg|_{\{n_j=n_1\}}. \quad (2.109)
\end{aligned}$$

## Calculation

The selection of the relevant terms leads to the basic expression for  $S_{\Phi}^{(2l,\tau^2,b)}$ , which reads

$$\tilde{S}_{\Phi}^{(p,\tau^2,b)} = \frac{1}{p} \int_0^\beta d\tau \int d\mathbf{r} \frac{1}{\beta V} \sum_n \sum_{\mathbf{k}} \left\{ \begin{array}{l} p-1 \text{ lines} \\ p-2 \text{ lines} \\ 1 \text{ line} \end{array} \right. \left\{ \begin{array}{l} \text{Tr} [\mathbb{G}_0(\mathbf{k}_1, n_1) \mathbb{F} \mathbb{G}_0(\mathbf{k}_1, n_2) (\hat{\tau}'_2) \mathbb{Q}_1 \mathbb{G}_0(\mathbf{k}_1, n_3) (\hat{\tau}'_2 + \hat{\tau}'_3) \mathbb{Q}_1 \\ \times \mathbb{G}_0(\mathbf{k}_1, n_4) \mathbb{F} \cdots \mathbb{G}_0(\mathbf{k}_1, n_p) \mathbb{F} + \\ + \mathbb{G}_0(\mathbf{k}_1, n_1) \mathbb{F} \mathbb{G}_0(\mathbf{k}_1, n_2) (\hat{\tau}'_2) \mathbb{Q}_1 \mathbb{G}_0(\mathbf{k}_1, n_3) \mathbb{F} \\ \times \mathbb{G}_0(\mathbf{k}_1, n_4) (\hat{\tau}'_2 + \hat{\tau}'_3 + \hat{\tau}'_4) \mathbb{Q}_1 \cdots \mathbb{G}_0(\mathbf{k}_1, n_p) \mathbb{F} \\ + \dots + \\ + \mathbb{G}_0(\mathbf{k}_1, n_1) \mathbb{F} \mathbb{G}_0(\mathbf{k}_1, n_2) (\hat{\tau}'_2) \mathbb{Q}_1 \mathbb{G}_0(\mathbf{k}_1, n_3) \mathbb{F} \\ \times \mathbb{G}_0(\mathbf{k}_1, n_4) \mathbb{F} \cdots \mathbb{G}_0(\mathbf{k}_1, n_p) (\hat{\tau}'_2 + \hat{\tau}'_3 + \dots + \hat{\tau}'_p) \mathbb{Q}_1 + \\ + \mathbb{G}_0(\mathbf{k}_1, n_1) \mathbb{F} \mathbb{G}_0(\mathbf{k}_1, n_2) \mathbb{F} \mathbb{G}_0(\mathbf{k}_1, n_3) (\hat{\tau}'_2 + \hat{\tau}'_3) \mathbb{Q}_1 \\ \times \mathbb{G}_0(\mathbf{k}_1, n_4) (\hat{\tau}'_2 + \hat{\tau}'_3 + \hat{\tau}'_4) \mathbb{Q}_1 \cdots \mathbb{G}_0(\mathbf{k}_1, n_p) \mathbb{F} \\ + \dots + \\ + \mathbb{G}_0(\mathbf{k}_1, n_1) \mathbb{F} \mathbb{G}_0(\mathbf{k}_1, n_2) \mathbb{F} \mathbb{G}_0(\mathbf{k}_1, n_3) (\hat{\tau}'_2 + \hat{\tau}'_3) \mathbb{Q}_1 \\ \times \mathbb{G}_0(\mathbf{k}_1, n_4) \mathbb{F} \cdots \mathbb{G}_0(\mathbf{k}_1, n_p) (\hat{\tau}'_2 + \hat{\tau}'_3 + \dots + \hat{\tau}'_p) \mathbb{Q}_1 + \\ + \dots + \\ + \mathbb{G}_0(\mathbf{k}_1, n_1) \mathbb{F} \mathbb{G}_0(\mathbf{k}_1, n_2) \mathbb{F} \mathbb{G}_0(\mathbf{k}_1, n_3) \mathbb{F} \mathbb{G}_0(\mathbf{k}_1, n_4) \mathbb{F} \times \dots \times \\ \times \mathbb{G}_0(\mathbf{k}_1, n_{p-1}) (\hat{\tau}'_2 + \hat{\tau}'_3 + \dots + \hat{\tau}'_{p-1}) \mathbb{Q}_1 \times \\ \times \mathbb{G}_0(\mathbf{k}_1, n_p) (\hat{\tau}'_2 + \hat{\tau}'_3 + \dots + \hat{\tau}'_p) \mathbb{Q}_1 \}_{\{n_j=n_1\}} \end{array} \right. , \quad (2.110)$$

where the curly brackets on the left group together the terms arising from the same line of expression (2.109). Again, the first simplification comes from the analysis of the expressions inside the trace signs. It is clear that, as was the case in all previous sections, only the contributions coming from terms with even  $p$  are non-zero. Therefore we can safely set  $p = 2l$  in the remainder of the derivation.

The presence of two  $\mathbb{Q}_1$  elements in each trace makes it impossible to reduce all traces to the same form by using the invariance of the trace for cyclical permutations and proceed as in the previous subsection.

Therefore here the combinatorial weights are obtained by explicitly calculating  $\tilde{S}_{\Phi}^{(2l,\tau^2,b)}$  for the few lowest- $l$  values. However, before proceeding, the total number of terms must be calculated so to give an upper bound to the order of the polynomials of  $l$  that constitute the combinatorial weights. We start by isolating the first curly bracket in (2.110) and highlighting just the operators  $\hat{\tau}$ , i.e.

$$\begin{aligned} & \cdots (\hat{\tau}'_2) \cdots (\hat{\tau}'_2 + \hat{\tau}'_3) \cdots + \\ & + \cdots (\hat{\tau}'_2) \cdots (\hat{\tau}'_2 + \hat{\tau}'_3 + \hat{\tau}'_4) \cdots \\ & + \dots + \\ & + \cdots (\hat{\tau}'_2) \cdots (\hat{\tau}'_2 + \hat{\tau}'_3 + \dots + \hat{\tau}'_{2l}) \cdots \end{aligned}$$

Labelling every line with the highest subscript  $j$  of an operator in the second parenthesis, the single operator  $\hat{\tau}'_2$  in the right parenthesis is combined with the  $j-1$  operators in the left one. The next curly bracket in (2.110) becomes

$$\begin{aligned} & \cdots (\hat{\tau}'_2 + \hat{\tau}'_3) \cdots (\hat{\tau}'_2 + \hat{\tau}'_3 + \hat{\tau}'_4) \cdots + \\ & + \cdots (\hat{\tau}'_2 + \hat{\tau}'_3) \cdots (\hat{\tau}'_2 + \hat{\tau}'_3 + \hat{\tau}'_4 + \hat{\tau}'_5) \cdots \\ & + \dots + \\ & + \cdots (\hat{\tau}'_2 + \hat{\tau}'_3) \cdots (\hat{\tau}'_2 + \hat{\tau}'_3 + \dots + \hat{\tau}'_{2l}) \cdots \end{aligned}$$

Following the same procedure for labelling the lines used for the terms in the first bracket for all brackets building up (2.110), the following general formula can be obtained for computing the total number of

terms:

$$N_{2l} = \sum_{j=2}^{2l} \sum_{i=1}^{j-2} (j-1)i = \frac{1}{6}l(l-1)(2l-1)(6l-1).$$

Considering the prefactor  $1/(2l)$  appearing in front of every term of  $\tilde{S}_{\Phi}^{(2l,\tau^2,b)}$  we can conclude that the combinatorial weights must be polynomials of  $l$  of (at most)  $3^d$  degree. Hereunder the expressions for  $\tilde{S}_{\Phi}^{(2l,\tau^2,b)}$  for a few small values of  $l$  are given:

$$\tilde{S}_{\Phi}^{(2,\tau^2,b)} = 0,$$

$$S_{\Phi}^{(4,\tau^2,b)} = \int_0^{\beta} d\tau \int d\mathbf{r} \frac{1}{\beta V} \sum_{\mathbf{k},n} \left[ \left( \lambda_0 + \frac{3}{2} \lambda_o \right) |\Phi|^2 \frac{\partial \Phi^*}{\partial \tau} \frac{\partial \Phi}{\partial \tau} + \left( \frac{1}{4} \lambda_0 + \frac{1}{4} \lambda_e + 3 \lambda_o \right) \left( \frac{\partial |\Phi|^2}{\partial \tau} \right) \right],$$

$$S_{\Phi}^{(6,\tau^2,b)} = \int_0^{\beta} d\tau \int d\mathbf{r} \frac{1}{\beta V} \sum_{\mathbf{k},n} \left( -\frac{|\Phi|^2}{\omega_n^2 + \xi^2} \right) \times \\ \times \left[ \left( 3 \lambda_0 + \frac{4}{3} \lambda_e + \frac{13}{3} \lambda_o \right) |\Phi|^2 \frac{\partial \Phi^*}{\partial \tau} \frac{\partial \Phi}{\partial \tau} + \left( \frac{7}{6} \lambda_0 + \frac{5}{3} \lambda_e + 28 \lambda_o \right) \left( \frac{\partial |\Phi|^2}{\partial \tau} \right) \right],$$

$$S_{\Phi}^{(8,\tau^2,b)} = \int_0^{\beta} d\tau \int d\mathbf{r} \frac{1}{\beta V} \sum_{\mathbf{k},n} \left( -\frac{|\Phi|^2}{\omega_n^2 + \xi^2} \right)^2 \times \\ \times \left[ \left( 3 \lambda_0 + 4 \lambda_e + \frac{17}{2} \lambda_o \right) |\Phi|^2 \frac{\partial \Phi^*}{\partial \tau} \frac{\partial \Phi}{\partial \tau} + \left( \frac{11}{4} \lambda_0 + \frac{23}{4} \lambda_e + 93 \lambda_o \right) \left( \frac{\partial |\Phi|^2}{\partial \tau} \right) \right],$$

where the functions  $\lambda_0$ ,  $\lambda_e$ , and  $\lambda_o$  depending on the fermionic (and bosonic) Matsubara frequencies are the same as those defined in (2.101)-(2.103). Writing the general expression for arbitrary  $l$  as

$$S_{\Phi}^{(2l,\tau^2,b)} = \int_0^{\beta} d\tau \int d\mathbf{r} \frac{1}{\beta V} \sum_{\mathbf{k},n} \left( -\frac{|\Phi|^2}{\omega_n^2 + \xi^2} \right)^{l-2} \times \\ \times \left[ \left( \alpha_l^{(1)} \lambda_0 + \beta_l^{(1)} \lambda_e + \eta_l^{(1)} \lambda_o \right) |\Phi|^2 \frac{\partial \Phi^*}{\partial \tau} \frac{\partial \Phi}{\partial \tau} + \left( \alpha_l^{(2)} \lambda_0 + \beta_l^{(2)} \lambda_e + \eta_l^{(2)} \lambda_o \right) \left( \frac{\partial |\Phi|^2}{\partial \tau} \right) \right],$$

the combinatorial weights can be written as

$$\begin{aligned} \alpha_l^{(1)} &= a_1^{(1)} l^3 + b_1^{(1)} l^2 + c_1^{(1)} l + d_1^{(1)}, \\ \beta_l^{(1)} &= a_2^{(1)} l^3 + b_2^{(1)} l^2 + c_2^{(1)} l + d_2^{(1)}, \\ \eta_l^{(1)} &= a_3^{(1)} l^3 + b_3^{(1)} l^2 + c_3^{(1)} l + d_3^{(1)}, \\ \alpha_l^{(2)} &= a_1^{(2)} l^3 + b_1^{(2)} l^2 + c_1^{(2)} l + d_1^{(2)}, \\ \beta_l^{(2)} &= a_2^{(2)} l^3 + b_2^{(2)} l^2 + c_2^{(2)} l + d_2^{(2)}, \\ \eta_l^{(2)} &= a_3^{(2)} l^3 + b_3^{(2)} l^2 + c_3^{(2)} l + d_3^{(2)}, \end{aligned}$$

and can be determined by solving the following systems of equations

$$\left\{ \begin{array}{l} \alpha_1^{(1)} = 0 \\ \alpha_2^{(1)} = 1 \\ \alpha_3^{(1)} = 3 \\ \alpha_4^{(1)} = 3 \end{array} \right\}, \quad \left\{ \begin{array}{l} \beta_1^{(1)} = 0 \\ \beta_2^{(1)} = 0 \\ \beta_3^{(1)} = 4/3 \\ \beta_4^{(1)} = 4 \end{array} \right\}, \quad \left\{ \begin{array}{l} \eta_1^{(1)} = 0 \\ \eta_2^{(1)} = 3/2 \\ \eta_3^{(1)} = 13/3 \\ \eta_4^{(1)} = 17/2 \end{array} \right\},$$

$$\left\{ \begin{array}{l} \alpha_1^{(2)} = 0 \\ \alpha_2^{(2)} = 1/4 \\ \alpha_3^{(2)} = 7/6 \\ \alpha_4^{(2)} = 11/4 \end{array} \right\}, \quad \left\{ \begin{array}{l} \beta_1^{(2)} = 0 \\ \beta_2^{(2)} = 1/4 \\ \beta_3^{(2)} = 5/3 \\ \beta_4^{(2)} = 23/4 \end{array} \right\}, \quad \left\{ \begin{array}{l} \eta_1^{(2)} = 0 \\ \eta_2^{(2)} = 3 \\ \eta_3^{(2)} = 28 \\ \eta_4^{(2)} = 93 \end{array} \right\}.$$

The resulting combinatorial weights are:

$$\begin{aligned} \alpha_l^{(1)} &= l - 1, \\ \beta_l^{(1)} &= \frac{2}{3}(l - 1)(l - 2), \\ \eta_l^{(1)} &= \frac{1}{6}(l - 1)(4l + 1), \\ \alpha_l^{(2)} &= (l - 1) \left( \frac{1}{3}l - \frac{5}{12} \right), \\ \beta_l^{(2)} &= (l - 1) \left( \frac{1}{4}l^2 - \frac{2}{3}l + \frac{7}{12} \right), \\ \eta_l^{(2)} &= \frac{1}{12}(l - 1)(3l^2 - 4l - 1). \end{aligned}$$

\* \* \*

The final expression for  $S_{\Phi}^{(2l,\tau^2,b)}$  is given by;

$$\begin{aligned} S_{\Phi}^{(2l,\tau^2,b)} &= \int_0^{\beta} d\tau \int d\mathbf{r} \frac{1}{\beta V} \sum_{\mathbf{k},n} \left( -\frac{|\Phi|^2}{\omega_n^2 + \xi^2} \right)^{l-2} \times \\ &\times \left\{ (l - 1) \left( \lambda_0 + \frac{2}{3}(l - 2)\lambda_e + \frac{1}{6}(4l + 1)\lambda_o \right) |\Phi|^2 \frac{\partial \Phi^*}{\partial \tau} \frac{\partial \Phi}{\partial \tau} + \right. \\ &\left. + \frac{(l - 1)}{12} [(4l - 5)\lambda_0 + (3l^2 - 8l + 7)\lambda_e + (3l^2 - 4l - 1)\lambda_o] \left( \frac{\partial |\Phi|^2}{\partial \tau} \right) \right\}. \end{aligned} \quad (2.111)$$

#### 2.6.4 Complete term $S_{\Phi}^{(\tau^2)}$

The contributions  $S_{\Phi}^{(2l,\tau^2,a)}$  and  $S_{\Phi}^{(2l,\tau^2,b)}$  can finally be brought together by summing (2.108) and (2.111), and the sum over the index  $l$  can be performed. The initial expression for the complete term  $S_{\Phi}^{(2l,\tau^2)}$  is

$$\begin{aligned} S_{\Phi}^{(2l,\tau^2)} &= -\frac{1}{2} \int_0^{\beta} d\tau \int d\mathbf{r} \frac{1}{\beta V} \sum_{\mathbf{k},n} \left( -\frac{|\Phi|^2}{\omega_n^2 + \xi^2} \right)^{l-2} \times \\ &\times \left\{ (\lambda_0 + (l - 1)\lambda_e) |\Phi|^2 \frac{\partial \Phi^*}{\partial \tau} \frac{\partial \Phi}{\partial \tau} + \right. \\ &\left. + \frac{1}{6} (l^2 - 1) [2\lambda_0 + (l - 2)\lambda_e + l\lambda_o] \left( \frac{\partial |\Phi|^2}{\partial \tau} \right) \right\}. \end{aligned}$$

## Calculation

The summation over  $l$  can be carried out for the two terms of the sum inside the curly brackets separately: in particular the results of the basic sums read

$$\begin{aligned}
& \sum_{l=1}^{\infty} \left( -\frac{|\Phi|^2}{\omega_n^2 + \xi^2} \right)^{l-2} (\lambda_0 + (l-1)\lambda_e) = \\
& = -\frac{(\omega_n^2 + \xi_k^2)^2 [|\Phi|^2(\lambda_0 - \lambda_e) + \lambda_0(\omega_n^2 + \xi_k^2)]}{|\Phi|^2(\omega_n^2 + \xi_k^2 + |\Phi|^2)}, \\
& \sum_{l=1}^{\infty} \left( -\frac{|\Phi|^2}{\omega_n^2 + \xi^2} \right)^{l-2} \frac{1}{6} (l^2 - 1) [2\lambda_0 + (l-2)\lambda_e + l\lambda_o] = \\
& = \frac{(\omega_n^2 + \xi_k^2)^2}{3(\omega_n^2 + \xi_k^2 + |\Phi|^2)^4} \times \\
& \times \left[ (|\Phi|^4 + 4|\Phi|^2(\omega_n^2 + \xi_k^2))(\lambda_0 - \lambda_e) + 3(\lambda_0 + \lambda_o)(\omega_n^2 + \xi_k^2)^2 \right].
\end{aligned}$$

Before proceeding to the fermionic Matsubara summations another step is necessary: the limit  $\Omega_m \rightarrow 0$  must be taken. To do this it is convenient to treat separately the terms proportional to  $\frac{\partial \Phi^*}{\partial \tau} \frac{\partial \Phi}{\partial \tau}$  and to  $\left( \frac{\partial |\Phi|^2}{\partial \tau} \right)^2$  and treat individually the terms involving  $\lambda_0$ ,  $\lambda_e$ , and  $\lambda_o$  respectively. In order to sketch the strategy employed to exploit the limiting procedure we concentrate on the contribution proportional to  $\left( \frac{\partial |\Phi|^2}{\partial \tau} \right)^2$ , which is the one that requires more care: for the term proportional to  $\lambda_0$ , i.e.

$$2 \frac{(\omega_n^2 + \xi_k^2)^2 (3\omega_n^2 + 3\xi_k^2 + |\Phi|^2)}{(\omega_n^2 + \xi_k^2 + |\Phi|^2)^2} \lambda_0$$

- the contribution of  $\lambda_0$  (2.101) is expanded in powers of  $\Omega_m$  around  $\Omega_m = 0$
- the coefficient of the second order term is isolated by exploiting

$$-\frac{\partial}{\partial \Omega_m^2} \left( 2 \frac{(\omega_n^2 + \xi_k^2)^2 (3\omega_n^2 + 3\xi_k^2 + |\Phi|^2)}{(\omega_n^2 + \xi_k^2 + |\Phi|^2)^2} \lambda_0 \right) \Big|_{\Omega_m=0}$$

- the final form of the contribution proportional to  $\lambda_0$  is

$$\begin{aligned}
M_n^{(1)} \equiv & -\frac{4(2\xi_k^2 + |\Phi|^2)}{3|\Phi|^2} \frac{1}{(\omega_n^2 + \xi_k^2 + |\Phi|^2)^3} - \frac{4\xi_k^2 - 2|\Phi|^2}{3|\Phi|^4} \frac{1}{(\omega_n^2 + \xi_k^2 + |\Phi|^2)^2} \\
& + \frac{2}{3|\Phi|^4} \frac{1}{(\omega_n^2 + \xi_k^2 + |\Phi|^2)} \tag{2.112}
\end{aligned}$$

Notice that the last expression was already manipulated in order to get rid of the dependence on the fermionic frequencies  $\omega_n$  in the numerators and make the Matsubara summations easier at a later stage: this manipulation will be applied to all terms in the following.

for the contribution proportional to  $\lambda_e$ , which reads

$$-\frac{|\Phi|^2 (\omega_n^2 + \xi_k^2)^2 (4\omega_n^2 + 4\xi_k^2 + |\Phi|^2)}{3(\omega_n^2 + \xi_k^2 + |\Phi|^2)^4} \lambda_e,$$

- the contribution of  $\lambda_e$  (2.102) is expanded in powers of  $\Omega_m$  and  $\Omega_k$  around  $\Omega_m = 0, \Omega_k = 0$ .
- the coefficient of the second order term is isolated by exploiting

$$-\frac{\partial}{\partial\Omega_m\partial\Omega_k} \left( -\frac{|\Phi|^2 (\omega_n^2 + \xi_k^2)^2 (4\omega_n^2 + 4\xi_k^2 + |\Phi|^2)}{3(\omega_n^2 + \xi_k^2 + |\Phi|^2)^4} \lambda_e \right) \Big|_{\Omega_m=0, \Omega_k=0}$$

- the final form of the contribution proportional to  $\lambda_e$  is

$$M_n^{(2)} \equiv \frac{2\xi_k^2 + |\Phi|^2}{(\omega_n^2 + \xi_k^2 + |\Phi|^2)^4} + \frac{1}{3|\Phi|^2} \frac{4\xi_k^2 - |\Phi|^2}{(\omega_n^2 + \xi_k^2 + |\Phi|^2)^3} + \frac{1}{3|\Phi|^4} \frac{2\xi_k^2 - |\Phi|^2}{(\omega_n^2 + \xi_k^2 + |\Phi|^2)^2} - \frac{1}{3|\Phi|^4} \frac{1}{(\omega_n^2 + \xi_k^2 + |\Phi|^2)}; \quad (2.113)$$

for the contribution proportional to  $\lambda_o$ , which reads

$$\frac{(\omega_n^2 + \xi_k^2)^4}{(\omega_n^2 + \xi_k^2 + |\Phi|^2)^4} \lambda_o,$$

- the contribution of  $\lambda_o$  (2.103) is expanded in powers of  $\Omega_m$  and  $\Omega_k$  around  $\Omega_m = 0, \Omega_k = 0$ .
- the coefficient of the second order term is isolated by exploiting

$$-\frac{\partial}{\partial\Omega_m\partial\Omega_k} \left( \frac{(\omega_n^2 + \xi_k^2)^4}{(\omega_n^2 + \xi_k^2 + |\Phi|^2)^4} \lambda_o \right) \Big|_{\Omega_m=0, \Omega_k=0}$$

- the final form of the contribution proportional to  $\lambda_o$  is

$$M_n^{(3)} \equiv -|\Phi|^2 \frac{1}{(\omega_n^2 + \xi_k^2 + |\Phi|^2)^4} + \frac{1}{(\omega_n^2 + \xi_k^2 + |\Phi|^2)^3}. \quad (2.114)$$

The component of  $S_{\Phi}^{(2l,\tau^2)}$  proportional to  $\frac{\partial\Phi^*}{\partial\tau} \frac{\partial\Phi}{\partial\tau}$  can be treated in the same way, resulting in

$$M_n^{(0)} \equiv \frac{2\xi_k + |\Phi|^2}{|\Phi|^4} \frac{1}{(\omega_n^2 + \xi_k^2 + |\Phi|^2)^2} - \frac{1}{|\Phi|^4} \frac{1}{\omega_n^2 + \xi_k^2 + |\Phi|^2}$$

In light of these results, the complete contribution to the action coming from second-order imaginary-time derivatives  $S_{\Phi}^{(2l,\tau^2)}$  can be written as

$$S_{\Phi}^{(2l,\tau^2)} = -\frac{1}{2} \int_0^\beta d\tau \int d\mathbf{r} \frac{1}{V} \sum_{\mathbf{k}} \frac{1}{\beta} \sum_n \left[ M_n^{(0)} \frac{\partial\Phi^*}{\partial\tau} \frac{\partial\Phi}{\partial\tau} + \left( M_n^{(1)} + M_n^{(2)} + M_n^{(3)} \right) \left( \frac{\partial|\Phi|^2}{\partial\tau} \right)^2 \right].$$

It is now possible to restore the dependence on the imbalance parameter  $\zeta$  by simply substituting the normal fermionic Matsubara frequencies  $\omega_n$  with their ‘‘shifted’’ version  $\nu_n$ . By observing the form of the arguments of the sum over the index  $n$ , it is clear that the Matsubara sums that need to be performed

are all of the form (2.77) and can therefore be easily solved in terms of the functions  $f_s(\beta, x, \zeta)$  with  $s = 1, 2, 3, 4$ . The result is

$$S_{\Phi}^{(2l, \tau^2)} = -\frac{1}{2} \int_0^{\beta} d\tau \int d\mathbf{r} \frac{1}{V} \sum_{\mathbf{k}} \left[ \left( \frac{2\xi_{\mathbf{k}} + |\Phi|^2}{|\Phi|^4} f_2(\beta, E_{\mathbf{k}}, \zeta) - \frac{1}{|\Phi|^4} f_1(\beta, E_{\mathbf{k}}, \zeta) \right) \frac{\partial \Phi^*}{\partial \tau} \frac{\partial \Phi}{\partial \tau} + \left( \frac{1}{3|\Phi|^4} f_1(\beta, E_{\mathbf{k}}, \zeta) + \frac{E_{\mathbf{k}}^2 - 3\xi_{\mathbf{k}}^2}{3|\Phi|^4} f_2(\beta, E_{\mathbf{k}}, \zeta) + \frac{4(2E_{\mathbf{k}}^2 - \xi_{\mathbf{k}}^2)}{3|\Phi|^2} f_3(\beta, E_{\mathbf{k}}, \zeta) + 2E_{\mathbf{k}}^2 f_4(\beta, E_{\mathbf{k}}, \zeta) \right) \left( \frac{\partial |\Phi|^2}{\partial \tau} \right)^2 \right].$$

The complete contribution  $S_{\Phi}^{(2l, \tau^2)}$  can be finally rewritten in the simple form

$$S_{\Phi}^{(2l, \tau^2)} = \int_0^{\beta} d\tau \int d\mathbf{r} \frac{1}{V} \sum_{\mathbf{k}} \left[ Q \frac{\partial \Phi^*}{\partial \tau} \frac{\partial \Phi}{\partial \tau} + \frac{R}{2} \left( \frac{\partial |\Phi|^2}{\partial \tau} \right)^2 \right],$$

where the new EFT coefficients  $Q$  and  $R$  are defined as

$$Q(|\Phi|^2) = \frac{1}{2|\Phi|^2} \int \frac{d\mathbf{k}}{(2\pi)^3} [f_1(\beta, E_{\mathbf{k}}, \zeta) - (E_{\mathbf{k}}^2 + \xi_{\mathbf{k}}^2) f_2(\beta, E_{\mathbf{k}}, \zeta)], \quad (2.115)$$

$$R(|\Phi|^2) = \int \frac{d\mathbf{k}}{(2\pi)^3} \left[ \frac{f_1(\beta, E_{\mathbf{k}}, \zeta) + (E_{\mathbf{k}}^2 - 3\xi_{\mathbf{k}}^2) f_2(\beta, E_{\mathbf{k}}, \zeta)}{3|\Phi|^4} + \right. \quad (2.116)$$

$$\left. + \frac{4(\xi_{\mathbf{k}}^2 - 2E_{\mathbf{k}}^2)}{3|\Phi|^2} f_3(\beta, E_{\mathbf{k}}, \zeta) + 2E_{\mathbf{k}}^2 f_4(\beta, E_{\mathbf{k}}, \zeta) \right]. \quad (2.117)$$

## 2.7 Complete effective field theory action

The results of the calculations performed in the previous sections can be finally collected to obtain the expression for the complete EFT action for a 3D system of ultracold Fermions with spin-imbalance, which reads

$$S_{EFT} = \int_0^{\beta} d\tau \int d\mathbf{r} \left[ \frac{1}{2} D \left( \frac{\partial \Phi^*}{\partial \tau} \Phi - \Phi^* \frac{\partial \Phi}{\partial \tau} \right) + Q \frac{\partial \Phi^*}{\partial \tau} \frac{\partial \Phi}{\partial \tau} + \frac{R}{2} \left( \frac{\partial |\Phi|^2}{\partial \tau} \right)^2 + \Omega_s + \frac{C}{2m} |\nabla_{\mathbf{r}} \Phi|^2 - \frac{E}{2m} (\nabla_{\mathbf{r}} |\Phi|^2)^2 \right], \quad (2.118)$$

where the definitions of the effective field theory coefficients  $\Omega_s$ ,  $C$ ,  $D$ ,  $E$ ,  $Q$ , and  $R$  are given, in terms of the modulus squared of the order parameter, by (2.39), (2.79), (2.95), (2.80), (2.115), and (2.117) respectively. Here these expressions are reported in order to

have an overview of the definitions:

$$\begin{aligned}
\Omega_s &= - \int \frac{d^3k}{(2\pi)^3} \left[ \frac{1}{\beta} \ln (2 \cosh (\beta E_{\mathbf{k}}) + 2 \cosh (\beta \zeta)) - \xi_{\mathbf{k}} - \frac{m|\Phi|^2}{k^2} \right] - \frac{m|\Phi|^2}{4\pi a_s}, \\
C &= \int \frac{d^3k}{(2\pi)^3} \frac{k^2}{3m} [f_2(\beta, E_{\mathbf{k}}, \zeta) - 4\xi_{\mathbf{k}}^2 |\Phi|^2 f_4(\beta, E_{\mathbf{k}}, \zeta)], \\
D &= \int \frac{d^3k}{(2\pi)^3} \frac{\xi_{\mathbf{k}}}{|\Phi|^2} [f_1(\beta, \xi_{\mathbf{k}}, \zeta) - f_1(\beta, E_{\mathbf{k}}, \zeta)], \\
E &= 2 \int \frac{d^3k}{(2\pi)^3} \frac{k^2}{3m} \xi_{\mathbf{k}}^2 f_4(\beta, E_{\mathbf{k}}, \zeta), \\
Q &= \frac{1}{2|\Phi|^2} \int \frac{d\mathbf{k}}{(2\pi)^3} [f_1(\beta, E_{\mathbf{k}}, \zeta) - (E_{\mathbf{k}}^2 + \xi_{\mathbf{k}}^2) f_2(\beta, E_{\mathbf{k}}, \zeta)], \\
R &= \int \frac{d\mathbf{k}}{(2\pi)^3} \left[ \frac{f_1(\beta, E_{\mathbf{k}}, \zeta) + (E_{\mathbf{k}}^2 - 3\xi_{\mathbf{k}}^2) f_2(\beta, E_{\mathbf{k}}, \zeta)}{3|\Phi|^4} + \right. \\
&\quad \left. + \frac{4(\xi_{\mathbf{k}}^2 - 2E_{\mathbf{k}}^2)}{3|\Phi|^2} f_3(\beta, E_{\mathbf{k}}, \zeta) + 2E_{\mathbf{k}}^2 f_4(\beta, E_{\mathbf{k}}, \zeta) \right].
\end{aligned}$$

# Chapter 3

## EFT description of Fermi superfluids

The previous chapter was devoted to the development of an effective field theory capable of describing the properties of a fermionic superfluid in terms of the bosonic order parameter, in a broad range of temperatures and across the BEC-BCS crossover. In the present chapter the first applications of the EFT will be considered.

In Section 3.1 the beyond mean-field fluctuations are considered and the spectrum of the collective excitations (Bogoliubov-Anderson modes) is obtained and described as a function of interaction and temperature. This is done by separating the mean-field and fluctuation contributions to the pairing field and then expanding the resulting action up to quadratic order in the fluctuations. The sound velocity  $c_s$  and the coefficient  $\lambda$  of the correction to the linear dispersion proportional to  $q^3$  are computed in terms of the EFT coefficients and compared to the predictions of other theoretical treatments [71–74].

Section 3.2 is instead devoted to the evaluation of the fluctuation contribution to the total particle density, obtained by correcting the saddle point density equation with the addition of a relevant fluctuation component by applying the Nozières Schmitt-Rink [45] approach. The behaviour of the critical temperature as a function of the interaction parameter  $(k_F a_s)^{-1}$  is analysed and the EFT predictions are compared with the results of the widely employed Gaussian pair fluctuations theory.

In Section 3.3 it is demonstrated how the correlation functions of any order can be obtained from the EFT action by introducing a generating functional. The condensate fraction and the pair correlation length, measuring the number of condensed pairs in the system and the typical size of a Cooper pair respectively, are evaluated at mean field level and the effects of interaction and temperature are described.

The results about the pair correlation length are used in Section 3.4 in order to obtain an indirect determination of the region of validity of the EFT. As highlighted in Chapter 2 the assumption at the core of the effective field theory is that the superfluid order parameter varies slowly in both time and space. To verify the validity of this hypothesis some results from Chapter 5 about the shape of a stable dark soliton in a Fermi superfluid are anticipated: in particular the typical size of the soliton, evaluated as the width at half height of the density dip, is compared to the size of a Cooper pair. The validity range of the EFT is identified with the domain in the  $\{T, \zeta, (k_F a_s)^{-1}\}$ -space where the pair correlation

length is substantially smaller than the soliton width.

The last part of the chapter, Section 3.5, is dedicated to the comparison, in the opportune limiting situations, between the EFT and other widely used effective theories: the Gross-Pitaevskii equation, valid at  $T = 0$  in the BEC regime, and the time-dependent Ginzburg-Landau treatment valid in the vicinity of the transition temperature. Finally in Subsection 3.5.3 a brief introduction to the Bogoliubov-de Gennes theory is given.

## 3.1 Collective excitations

In this section the spectra of the collective excitation modes of a system of ultracold fermions are calculated in the context of the effective field theory developed in Chapter 2. The theoretical treatment employed here to study the corrections to the mean field theory caused by the contribution of fluctuations aims to establish a correspondence between the EFT and the Gaussian pair fluctuations (GPF) approach. Before proceeding a remark must be made: the literature about the GPF treatment of beyond mean field effects can be classified in two categories. The fluctuations about the saddle point are introduced by writing the pairing field as

$$\Phi(x, \tau) = \Delta + \varphi(x, t), \quad \Phi^*(x, \tau) = \Delta^* + \varphi^*(x, t). \quad (3.1)$$

Here  $\varphi(x, t)$  describes the fluctuations while  $\Delta$  is the constant solution of the saddle-point gap equation for a uniform system

$$\frac{\partial \Omega_{sp}}{\partial \Delta} = 0, \quad (3.2)$$

where  $\Omega_{sp}$  is the saddle point thermodynamic potential already encountered in Section 2.2. Denoting the fluctuation contributions to the thermodynamic potential with  $\Omega_{fl}$ , the total thermodynamic potential can be written as

$$\Omega = \Omega_{sp} + \Omega_{fl} \quad (3.3)$$

The two main approaches to the treatment of Gaussian fluctuations differ in the way this quantity is treated in relation to the number equation. The total density and the density of the excess component particles are related to the total thermodynamic potential through

$$n = - \left. \frac{\partial \Omega}{\partial \mu} \right|_{T, \zeta},$$

$$\delta n = - \left. \frac{\partial \Omega}{\partial \zeta} \right|_{T, \mu}.$$

when inserting (3.3) into the last expression, this becomes

$$n = - \left. \frac{\partial \Omega_{sp}}{\partial \mu} \right|_{T, \zeta} - \left. \frac{\partial \Omega_{fl}}{\partial \mu} \right|_{T, \zeta},$$

$$\delta n = - \left. \frac{\partial \Omega_{sp}}{\partial \zeta} \right|_{T, \mu} - \left. \frac{\partial \Omega_{fl}}{\partial \zeta} \right|_{T, \mu}.$$

However, when we consider explicitly the dependence of  $\Omega$  on the pairing field, an additional term has to be considered, i.e.

$$n = - \left. \frac{\partial \Omega_{sp}}{\partial \mu} \right|_{T,\zeta,\Delta} - \left. \frac{\partial \Omega_{fl}}{\partial \mu} \right|_{T,\zeta,\Delta} - \left. \frac{\partial \Omega_{fl}}{\partial \Delta} \right|_{T,\zeta,\mu} \frac{\partial \Delta}{\partial \mu} \Big|_{T,\zeta}, \quad (3.4)$$

$$\delta n = - \left. \frac{\partial \Omega_{sp}}{\partial \zeta} \right|_{T,\mu,\Delta} - \left. \frac{\partial \Omega_{fl}}{\partial \zeta} \right|_{T,\mu,\Delta} - \left. \frac{\partial \Omega_{fl}}{\partial \Delta} \right|_{T,\zeta,\mu} \frac{\partial \Delta}{\partial \zeta} \Big|_{T,\mu}. \quad (3.5)$$

The two main approaches in the context of the GPF theory are the NSR treatment, introduced by Nozières and Schmitt-Rink [45], and the full GPF treatment (sometimes referred to as NSR-2). In particular the first retains just the first two terms in the right hand side of (3.4) and (3.5), while the second considers the full equations. Up to now no agreement has been found in the theoretical community about which of the two approaches is the best: each one has proven to give better predictions in specific situations but worse in others. References in which the full GPF method is used are for example [75, 76] by Hu *et al.*, recent papers [77, 78] by Randeria *et al.*, [79] by Keeling *et al.*, [80] by Lerch *et al.*, or [69, 81] by Tempere *et al.*. For references based on the application of the NSR method the reader is addressed to the work by Strinati *et al.* [82–85], by Ohashi *et al.* [86–88], or to earlier papers by Randeria *et al.* [46]. A brief discussion of the advantages and disadvantages of each method is included in the already mentioned paper [81]; the review article by Levin *et al.* [89] offers instead a more extended and detailed presentation of the principal methods to treat fluctuations beyond mean field.

In the present work a hybrid between the EFT and the standard NSR method is adopted. In fact it has been demonstrated that the application of the full GPF treatment to the standard fluctuation action and, even more significantly to the EFT action, can lead to a non-physical negative contribution to the fluctuation correction  $n_{fl}$  to the density.

The starting point to add fluctuations to the mean field treatment is to insert the shift (3.1) into the expression of the EFT action (2.118). This results in

$$\begin{aligned} S_{EFT}^{(fl)} = \int_0^\beta d\tau \int d\mathbf{r} \left[ \right. \\ & \frac{1}{2} D ((\Delta + \varphi)(\Delta^* + \varphi^*)) \left( \frac{\partial(\Delta^* + \varphi^*)}{\partial \tau} (\Delta + \varphi) - (\Delta^* + \varphi^*) \frac{\partial(\Delta + \varphi)}{\partial \tau} \right) + \\ & + Q \frac{\partial(\Delta^* + \varphi^*)}{\partial \tau} \frac{\partial(\Delta + \varphi)}{\partial \tau} - \frac{R}{2} \left( \frac{\partial(\Delta + \varphi)(\Delta^* + \varphi^*)}{\partial \tau} \right)^2 + \\ & + \Omega_s ((\Delta^* + \varphi^*)(\Delta + \varphi)) + \frac{C}{2m} [\nabla_{\mathbf{r}}(\Delta^* + \varphi^*) \nabla_{\mathbf{r}}(\Delta + \varphi)] + \\ & \left. - \frac{E}{2m} [\nabla_{\mathbf{r}}((\Delta^* + \varphi^*)(\Delta + \varphi))]^2 \right], \quad (3.6) \end{aligned}$$

where, on the basis of the discussion of Chapter 2, the full dependence of the EFT coefficients  $D$  and  $\Omega_s$  on  $|\Phi|^2$  has been considered. Collecting the terms up to second order in

the fluctuations the quadratic part of the action takes the form

$$\begin{aligned}
S_{EFT}^{(quad)} = \int_0^\beta d\tau \int d\mathbf{r} \left[ \right. \\
& \frac{1}{2} \tilde{D} (|\Delta|^2) \left( \frac{\partial \varphi^*}{\partial \tau} \varphi - \varphi^* \frac{\partial \varphi}{\partial \tau} \right) + Q \frac{\partial \varphi^*}{\partial \tau} \frac{\partial \varphi}{\partial \tau} - \frac{R}{2} \left( \frac{\partial \varphi^*}{\partial \tau} \Delta + \Delta^* \frac{\partial \varphi}{\partial \tau} \right)^2 + \\
& + W (|\Delta|^2) (|\varphi|^2) + U (|\Delta|^2) \left( \frac{1}{2} \varphi^2 + \frac{1}{2} (\varphi^*)^2 \right) + \frac{C}{2m} [\nabla_{\mathbf{r}} \varphi^* \cdot \nabla_{\mathbf{r}} \varphi] + \\
& \left. - \frac{E}{2m} (\Delta \nabla_{\mathbf{r}} \varphi^* + \Delta^* \nabla_{\mathbf{r}} \varphi)^2 \right]. \tag{3.7}
\end{aligned}$$

Here the new coefficients  $A$ ,  $\tilde{D}$ ,  $U$  and  $W$  are introduced as:

$$A = \frac{\partial \Omega_s(|\Delta|^2)}{\partial |\Delta|^2}, \quad \tilde{D} = \frac{\partial [|\Delta|^2 D(|\Delta|^2)]}{\partial |\Delta|^2}, \tag{3.8}$$

$$U = |\Delta|^2 \frac{\partial^2 \Omega(|\Delta|^2)}{\partial (|\Delta|^2)^2}, \quad W = A + U. \tag{3.9}$$

The coefficients  $U$  and  $W$  are in principle different but, when the gap equation is applied they become equal since  $A = \partial \Omega_{sp} / \partial |\Delta|^2$  is nothing but the left hand side of the saddle-point gap equation (3.2). Even if this simplification is possible, the coefficients will be kept distinct because, proceeding with the NSR-scheme, when taking derivatives of  $U$  and  $W$  with respect to the chemical potential to compute the fluctuation correction to the density, the derivative of the difference  $W - U = A$  may give non-zero contributions. It is worth remarking that the terms of order zero in the fluctuations add up to a constant contribution to the action that does not affect the physics of the system. The terms of order one on the other hand identically vanish, as expected.

By using the Fourier expansion for the fluctuation coordinates, i.e.

$$\begin{aligned}
\varphi(\mathbf{r}, \tau) &= \frac{1}{\sqrt{\beta V}} \sum_{\mathbf{q}, m} e^{i\mathbf{q} \cdot \mathbf{r} - i\Omega_m \tau} \varphi_{\mathbf{q}, m} \\
\varphi^*(\mathbf{r}, \tau) &= \frac{1}{\sqrt{\beta V}} \sum_{\mathbf{q}, m} e^{-i\mathbf{q} \cdot \mathbf{r} + i\Omega_m \tau} \varphi_{\mathbf{q}, m}^*
\end{aligned}$$

the quadratic action can be rewritten in reciprocal space notation as

$$S_{EFT}^{(quad)} = \frac{1}{2} \sum_{\mathbf{q}, m} \begin{pmatrix} \varphi_{\mathbf{q}, m}^* & \varphi_{-\mathbf{q}, -m} \end{pmatrix} \mathbb{M}(q, i\Omega_n) \begin{pmatrix} \varphi_{\mathbf{q}, m} \\ \varphi_{-\mathbf{q}, -m}^* \end{pmatrix}, \tag{3.10}$$

The matrix  $\mathbb{M}(q, i\Omega_n)$  is determined, in terms of the EFT coefficients, by:

$$\mathbb{M}(q, i\Omega_n) = \begin{pmatrix} W + \frac{C}{2m} q^2 - i\Omega_m \tilde{D} + \Omega_m^2 Q & U - |\Delta|^2 \left( \frac{E}{m} q^2 + R \Omega_m^2 \right) \\ U - |\Delta|^2 \left( \frac{E}{m} q^2 + R \Omega_m^2 \right) & W + \frac{C}{2m} q^2 + i\Omega_m \tilde{D} + \Omega_m^2 Q \end{pmatrix}. \tag{3.11}$$

It is worth noticing that simple relations exist between the different elements of the matrix, i.e.

$$M_{22}(q, i\Omega_n) = M_{11}(q, -i\Omega_n), \quad M_{21}(q, i\Omega_n) = M_{12}(q, i\Omega_n). \quad (3.12)$$

The spectrum of bosonic excitations is determined after the transformation  $i\Omega_m \rightarrow \omega$  by solving the equation

$$\det \mathbb{M}(q, \omega) = 0. \quad (3.13)$$

The solution is then expanded in powers of  $q$  up to the fourth order, resulting in

$$\omega_q^2 = c_s^2 q^2 + \left(\frac{1}{2m}\right)^2 \lambda q^4 + O(q^6). \quad (3.14)$$

In accordance with the Goldstone theorem the dispersion relation for the Bogoliubov excitation is linear at small momenta, i.e.  $\omega_q = c_s q + \dots$ : this relation introduces the sound velocity  $c_s$  which will be one of the main focuses of the present chapter. In addition the first correction, due to the terms in (3.14) that are quartic in  $q$  will be computed. The sound velocity can be readily obtained by taking the square root of the coefficient at  $q^2$  in (3.14):

$$c_s = \sqrt{2U \frac{C + |\Delta|^2 E}{\tilde{D}^2 + 2U(Q + |\Delta|^2 R)}}. \quad (3.15)$$

The second coefficient, denoted with  $\lambda$ , is instead given by

$$\lambda = \tilde{D}^2 \frac{(C + 2|\Delta|^2 E) \left( C \left( \tilde{D}^2 + 4|\Delta|^2 UR \right) - 2|\Delta|^2 E \left( \tilde{D}^2 + 4UQ \right) \right)}{\left( \tilde{D}^2 + 2U(Q + |\Delta|^2 R) \right)^3} \quad (3.16)$$

where, in the last two expressions we have set  $U = W$  since in this context  $A = 0$ . The dispersion relation of the pair excitation (the Bogoliubov-Anderson mode) can be finally written as

$$\hbar\omega_q = \hbar q \sqrt{c_s^2 + \lambda \left(\frac{\hbar q}{2m}\right)^2}. \quad (3.17)$$

where the factors  $\hbar$  have been momentarily restored to get a better picture of the units in play. The expansion of the square root in powers of  $q$  up to second order leads to the following form for the energy of the collective excitations:

$$\hbar\omega_q = \hbar c_s q \left[ 1 + \frac{\lambda}{8} \left(\frac{\hbar q}{c_s m}\right)^2 + \dots \right]. \quad (3.18)$$

This expression highlights the fact that the first correction to the linear dispersion is due to terms in  $q^3$  and makes it easier to compare the notation with that of other articles, e.g. [74], where moreover the coefficient  $\lambda$  is named  $\gamma$ .

The behaviour of the sound velocity  $c_s$  as a function of the interaction parameter  $(k_F a_s)^{-1}$

is depicted in Fig. 3.1 for different temperatures. It is important to notice that the BEC limit of  $c_s \rightarrow (v_F/2)\sqrt{\mu_B/m_B}$  [90] and the BCS limit of  $c_s \rightarrow 1/\sqrt{3}v_F$  are both correctly reproduced. In addition the EFT data for  $T = 0$  have been compared with the calculations by Salasnich *et al.* [71] obtained in the framework of Gaussian pair fluctuations theory: a good agreement is found throughout the entire interaction domain, and in particular at unitarity and on the BCS side of the resonance.

The coefficient  $\lambda$  of the term proportional to  $q^3$  in (3.18) can be interpreted, as will become clearer in Chapter 4, as a correction to the mass of the bosonic excitation, which will be defined as  $m_B = m/\sqrt{\lambda}$ . Fig. 3.2 shows the behaviour of  $\lambda$  across the BEC-BCS crossover. The dependence on temperature is found to be very weak and becomes sizable just in the BCS regime. The BEC limit of  $\lambda \rightarrow 1/4$ , which in turn means that  $m_B \rightarrow 2m$ , is correctly retrieved. A remark must be added in regard of the behaviour of  $\lambda$ : it appears that the EFT cannot capture the fact that  $\lambda$  is expected to assume large negative values on the BCS side of the resonance, as predicted in [72–74]. This emerges clearly from Fig. 3.3 where the EFT predictions for  $\lambda$  across the BEC-BCS crossover are compared to those of Kurkjian *et al.* [74]. While the two curves match in the BEC limit, going towards unitarity they separate with the EFT data (full black line) remaining always positive, while the red dashed line representing the results of [74] bends down and reaches negative values in the near BCS limit.

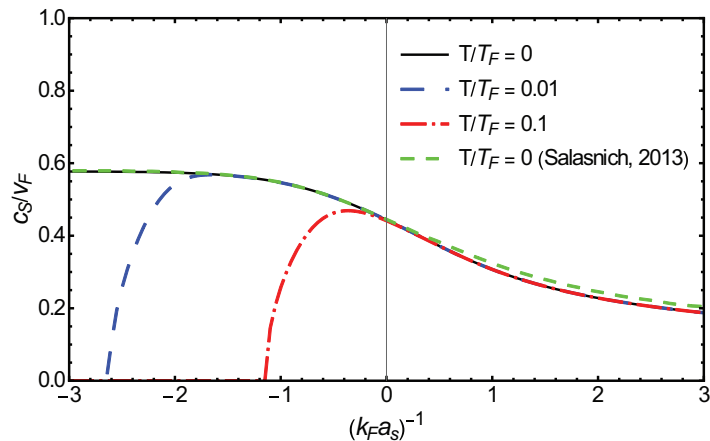


Figure 3.1: Sound velocity as a function of the interaction parameter  $(k_F a_s)^{-1}$  in different conditions of temperature, i.e.  $T = 0$  (black full line),  $T = 0.01T_F$  (blue dashed line),  $T = 0.1T_F$  (red dot-dashed line). The EFT values for  $c_s$  are shown across the entire BEC-BCS crossover and compared to the prediction by Salasnich *et al.* [71] (green finely-dashed line). The velocity is plotted in units of the Fermi velocity  $v_F = k_F/m$ .

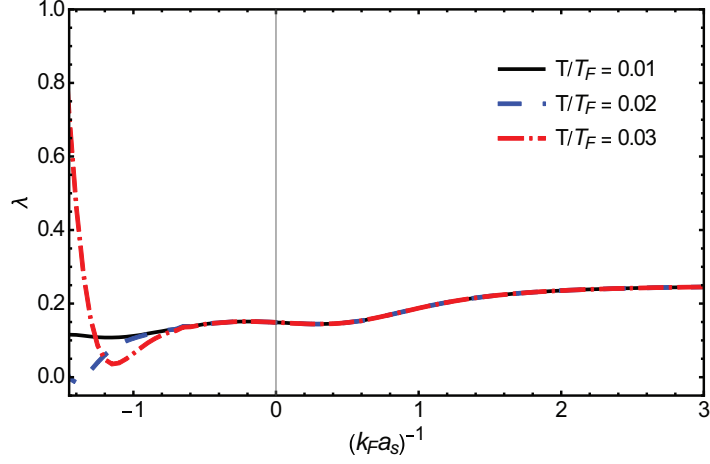


Figure 3.2: Coefficient  $\lambda$  of the  $q^3$  term in the dispersion relation  $\omega_q$  (3.18) as a function of the interaction parameter  $(k_F a_s)^{-1}$  across the BEC-BCS crossover in different conditions of temperature, i.e.  $T = 0$  (black full line),  $T = 0.01T_F$  (blue dashed line),  $T = 0.1T_F$  (red dot-dashed line).

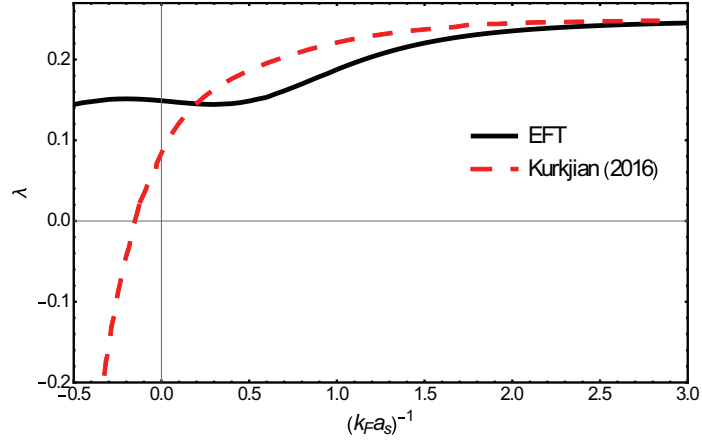


Figure 3.3: The EFT predictions for the coefficient  $\lambda$  of the  $q^3$  term in the dispersion relation  $\omega_q$  (3.18) (full black line) are compared to the analogous data from [74] (red dashed line) as a function of the interaction parameter  $(k_F a_s)^{-1}$  across the BEC-BCS crossover.

## 3.2 Critical temperature

The next goal of this chapter is to study the equation of state for a Fermi superfluid within the EFT formalism. This in turn allows us to determine the critical temperature and to describe the temperature dependence of different parameters of the system in the superfluid state.

### 3.2.1 Fluctuation contribution to the density

As mentioned earlier, in the present treatment a combination of EFT formalism and NSR approach is employed: the equation of state is obtained as a joint solution of the saddle-point gap equation (2.30),

$$\frac{\partial \Omega_{sp}}{\partial \Delta} = 0,$$

and the density equation,

$$n = -\frac{\partial \Omega}{\partial \mu}, \quad (3.19)$$

where  $\Omega = \Omega_{sp} + \Omega_{fl}$  is a sum of the saddle-point and fluctuation contributions to the thermodynamic potentials. The density is in turn subdivided into the two corresponding components:

$$n = n_{sp} + n_{fl}, \quad n_{sp} = -\frac{\partial \Omega_{sp}}{\partial \mu}, \quad n_{fl} = -\frac{\partial \Omega_{fl}}{\partial \mu}. \quad (3.20)$$

The saddle-point expression for the density was given in Chapter 2 in equation (2.31). In the following we will focus on the evaluation of the fluctuation correction to that expression. As already mentioned, this will be determined by adopting the NSR scheme, i.e. the derivative  $\frac{\partial \Omega}{\partial \mu}$  is considered a partial derivative keeping  $\Delta$  as an independent parameter and the third term on the right hand side of (3.4) and (3.5) is neglected. According to (3.20) the fluctuation contribution to the fermion density is obtained as minus the derivative with respect to the chemical potential of the component of the grand canonical thermodynamic potential due to fluctuations: this is given by

$$\begin{aligned} \Omega_{fl}(T, \mu, \zeta; \Delta) &= \frac{1}{2\beta} \sum_{\mathbf{q}, m} \ln \{ \det [\mathbb{M}(\mathbf{q}, i\Omega_m)] \} \\ &= \frac{1}{2\beta} \sum_{\mathbf{q}, m} \ln [\Gamma(\mathbf{q}, i\Omega_m)] \end{aligned} \quad (3.21)$$

where,  $\Gamma(\mathbf{q}, i\Omega_m)$  is defined exploiting the relations between the elements of  $\mathbb{M}(\mathbf{q}, i\Omega_m)$  (3.12), as

$$\Gamma(\mathbf{q}, i\Omega_m) = M_{1,1}(\mathbf{q}, i\Omega_m) M_{1,1}(\mathbf{q}, -i\Omega_m) - M_{1,2}(\mathbf{q}, i\Omega_m) M_{1,2}(\mathbf{q}, -i\Omega_m).$$

The logarithm of the determinant of  $\mathbb{M}(\mathbf{q}, i\Omega_m)$  in (3.21) appears as a consequence of the Gaussian integration over the bosonic variables  $\bar{\varphi}$  and  $\varphi$ : a similar situation was encountered already in Chapter 2. The fluctuation contribution to the total particle density is related to  $\Omega_{fl}$  through (3.20). To compute this quantity also the derivatives of the elements of  $\mathbb{M}$  with respect to  $\mu$  are needed. To simplify the notation in the following calculations this sort of derivatives will be indicated by the subscript  $\mu$ , e.g.  $U_\mu \equiv \partial U / \partial \mu$ .

With the additional substitution  $i\Omega_m \rightarrow z$  the derivatives read

$$\frac{\partial M_{1,1}(\mathbf{q}, z)}{\partial \mu} = W_\mu + C_\mu q^2 - \tilde{D}_\mu z - Q_\mu z^2 = U_\mu + A_\mu + C_\mu q^2 - \tilde{D}_\mu z - Q_\mu z^2, \quad (3.22)$$

$$\frac{\partial M_{1,2}(\mathbf{q}, z)}{\partial \mu} = U_\mu - 2E_\mu q^2 + R_\mu z^2. \quad (3.23)$$

On the other hand, for the matrix elements, the simplification  $U = W$  discussed in the previous section can be exploited:

$$M_{1,1}(\mathbf{q}, z) = U + \frac{C}{2m} q^2 - \tilde{D}z - Qz^2, \quad M_{1,2}(\mathbf{q}, z) = U - |\Delta|^2 \left( \frac{E}{m} q^2 + Rz^2 \right). \quad (3.24)$$

Taking the derivative of (3.21) the fluctuation contribution to the density yields:

$$n_{fl} = -\frac{1}{4\pi^2} \frac{1}{\beta} \sum_{m=-\infty}^{\infty} \int_0^\infty q^2 dq J(\mathbf{q}, i\Omega_m) \quad (3.25)$$

where the function  $J(\mathbf{q}, z)$  is defined as

$$J(\mathbf{q}, z) \equiv \frac{1}{\Gamma(\mathbf{q}, z)} \left[ M_{1,1}(\mathbf{q}, -z) \frac{\partial M_{1,1}(\mathbf{q}, z)}{\partial \mu} + \frac{\partial M_{1,1}(\mathbf{q}, -z)}{\partial \mu} M_{1,1}(\mathbf{q}, z) + \right. \\ \left. - 2M_{1,2}(\mathbf{q}, -z) \frac{\partial M_{1,2}(\mathbf{q}, z)}{\partial \mu} \right] \quad (3.26)$$

When expanding the numerator of (3.26) in powers of  $(q, z)$ , only the terms consistent with the long-wavelength approximation at the basis of the EFT must be kept. These terms are those up to the second order in powers of  $q$  and to first order in powers of  $z$ . This last condition is set because  $z$  is proportional to  $\omega_{\mathbf{q}}$  which, for large values of the momentum  $q$  is in turn proportional to  $q^2$  (as can be easily verified by expanding (3.17) in powers of  $q$  for  $q \rightarrow \infty$ ). Due to symmetry reasons, the linear terms in  $z$  do not give contributions to the summation over  $m$ , therefore the numerator of  $J(\mathbf{q}, z)$  (3.26) can be rewritten in terms of the EFT coefficients as

$$UA_\mu + \left[ C(U_\mu + A_\mu) + C_\mu U + 2(EU_\mu + E_\mu U) + \right. \\ \left. - v_s^2 \left( \tilde{D}\tilde{D}_\mu + Q(U_\mu + A_\mu) + U(Q_\mu + R_\mu) + RU_\mu \right) \right] q^2. \quad (3.27)$$

To simplify the notation, the terms are distinguished in function of their dependence on  $q$  and on the sound velocity  $c_s$ : by introducing the coefficients

$$\alpha_1 = UA_\mu, \quad (3.28a)$$

$$\alpha_2 = CA_\mu + U(C_\mu + 2|\Delta|^2 E_\mu) + (C + 2|\Delta|^2 E)U_\mu, \quad (3.28b)$$

$$\alpha_3 = \tilde{D}\tilde{D}_\mu + (Q + |\Delta|^2 R)U_\mu + U(Q_\mu + |\Delta|^2 R_\mu) + QA_\mu, \quad (3.28c)$$

formula (3.27) can be rewritten as:

$$\alpha_1 + (\alpha_2 - c_s^2 \alpha_3) q^2. \quad (3.29)$$

In the same way the denominator of (3.26),  $\Gamma(\mathbf{q}, z)$ , is expanded about the poles in  $z = \pm\omega_{\mathbf{q}}$ , where  $\omega_{\mathbf{q}}$  is the pair excitation frequency (3.17). The result is:

$$\Gamma(\mathbf{q}, z) \approx - \left( \tilde{D}^2 + 2U(Q + |\Delta|^2 R) \right) (z^2 - \omega_{\mathbf{q}}^2).$$

Thus the fluctuation contribution to the density becomes:

$$\begin{aligned} n_{fl} &= \frac{1}{\beta} \sum_{m=-\infty}^{\infty} \frac{1}{2\pi^2} \int_0^{\infty} q^2 dq \frac{\alpha_1 + (\alpha_2 - c_s^2 \alpha_3) q^2}{\tilde{D}^2 + 2U(Q + |\Delta|^2 R)} \frac{1}{(i\Omega_m)^2 - \omega_{\mathbf{q}}^2} = \\ &= \frac{1}{\beta} \sum_{m=-\infty}^{\infty} \frac{1}{4\pi^2} \int_0^{\infty} q^2 dq \frac{\alpha_1 + (\alpha_2 - c_s^2 \alpha_3) q^2}{\tilde{D}^2 + 2U(Q + |\Delta|^2 R)} \frac{1}{\omega_{\mathbf{q}}} \left( \frac{1}{i\Omega_m - \omega_{\mathbf{q}}} - \frac{1}{i\Omega_m + \omega_{\mathbf{q}}} \right). \end{aligned}$$

This expression can be further simplified by using the symmetry  $m \leftrightarrow -m$ : for a generic function  $f$  the equality

$$\sum_{m=-\infty}^{\infty} [f(i\Omega_m) + f(-i\Omega_m)] = 2 \sum_{m=-\infty}^{\infty} f(i\Omega_m)$$

holds, therefore the quantity  $n_{fl}$  can be again simplified and reads

$$n_{fl} = \frac{1}{\beta} \sum_{m=-\infty}^{\infty} \frac{1}{2\pi^2} \int_0^{\infty} q^2 dq \frac{\alpha_1 + (\alpha_2 - c_s^2 \alpha_3) q^2}{\tilde{D}^2 + 2U(Q + |\Delta|^2 R)} \frac{1}{\omega_{\mathbf{q}}} \left( \frac{1}{i\Omega_m - \omega_{\mathbf{q}}} \right).$$

The Matsubara sum over the bosonic frequencies  $\Omega_m$  is performed by transforming it into a contour integration in the standard way [68, 91], i.e.

$$\frac{1}{\beta} \sum_{m=-\infty}^{\infty} f(i\Omega_m) = \frac{1}{\pi} \int_{-\infty}^{\infty} d\omega \frac{\text{Im} f(\omega + i\delta)}{e^{\beta\omega} - 1}, \quad \delta \rightarrow +0 \quad (3.30)$$

Therefore the final result for the fluctuation contribution to the density is

$$n_{fl} = - \frac{1}{2\pi^2} \frac{1}{\tilde{D}^2 + 2U(Q + |\Delta|^2 R)} \int_0^{\infty} q^2 dq \frac{1}{\omega_{\mathbf{q}}} \frac{\alpha_1 + (\alpha_2 - c_s^2 \alpha_3) q^2}{e^{\beta\omega_{\mathbf{q}}} - 1}, \quad (3.31)$$

or, restoring the explicit dependence on the EFT coefficients,

$$\begin{aligned} n_{fl} &= - \frac{1}{2\pi^2} \frac{1}{\tilde{D}^2 + 2U(Q + R)} \int_0^{\infty} q^2 dq \frac{1}{\omega_{\mathbf{q}}} \frac{1}{e^{\beta\omega_{\mathbf{q}}} - 1} \\ &\times \left\{ U \frac{\partial A}{\partial \mu} + \left[ \frac{\partial}{\partial \mu} (WC + 2UE) - \frac{c_s^2}{2} \frac{\partial}{\partial \mu} \left( \tilde{D}^2 + 2(WQ + U|\Delta|^2 R) \right) \right] q^2 \right\}. \quad (3.32) \end{aligned}$$

### 3.2.2 Results for the critical temperature

The coupled solution of the gap equation and of the number equation (3.20) with the fluctuation correction to the density  $n_{fl}$  given by (3.32) enables us to evaluate the critical temperature  $T_c$  at which pairing occurs.

The behaviour of this quantity is analysed in Fig. 3.4 as a function of the interaction parameter  $(k_F a_s)^{-1}$  across the BEC-BCS crossover. The EFT results are compared to the predictions of the mean-field theory, as well as to those of the NSR treatment in two different implementations, by Perali *et al.* [84], and by Sá de Melo *et al.* [46] respectively. It appears clear that the mean-field calculations give quantitatively good results only limited to the BCS regime and increasingly overestimate  $T_c$  going towards the BEC side of the resonance. The other three approaches all agree in the BEC limiting case, but show sizable differences in the intermediate interaction range and in the BCS limit where the transition temperature determined in the implementation of the NSR scheme by Sá de Melo appears to be lower than in the other approaches. On the other hand at unitarity and in the near-BEC regime the predictions the present EFT and of Sá de Melo's NSR theory remain close to each other while the NSR treatment by Perali predicts a higher  $T_c$ .

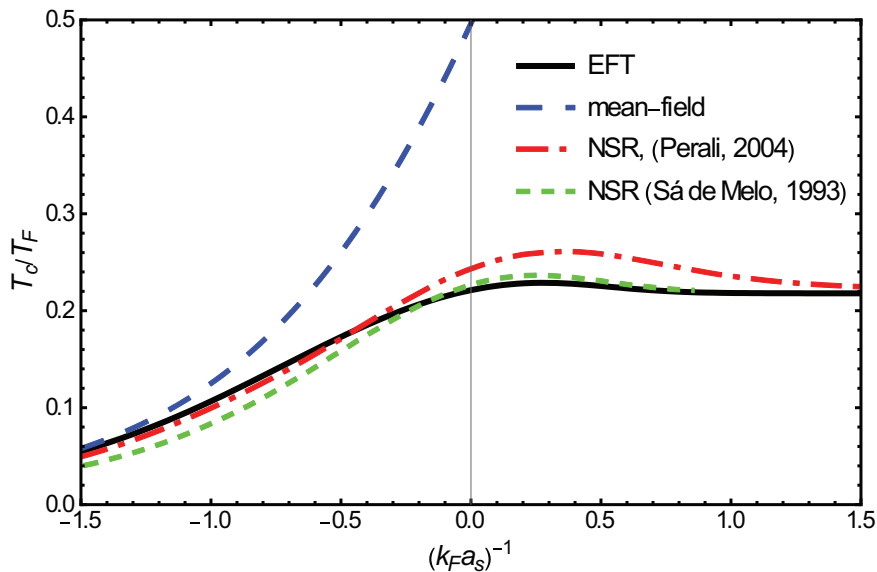


Figure 3.4: Critical temperature (in units of the Fermi temperature  $T_F$ ) as a function of the interaction parameter  $(k_F a_s)^{-1}$  across the BEC-BCS crossover. The predictions of the effective field theory developed in this work (full black line) are compared to the results of the mean-field theory (blue dashed line), the implementation of the NSR scheme by Perali *et al.* [84] (red dot-dashed line) and the implementation of the NSR scheme by Sá de Melo *et al.* [46] (green fine-dashed line).

### 3.3 Correlation functions: condensate density and correlation length

The present section is dedicated to the calculation of two relevant quantities in the description of a fermionic superfluid:

- the condensate fraction, which gives a measure of the number of particles that take part in the pairing mechanism;
- the pair correlation length, that is an estimate of the characteristic size of the Cooper pairs forming the fermionic condensate.

Both these quantities can be calculated in terms of correlation functions: in the following we will show how fermionic correlation functions of all orders can be obtained with the use of a generating functional.

The calculations exploited in this section are at mean-field level: the expressions obtained will then be used in Chapter 4 where a simple model to study the polaronic effects produced by an impurity in a Fermi superfluid is developed. The corrections to these correlation functions due to beyond-mean-field effects are outside the scope of the present work, but many studies can be found in literature, e.g. in [92] for the condensate density and in [93,94] for the pair correlation length.

#### 3.3.1 Generating functional

The generating functional necessary to calculate the fermionic correlation functions can be obtained by modifying the partition sum (2.3) with the inclusion of sinks and sources  $\bar{\lambda}$ , and  $\lambda$ :

$$\tilde{Z}[\bar{\lambda}, \lambda] = \int \mathcal{D}\bar{\psi} \int \mathcal{D}\psi e^{-\tilde{S}[\bar{\psi}, \psi; \bar{\lambda}, \lambda]}, \quad (3.33)$$

where the extended action  $\tilde{S}$  is defined as

$$\begin{aligned} \tilde{S} = & \int_0^\beta d\tau \int d\mathbf{r} \sum_{\sigma=\uparrow, \downarrow} \bar{\psi}_\sigma(\mathbf{r}, \tau) \left( \frac{\partial}{\partial \tau} - \nabla_{\mathbf{r}}^2 - \mu_\sigma \right) \psi_\sigma(\mathbf{r}, \tau) \\ & + g \int_0^\beta d\tau \int d\mathbf{r} \bar{\psi}_\uparrow(\mathbf{r}, \tau) \bar{\psi}_\downarrow(\mathbf{r}, \tau) \psi_\downarrow(\mathbf{r}, \tau) \psi_\uparrow(\mathbf{r}, \tau) \\ & - \int_0^\beta d\tau \int d\mathbf{r} [\bar{\lambda}_\uparrow(\mathbf{r}, \tau) \psi_\uparrow(\mathbf{r}, \tau) + \bar{\psi}_\uparrow(\mathbf{r}, \tau) \lambda_\uparrow(\mathbf{r}, \tau) \\ & - \bar{\lambda}_\downarrow(\mathbf{r}, \tau) \psi_\downarrow(\mathbf{r}, \tau) - \bar{\psi}_\downarrow(\mathbf{r}, \tau) \lambda_\downarrow(\mathbf{r}, \tau)]. \end{aligned} \quad (3.34)$$

Since the starting action was an even function of fermionic Grassmann variables, to insure consistency and preserve the symmetry properties, also the sources  $\lambda_\downarrow(\mathbf{r}, \tau)$ ,  $\lambda_\uparrow(\mathbf{r}, \tau)$ ,  $\bar{\lambda}_\uparrow(\mathbf{r}, \tau)$ , and  $\bar{\lambda}_\downarrow(\mathbf{r}, \tau)$  must be grassmanian symbols.

The generating functional is defined in terms of the normal and extended partition sums as the normalised expression

$$P[\bar{\lambda}, \lambda] = \frac{\tilde{Z}[\bar{\lambda}, \lambda]}{Z}, \quad (3.35)$$

which becomes unity when all the sources are switched off, i.e. when all  $\{\bar{\lambda}, \lambda\}$  are equal to zero. The explicit form for  $P[\bar{\lambda}, \lambda]$  is:

$$P[\bar{\lambda}, \lambda] = \left\langle \exp \left[ \int_0^\beta d\tau \int d\mathbf{r} \left[ \bar{\lambda}_\uparrow(\mathbf{r}, \tau) \psi_\uparrow(\mathbf{r}, \tau) + \bar{\psi}_\uparrow(\mathbf{r}, \tau) \lambda_\uparrow(\mathbf{r}, \tau) - \bar{\lambda}_\downarrow(\mathbf{r}, \tau) \psi_\downarrow(\mathbf{r}, \tau) - \bar{\psi}_\downarrow(\mathbf{r}, \tau) \lambda_\downarrow(\mathbf{r}, \tau) \right] \right] \right\rangle. \quad (3.36)$$

In the last expression the symbols  $\langle \dots \rangle$  indicate an average taken in terms of the normal fermionic action  $S$ . In the remainder of this section we will show how the generating functional can be instead expressed in terms of an average taken with respect to the effective field action derived in Chapter 2.

In order to have a simpler notation, further on, we drop the arguments  $(\mathbf{r}, \tau)$  of the fields appearing in the action. As a consequence the expressions for the quantities  $\tilde{S}$  and  $P[\bar{\lambda}, \lambda]$  in the compact notation read

$$\begin{aligned} \tilde{S} &= \int_0^\beta d\tau \int d\mathbf{r} \sum_{\sigma=\uparrow, \downarrow} \bar{\psi}_\sigma \left( \frac{\partial}{\partial \tau} - \nabla_{\mathbf{r}}^2 - \mu_\sigma \right) \psi_\sigma \\ &+ g \int_0^\beta d\tau \int d\mathbf{r} \bar{\psi}_\uparrow \bar{\psi}_\downarrow \psi_\downarrow \psi_\uparrow - \int_0^\beta d\tau \int d\mathbf{r} (\bar{\lambda}_\uparrow \psi_\uparrow + \bar{\psi}_\uparrow \lambda_\uparrow - \bar{\lambda}_\downarrow \psi_\downarrow - \bar{\psi}_\downarrow \lambda_\downarrow), \end{aligned} \quad (3.37)$$

and

$$P[\bar{\lambda}, \lambda] = \left\langle \exp \left[ \int_0^\beta d\tau \int d\mathbf{r} (\bar{\lambda}_\uparrow \psi_\uparrow + \bar{\psi}_\uparrow \lambda_\uparrow - \bar{\lambda}_\downarrow \psi_\downarrow - \bar{\psi}_\downarrow \lambda_\downarrow) \right] \right\rangle \quad (3.38)$$

respectively.

Performing the Hubbard-Stratonovich transformation on the original action produces the same results obtained in the derivation carried out in Chapter 2 and the extended action can be written as:

$$\begin{aligned} \tilde{S} &= \int_0^\beta d\tau \int d\mathbf{r} \sum_{\sigma=\uparrow, \downarrow} \bar{\psi}_\sigma \left( \frac{\partial}{\partial \tau} - \nabla_{\mathbf{r}}^2 - \mu_\sigma \right) \psi_\sigma \\ &+ \int_0^\beta d\tau \int d\mathbf{r} (\Phi^* \psi_\uparrow \psi_\downarrow + \Phi \bar{\psi}_\downarrow \bar{\psi}_\uparrow) \\ &- \int_0^\beta d\tau \int d\mathbf{r} \frac{1}{g} \Phi^* \Phi + \delta S[\bar{\lambda}, \lambda]. \end{aligned} \quad (3.39)$$

This extended HS action differs from the HS action (2.8) just by the presence of the terms involving the sources  $\bar{\lambda}$ , and  $\lambda$ , i.e.

$$\delta S[\bar{\lambda}, \lambda] = - \int_0^\beta d\tau \int d\mathbf{r} (\bar{\lambda}_\uparrow \psi_\uparrow + \bar{\psi}_\uparrow \lambda_\uparrow - \bar{\lambda}_\downarrow \psi_\downarrow - \bar{\psi}_\downarrow \lambda_\downarrow). \quad (3.40)$$

Reintroducing the fermionic Nambu spinors  $\bar{\Psi}$  and  $\Psi$  (2.7), together with the additional spinors involving the sources

$$\Lambda \equiv \begin{pmatrix} \lambda_{\uparrow} \\ \bar{\lambda}_{\downarrow} \end{pmatrix}, \quad \bar{\Lambda} \equiv (\bar{\lambda}_{\uparrow}, \lambda_{\downarrow}),$$

in matrix notation, the extended action becomes:

$$\tilde{S} = - \int_0^{\beta} d\tau \int d\mathbf{r} \left[ \bar{\Psi} [\mathbb{G}^{-1}(\mathbf{r}, \tau)] \Psi - (\bar{\Psi}\Lambda + \bar{\Lambda}\Psi) - \frac{1}{g}\Phi^*\Phi \right], \quad (3.41)$$

where the inverse fermion propagator  $\mathbb{G}^{-1}(\mathbf{r}, \tau)$  already encountered in (2.9) was introduced. The action written in this way still poses the problem of the integration of the fermionic variables, which is complicated by the presence of the terms in  $\bar{\Lambda}$  and  $\Lambda$ . This issue can be solved by performing a shift of the fermionic variables and by requiring that the terms that couple the sources to the fermionic fields, i.e. the terms involving products of the form  $\bar{\lambda}_{\uparrow}\psi_{\uparrow}$ ,  $\bar{\psi}_{\uparrow}\lambda_{\uparrow}$ ,  $\bar{\lambda}_{\downarrow}\psi_{\downarrow}$ ,  $\bar{\psi}_{\downarrow}\lambda_{\downarrow}$ , must vanish. The result of this shift is

$$\tilde{S} \rightarrow \tilde{S}' = - \int_0^{\beta} d\tau \int d\mathbf{r} \left[ \bar{\Psi}' [\mathbb{G}^{-1}(\mathbf{r}, \tau)] \Psi' - \frac{1}{g}\Phi^*\Phi - \bar{\Lambda}\mathbb{G}\Lambda \right]. \quad (3.42)$$

where  $\bar{\Psi}'$  and  $\Psi'$  represent the new shifted fermionic Nambu spinors. Since the shift of the fermionic variables does not affect the result of the integration in the partition sum, from now on the primes can (and will) be safely dropped. The new action  $S'$  is related to the action  $S$  (2.8) through

$$\tilde{S}' = S + \delta S [\bar{\lambda}, \lambda], \quad (3.43)$$

where the term  $\delta S [\bar{\lambda}, \lambda]$  is defined as

$$\delta S [\bar{\lambda}, \lambda] = - \int_0^{\beta} d\tau \int d\mathbf{r} \int_0^{\beta} d\tau' \int d\mathbf{r}' \bar{\Lambda}(\mathbf{r}', \tau') \mathbb{G}(\mathbf{r}', \tau' | \mathbf{r}, \tau) \Lambda(\mathbf{r}, \tau) \quad (3.44)$$

As intended, the source term  $\delta S$  does not depend on the original fermionic fields  $\bar{\Psi}$  and  $\Psi$  anymore but only on the pair field  $\Phi^*, \Phi$ . The sources were thus successfully decoupled from the fermionic part of the action.

The fermionic part of the action is now exactly equal to the one treated in detail in Chapter 2 and can be therefore replaced by the EFT action (2.118). Hence the generating functional can be expressed as an average with respect to the effective bosonic action rather than to the fermionic one. The resulting form for  $P [\bar{\lambda}, \lambda]$  is

$$\begin{aligned} P [\bar{\lambda}, \lambda] &= \left\langle e^{-\delta S [\bar{\lambda}, \lambda]} \right\rangle_{S_{EFT}} = \left\langle e^{\int_0^{\beta} d\tau \int d\mathbf{r} \bar{\Lambda}\mathbb{G}\Lambda} \right\rangle_{S_{EFT}} \\ &= \left\langle \exp \left[ \int_0^{\beta} d\tau \int d\mathbf{r} \int_0^{\beta} d\tau' \int d\mathbf{r}' \bar{\Lambda}(\mathbf{r}', \tau') \mathbb{G}(\mathbf{r}', \tau' | \mathbf{r}, \tau) \Lambda(\mathbf{r}, \tau) \right] \right\rangle_{S_{EFT}}. \end{aligned} \quad (3.45)$$

This functional allows to determine any correlation function of the fermion variables at any order through the calculation functional derivatives of the generating functional with respect to the sources  $\hat{\lambda}$  and  $\lambda$  followed by the limit  $\hat{\lambda} \rightarrow 0$  and  $\lambda \rightarrow 0$ . For example in the present chapter we will focus on the determination of the correlation functions that provide the condensate density and the pair correlation length which are given by

$$\langle \psi_{\uparrow}(\mathbf{r}, \tau) \psi_{\downarrow}(\mathbf{r}', \tau) \rangle = - \frac{\delta}{\delta \bar{\lambda}_{\uparrow}(\mathbf{r}, \tau)} P[\bar{\lambda}, \lambda] \frac{\delta}{\delta \bar{\lambda}_{\downarrow}(\mathbf{r}', \tau')} \Big|_{\bar{\lambda}, \lambda=0}, \quad (3.46)$$

and

$$\begin{aligned} & \left\langle \hat{\psi}_{\uparrow}(\mathbf{r}, \tau) \hat{\psi}_{\downarrow}(\mathbf{r}', \tau) \psi_{\downarrow}(\mathbf{r}', \tau) \psi_{\uparrow}(\mathbf{r}, \tau) \right\rangle = \\ & = \frac{\delta}{\delta \lambda_{\downarrow}(\mathbf{r}', \tau)} \frac{\delta}{\delta \lambda_{\uparrow}(\mathbf{r}, \tau)} P[\bar{\lambda}, \lambda] \frac{\delta}{\delta \bar{\lambda}_{\uparrow}(\mathbf{r}, \tau)} \frac{\delta}{\delta \bar{\lambda}_{\downarrow}(\mathbf{r}', \tau')} \Big|_{\bar{\lambda}, \lambda=0}. \end{aligned} \quad (3.47)$$

### 3.3.2 Condensate fraction

Inserting the explicit expression (3.45) of the generating functional in terms of the EFT action into the definition of the condensate density (3.46), we obtain the relation between the fermion and boson average:

$$\langle \psi_{\uparrow}(\mathbf{r}, \tau) \psi_{\downarrow}(\mathbf{r}', \tau) \rangle = - \langle \mathbb{G}_{12}(\mathbf{r}, \tau | \mathbf{r}', \tau) \rangle_{SEFT}, \quad (3.48)$$

where  $\mathbb{G}_{12}$  indicates the  $\{1, 2\}$  element of the matrix representation of the fermionic Green's function (2.9) encountered in Chapter 2. It is important to remark that the last expression is independent of the sources  $\bar{\lambda}, \lambda$ . This is a consequence of the procedure for calculating averages described at the end of the previous section which requires that, after the functional derivatives with respect to the sources  $\bar{\lambda}, \lambda$ , these must be set equal to 0. The expression for the condensate density is [68, 95]:

$$n_c = \frac{1}{V} \int d\mathbf{r} \int d\mathbf{r}' |\langle \mathbb{G}_{12}(\mathbf{r}, \tau | \mathbf{r}', \tau) \rangle_{EFT}|^2. \quad (3.49)$$

In order to obtain a closed form for  $n_c$  is now convenient to move to Fourier representation: this can be done by again following the derivation of Chapter 2. The Fourier representation of  $\mathbb{G}_{12}(\mathbf{r}, \tau | \mathbf{r}', \tau)$ , is given by

$$\mathbb{G}_{12}(\mathbf{r}, \tau | \mathbf{r}', \tau') = \frac{1}{\beta V} \sum_{\mathbf{k}', n'} \sum_{\mathbf{k}, n} \mathbb{G}_{12}(\mathbf{k}, n | \mathbf{k}', n') e^{-i\mathbf{k}' \cdot \mathbf{r}' + i\omega_{n'} \tau'} e^{i\mathbf{k} \cdot \mathbf{r} - i\omega_n \tau} \quad (3.50)$$

In turn formula (3.49) becomes

$$\begin{aligned}
n_c &= \frac{1}{\beta^2 V^3} \int d\mathbf{r} \int d\mathbf{r}' \sum_{\mathbf{k}', n'} \sum_{\mathbf{k}, n} \langle \mathbb{G}_{12}(\mathbf{k}, n | \mathbf{k}', n') \rangle_{SEFT} e^{-i\mathbf{k}' \cdot \mathbf{r}' + i\omega_{n'} \tau} e^{i\mathbf{k} \cdot \mathbf{r} - i\omega_n \tau} \\
&\quad \times \sum_{\mathbf{k}'_1, n'_1} \sum_{\mathbf{k}_1, n_1} \langle \mathbb{G}_{12}^*(\mathbf{k}_1, n_1 | \mathbf{k}'_1, n'_1) \rangle_{SEFT} e^{i\mathbf{k}'_1 \cdot \mathbf{r}' - i\omega_{n'_1} \tau} e^{-i\mathbf{k}_1 \cdot \mathbf{r} + i\omega_{n_1} \tau} \\
&= \frac{1}{V \beta^2} \sum_{\mathbf{k}', n'} \sum_{\mathbf{k}, n} \sum_{n'_1} \sum_{n_1} \langle G_{12}(\mathbf{k}, n | \mathbf{k}', n') \rangle_{Seff} \langle G_{12}^*(\mathbf{k}, n_1 | \mathbf{k}', n'_1) \rangle_{Seff} \\
&\quad \times e^{-i(\omega_n + \omega_{n'_1} - \omega_{n_1} - \omega_{n'}) \tau}.
\end{aligned}$$

Since the system under consideration is stationary, the condensate fraction  $n_c$  must be independent on time, therefore we can set

$$n + n'_1 - n' - n_1 = 0 \quad \implies \quad n - n' = n_1 - n'_1.$$

and the expression for the condensate density is simplified. Renaming the indices by setting  $m \equiv n - n' = n_1 - n'_1$ , we obtain

$$n_c = \frac{1}{V \beta^2} \sum_{\mathbf{q}, m} \sum_{\mathbf{k}, n, n'} \langle G_{12}(\mathbf{k}, n | \mathbf{k} + \mathbf{q}, n + m) \rangle_{SEFT} \langle G_{12}^*(\mathbf{k}, n' | \mathbf{k} + \mathbf{q}, n' + m) \rangle_{SEFT} \quad (3.51)$$

The last necessary step to calculate the saddle-point expression for the condensate density is to recall the saddle-point form of the inverse fermion propagator, which is given by

$$\mathbb{G}_{sp}^{-1}(\mathbf{k}, n | \mathbf{k}', n') = \delta_{n', n} \delta_{\mathbf{k}', \mathbf{k}} \begin{pmatrix} i\omega_n - \xi_{\mathbf{k}} + \zeta & -\Delta \\ -\Delta & i\omega_n + \xi_{\mathbf{k}} + \zeta \end{pmatrix}, \quad (3.52)$$

The fermionic Green's function can be obtained by simply inverting the previous matrix, and reads

$$\mathbb{G}_{sp}(\mathbf{k}, n | \mathbf{k}', n') = -\delta_{n', n} \delta_{\mathbf{k}', \mathbf{k}} \begin{pmatrix} \frac{i\omega_n + \xi_{\mathbf{k}} + \zeta}{(\omega_n - i\zeta)^2 + \xi_{\mathbf{k}}^2 + \Delta^2} & \frac{\Delta}{(\omega_n - i\zeta)^2 + \xi_{\mathbf{k}}^2 + \Delta^2} \\ \frac{\Delta}{(\omega_n - i\zeta)^2 + \xi_{\mathbf{k}}^2 + \Delta^2} & \frac{i\omega_n - \xi_{\mathbf{k}} + \zeta}{(\omega_n - i\zeta)^2 + \xi_{\mathbf{k}}^2 + \Delta^2} \end{pmatrix} \quad (3.53)$$

Hence the condensate density at saddle-point level can be written, in terms of the Matsubara frequency  $\omega_n$ , as

$$n_c^{(sp)} = \Delta^2 \int \frac{d\mathbf{k}}{(2\pi)^3} \left( \frac{1}{\beta} \sum_n \frac{1}{(\omega_n - i\zeta)^2 + E_{\mathbf{k}}^2} \right)^2.$$

The computation of the Matsubara sum yields the final expression for  $n_c$ , i.e.:

$$\begin{aligned}
n_c^{(sp)} &= \Delta^2 \int \frac{d\mathbf{k}}{(2\pi)^3} \frac{1}{4E_{\mathbf{k}}^2} \left( \frac{\sinh(\beta E_{\mathbf{k}})}{\cosh(\beta E_{\mathbf{k}}) + \cosh(\beta \zeta)} \right)^2 = \\
&= \frac{\Delta^2}{2\pi^2} \int_0^\infty k^2 dk [f_1(\beta, E_{\mathbf{k}}, \zeta)]^2
\end{aligned} \quad (3.54)$$

which coincides with the well known result found in literature [92, 95].

The condensate fraction  $\nu_c$  is defined as the ratio between (twice) the condensate density and the total density, i.e.

$$\nu_c \equiv 2n_c/n. \quad (3.55)$$

The factor 2 in the definition has been added to normalise the condensate fraction to 1. As discussed in reference to the solution of the number equation, we consider the total density  $n$  to be normalised to the value  $n = 1/(3\pi^2)$ , therefore the condensate fraction is given by

$$\nu_c^{(sp)} = \frac{3}{2}\Delta^2 \int_0^\infty k^2 dk [f_1(\beta, E_{\mathbf{k}}, \zeta)]^2 \quad (3.56)$$

Figure 3.5 shows the behaviour of  $\nu_c$  in different temperature conditions across the BEC-BCS crossover. As expected, in the extreme BEC limit the fraction approaches 1, i.e. all the particles of the system are paired and the tightly bound bosonic molecules that they form are all condensed. While the value of  $\nu_c$  in the BEC regime is weakly affected by temperature, the presence of unpaired particles due to finite temperature, reduces the number of atoms that participate to the pairing in other regimes. In particular it can be observed that at higher temperatures the condensate fraction on the BCS side of the resonance is completely suppressed: this is due to the fact that at finite temperatures no superfluid order can be achieved in said interaction region.

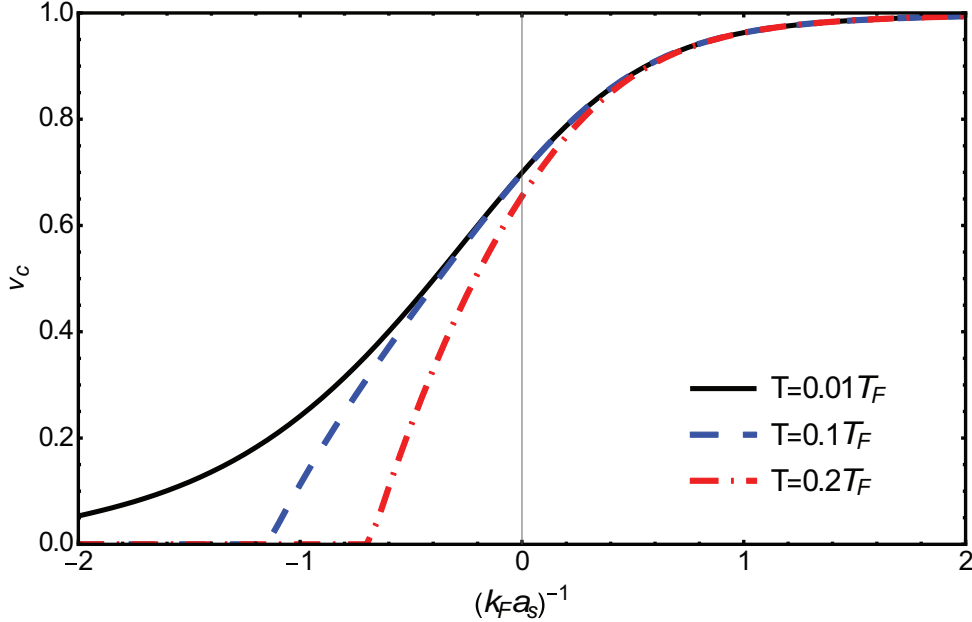


Figure 3.5: Saddle-point condensate fraction across the BEC-BCS crossover at different temperatures:  $T = 0.01T_F$  (full black line),  $T = 0.1T_F$  (blue dashed line), and  $T = 0.2T_F$  (red dot-dashed line).

### 3.3.3 Pair correlation length

The pair correlation length represents an estimate of the typical size of a Cooper pair. In this section we will proceed to its calculation by employing the generating functional method described at an earlier stage in this chapter. Following the theoretical description given in [93,94] the pair correlation length is determined in terms of the correlation function

$$g_{\uparrow\downarrow}(\mathbf{r}) = \left\langle \bar{\psi}_{\uparrow}\left(\mathbf{R} + \frac{\mathbf{r}}{2}\right) \bar{\psi}_{\downarrow}\left(\mathbf{R} - \frac{\mathbf{r}}{2}\right) \psi_{\downarrow}\left(\mathbf{R} - \frac{\mathbf{r}}{2}\right) \psi_{\uparrow}\left(\mathbf{R} + \frac{\mathbf{r}}{2}\right) \right\rangle - \left(\frac{n}{2}\right)^2, \quad (3.57)$$

(where  $n$  is the fermionic density), as

$$\xi_{pair} = \left( \frac{\int d\mathbf{r} \mathbf{r}^2 g_{\uparrow\downarrow}(\mathbf{r})}{\int d\mathbf{r} g_{\uparrow\downarrow}(\mathbf{r})} \right)^{1/2}. \quad (3.58)$$

In expression (3.57) the space dependence is described by separating the center of mass coordinate  $\mathbf{R}$  and the relative coordinate  $\mathbf{r}$ . It is demonstrated [93] that at the mean-field level the pair correlation function  $g_{\uparrow\downarrow}$  can be factorised as a product of single particle averages as

$$\begin{aligned} g_{\uparrow\downarrow}^{(sp)}(\mathbf{r}) &= \left\langle \psi_{\downarrow}\left(\mathbf{R} - \frac{\mathbf{r}}{2}\right) \psi_{\uparrow}\left(\mathbf{R} + \frac{\mathbf{r}}{2}\right) \right\rangle \left\langle \bar{\psi}_{\uparrow}\left(\mathbf{R} + \frac{\mathbf{r}}{2}\right) \bar{\psi}_{\downarrow}\left(\mathbf{R} - \frac{\mathbf{r}}{2}\right) \right\rangle = \\ &= \left| \left\langle \psi_{\downarrow}\left(\mathbf{R} - \frac{\mathbf{r}}{2}\right) \psi_{\uparrow}\left(\mathbf{R} + \frac{\mathbf{r}}{2}\right) \right\rangle \right|^2. \end{aligned} \quad (3.59)$$

Since the system under consideration is uniform, this quantity must be independent of the center of mass coordinate  $\mathbf{R}$ , therefore the previous expression can be further simplified to give

$$g_{\uparrow\downarrow}^{(sp)}(\mathbf{r}) = \left| \left\langle \psi_{\downarrow}\left(-\frac{\mathbf{r}}{2}\right) \psi_{\uparrow}\left(\frac{\mathbf{r}}{2}\right) \right\rangle \right|^2. \quad (3.60)$$

Following the procedure outlined in the previous section, it is convenient to write the expressions at the numerator and at the denominator of (3.58) in reciprocal space notation. It is straightforward to observe that the expression at the denominator coincides exactly with the one of the condensate density  $n_c$  (3.54). For what concerns the numerator we have

$$\begin{aligned} \int d\mathbf{r} \mathbf{r}^2 g_{\uparrow\downarrow}(\mathbf{r}) &= \Delta^2 \int \frac{d\mathbf{k}}{(2\pi)^3} \left( \nabla_{\mathbf{k}} \frac{1}{2E_{\mathbf{k}}} \frac{\sinh(\beta E_{\mathbf{k}})}{\cosh(\beta E_{\mathbf{k}}) + \cosh(\beta\zeta)} \right)^2 \\ &= \Delta^2 \int \frac{d\mathbf{k}}{(2\pi)^3} [\nabla_{\mathbf{k}} f_1(\beta, E_{\mathbf{k}}, \zeta)]^2. \end{aligned} \quad (3.61)$$

Remembering the recursive relation (2.78) that relates the functions  $f_s(\beta, E_{\mathbf{k}}, \zeta)$  with different indices  $s$ , the last line can be again simplified and becomes

$$\Delta^2 \int \frac{d\mathbf{k}}{(2\pi)^3} [\nabla_{\mathbf{k}} f_1(\beta, E_{\mathbf{k}}, \zeta)]^2 = \Delta^2 \int \frac{d\mathbf{k}}{(2\pi)^3} [-4\mathbf{k} \cdot \xi_{\mathbf{k}} f_2(\beta, E_{\mathbf{k}}, \zeta)]^2$$

Exploiting the spherical symmetry of the system the final expression for the mean-field pair correlation length finally reads

$$\xi_{pair} = \left( \frac{\int_0^\infty k^2 dk [4k \xi_k f_2(\beta, E_k, \zeta)]^2}{\int_0^\infty k^2 dk [f_1(\beta, E_k, \zeta)]^2} \right)^{1/2}. \quad (3.62)$$

The pair correlation length will be used in the following section to test the reliability of the predictions of the EFT. From the comparison between  $\xi_{pair}$ , which measures the typical size of the Cooper pairs, and the width of the solitons examined in that context, the region of validity of the EFT can be identified. The theory presented in this thesis is based on the hypothesis that the order parameter varies slowly in both time and space: it can therefore be assumed that the analysis is valid when the characteristic length scale of object under consideration (in this case the soliton) is larger than the size of the Cooper pairs.

Figure 3.6 depicts the dependence of  $\xi_{pair}$  on the interaction parameter  $(k_F a_s)^{-1}$  across the BEC-BCS crossover. As was the case for the condensate fraction, the effect of temperature is negligible in the BEC limit, but becomes more substantial at unitarity and in the BCS regime. In particular the size of the Cooper pairs is reduced as the temperature increases. The two data sets relative to higher temperatures in the figure do not span the entire interaction regime because in those temperature conditions the superfluid order parameter drops to zero for large negative values of  $(k_F a_s)^{-1}$ .

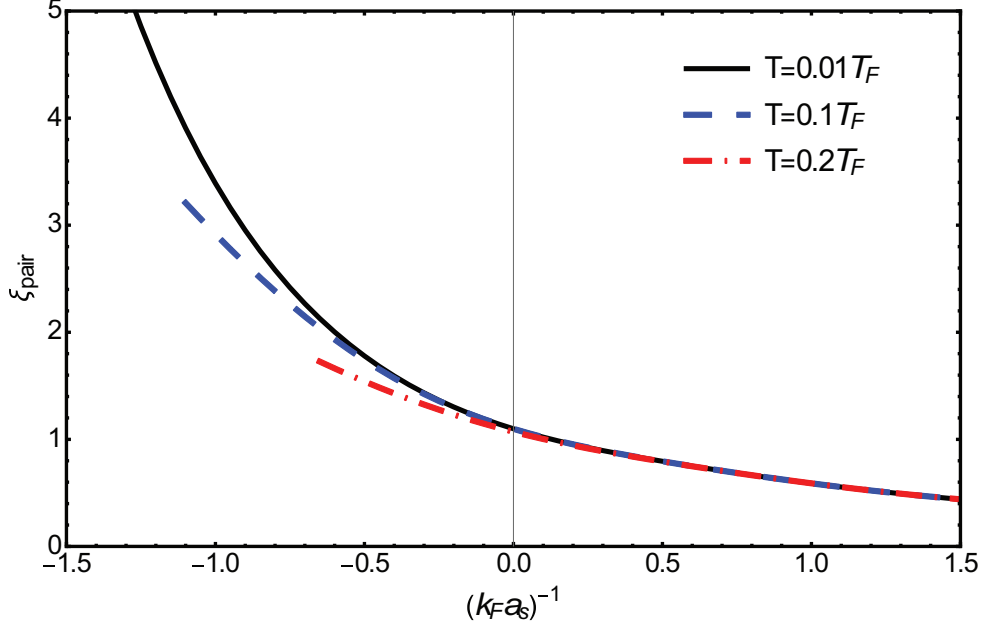


Figure 3.6: Saddle-point pair correlation length across the BEC-BCS crossover at different temperatures:  $T = 0.01T_F$  (full black line),  $T = 0.1T_F$  (blue dashed line), and  $T = 0.2T_F$  (red dot-dashed line).

### 3.4 Validity range of the EFT

In this section the correlation functions calculated in the previous section will be employed in order to obtain an indirect determination of the validity domain of the effective field theory derived in the present work. To do so we are going to anticipate some results about the shape of dark solitons in Fermi superfluid that will be discussed in full detail in Chapter 5.

In Chapter 2 it was repeatedly highlighted that one of the cornerstones on which the effective field theory presented in this thesis is built is the assumption that the order parameter changes slowly in both time and space, corresponding to a long-wavelength approximation. In order to verify the validity of this hypothesis we consider the system consisting of a dark soliton in a uniform fermionic superfluid. This appears as dip in the density profile of the condensate with width and depth determined by the conditions of temperature, imbalance, and interaction, i.e. by the combination of parameters  $\{\beta, \zeta, (k_F a_s)^{-1}\}$ . A detailed analysis of the dependence of the soliton properties on these three parameters will be carried out in the following chapter.

One way to indirectly verify the slow variation hypothesis at the basis of the EFT is to compare the characteristic length scale for the uniform system, i.e. the typical size  $\xi_{pair}$  of the Cooper pairs, to the characteristic length relative to the particular phenomenon that is being examined, i.e. the soliton width. The soliton width is closely related to the phase coherence length or healing length. According to this reasoning the region of validity of the EFT can be therefore identified as the region of the  $\{\beta, \zeta, (k_F a_s)^{-1}\}$ -space for which the size of the soliton is much larger than  $\xi_{pair}$ . As already mentioned, the typical size of the Cooper pairs can be estimate by calculating the correlation length  $\xi_{pair}$  (often referred to as Pippard length [91]). This quantity was studied in detail in Section 3.3 by using a generating functional to calculate the necessary four-fermion correlation function. Here we report just its expression obtained in the context of the present EFT, which reads:

$$\xi_{pair} = \sqrt{\frac{\int dk k^2 (4k \xi_k f_2(\beta, E_{\mathbf{k}}, \zeta))^2}{\int dk k^2 (f_1(\beta, E_{\mathbf{k}}, \zeta))^2}}. \quad (3.63)$$

To describe the characteristic size of the soliton two different estimates are considered (and compared): in addition to the width at half height of the soliton dip  $\xi_n$  (that will represent the main measure of the width in the analysis of Chapter 5), here also the phase coherence length  $\xi_{phase}$  will be studied. In the case of a black soliton (with velocity  $v_S = 0$ ),  $\xi_{phase}$  is determined by making an ansatz on the shape of the spatial profile of the order parameter: employing as a trial function for the amplitude modulation of the form

$$\Phi(x) = \Phi_{\infty} a(x), \quad a(x) = \tanh\left(\frac{x}{\sqrt{2}\xi_{var}}\right), \quad (3.64)$$

the free energy of the system is then minimised with respect to the variational parameter  $\xi_{var}$ . As discussed in [93] a rescaling coefficient is needed in order to connect the variational parameter  $\xi_{var}$  to the healing length  $\xi_{phase}$ . To this purpose, the convention of rescaling

$\xi_{var}$  to the value of  $\xi_{phase}$  at  $T = 0$  in the BCS limit was adopted, obtaining the relation  $\xi_{phase} = 1.175 \xi_{var}$ .

Fig.3.7 shows the comparison between the characteristic size of the soliton and of the Cooper pairs as a function of the interaction parameter  $(k_F a_s)^{-1}$  across the BEC-BCS crossover. The two plots are relative to two different temperature regimes: in particular, the left panel focuses on the situation in which the temperature is much lower than the critical temperature ( $T/T_c = 0.1$ ), while the right panel considers the ‘‘Ginzburg-Landau’’ typical regime where the temperature is close to  $T_c$ , i.e.  $T/T_c = 0.95$ . In the high temperature situation (Fig.3.7(right panel)) it emerges that the soliton width remains substantially larger than the Cooper pair size in the entire interaction regime, thus guaranteeing a good degree of reliability for the EFT. On the other hand, in the low temperature configuration (Fig. 3.7(left panel)) the same conclusion remains true only on the BEC side of the resonance. When moving towards unitarity and further on towards the BCS regime the soliton width approaches more and more closely the pair correlation length until the two quantities become practically equal. Another observation that must be made is that the two different evaluations of the soliton size, i.e.  $\xi_{phase}$  and  $\xi_n$  are in extremely good agreement in both the BEC and the BCS limit, but a difference can be seen when considering intermediate interaction regimes: such a discrepancy can be explained by considering the ansatz (3.64) on the form of the trial function used to determine  $\xi_{phase}$ . In fact, while in both the BEC [96, 97] and BCS [98] limits the amplitude modulation of the soliton is expected to be modeled by a hyperbolic tangent, the same is not in general true at unitarity and in the intermediate regimes. To have a more comprehensive picture of the domain of validity of the effective field theory presented in this thesis, in Fig.3.8 the ratio between the pair correlation length  $\xi_{pair}$  and the healing length  $\xi_{phase}$  is plotted as a function of both the temperature (normalised to the critical temperature) and the interaction parameter  $(k_F a_s)^{-1}$ . The color runs from a lighter, to a darker shade as the ratio  $\xi_{pair}/\xi_{phase}$  decreases. Therefore the region of reliability of the EFT can be identified with the dark blue/purple region of the contour plot. The result is consistent with what discussed before: the EFT proves to be fully reliable at high enough temperatures, but, as the temperature decreases, its validity is not guaranteed on the BCS side of the resonance.

In order to understand the effect of population imbalance on the validity range of the EFT, in Fig. 3.9 the ratio  $\xi_{pair}/\xi_{phase}$  is plotted as a function of the imbalance parameter  $\zeta$  and again of temperature (this time normalised to the Fermi temperature). The imbalance does not affect substantially the ratio between the two length scales in the vast majority of the configuration. Only in a small region of the  $\{\zeta, T/T_F\}$  space a non monotonic behaviour is observed. This feature is a consequence of the nature of the dependence of the order parameter on imbalance (see for reference the inset of figure 5.10 in Chapter 5): the modulus of the order parameter as a function of  $\zeta$  varies slowly in the entire domain of values of imbalance until a critical value  $\zeta^{(crit)}$  is closely approached. Only at that point the field  $\Phi$  shows a sudden change as it abruptly drops to zero.

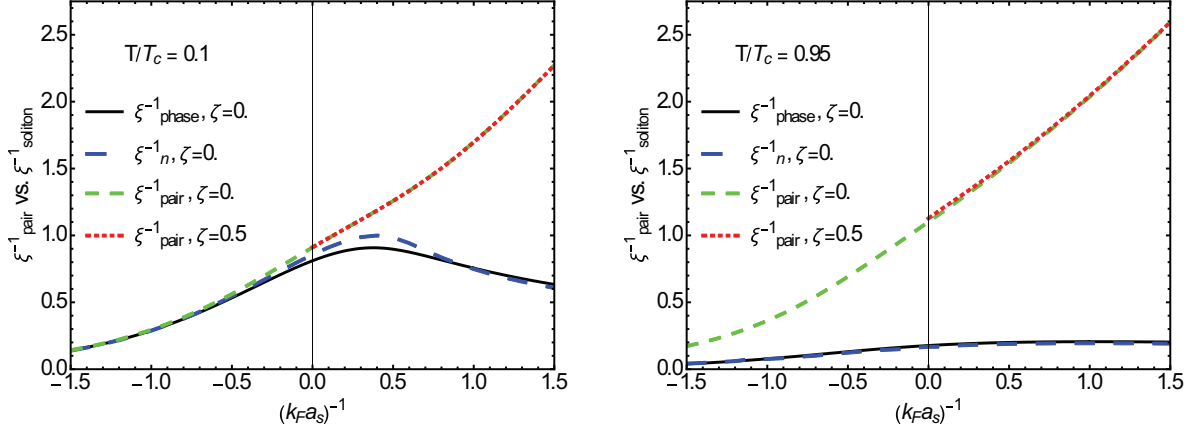


Figure 3.7: (left panel) Comparison between inverse pair correlation length and inverse soliton width (in units of  $k_F$ ) across the BEC-BCS crossover for  $T/T_c = 0.1$ . The full black line represents the inverse healing length without imbalance. The dashed blue line describes the inverse soliton width. The dashed green line represents the inverse pair correlation length. The dotted red line represents the inverse pair correlation length with imbalance  $\zeta = 0.5E_F$ . (right panel) Comparison between inverse pair correlation length and inverse soliton width across the BEC-BCS crossover for  $T/T_c = 0.95$ : the dashing/color code is the same as for (a).

## 3.5 Comparison with other theoretical approaches

### 3.5.1 BEC limit

The goal of this subsection is to demonstrate that the EFT naturally retrieves the results predicted by the Gross-Pitaevskii equation in the BEC limit, when the fermion pairs become tightly bound bosonic dimers. To begin with, it is important to notice that the terms with second order time derivatives, i.e. those involving coefficients  $Q$  and  $R$ , do not have a counterpart in the Gross-Pitaevskii equation. For the moment they will be therefore ignored: later this simplification will be justified by demonstrating that such terms become negligible in the BEC limit. In order to obtain the equation of motion that governs the real-time dynamics of the system, the simplified version ( $Q = 0$ ,  $R = 0$ ) of the effective field action (2.118) must be converted from Euclidean- to real-time notation. This is done by exploiting the formal replacement

$$\tau \rightarrow it, \quad S(\beta) \rightarrow iS(t_a, t_b).$$

The real-time action is given in terms of the real-time Lagrangian density  $\mathcal{L}$  by

$$S(t_a, t_b) = \int_{t_a}^{t_b} dt \int d\mathbf{r} \mathcal{L},$$

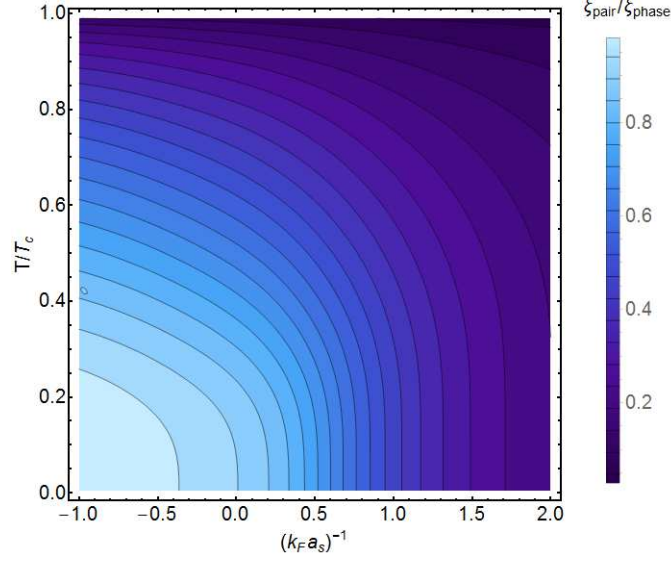


Figure 3.8: Contour plot depicting the behaviour of the ratio  $\xi_{pair}/\xi_{phase}$  between the pair correlation length and the variationally determined healing length as a function of the inverse scattering length  $a_s$  and the temperature. The values of the scattering length span the entire BEC-BCS crossover, while the temperature range goes from 0 to the critical temperature  $T_c$ .

where  $\mathcal{L}$  is defined as

$$\mathcal{L} = \frac{i}{2} D \left( \frac{\partial \Phi^*}{\partial t} \Phi - \Phi^* \frac{\partial \Phi}{\partial t} \right) + \Omega_s + \frac{C}{2m} |\nabla_r \Phi|^2 - \frac{E}{2m} (\nabla_r |\Phi|^2)^2.$$

The equation of motion can be therefore simply obtained from the Euler-Lagrange equations

$$\frac{\partial \mathcal{L}}{\partial \Phi} - \frac{\partial}{\partial t} \frac{\partial \mathcal{L}}{\partial (\partial_t \Phi)} = 0,$$

and is found to read

$$i \tilde{D} \frac{\partial \Phi}{\partial t} = -\frac{C}{2m} \nabla_r^2 \Phi + \left( A + \frac{E}{m} \nabla_r^2 |\Phi|^2 \right) \Phi. \quad (3.65)$$

The additional coefficients  $A$  and  $\tilde{D}$  appearing in the previous expression are the modified EFT coefficient already encountered in (3.8). To cast the equation of motion (3.65) into a form that more closely resembles the Gross-Pitaevskii equation it is convenient to divide both sides of the equality by  $\tilde{D}$ : this leads to

$$i \frac{\partial \Phi}{\partial t} = -\frac{C}{2m \tilde{D}} \nabla_r^2 \Phi + \left( \frac{A}{\tilde{D}} + \frac{E}{m \tilde{D}} \nabla_r^2 |\Phi|^2 \right) \Phi.$$

The first term in the left hand side of the last equation, i.e. the kinetic term, has the same form of the kinetic term in the GP equation, but with a prefactor given by the ratio  $C/\tilde{D}$ .

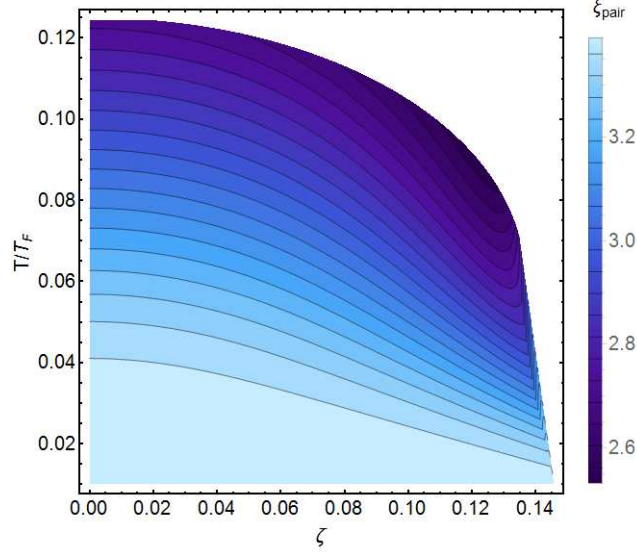


Figure 3.9: Dependence of the pair correlation length on the imbalance parameter  $\zeta$  and temperature  $T$  at  $(k_F a_s)^{-1} = -1$  on the BCS side of the resonance. The non-monotonic behaviour of  $\xi_{pair}(\zeta)$  is apparent. Lengths are in units of  $k_F^{-1}$  and  $\zeta$  is in units of  $E_F$ .

From Fig.3.10(a) it appears that this ratio tends to 1/2 in the BEC limit, suggesting that this term now describes the kinetic energy of a particle of mass  $M = 2m$ . On the other hand, panel (b) of Fig.3.10 shows how the term proportional to the EFT coefficient  $E$  becomes less and less relevant as the interaction becomes stronger.

The last term that needs to be taken into consideration is  $(A/\tilde{D})\Phi$ . This needs to reproduce the nonlinear term of the GP equation which reads  $U|\Phi|^2\Phi$ , where  $U$  represents the coupling constant for the boson-boson interaction. The expansion of the thermodynamic potential  $\Omega_s$  in powers of the order parameter can be written as

$$\Omega_s(|\Phi|^2) = \Omega(0) + a|\Phi|^2 + \frac{1}{2}b|\Phi|^4 + \dots \quad (3.66)$$

From the definition of  $A$  (3.8) we can deduce the equality

$$A = a + b|\Phi|^2 + \dots$$

and, in turn, the coefficients  $a$  and  $b$  can be written in terms of  $A$  as

$$a = A|_{|\Phi|=0} \quad b = \left. \frac{\partial A(|\Phi|^2)}{\partial |\Phi|^2} \right|_{|\Phi|=0}$$

As discussed in [1] the coefficients  $a$  and  $b$  obtained in such way exactly reproduce those obtained in the time-dependent Ginzburg-Landau treatment by Sà de Melo *et al.* in [46]. In the same paper it is demonstrated how, in the strong coupling BEC limit, the contribution

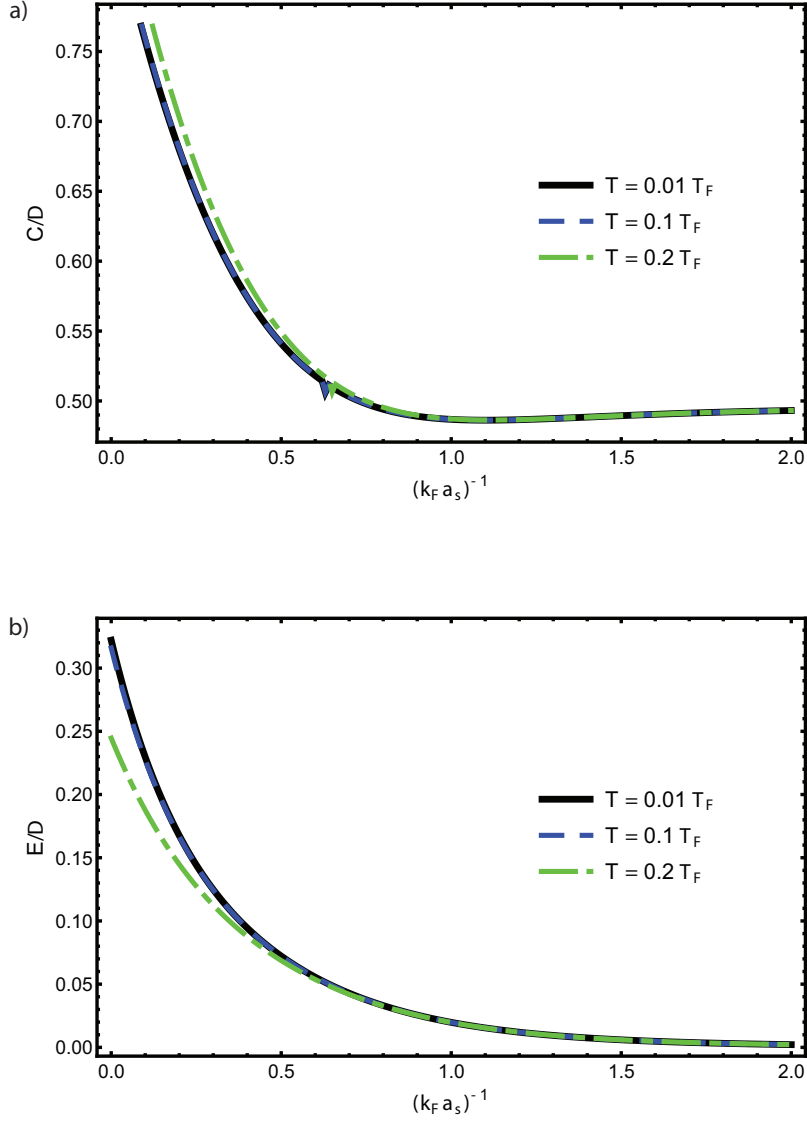


Figure 3.10: The ratios  $C/\tilde{D}$  and  $E/\tilde{D}$  are displayed in function of the interaction parameter  $(k_F a_s)^{-1}$  for three different values of the temperature. The ratio  $C/\tilde{D}$  tends to the value  $1/2$  thus reproducing the numerical prefactor of the kinetic term for a boson of mass  $M = 2m$ . The quantity  $E/\tilde{D}$  tends instead to 0 as the coupling becomes stronger.

$(a|\Phi|^2 + \frac{1}{2}b|\Phi|^4)/d$  correctly tends to the nonlinear term  $U|\Phi|^2\Phi$ , with

$$U = \frac{8\pi k_F a_s}{2m} = \frac{4\pi k_F a_B}{M}$$

i.e. the interaction strength for a boson of mass  $M$  and effective s-wave boson-boson scattering length  $a_B = 2a_F$ . The same procedure leads to the same conclusion in the context of the present effective field theory.

In light of this discussion we can conclude that, in the BEC limit (and for values of  $|\Phi|$  small enough that  $\Omega_s$  is well approximated by its expansion up to quartic order (3.66)), the EFT equation of motion (3.65) reduces to the Gross-Pitaevskii equation for composite bosons of mass  $M = 2m$  that interact through a *s-wave* contact potential described by the scattering length  $a_B = 2a_F$ .

At the beginning of the present subsection the terms with time derivatives of order (or power) higher than one were neglected. The complete equation of motion accounting for the presence of these contributions is given in [1]: later in the thesis it will be made clear that the coefficients of terms with second order derivatives can be considered constants and equal to their value in the uniform system configuration. This simplification leads us to understand that the coefficient ratios which weight the contributions coming from the extra terms in the equation of motion are  $Q/\tilde{D}$  and  $R/\tilde{D}$ . The two panels of Fig.3.11 confirm the validity of the hypothesis that the terms of the EFT action (2.118) proportional to  $Q$  and  $R$  can be neglected in the deep BEC limit.

### 3.5.2 EFT vs. time-dependent Ginzburg-Landau theory

At the start of Chapter 2 it was stated that the present effective field theory is inspired by the Ginzburg-Landau approach. This assertion is true in the sense that both theories describe the system of ultracold fermions in terms of a macroscopic wavefunction (identified with the order parameter), and – from a mathematical point of view – follow a similar path in the treatment of the corrections to the mean-field theory. Moreover the analysis of Fig. 3.8 indicates that at unitarity and in the BCS regime the reliability range of the EFT reduces to the vicinity of  $T_c$  similarly to the GL treatment. In this section we show that a more careful comparison between the two approaches leads to the revelation of a crucial difference.

As mentioned in the previous subsection the coefficients  $a$  and  $b$  of the quadratic and quartic terms (in  $|\Phi|$ ) of the time-dependent Ginzburg-Landau theory developed in [46] can be exactly reproduced in the context of the present effective field theory when the limit of small order parameter i.e  $|\Phi| \rightarrow 0$  is taken. While the same is true for the coefficient  $c$  of the kinetic term, a particular attention must be given to the coefficient  $d$  of the term involving the first-order time derivative. The counterpart of  $d$  in the present EFT is  $\tilde{D}$  but, even in the small- $|\Phi|$  limit, these two coefficients remain substantially different. On the one hand  $\tilde{D}$  is always real across the entire interaction domain; on the other hand, from the definition of  $d$  in [46], it is immediately clear that this coefficient has a non-zero imaginary part. In particular the imaginary part of  $d$  is dominant in the weak coupling BCS side of the Feshbach resonance, meaning that the dynamics of  $\Phi$  in this regime is essentially damped. When the coupling becomes stronger, in the BEC regime,  $\text{Im}(d)$  tends to 0, and, in the small- $\Phi$  limit,  $\text{Re}(d) \rightarrow \tilde{D}$ , so the dynamics of  $\Phi$  is propagative and the analogy between EFT, TDGL, and Gross-Pitaevskii theory is restored. It is worth mentioning that the behaviour of the imaginary part of the coefficient  $d$  predicted in [46] was retrieved also by Machida and Toyama [62] who independently derived a time-dependent Ginzburg-Landau treatment for fermionic gases in the BEC-BCS crossover starting from the fermion-boson

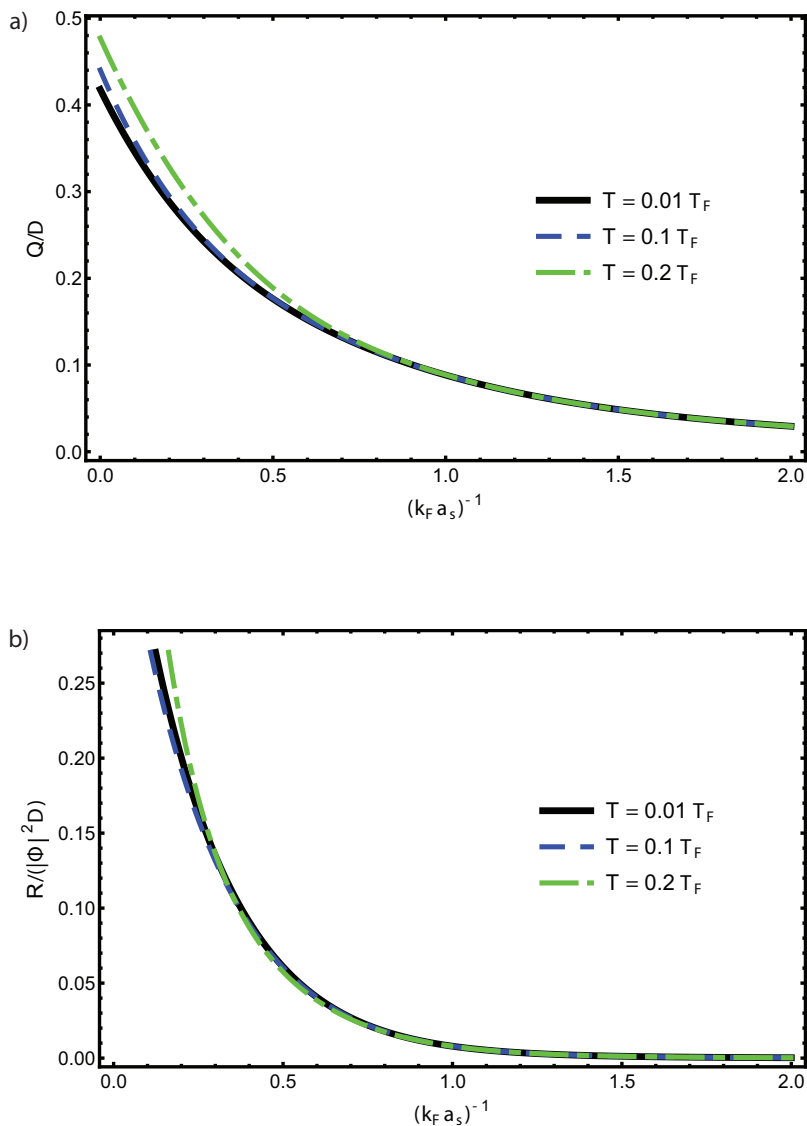


Figure 3.11: The ratios  $Q/\tilde{D}$  and  $R/\tilde{D}$  are displayed in function of the interaction parameter  $(k_F a_s)^{-1}$  for three different values of the temperature. Both quantities tends instead 0 as the coupling becomes stronger.

model.

### 3.5.3 Bogoliubov-de Gennes theory

In Chapter 5 we are often going to compare the EFT predictions with the results available in the literature based on the numerical solution of the Bogoliubov-de Gennes (BdG) equations. These results are expected to be reliable across the BEC-BCS crossover but, on the downside, require a large amount of computation time and memory. For comparison

a calculation that can take a whole day following the BdG approach can be reduced to minutes if performed in the framework of an effective field theory [99].

This subsection is therefore devoted to give a brief overview of the BdG theory. In the mean field approximation, following the derivation of [100], the BCS Hamiltonian for a balanced system in absence of external confinement can be written as:

$$\begin{aligned} \hat{H}_{BCS} = \sum_{\sigma} \int d\mathbf{r} \hat{\psi}_{\sigma}^{\dagger}(\mathbf{r}) \left( -\frac{\hbar\nabla^2}{2m} - \mu \right) \hat{\psi}_{\sigma}(\mathbf{r}) + \\ - \int d\mathbf{r} \left\{ \Delta(\mathbf{r}) \left[ \hat{\psi}_{\uparrow}^{\dagger}(\mathbf{r}) \hat{\psi}_{\downarrow}^{\dagger}(\mathbf{r}) - \frac{1}{2} \langle \hat{\psi}_{\uparrow}^{\dagger}(\mathbf{r}) \hat{\psi}_{\downarrow}^{\dagger}(\mathbf{r}) \rangle \right] + h.c. \right\} \end{aligned} \quad (3.67)$$

where the term of the form  $\Delta \langle \hat{\psi}_{\uparrow}^{\dagger} \hat{\psi}_{\downarrow}^{\dagger} \rangle$  in the second line is introduced to avoid double counting. The Hamiltonian (3.67) can be diagonalized by performing the Bogoliubov-Valatin transformation on the field operators  $\hat{\psi}_{\sigma}^{\dagger}(\mathbf{r})$  and  $\hat{\psi}_{\sigma}(\mathbf{r})$ , i.e.

$$\hat{\psi}_{\sigma}^{\dagger}(\uparrow) = \sum_n \left[ u_n^*(\mathbf{r}) \hat{\gamma}_{n\uparrow}^{\dagger} + v_n(\mathbf{r}) \hat{\gamma}_{n\downarrow} \right] \quad \hat{\psi}_{\sigma}^{\dagger}(\downarrow) = \sum_n \left[ u_n^*(\mathbf{r}) \hat{\gamma}_{n\downarrow}^{\dagger} + v_n(\mathbf{r}) \hat{\gamma}_{n\uparrow} \right] \quad (3.68)$$

$$\hat{\psi}_{\sigma}(\uparrow) = \sum_n \left[ u_n(\mathbf{r}) \hat{\gamma}_{n\uparrow} + v_n^*(\mathbf{r}) \hat{\gamma}_{n\downarrow}^{\dagger} \right] \quad \hat{\psi}_{\sigma}(\downarrow) = \sum_n \left[ u_n(\mathbf{r}) \hat{\gamma}_{n\downarrow} + v_n^*(\mathbf{r}) \hat{\gamma}_{n\uparrow}^{\dagger} \right]. \quad (3.69)$$

The original fermionic field operators are hence rewritten as linear combinations of the new operators  $\hat{\gamma}_{\sigma}^{\dagger}$  and  $\hat{\gamma}_{\sigma}$ , which should still satisfy the fermionic anticommutation relations

$$\left\{ \hat{\gamma}_{n\sigma}, \hat{\gamma}_{m\sigma'}^{\dagger} \right\} = \delta_{nm} \delta_{\sigma\sigma'} \quad \left\{ \hat{\gamma}_{n\sigma}, \hat{\gamma}_{m\sigma'} \right\} = 0.$$

From the anticommutation relations for  $\hat{\psi}_{\sigma}^{\dagger}(\mathbf{r})$  and  $\hat{\psi}_{\sigma}(\mathbf{r})$  the additional condition

$$\sum_n \left[ u_n^*(\mathbf{r}) u_n(\mathbf{r}') + v_n(\mathbf{r}) v_n^*(\mathbf{r}') \right] = \delta(\mathbf{r} - \mathbf{r}')$$

is obtained.

After the transformations (3.68) and (3.69), the Hamiltonian (3.67) results in

$$\hat{H}_{BCS} = (E_0 - \mu N) + \sum_{n,\sigma} \epsilon_n \hat{\gamma}_{n\sigma}^{\dagger} \hat{\gamma}_{n\sigma} \quad (3.70)$$

The requirement that the operators  $\hat{\gamma}_{\sigma}^{\dagger}$  and  $\hat{\gamma}_{\sigma}$  diagonalize the Hamiltonian (3.67) finally leads to the Bogoliubov-de Gennes equations

$$\begin{pmatrix} -\frac{\hbar\nabla^2}{2m} - \mu & \Delta(\mathbf{r}) \\ \Delta^*(\mathbf{r}) & -\frac{\hbar\nabla^2}{2m} - \mu \end{pmatrix} \begin{pmatrix} u_n(\mathbf{r}) \\ v_n(\mathbf{r}) \end{pmatrix} = \epsilon_n \begin{pmatrix} u_n(\mathbf{r}) \\ v_n(\mathbf{r}) \end{pmatrix} \quad (3.71)$$

which determine the amplitudes  $u_n$  and  $v_n$ . The order parameter  $\Delta(\mathbf{r})$  is in general a complex, position dependent function and is determined by the self-consistency equation

$$\Delta(\mathbf{r}) = -g \langle \hat{\psi}_{\downarrow}(\mathbf{r}) \hat{\psi}_{\uparrow}(\mathbf{r}) \rangle = g \langle \hat{\psi}_{\uparrow}(\mathbf{r}) \hat{\psi}_{\downarrow}(\mathbf{r}) \rangle. \quad (3.72)$$

In conclusion the BdG equations represent an extension of the standard BCS treatment useful to describe non-uniform configurations of a Fermi superfluid such as quantized vortices, or solitons. A comparison between the vortex profiles calculated within the BdG approach [101] and within the EFT presented in this thesis was reported in [1]: in Fig. 3.12 we report the results. Consistently with the discussion about the validity domain of Section 3.4, it emerges that the EFT results agree with those of the BdG approach if the ratio  $T/T_c$  is large or the interaction is tuned towards the BEC regime. A sizable disagreement is found at unitarity and in the BCS regime for low temperatures.

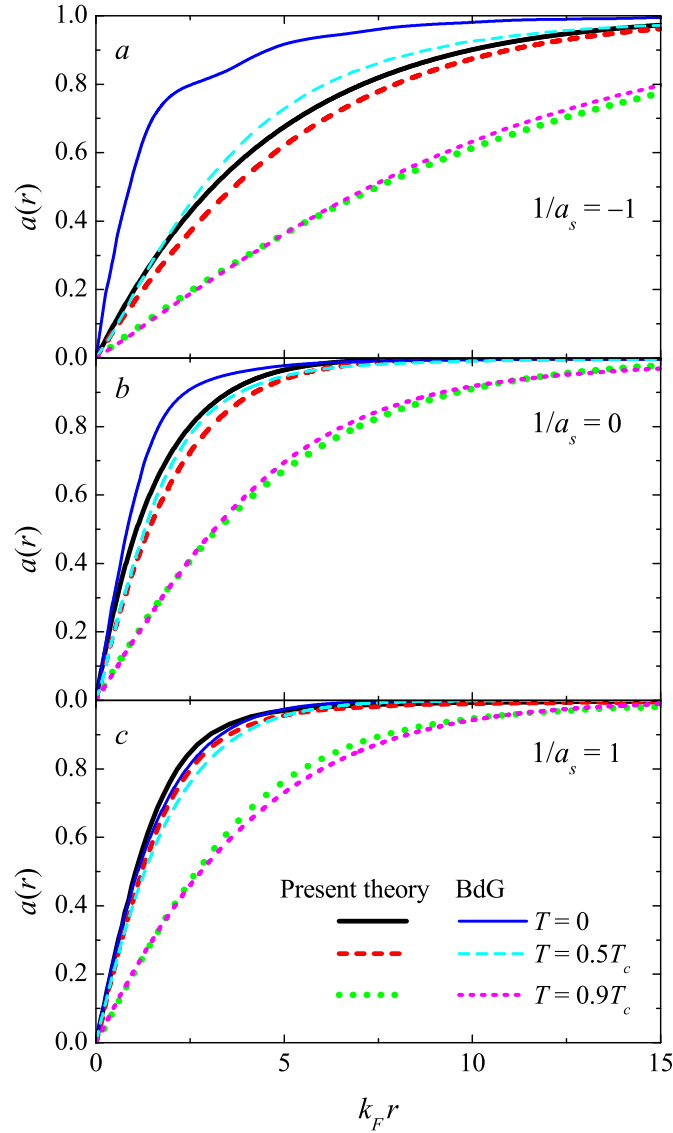


Figure 3.12: Amplitude modulation function of the order parameter  $a(r) = |\Phi(r)|/|\Phi(\infty)|$  for a vortex at different temperatures and scattering lengths. The results of the present EFT (heavy curves) are compared with the BdG data of reference [101] (thin curves).



## Chapter 4

# EFT applied to polarons in Fermi superfluids

The polaron concept was first introduced by Landau [28] as a quasiparticle consisting of an electron and the polarization cloud that it drags along while moving in a polar crystal. Since then, many different physical systems – ranging from solid state to high energy physics – have been mapped on the polaron problem. Among these realisations, one that has been the focus of much attention in the recent years is the BEC polaron, i.e. a quasiparticle arising from the interaction of an impurity with the Bogoliubov excitations of a Bose-Einstein condensate.

The theoretical descriptions of the polaron problem can be classified according to the strength of the impurity-boson interaction for which they are valid. The weak coupling regime has been mostly studied by means of a perturbative treatment first developed by Fröhlich [30] or by a canonical transformation proposed by Lee-Low-Pines [29] based on a suggestion by Tomonaga [50, 102]. For the strong coupling regime the treatments, introduced by Landau and Pekar [31] and by Bogoliubov and Tyablikov [103], are based respectively on the use of a trial localized wavefunction and again on a canonical transformation. In addition an all-coupling theory was developed by Feynman based on the path integral formalism [67], the results of which were more recently reproduced by using the diagrammatic Monte Carlo method [104]. All these treatments were later applied to the case of the BEC polaron – see for example [5, 6] for weak coupling, [7–11] for strong coupling, and [12] for all coupling. In addition, also a renormalisation group study [13] and a Quantum Monte Carlo treatment [14] both applicable to all coupling regimes were developed. In 2015 an experimental setup suitable to investigate the BEC polaron was engineered consisting of Cs neutral impurities coupled to a Rb Bose-Einstein condensate [105]; one year later two groups achieved the experimental realisation of a BEC polaron in a system of  $^{87}\text{Rb}$  with  $^{40}\text{K}$  fermionic impurities [106], and of  $^{39}\text{K}$  with impurities of the same species but in a different hyperfine state [107].

In the context of Fermi gases, polaronic effects are expected in highly imbalanced Fermi gases in the extreme limit of a single down-spin particle coupled to an ideal gas of up-spins; the so called Fermi polaron has been examined both from a theoretical [108–111] and from

an experimental point of view [112, 113]. Recently, a polaron-like problem has also been studied in the context of a fermionic system consisting of three spin populations by using a variational approach [114].

In this section a different version of the polaron problem in a Fermi system is proposed. In particular we consider the interaction of a single impurity atom with the collective excitations of a fermionic superfluid by mapping it on the same Hamiltonian used in the BEC polaron case. This ansatz is in principle valid only in the extreme BEC side of the Feshbach resonance where the main contribution to the physics of the system should come from the Bogoliubov excitations on top of a molecular BEC. In the framework of the effective field theory derived in Chapter 2 this molecular condensate is described by a macroscopic wavefunction. The description in terms of a macroscopic wavefunction remains valid also when moving away from the BEC limit and towards unitarity, provided the coefficients of the field equation are properly adapted. This fact was used in Section 3.1 to calculate the dispersion relation for the Bogoliubov excitations of the superfluid, accounting for the effect of interaction, as the system goes across the BEC-BCS crossover. In turn, this enables us to study how the properties of the BEC polaron change when the underlying condensate no longer consists of pointlike bosons, but of Cooper pairs. The polaron problem is then studied in the weak coupling limit by employing the well known  $T = 0$  perturbative treatment and the behaviour of effective mass and polaronic coupling constant is examined as function of the impurity-boson interaction and of the fermion-fermion interaction in the underlying superfluid. In experiments investigating impurities in Bose Einstein condensates, the polaronic coupling constant can be tuned by acting on the bare boson-boson and boson-impurity scattering lengths. Although methods have been proposed that could boost the polaronic coupling constant and make the strong-coupling regime accessible [105, 115], up to now only the weak coupling situation has been achieved, hence motivating our focus on this interaction regime.

## 4.1 Mapping the fermionic problem on the BEC-polaron problem

The problem of a single impurity in a Bose-Einstein condensate can be described by an Hamiltonian of the form

$$\hat{H} = E_{GP} + g_{IB}N_c + \frac{\hat{p}^2}{2m_I} + \sum_{\mathbf{q}} \hbar\omega_{\mathbf{q}}\hat{\alpha}_{\mathbf{q}}^{\dagger}\hat{\alpha}_{\mathbf{q}} + g_{IB}\sqrt{N_c} \sum_{\mathbf{q}} \sqrt{\frac{\epsilon_{\mathbf{q}}}{\hbar\omega_{\mathbf{q}}}} e^{-i\mathbf{q}\cdot\hat{\mathbf{r}}} \left( \hat{\alpha}_{\mathbf{q}} + \hat{\alpha}_{-\mathbf{q}}^{\dagger} \right) \quad (4.1)$$

where  $E_{GP}$  represents the Gross-Pitaevskii energy of the condensate,  $N_c$  is the number of particles in the condensate,  $\frac{\hat{p}^2}{2m_I}$  is the kinetic energy of the impurity of mass  $m_I$ , and  $\epsilon_{\mathbf{q}} = \frac{\hbar^2\mathbf{q}^2}{2m_B}$  is the dispersion for a free boson of mass  $m_B$ . In the last two terms,  $\alpha_{\mathbf{q}}^{\dagger}$  ( $\alpha_{\mathbf{q}}$ ) and  $\omega_{\mathbf{q}}$  are respectively the creation (annihilation) operators and dispersion relation for the Bogoliubov excitations of the bosonic condensate (that play the role of the phonons in

analogy with the solid state Fröhlich polaron case). The boson-impurity and boson-boson contact interactions are assumed to be  $s$ -wave and are governed respectively by the coupling constants  $g_{IB}$  and  $g_{BB}$  that can be related to the corresponding scattering lengths  $a_{IB}$  and  $a_{BB}$  through the solution of the Lippmann-Schwinger equation. The fermionic superfluid is described by the EFT action (2.118) but, in order to avoid confusion, in the present section the fermion-fermion scattering length will be denoted with  $a_{FF}$  (instead of the usual  $a_S$ ) and the fermion mass with  $m_F$  (instead of the usual  $m$ ).

Superfluid Fermi gases exhibit bosonic collective excitations (turning into the usual Bogoliubov modes in the BEC limit), as well as fermionic excitations (turning into broken Cooper pairs in the BCS limit). However, if one stays away from the BCS limit, the fermionic excitations are strongly gapped and hence suppressed at low temperatures. Therefore we only consider the dressing of the impurity by the bosonic collective excitations. This implies that we do not wander too far away from the BEC regime, and that our results are restricted to temperatures well below the superfluid critical temperature. In this context, the Hamiltonian (4.1) is assumed to remain valid. As mentioned above the goal of this section is to describe the system away from the extreme BEC limit by employing the Hamiltonian (4.1) with a modified dispersion relation for the bosonic excitation modes and with a modified condensate density. Both the dispersion relation and the condensate density now depend on the fermionic interaction strength  $1/a_{FF}$ .

The number of particles in the condensate  $N_c = Vn_c$  in (4.1) is calculated via the appropriate expression for a fermionic system that was derived, at saddle point level, in Section 3.3.

For what concerns the “phonon” dispersion  $\omega_{\mathbf{q}}$ , Section 3.1 the spectrum of collective excitations for an ultracold Fermi gas was calculated up to third order in  $q$ , resulting in the dispersion relation (3.17) that we report here for convenience

$$\hbar\omega_{\mathbf{q}} = \hbar q \sqrt{c_s^2 + \lambda \left( \frac{\hbar q}{2m_F} \right)^2}. \quad (4.2)$$

With the introduction of the interaction-dependent mass for the bosonic excitation  $m_B(\lambda) = m_F/\sqrt{\lambda}$  and the characteristic length  $\xi \equiv \frac{\hbar}{\sqrt{2m_B(\lambda)c_s}}$ , the last expression becomes

$$\hbar\omega_{\mathbf{q}} = \frac{\hbar^2}{2m_B(\lambda)} q \sqrt{q^2 + 2/\xi^2}. \quad (4.3)$$

Thanks to the expressions for  $c_s$  (3.15) and  $\lambda$  (3.16) derived in the early stages of the present chapter in terms of the EFT coefficients, equation (4.3) can describe the dispersion relation for the collective excitations of the Fermi superfluid in different interaction configurations across the BEC-BCS crossover. Before proceeding with the theoretical treatment, the coefficient  $\lambda$  deserves a further remark: as it becomes clear from the definition of  $m_B(\lambda)$ ,  $\lambda$  can be interpreted as a correction to the mass of the collective excitation. Fig. 3.2 shows the behaviour of this quantity across the BEC-BCS crossover for different temperatures: as already mentioned, in the BEC limit the value of  $\lambda$  tends to  $1/4$  thus making the mass

of the bosonic excitation tend to the expected BEC value of  $m_B^{(BEC)} = 2m_F$ . Given this consideration we use the quantity  $m_B(\lambda)$  to define the energy  $\epsilon_{\mathbf{q}}$  (that in the BEC polaron case represented the dispersion for a free boson) as  $\epsilon_{\mathbf{q}} \equiv \frac{\hbar^2 q^2}{2m_B(\lambda)}$ .

Finally it has to be noted that in principle both the boson-boson and impurity-boson scattering lengths  $a_{BB}$  and  $a_{IB}$  could be related to the fermion-fermion scattering length (see for example [83, 116, 117]) but this would require a systematic treatment that lies beyond the scope of the present work. However, these quantities will combine into a dimensionless coupling strength, as a function of which we will study the results of our formalism.

## 4.2 Weak coupling limit for an impurity in a BEC condensate

In order to study the weak coupling regime for the system consisting of an impurity interacting with the collective Bogoliubov excitations of a fermionic superfluid at  $T = 0$  we employ second order perturbation theory [5]. The operator part of the Hamiltonian (4.1) is divided in an unperturbed part

$$\hat{H}_0 = \frac{\hat{p}^2}{2m_I} + \sum_{\mathbf{q}} \hbar\omega_{\mathbf{q}} \hat{\alpha}_{\mathbf{q}}^\dagger \hat{\alpha}_{\mathbf{q}} \quad (4.4)$$

accounting for the kinetic energy of the free impurity and the gas of non-interacting collective excitations, plus a perturbation component

$$\hat{V} = g_{IB} \sqrt{N_c} \sum_{\mathbf{q}} \sqrt{\frac{\epsilon_{\mathbf{q}}}{\hbar\omega_{\mathbf{q}}}} e^{-i\mathbf{q}\cdot\hat{\mathbf{r}}} \left( \hat{\alpha}_{\mathbf{q}} + \hat{\alpha}_{-\mathbf{q}}^\dagger \right). \quad (4.5)$$

We start from an unperturbed state of the form  $|\psi_{\mathbf{k}}\rangle |\emptyset\rangle$  consisting of a free impurity described by a plane-wave eigenfunction  $\psi_{\mathbf{q}} = e^{i\mathbf{k}\cdot\mathbf{r}}/\sqrt{V}$  and the vacuum state for the Bogoliubov excitations of the pair condensate  $|\emptyset\rangle$ , with energy  $E_{\mathbf{k}}^{(0)} = \langle\emptyset| \langle\psi_{\mathbf{k}}| H_0 |\psi_{\mathbf{k}}\rangle |\emptyset\rangle = \frac{\hbar^2 k^2}{2m_I}$ . The first order correction to the energy  $\Delta E_{\mathbf{k}}^{(1)}$  is identically zero while the second order correction  $\Delta E_{\mathbf{k}}^{(2)}$  is

$$\Delta E_{\mathbf{k}}^{(2)} = \sum_{|exc\rangle \neq |\psi_{\mathbf{k}}\rangle |\emptyset\rangle} \frac{\left| \langle exc | \hat{V} |\psi_{\mathbf{k}}\rangle |\emptyset\rangle \right|^2}{E_{\mathbf{k}}^{(0)} - E_{exc}^{(0)}}. \quad (4.6)$$

The only excited states  $|exc\rangle$  contributing to this quantity are those consisting of the free impurity plus a single Bogoliubov excitation, therefore the second order energy correction is

$$\Delta E_{\mathbf{k}}^{(2)} = N_c g_{IB}^2 \sum_{\mathbf{q}} \frac{\sqrt{\frac{q^2}{q^2 + 2/\xi^2}}}{\left[ \frac{\hbar^2 \mathbf{k}\cdot\mathbf{q}}{m_I} - \frac{\hbar^2 q^2}{2m_I} - \frac{\hbar^2}{2m_B} q \sqrt{q^2 + \frac{2}{\xi^2}} \right]}, \quad (4.7)$$

where in the last line we have introduced the expression for the Bogoliubov dispersion  $\omega_{\mathbf{q}}$  in terms of the healing length  $\xi$  given in (4.3). Substituting the sum over momenta  $\mathbf{q}$  with an integral and expanding the integrand in powers of the momentum  $k$  of the impurity leads to

$$\begin{aligned} \Delta E_{\mathbf{k}}^{(2)} = & -N_c \left( g_{IB}^{(0)} \right)^2 \frac{V}{(2\pi)^2} \int_0^\infty dQ 2Q^2 \times \\ & \times \left[ \frac{\sqrt{\frac{Q^2}{Q^2 + \frac{2}{\xi^2}}}}{\frac{\hbar^2 Q^2}{2m_I} + \frac{\hbar^2}{2m_B(\lambda)^2} Q \sqrt{Q^2 + \frac{2}{\xi^2}}} + \left( \frac{\hbar^2 Q K}{2m_I} \right)^2 \frac{\sqrt{\frac{Q^2}{Q^2 + \frac{2}{\xi^2}}}}{3 \left( \frac{\hbar^2 Q^2}{2m_I} + \frac{\hbar^2}{2m_B(\lambda)} Q \sqrt{Q^2 + \frac{2}{\xi^2}} \right)^3} + \dots \right] \end{aligned} \quad (4.8)$$

where the dimensionless variables  $Q$  (and  $K$ ) are defined as  $Q = \xi q$  (and  $K = \xi k$ ). The term constant in  $K$  is divergent for large values of  $Q$ . This divergence is removed by including the regularised form of the boson-impurity coupling constant  $g_{IB}$ .

The solution of the Lippmann-Schwinger equation up to second perturbative order gives

$$g_{IB} = \frac{2\pi\hbar^2 a_{IB}}{V m_R(\lambda)} + \alpha \frac{\epsilon_0}{4\pi} \left( \frac{m_I}{m_R(\lambda)} \right)^2 \int dQ \frac{m_R(\lambda)}{m_I} \quad (4.9)$$

where we have introduced, in analogy with the case of an impurity in a BEC, the modified reduced mass  $m_R(\lambda) = \left( \frac{1}{m_B(\lambda)} + \frac{1}{m_I} \right)^{-1}$ , the energy unit  $\epsilon_0 = \frac{\hbar^2}{m_I \xi^2}$ , and the interaction parameter

$$\alpha = \frac{a_{IB}^2}{a^* \xi} \quad (4.10)$$

The quantity  $a^*$  is defined as  $a^* = 1/(16\pi n_c c_s^2/\epsilon_0^2)$ : in analogy with the BEC polaron case [12] – where the polaronic coupling constant is defined as  $\alpha = a_{IB}^2/(a_{BB}\xi)$  – we expect it to represent a dimensionless coupling parameter expressing the strength of the interaction between the impurity and the bosonic modes of the pair condensate. Substituting (4.9) and (4.10) in the term  $N_c g_{IB}$  of the Hamiltonian provides us with the regularisation necessary to have a converging integral for the energy that now reads

$$\begin{aligned} E_{\mathbf{k}}^{(2)} = & E_{GP} + \frac{2\pi\hbar^2 a_{IB}}{m_R(\lambda)} n_c + \frac{K^2}{2} \epsilon_0 + \\ & + \alpha \frac{\epsilon_0}{4\pi} \left( \frac{m_I}{m_R(\lambda)} \right)^2 \int_0^\infty dQ Q^2 \times \\ & \times \left[ \frac{m_R(\lambda)/m_I}{Q^2} - \frac{\sqrt{\frac{Q^2}{Q^2 + 2}}}{Q^2 + \frac{m_I}{m_B(\lambda)} Q \sqrt{Q^2 + 2}} - K^2 Q^2 \frac{\sqrt{\frac{Q^2}{Q^2 + 2}}}{3 \left( Q^2 + \frac{m_I}{m_B(\lambda)} Q \sqrt{Q^2 + 2} \right)^3} + \dots \right] \end{aligned} \quad (4.11)$$

It is important to notice that the previous expression is consistent with the theoretical predictions for the weak coupling BEC polaron obtained from the all-coupling Feynman treatment: see for reference equation (22) in [12].

### 4.3 Interaction parameter and effective mass of the polaron

As it is clear from (4.11), the dimensionless parameter  $\alpha$  – often referred to as the polaronic coupling constant – is the quantity that determines the magnitude of the perturbative corrections to the energy. Figure 4.1 depicts its dependence on the fermion-fermion interaction parameter  $(k_F a_{FF})^{-1}$  in the BEC-BCS crossover. A monotonic increase is found for  $\alpha$  as the system approaches the BEC side of the Feshbach resonance. Moreover its value at fixed  $(k_F a_{FF})^{-1}$  increases with  $a_{IB}$ . As expected, when the boson-impurity scattering length  $a_{IB}$  is equal to zero  $\alpha$  is also identically zero as the impurity does not interact with the superfluid.

From the expression for the energy (4.11), also the effective mass of the polaron  $m^*$  can be calculated by using the definition

$$\frac{1}{m^*} = \frac{1}{\hbar^2} \left. \frac{\partial^2 (E_{\mathbf{k}}^{(2)})}{\partial k^2} \right|_{k \rightarrow 0} \quad (4.12)$$

Inserting the explicit expression (4.11) for  $E_{\mathbf{k}}^{(2)}$  in the last equation and solving for  $m^*$  we obtain

$$m^* = m_I \left( 1 - \alpha \frac{\epsilon_0}{4\pi} \left( \frac{m_I}{m_R(\lambda)} \right)^2 \int_0^\infty dQ Q^4 \frac{\sqrt{\frac{Q^2}{Q^2+2}}}{3 \left( Q^2 + \frac{m_I}{m_B(\lambda)} Q \sqrt{Q^2+2} \right)^3} \right)^{-1} \quad (4.13)$$

Figure 4.2 shows the behaviour of the ratio between the effective mass of the polaron and the mass of the impurity across the BEC-BCS crossover for fixed values of  $a_{IB}$ . A maximum for the ratio  $m^*/m_I$  is found for small positive values of the interaction parameter  $(k_F a_{FF})^{-1}$ . Similar to the case of the interaction parameter  $\alpha$ , as could be intuitively expected, also the value of the effective mass at fixed fermion-fermion interaction strength increases with the boson-impurity scattering length.

From both Fig.4.1 and Fig.4.2 it appears that a region of major relevance in the domain of values of the interaction parameter is the one around  $(k_F a_{FF})^{-1} \sim 0.4$ . For the polaronic coupling constant  $\alpha$  this is the region where a marked change in the slope of the curves in Fig.4.1 is observed. On the other hand, considering the behaviour of the effective mass, from Fig.4.2 we notice that the maximum of the ratio  $m^*/m_I$  is also localised around this position. The importance of this region of the interaction parameter domain was also pointed out in reference [3] where a peak in the inverse pair coherence length is detected suggesting a direct link between the appearance of particular features in this range of values of  $(k_F a_{FF})^{-1}$  and the intrinsic nature of the system.

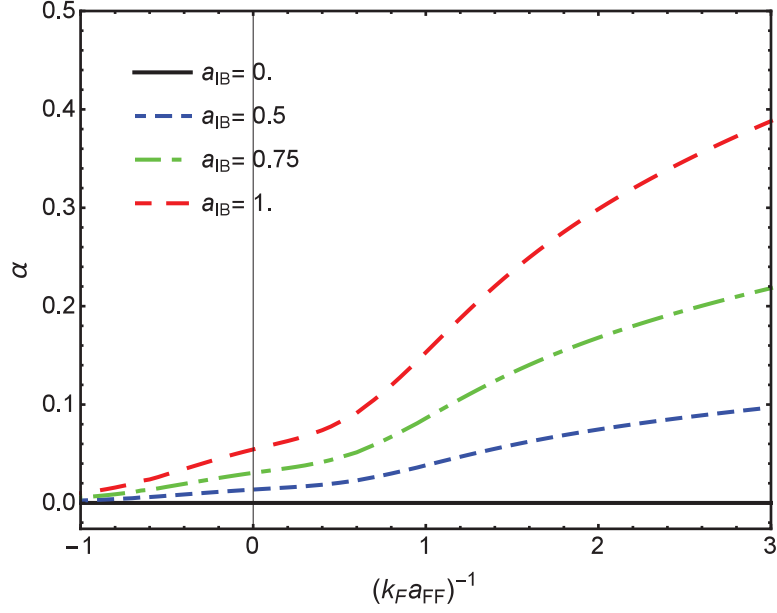


Figure 4.1: Dependence of the dimensionless interaction parameter  $\alpha$  on the fermion-fermion interaction strength  $(k_F a_{FF})^{-1}$  across the BEC-BCS crossover for different values of the boson-impurity scattering length at  $T = 0$

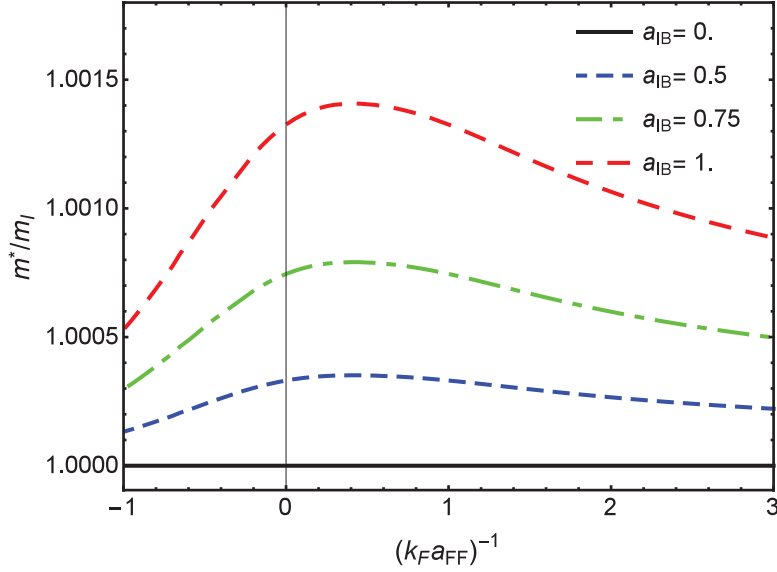


Figure 4.2: Ratio between the effective mass of the polaron and the mass of the impurity as a function of the fermionic interaction parameter  $(k_F a_{FF})^{-1}$  for different values of  $a_{IB}$  at  $T = 0$ .

## 4.4 Discussion and conclusions

In this section we have studied a system composed by a single impurity atom interacting with the collective excitations of a fermionic superfluid by employing the Fröhlich-like

Hamiltonian widely used to study the similar BEC polaron problem and extending its validity – in principle limited to the extreme BEC side of the Feshbach resonance – to a wider region of the BEC-BCS crossover. This was done by employing the  $(k_F a_{FF})^{-1}$ -dependent form of the dispersion relations for the Bogoliubov excitations of the Fermi superfluid obtained in Section 3.1 in the context of the effective field theory derived in Chapter 2. The system was studied in the weak coupling regime in perturbation theory. In order for this kind of treatment to be valid we had to restrict the analysis to the  $T = 0$  situation. However, as discussed in Section 3.4 as well as in [3] in regard to dark solitons, this requirement on the temperature introduces a limitation on the reliability of the EFT away from the BEC limit. Given this consideration we remark that the results at unitarity and in the BCS regime can be seen just as qualitative predictions.

The main focus of this section was the calculation of the effective mass of the polaron and the analysis of how it changes as one moves away from the extreme BEC limit. For a fixed value of the fermion-fermion interaction strength  $(k_F a_{FF})^{-1}$  the effective mass is shown to slightly increase with the impurity-boson scattering length. The behaviour across the BEC-BCS crossover is not monotonic: in particular a broad peak in the value of  $m^*$  is found on the near BEC side of the resonance. In the extreme BEC limit the results of the BEC polaron problem are correctly retrieved. The polaron effective mass has already been successfully measured in experiments on ionic crystals and polar semiconductors [118]. The recently achieved experimental realisation of the BEC polaron [106, 107] opens the door to the possibility of measuring this property also in systems like the one considered in the present work.

Also the variation of the polaronic coupling parameter  $\alpha$  was studied as a function of the fermion-fermion interaction, finding a monotonic increase as the system goes from the BCS towards the BEC regime.

# Chapter 5

## EFT applied to dark solitons in Fermi superfluids

### 5.1 Introduction

The goal of the present chapter is to study the properties of dark solitons in superfluid fermionic systems in the framework of the effective field theory developed in Chapter 2.

Solitons are nonlinear localized excitations that propagate through a medium without changing their shape. They have been studied in an extremely broad range of fields, from fluid dynamics to quantum optics. Starting in the early 2000's, Bose Einstein condensates were added to the list of fields in which solitons can be examined from both a theoretical [96,97] and an experimental [119–122] point of view. The first lab realisation of soliton-like excitations in Fermi systems is even more recent, dating back to 2013; however the theoretical literature investigating this phenomenon is already extended [123–126]. The main technique employed to create dark solitons in experiments with cold gases is called “phase imprinting” [119–122, 127, 128]: after the atomic cloud is cooled and confined, laser light is shone on one half of it thus locally changing the phase of the superfluid order parameter. This results in a phase jump between the two halves of the condensate and, in turn, in the appearance of the desired soliton. In a 3D system this appears as a region (plane) of lower particle density that can be detected with appropriate imaging methods. For what concerns Bose Einstein condensates the most employed technique is absorption imaging after a time-of-flight expansion [119–122]; for fermionic systems in addition a rapid ramp towards the BEC side of the resonance is required during the time-of flight expansion in order to improve the contrast [127, 128].

The stability of solitons in cold atom systems has been widely investigated from a theoretical point of view: for what concerns Bose Einstein condensates it was demonstrated [129–131] that, while solitons in 1D configurations are stable, in higher dimensionalities they are subject to a transverse instability mechanism that drastically limits their lifetime. This decay process is commonly known as snake instability, as it was named for the first time in an article by Zakharov and Rubenchik in 1974 [132]: after the soliton is created

inside the atomic cloud, the depletion plane starts oscillating until it breaks leaving a cascade of decay products behind. Stable solitons in 3D systems were predicted in BECs subject to an external potential [133], and in dipolar BECs [134, 135]; moreover stable Jones-Roberts solitons were recently created by imprinting a triangular phase pattern on a three dimensional BEC [136]. The first experimental observation of the soliton decay in BECs was performed in 2014 [137]. For what concerns fermionic systems theorists have analyzed the snake instability mechanism by employing different methods, e.g. the hydrodynamic approximation, the RPA approach, the numerical solution of the time-dependent Bogoliubov-de Gennes equations [138], and calculations [139] based on a coarse-grained version of the BdG equations introduced in [99]. The experimental observation proved to be more challenging: in particular in the first experiment on dark solitons in Fermi superfluids performed in 2013 at MIT [127], solitary waves were detected and were at first identified as solitons, but their surprisingly high effective mass and long lifetime led to a reinterpretation of the results as solitonic vortices, product of the decay through snake instability of a short lived dark soliton [128]. More recently the cascade of excitations generated by the death of a dark soliton was more precisely described and detected [140]. A way to stabilise the solitonic excitation against this transverse instability is to make the confinement in the directions perpendicular to the propagation very tight, so that the geometry of the system is reduced to a quasi-1D configuration. At a later stage in this work a possible alternative method is discussed which could lead to soliton stabilisation through spin-imbalance, without compromising the 3D nature of the system.

In the first part of the chapter, from Section 5.2 to Section 5.3, the properties of stable dark solitons will be described by analysing the order parameter and density profiles: the main references for this part of the thesis are [3, 70]. Considering excitations moving at constant speed in a quasi-1D geometry it will be shown that the equations of motion for amplitude and phase of the pair field admit an exact analytic solution. This, in turn, gives access to the calculation of the density profile of the atomic cloud, which will be examined in various conditions of temperature and interaction. Spin imbalance and soliton velocity are two additional parameters that can be varied and produce changes in the density profile. In particular, finite temperature and/or a nonzero imbalance prevent a portion of the particles of the system from forming Cooper pairs, and the soliton core is a convenient place where these unpaired particles can be stored.

Finally some of the main dynamic properties of solitons are derived and compared to the data available from literature. In addition the importance of the inclusion of the higher-than-first order time derivatives in the EFT action of the system is discussed.

The second part of the chapter, starting from Section 5.4, is instead dedicated to the description of the snake instability mechanism responsible for dark soliton decay: these results were reported in the manuscript [4]. The stable soliton solution is modified by adding a transverse perturbation, and the spectrum of the instability is obtained. The snake instability is a long wavelength phenomenon, therefore the inverse of the minimum momentum  $k_c$  for which the imaginary part of the perturbation frequency becomes zero, i.e.  $k_c^{-1}$ , can be used to estimate the maximum transverse size of the system necessary to observe a stable wave. This estimate is then compared to the other data available

in literature such as hydrodynamic approximation, RPA, time dependent Bogoliubov-de Gennes simulations, and recent theoretical predictions based on the coarse-grained version of the BdG equations. The EFT results show a reliable behaviour across the entire BEC-BCS crossover, nicely capturing the change in the relevant length scales from the pair coherence length in the BCS regime to the healing length in the BEC limit. Also the presence of imbalance is considered: it is demonstrated that the maximum transverse size for a soliton to be stable is larger in a system with unequal spin populations with respect to a balanced system. This in principle provides experimentalists with a method to stabilise solitons without making the transverse confinement extremely tight and therefore reducing the dimensionality of the system.

Finally Section 5.6 hosts the conclusions of the study carried out in the present chapter together with a brief summary of the results obtained.

## 5.2 Model

In Chapter 2, the effective field theory real-time action  $S_{EFT}$  was derived: the final expression for this quantity was given in (2.118) and reads:

$$S_{EFT} = \int_0^\beta d\tau \int d\mathbf{r} \left[ \frac{1}{2} D \left( \frac{\partial \Phi^*}{\partial \tau} \Phi - \Phi^* \frac{\partial \Phi}{\partial \tau} \right) + Q \frac{\partial \Phi^*}{\partial \tau} \frac{\partial \Phi}{\partial \tau} + \frac{R}{2} \left( \frac{\partial |\Phi|^2}{\partial \tau} \right) + \Omega_s + \frac{C}{2m} |\nabla_{\mathbf{r}} \Phi|^2 - \frac{E}{2m} (\nabla_{\mathbf{r}} |\Phi|^2)^2 \right].$$

The goal of this section is to obtain a soliton solution for the equations of motion for the field  $\Phi$  and describe the dynamics of the excitation. In order to achieve this objective, as already mentioned in Subsection 3.5.1 it is necessary to move from the imaginary-time formalism to the real-time one. In the aforementioned Section this derivation was briefly sketched for the simplified action without second order imaginary-time derivatives: here the procedure will be applied to the most general case. The formal replacements that need to be exploited are

$$\tau \longrightarrow it, \quad (5.1)$$

$$S_{EFT}(\beta) \longrightarrow -i S_{EFT}(t_B, t_A) \quad (5.2)$$

the first substitution modifies the imaginary-time derivatives according to  $\frac{\partial}{\partial \tau} \rightarrow -i \frac{\partial}{\partial t}$ , thus the action becomes

$$S_{EFT}(\beta) = -i \int dt \int d\mathbf{r} \left[ i \frac{D}{2} \left( \bar{\Phi} \frac{\partial \Phi}{\partial t} + \frac{\partial \bar{\Phi}}{\partial t} \Phi \right) + Q \frac{\partial \Phi}{\partial t} \frac{\partial \bar{\Phi}}{\partial t} - \frac{R}{2} \left( \frac{\partial |\Phi|^2}{\partial t} \right)^2 - \mathcal{H} \right], \quad (5.3)$$

where the terms not involving time derivatives were collected by defining

$$\mathcal{H} = \Omega_s + \frac{C}{2m} |\nabla_{\mathbf{r}} \Phi|^2 - \frac{E}{2m} (\nabla_{\mathbf{r}} |\Phi|^2)^2 \quad (5.4)$$

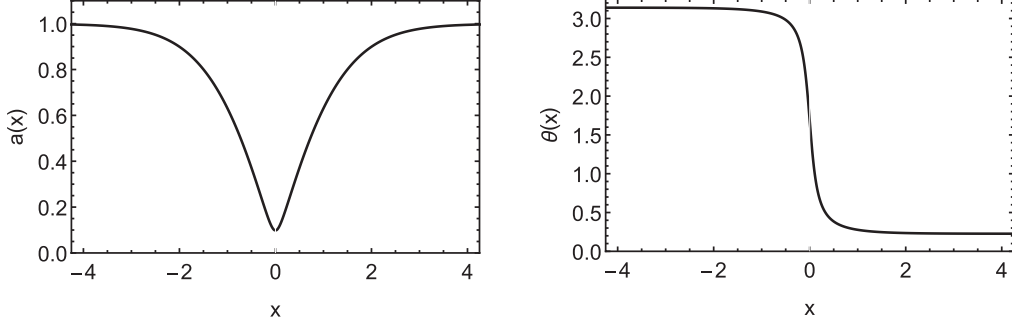


Figure 5.1: Typical amplitude (left) and phase (right) profiles of the order parameter  $\Phi$  for a dark soliton in a fermionic superfluid. The sets are calculated in the case of a balanced system ( $\zeta = 0$ ) for a soliton of velocity  $v_S = 0.1v_F$ , at temperature  $T = 0.01T_F$ , and interaction strength  $(k_F a_s)^{-1} = 0.25$ .

The second substitution, i.e. (5.2), ultimately leads to the final expression for the real-time action:

$$S_{EFT}(t_B, t_A) = \int_{t_A}^{t_B} dt \int d\mathbf{r} \left[ i \frac{D}{2} \left( \bar{\Phi} \frac{\partial \Phi}{\partial t} + \frac{\partial \bar{\Phi}}{\partial t} \Phi \right) + Q \frac{\partial \Phi}{\partial t} \frac{\partial \bar{\Phi}}{\partial t} - \frac{R}{2} \left( \frac{\partial |\Phi|^2}{\partial t} \right)^2 - \mathcal{H} \right] \quad (5.5)$$

From the relation between the action and the Lagrangian density  $\mathcal{L}$ , which is given by

$$S(t_B, t_A) = \int_{t_A}^{t_B} dt \int d\mathbf{r} \mathcal{L},$$

the explicit expression for  $\mathcal{L}$  can be written as

$$\begin{aligned} \mathcal{L} &= i \frac{D}{2} \left( \bar{\Phi} \frac{\partial \Phi}{\partial t} + \frac{\partial \bar{\Phi}}{\partial t} \Phi \right) + Q \frac{\partial \Phi}{\partial t} \frac{\partial \bar{\Phi}}{\partial t} - \frac{R}{2} \left( \frac{\partial |\Phi|^2}{\partial t} \right)^2 \\ &\quad - \Omega_s(\Phi) - \frac{C}{2m} (\nabla_{\mathbf{r}} \bar{\Phi} \cdot \nabla_{\mathbf{r}} \Phi) + \frac{E}{2m} (\nabla_{\mathbf{r}} |\Phi|^2)^2 \\ &= i \frac{D}{2} \left( \bar{\Phi} \frac{\partial \Phi}{\partial t} + \frac{\partial \bar{\Phi}}{\partial t} \Phi \right) + Q \frac{\partial \Phi}{\partial t} \frac{\partial \bar{\Phi}}{\partial t} - \frac{R}{2} \left( \frac{\partial |\Phi|^2}{\partial t} \right)^2 - \mathcal{H} \end{aligned} \quad (5.6)$$

As can be seen from Fig.5.1, the two main signatures of a soliton in a quantum gas are:

- a localised change in the amplitude profile of the order parameter. If the order parameter has a dip the soliton is called dark (or grey); if the order parameter exhibits a peak the soliton is called bright.
- a sudden jump in the phase profile of the order parameter.

In order to account for the presence of a soliton a formalism is needed that can account for both these features: therefore the order parameter  $\Phi(\mathbf{r}, t)$  is considered as the product of an amplitude factor and a phase factor as

$$\Phi(\mathbf{r}, t) \equiv |\Phi(\mathbf{r}, t)| e^{i\theta(\mathbf{r}, t)} \quad (5.7)$$

Moreover the amplitude factor can be split in two subfactors in order to highlight the change with respect to its background value (i.e. the value it assumes in the case of a uniform system) due to the presence of the solitonic excitation, namely

$$|\Phi(\mathbf{r}, t)| = a(\mathbf{r}, t) |\Phi_\infty| \quad (5.8)$$

where  $|\Phi_\infty|$  represents the background value of the order parameter while  $a(\mathbf{r}, t)$  describes the coordinate-dependent modulation of the amplitude. We can now introduce the regularised version of  $\mathcal{L}$  that is obtained by substituting  $\mathcal{H}$  with  $\bar{\mathcal{H}} = \mathcal{H} - \Omega_s(\Phi_\infty)$ . Performing this subtraction does not change the physics of the system since this operation can be seen just as a redefinition of the zero-energy. The consequence of this redefinition is that all the values of the energy considered in the following are in fact energy differences calculated with respect to the energy of the uniform system. After the substitutions (5.7) and (5.8), the regularised Lagrangian density (that from now on will simply be denoted with  $\mathcal{L}$ , dropping the “bar”-symbol for the sake of notational clarity) becomes

$$\begin{aligned} \mathcal{L} &= -\kappa(a)a^2\frac{\partial\theta}{\partial t} + Q|\Phi_\infty|^2 \left[ \left(\frac{\partial a}{\partial t}\right)^2 + a^2 \left(\frac{\partial\theta}{\partial t}\right)^2 \right] - \frac{R}{2}4|\Phi_\infty|^4 a^2 \left(\frac{\partial a}{\partial t}\right)^2 - \mathcal{H} = \\ &= -\kappa(a)a^2\frac{\partial\theta}{\partial t} + Q|\Phi|^2 \left(\frac{\partial\theta}{\partial t}\right)^2 + (Q - 2R|\Phi_\infty|^2 a^2) |\Phi_\infty|^2 \left(\frac{\partial a}{\partial t}\right)^2 + \\ &\quad - \left[ \Omega_s(\Phi) - \Omega_s(\Phi_\infty) + \frac{1}{2}\rho_{qp}(a) (\nabla_{\mathbf{r}}a)^2 + \frac{1}{2}\rho_{sf}(a) (\nabla_{\mathbf{r}}\theta)^2 \right] \end{aligned} \quad (5.9)$$

The coefficient  $\kappa(a)$  of the term with first order time-derivative, the quantum pressure coefficient  $\rho_{qp}(a)$  and the superfluid density  $\rho_{sf}(a)$  are defined, in terms of the EFT coefficients  $C$  (2.79),  $D$  (2.95) and  $E$  (2.80), as

$$\kappa(a) = D(a) |\Phi_\infty|^2 \quad (5.10)$$

$$\rho_{sf}(a) = \frac{C(a)}{m} |\Phi|^2 \quad (5.11)$$

$$\rho_{qp}(a) = \frac{C(a) - 4|\Phi|^2 E(a)}{m} |\Phi_\infty|^2, \quad (5.12)$$

in the same way as in [70], [1], and [3]. The superfluid density is associated with phase stiffness, and it can be identified with the prefactor of  $(\nabla_{\mathbf{r}}\theta)^2/2$ . The quantum pressure typically characterises the energy cost of amplitude changes of the wavefunction. It acts as a pressure, for example counteracting the confinement of the wavefunction to smaller volumes. In analogy with the  $\rho_{sf}$ , we then denote the prefactor of the  $(\nabla_{\mathbf{r}}a)^2/2$  term by  $\rho_{qp}$ .

In general it is impossible to find a closed-form solution for the equations of motion corresponding to the Lagrangian (5.9). However in the remainder of this section we will demonstrate how a simple solution can be found under the assumption that the soliton propagates with constant velocity  $v_S$  along the direction  $x$ . This hypothesis is not very

accurate when it comes to describe the typical situation investigated in experiments on dark solitons in ultracold quantum gases: in fact the presence of a harmonic trapping potential is expected to cause an acceleration of the soliton. Nevertheless our assumption is expected to become more accurate in the case of an elongated condensate, i.e. when the trapping along the  $x$  direction is weak. Also, recent progress in experiments [141] has introduced the possibility to confine the atomic cloud by using box-like potentials, making the present treatment extremely reliable. Under the aforementioned assumption, the space-time dependence of the order parameter is simplified according to the relation

$$f(x, t) = f(x - v_S t). \quad (5.13)$$

This enables us to eliminate the time derivatives and replace them with spatial derivatives using the equality

$$\frac{\partial f(x - v_S t)}{\partial t} = -v_S \frac{\partial f(x)}{\partial x}$$

Hence, after substituting

$$a(x, t) \longrightarrow a(x - v_S t) \quad \theta(x, t) \longrightarrow \theta(x - v_S t),$$

the Lagrangian becomes

$$\begin{aligned} \mathcal{L} = & \kappa(a) a^2 v_S \frac{\partial \theta}{\partial x} + Q v_S^2 |\Phi|^2 \left( \frac{\partial \theta}{\partial x} \right)^2 + (Q - 2R |\Phi_\infty|^2 a^2) v_S^2 |\Phi_\infty|^2 \left( \frac{\partial a}{\partial x} \right)^2 + \\ & - [\Omega_s(a) - \Omega_s(a_\infty)] - \frac{1}{2} \rho_{qp}(a) \left( \frac{\partial a}{\partial x} \right)^2 - \frac{1}{2} \rho_{sf}(a) \left( \frac{\partial \theta}{\partial x} \right)^2. \end{aligned} \quad (5.14)$$

Defining the modified (velocity dependent) superfluid density and quantum pressure coefficient as

$$\tilde{\rho}_{sf}(a) = \rho_{sf}(a) - 2Q v_S^2 |\Phi|^2, \quad (5.15)$$

$$\tilde{\rho}_{qp}(a) = \rho_{qp}(a) - 2(Q - 2R |\Phi_\infty|^2 a^2) v_S^2 |\Phi_\infty|^2, \quad (5.16)$$

we can recast the Lagrangian density in the same form as in [1, 3, 70], i.e.

$$\mathcal{L} = \kappa(a) a^2 v_S \frac{\partial \theta}{\partial x} - [\Omega_s(a) - \Omega_s(a_\infty)] - \frac{1}{2} \tilde{\rho}_{qp}(a) \left( \frac{\partial a}{\partial x} \right)^2 - \frac{1}{2} \tilde{\rho}_{sf}(a) \left( \frac{\partial \theta}{\partial x} \right)^2. \quad (5.17)$$

The equation of motion for the phase and the amplitude can now be derived by solving the Lagrange equations for  $\mathcal{L}$  (5.17). The equation of motion for the phase can be easily be found to be

$$\frac{\partial}{\partial x} \left[ \kappa(a) a^2 v_S - \tilde{\rho}_{sf}(a) \left( \frac{\partial \theta}{\partial x} \right) \right] = 0 \quad (5.18)$$

The solution of this equation is

$$\frac{\partial \theta}{\partial x} = \frac{\kappa(a)a^2 v_S + c}{\tilde{\rho}_{sf}(a)} \quad (5.19)$$

with  $c$  a constant whose value can be fixed by imposing the boundary condition for a dark soliton

$$\frac{\partial \theta}{\partial x} \rightarrow 0 \quad \text{for } x \rightarrow \pm\infty,$$

stating that the velocity field goes to zero at infinity. This leads to

$$\frac{\kappa(a_\infty)a_\infty^2 v_S + c}{\tilde{\rho}_{sf}(a_\infty)} = 0.$$

Remembering that  $a_\infty = 1$  and defining the bulk value of  $\kappa(a)$  as  $\kappa_\infty \equiv \kappa(a_\infty)$  the value of the constant  $c$  results  $c = -\kappa_\infty v_S$ . Therefore

$$\frac{\partial \theta}{\partial x} = \frac{v_S}{\tilde{\rho}_{sf}(a)} (\kappa(a)a^2 - k_\infty). \quad (5.20)$$

From the last expression it follows that the phase profile of the order parameter in presence of a dark soliton is described by

$$\theta(x) = v_S \int_{-\infty}^x dx' \frac{\kappa(a(x'))a(x')^2 - \kappa_\infty}{\tilde{\rho}_{sf}(a(x'))}. \quad (5.21)$$

The Lagrange equation for the amplitude is

$$\begin{aligned} & \frac{\partial}{\partial a} (\kappa(a)a^2 v_S) \frac{\partial \theta}{\partial x} - \frac{\partial \Omega_s}{\partial a} - \frac{1}{2} \frac{\partial \tilde{\rho}_{qp}}{\partial a} \left( \frac{\partial a}{\partial x} \right)^2 - \frac{\partial}{\partial x} \left( \tilde{\rho}_{qp} \frac{\partial a}{\partial x} \right) - \frac{1}{2} \frac{\partial \tilde{\rho}_{sf}}{\partial a} \left( \frac{\partial \theta}{\partial x} \right)^2 = 0 \\ \implies & - \frac{\partial}{\partial x} \left( \tilde{\rho}_{qp} \frac{\partial a}{\partial x} \right) = \frac{1}{2} \frac{\partial \tilde{\rho}_{qp}}{\partial a} \left( \frac{\partial a}{\partial x} \right)^2 + \frac{\partial \Omega_s}{\partial a} - \frac{\partial}{\partial a} (\kappa(a)a^2 v_S) \frac{\partial \theta}{\partial x} + \frac{1}{2} \frac{\partial \tilde{\rho}_{sf}}{\partial a} \left( \frac{\partial \theta}{\partial x} \right)^2 \end{aligned}$$

Inserting in the last expression the solution (5.20) for  $\frac{\partial \theta}{\partial x}$ , we find

$$- \frac{\partial}{\partial x} \left( \tilde{\rho}_{qp} \frac{\partial a}{\partial x} \right) = \frac{1}{2} \frac{\partial \tilde{\rho}_{qp}}{\partial a} \left( \frac{\partial a}{\partial x} \right)^2 + \frac{\partial \Omega_s}{\partial a} - \frac{1}{2} v_S^2 \frac{\partial}{\partial a} \left( \frac{[\kappa(a)a^2 - k_\infty]^2}{\tilde{\rho}_{sf}} \right) \quad (5.22)$$

The boundary conditions for the amplitude are

$$\left. \frac{\partial a}{\partial x} \right|_{x \rightarrow \pm\infty} = 0, \quad a_\infty = 1.$$

It is convenient to notice that equation (5.22) does not allow for a straightforward solution for  $a$  as a function of  $x$  but can still be solved if we look for a solution for  $x$  as a function of  $a$  instead. This leads to the solution

$$x = \pm \frac{1}{\sqrt{2}} \int_{a_0}^a da' \frac{\sqrt{\tilde{\rho}_{qp}(a')}}{\sqrt{X(a') - v_S^2 \tilde{Y}(a')}} \quad (5.23)$$

where the auxiliary functions

$$\begin{aligned} X(a) &\equiv \Omega_s(a) - \Omega_s(a_\infty), \\ \tilde{Y}(a) &\equiv \frac{[\kappa(a)a^2 - \kappa_\infty]^2}{2\tilde{\rho}_{sf}(a)}, \end{aligned}$$

were introduced to simplify the notation. Furthermore, from (5.23) we deduce that the amplitude in the center of the soliton  $a_0 \equiv a(x=0)$  is given by the solution of

$$X(a_0) - v_S^2 \tilde{Y}(a_0) = 0. \quad (5.24)$$

In conclusion the phase and amplitude profiles of the order parameter for a dark soliton in a Fermi superfluid can be completely determined, given the input values of inverse temperature  $\beta$ , imbalance parameter  $\zeta$ , and soliton velocity  $v_S$  by solving (5.21), (5.23), and (5.24) respectively.

Before proceeding to the study and analysis of the order parameter profiles resulting from the solution of the equations derived in this section, it is necessary to make a further remark. One of the cornerstones of the effective field theory derived in Chapter 2 is a gradient expansion of the order parameter up to second order in both space and (imaginary-)time derivatives. It is therefore necessary to carefully consider whether the dependence of the EFT coefficients on the order parameter must or must not be taken into account, in order to assure that the treatment that will be carried out in the following sections remains inside the limits of approximation. From the analysis of the full expression for the EFT action (2.118) it emerges that, for the coefficients of zeroth and first order in the gradients, i.e. for the thermodynamic potential  $\Omega_s$  and the coefficient  $D$ , the full  $\Phi$ -dependence must be considered. On the other hand, the coefficients of the terms involving higher-than-first order gradients (in both time and space), i.e.  $C$ ,  $E$ ,  $Q$ , and  $R$ , have to be considered constant and equal to their value in the case of a uniform system.

## 5.3 Results for a stable soliton

This section is devoted to the presentation of the results obtained in the framework of the theoretical treatment developed in the previous section for the study of dark solitons in fermionic superfluids. In particular, given the approximation (5.13), the data presented in this section are to be intended as relative to dark solitons moving with velocity  $v_S$  in a quasi-1D superfluid. In subsection 5.3.1 the equations (5.21) and (5.23) for the phase and amplitude profile of the order parameter are solved, and the basic features of the resulting profiles are described for different configurations of temperature, population imbalance and soliton velocity. A part of the subsection is also dedicated to the analysis of the relevance of the corrections due to the inclusion of terms involving higher-than-first order time derivatives into the action of the system (2.118).

Subsection 5.3.2 is instead devoted to the study of some of the dynamical properties of the solitonic excitations: in particular, for what concerns the effective mass of the dark

soliton a disagreement between the predictions of the present EFT and other theoretical approaches is detected and discussed.

### 5.3.1 Shape of the soliton

The solution of equations (5.21) and (5.23) results in the determination of a spatial profile for the order parameter showing the characteristic dip in the amplitude and jump in the phase that were sketched in Fig.5.1. The decrease of  $a(x)$  where the soliton is located corresponds to a dip in the density of the condensate cloud, which can be detected with appropriate imaging techniques in experiment. In order to calculate the density profile of the fermionic system starting from the spatial distributions  $a(x)$  and  $\theta(x)$ , the mean-field local density approximation (LDA) is employed. Using the relation

$$n^{(\text{LDA})} = -\frac{\partial\Omega_s}{\partial\mu}, \quad (5.25)$$

with the space profile of  $\Phi(x)$  as an input, the density profile is obtained. Corrections to these profiles due to the inclusion of fluctuations were discussed in [70] but are not considered in the present work.

Before starting to observe the effects of other tunable parameters such as imbalance or soliton velocity, it is worth remarking an aspect that is due just to the temperature and interaction regime. When a black soliton (a stationary soliton with  $v_S = 0$ ) is considered, the phase profile is a step function that shows a sudden jump in  $x = 0$  from the value  $\theta = \pi$  to  $\theta = 0$ , while the amplitude profile shows the characteristic dip and goes to 0 at the soliton center. The fact that  $\Phi(0)$  is zero means that there are no fermionic pairs in the center of the soliton. Comparing the amplitude profile to the density profile, as done in Fig.5.2, shows that the latter is non-zero in  $x = 0$ . This is a first indication that the filling of the soliton core is partly due to the presence of unpaired particles. At non-zero temperature, pair-breaking excitations appear in the BCS regime. These act as a “normal” component that starts to fill the soliton core, as is evident from Fig.5.2. As the system is tuned towards the BEC regime, these pair-breaking excitations become strongly gapped, leading to less unpaired particles and a total density that follows the condensate density. It should be noted that, as the fermionic system becomes more and more similar to a real Bose Einstein condensate of tightly bound fermion pairs, i.e. as the interaction is tuned towards the deep BEC regime and the temperature is set to a value substantially lower than the critical one  $T_c$ , one expects that the square of the order parameter becomes equivalent to the (bosonic) particle density. To prove this point, in figure 5.3 the density at the center of the soliton is plotted as a function of the temperature for different interaction strengths. It is immediately clear that in the situation in which the system most closely resembles a real BEC the density at the center of the black soliton becomes zero, same as the amplitude of order parameter.

In order to find more evidence about the nature of the particles that are stored in the core of the soliton it is useful to introduce a population imbalance. Doing so increases the number of particles that can not participate in the pairing mechanism. To this regard, in

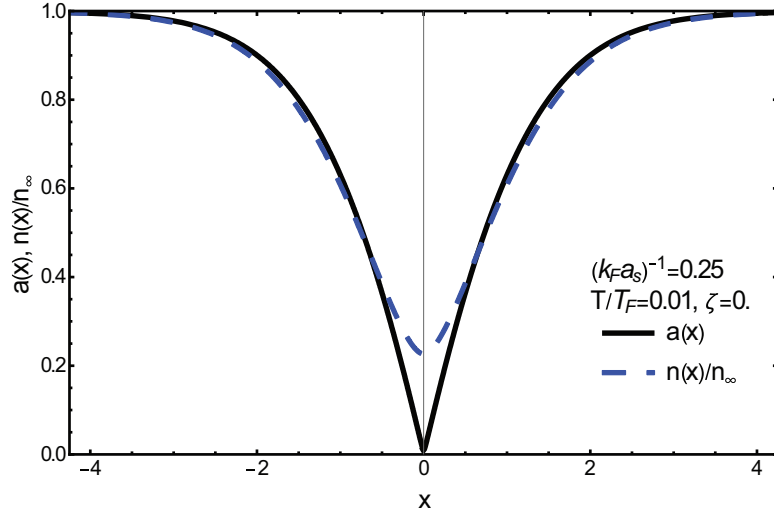


Figure 5.2: Amplitude profile (full black line) and corresponding density profile (blue dashed line) for a dark soliton at  $T = 0.01T_F$ ,  $\zeta = 0$ , in the near BEC regime, i.e.  $(k_F a_s)^{-1} = 0.25$ . It is important to notice that at the soliton center a non-zero fermion density is found while the order parameter is zero, thus giving a first evidence of the fact that the soliton core is filled by unpaired fermions.

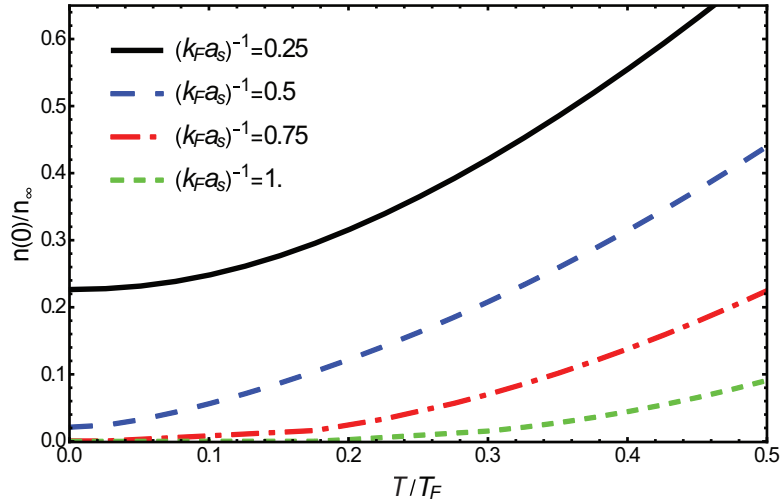


Figure 5.3: Fermion density at the center of a black soliton for different values of the interaction parameter, ranging from the near BEC regime with  $(k_F a_s)^{-1} = 0.25$  (black full line) to the deep BEC regime with  $(k_F a_s)^{-1} = 1$  (green dotted line), with the intermediate configurations  $(k_F a_s)^{-1} = 0.5$  (blue dashed line) and  $(k_F a_s)^{-1} = 0.75$  (red dot-dashed line).

Figure 5.4 the fermion density profile of a dark soliton of velocity  $v_S = 0.2v_F$ <sup>1</sup> (normalised to the bulk density) is shown as a function of the distance from its center, for different values of the imbalance parameter  $\zeta$ . Consistently with the hypothesis made above about the filling of the soliton core by unpaired particles, it can be observed that the presence of imbalance increases the density at the soliton center. For increasing values of  $\zeta$ , the soliton gets filled with a growing amount of particles, becoming shallower and broader at the same time. The inset of Fig. 5.4, highlights this last aspect in particular: the inverse soliton width (measured at half the height of the density dip)  $\xi_n^{-1}$  is seen to decrease when the value of  $\zeta$  increases; this effect takes place in all interaction regimes, as demonstrated by the three different data sets plotted in the inset which show the BCS (blue dot-dashed line), unitarity (green dashed line) and BEC regime (red full line) respectively.

Figures 5.5-5.6 also show the fermion density profile, for different values of velocity  $v_S$  and temperature  $T/T_F$  respectively. As it was the case for imbalance, also an increase in temperature makes the soliton shallower and broader: this can be intuitively understood because at higher temperatures less particles are available for forming Cooper pairs. A similar filling effect is observed when the soliton velocity becomes higher. In particular it is worth remarking that for high velocities the contribution of terms with higher-than-first order time derivatives in the EFT action (2.118) becomes sizable and cannot be neglected. This point is briefly discussed later on in a separate subsection.

The soliton core filling for increasing spin imbalance can be examined more specifically by considering the spatial distribution of the density difference  $\delta n(x)$  between the “spin-up” and “spin-down” populations. In figure 5.7 the  $\delta n(x)$  profile, normalised to the value at the soliton center  $\delta n(0)$ , is plotted for different levels of imbalance. The bottom inset indicates that the peak density difference  $\delta n(0)$  increases almost monotonously with  $\zeta$  across the BEC-BCS crossover.

As the imbalance between the two spin populations increases, so does the amount of unpaired particles that cannot participate in the superfluid state of condensed pairs. At finite temperatures, a part of these normal state particles coexist with the condensate in the form of a thermal gas, but any additional majority component particles have to be spatially removed from the pair condensate. The soliton dip offers a convenient location where the excess normal state particles can be accommodated, and therefore it fills up with an increasing quantity of unpaired atoms as the population imbalance becomes higher. Correspondingly to the broadening of the soliton density dip observed in Fig. 5.4, the upper inset of Fig. 5.7 shows that also the width of the  $\delta n(x)/\delta n(0)$  curves increases with  $\zeta$ .

Again changes in temperature and/or soliton velocity strongly affect the distribution of the excess component density in a way that is consistent with the previous observations regarding the fermion density, as it can be seen from Figure 5.8 and 5.9 respectively. In this regard it is worth remarking that a decrease in temperature produces an enhancement of the degree of localisation for the distribution of excess-spin component particles.

The insets of Fig.5.5 and Fig.5.8 focus on the width  $\xi_n$  of the soliton and the width  $\xi_{\delta n}$  of

---

<sup>1</sup>Notice that the Fermi velocity in the natural units used throughout this work is  $v_F = k_F/m = 2$ .

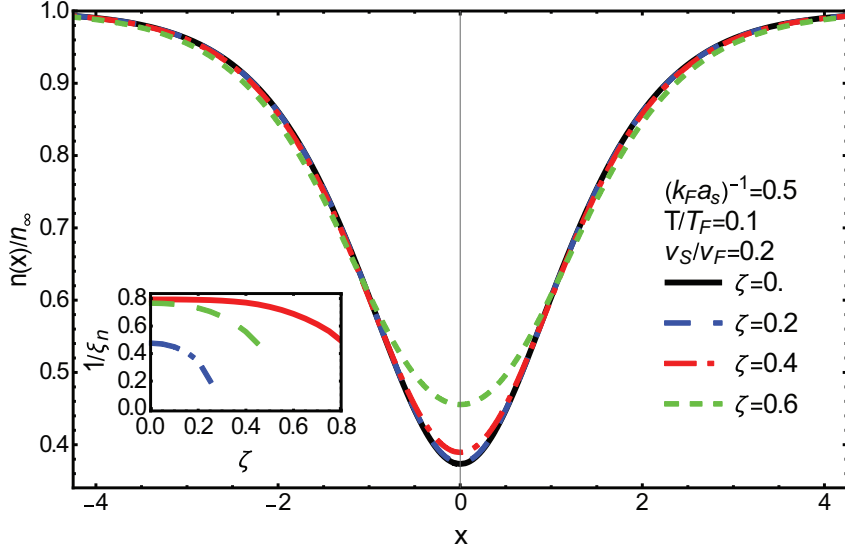


Figure 5.4: Density profiles at  $T = 0.1T_F$ ,  $v_S = 0.4$  on the BEC side of the resonance  $(k_F a_s)^{-1} = 0.5$  for different values of the imbalance parameter  $\zeta$ . The inset show the behaviour of the inverse soliton width  $(\xi_n)^{-1}$  in the BCS (blue dot-dashed line), unitarity (green dashed line) and BEC (red line) regimes as a function of  $\zeta$ . The position  $x$  and widths  $\xi_n$  are given in units of  $k_F^{-1}$ , the imbalance parameter  $\zeta$  is in units of  $E_F$  and the velocities are in units of  $v_F$ .

the excess component population. A critical value of the soliton velocity can be determined for which the depth of the profiles  $n(x)$  and  $\delta n(x)$  goes to zero and, at the same time, the width goes to infinity. in Fig.5.10 the effect of imbalance on this critical width is examined for three different interaction regimes spanning the BEC-BCS crossover. The comparison with the behaviour of the mean field bulk value of the order parameter as a function of imbalance in the same regimes (inset) clearly demonstrates that the value of the imbalance parameter  $\zeta$  for which the critical velocity  $v_S^{(crit)}$  goes to zero is the same  $\zeta^{(crit)}$  for which the normal state becomes more energetically favorable than the superfluid one, i.e. the minimum of the free energy corresponds to  $\Phi_\infty = 0$ .

To conclude the discussion about the shape properties of stable dark solitons in quasi-1D systems, in Fig.5.11 the inverse width of the soliton is plotted as a function of the interaction parameter  $(k_F a_s)^{-1}$  across the BEC-BCS crossover. The different stroke-color combinations identify various conditions of imbalance, making clear that the imbalance substantially affects the shape of the soliton in the intermediate and BCS regime while leaving them unchanged as the BEC limit is approached. In all situations, with or without imbalance, the maximum width and the maximum depth of the soliton are reached in the near-BEC regime around  $(k_F a_s)^{-1} = 0.4$ .

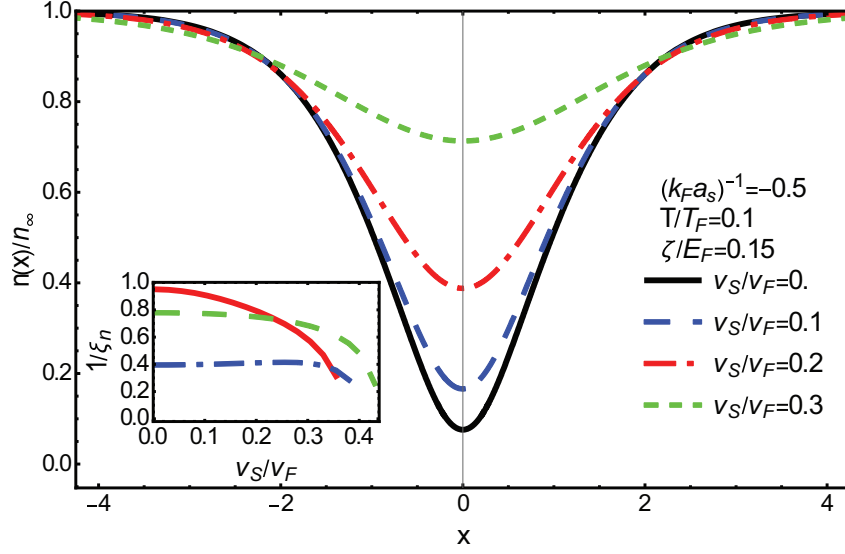


Figure 5.5: Density profiles at  $T = 0.1T_F$ ,  $\zeta = 0.15$  on the BEC side of the resonance  $(k_F a_s)^{-1} = 0.5$  for different values of the soliton velocity. The insets show the behaviour of the inverse soliton width  $(\xi_n)^{-1}$  in the BCS (blue dot-dashed line), unitarity (green dashed line) and BEC (red line) regimes as a function of  $v_S$ . The position  $x$  and widths  $\xi_n$  are given in units of  $k_F^{-1}$ , the imbalance parameter  $\zeta$  is in units of  $E_F$  and the velocities are in units of  $v_F$ .

### Remark: relevance of the terms in $Q$ and $R$

In Section 5.2 it was demonstrated how the inclusion of the terms of the action involving imaginary-time derivatives of order higher than one produces equations for the amplitude and phase profiles of the order parameter that have the same form as those obtained in the simplified case (with just first order derivatives) [1, 3, 70] provided that the standard superfluid density  $\rho_{sf}$  (5.11) and quantum pressure coefficient  $\rho_{qp}$  (5.12) are replaced by their modified velocity-dependent versions  $\tilde{\rho}_{sf}$  (5.15) and  $\tilde{\rho}_{qp}$  (5.16) respectively. From the explicit expressions it is clear that the additional terms in  $\tilde{\rho}_{sf}$  and  $\tilde{\rho}_{qp}$  are proportional to the square of the soliton velocity  $v_S$ , therefore it is immediate to conclude that for a black soliton, i.e. when  $v_S = 0$ , the terms of the action with higher-than-first order imaginary-time derivatives do not give any contribution to the physics of the system. The stability of stationary solitons is going to be the main topic of Sections 5.4-5.5 later in this chapter: according to the previous discussion in the theoretical treatment the terms proportional to the EFT coefficients  $Q$  and  $R$  will be neglected at that stage.

To give a clearer picture of the effect of the inclusion of the terms with imaginary-time derivatives of order higher than one in the action of the system, it is useful to examine how this affects the order parameter profile. Figure 5.12 shows the value of the amplitude modulation coefficient  $a$  calculated at the center of the soliton, namely  $a_0$ , as a function of the soliton velocity, in the BEC (black and blue lines) and BCS (red and green lines)

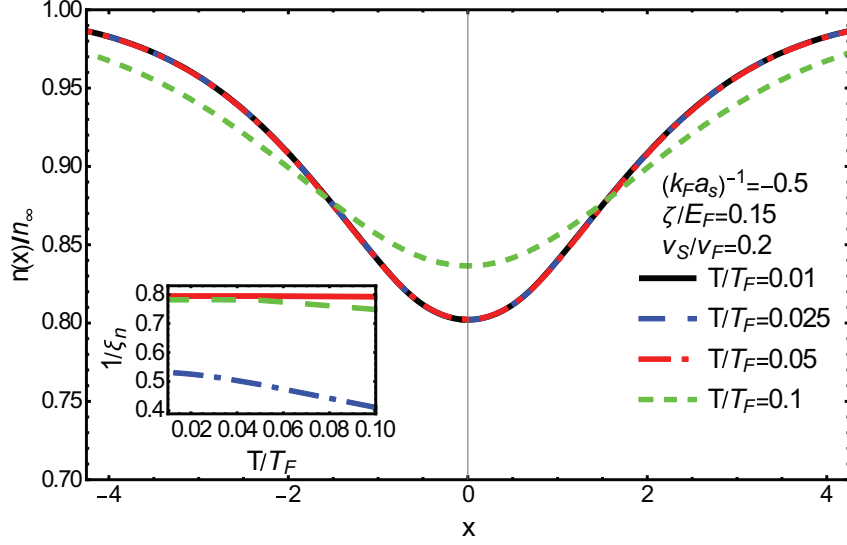


Figure 5.6: Density profiles at  $\zeta = 0.15$ ,  $v_S = 0.4$  on the BCS side of the resonance  $(k_F a_s)^{-1} = -0.5$  for different values of the temperature. The insets show the behaviour of the inverse soliton width  $(\xi_n)^{-1}$  in the BCS (blue dot-dashed line), unitarity (green dashed line) and BEC (red line) regimes as a function of  $T$ . The position  $x$  and widths  $\xi_n$  are given in units of  $k_F^{-1}$ , the imbalance parameter  $\zeta$  is in units of  $E_F$  and the velocities are in units of  $v_F$ .

regimes respectively. The dashed lines are relative to the complete action with  $Q \neq 0$  and  $R \neq 0$ , while the full lines describe the simplified case with  $Q = 0$  and  $R = 0$ . In both interaction configurations the contribution from the terms in  $Q$  and  $R$  becomes more relevant as the soliton velocity increases.

The same behaviour can be observed when the profile of the amplitude modulation  $a$  of the order parameter is considered as a function of the spatial coordinate  $x$ , as it is done in Fig.5.13. There the amplitude profile  $a(x)$  in two different velocity regimes –  $v_S = 0.1$  (black and blue lines) and  $v_S = 0.5$  (red and green lines) – are shown in the situation with (dashed lines) and without (full lines) the inclusion of higher-than-first order time derivatives in the EFT action. Again it can be noticed that for small velocities the difference in the amplitude profiles between the two situations is extremely small, but as the velocity becomes larger, a sizable effect is observed. This behaviour becomes even apparent when the insets of the plot are taken into consideration: the insets show the absolute value of the difference between the curves calculated with and without the terms in  $Q$  and  $R$ . The maximum value of such difference in the case of high soliton velocity ( $v_S = 0.5$ ) is two orders of magnitude larger than the one for  $v_S = 0.1$ .

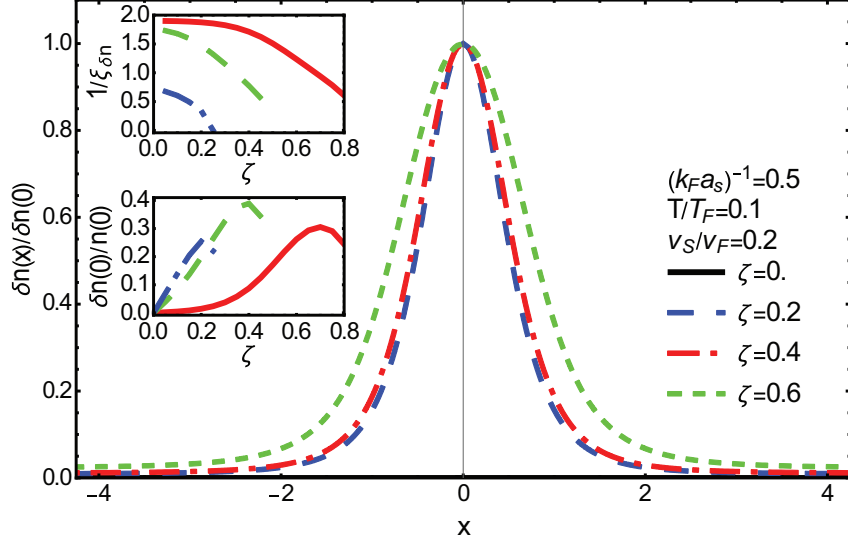


Figure 5.7: Excess component density at  $T = 0.1T_F$ ,  $v_S = 0.4$  on the BEC side of the resonance  $(k_F a_s)^{-1} = 0.5$  for different values of the imbalance. The left [right] insets show the behaviour of the ratio  $\delta n(0)/n(0)$  [inverse width  $(\xi_{\delta n})^{-1}$  of the excess component distribution] in the BCS (blue dot-dashed line), unitarity (green dashed line) and BEC (red line) regimes as a function of the imbalance. The position  $x$  and widths  $\xi_n$  are given in units of  $k_F^{-1}$ , the imbalance parameter  $\zeta$  is in units of  $E_F$  and the velocities are in units of  $v_F$ .

### 5.3.2 Dynamical properties

Up to this point only features of the soliton connected to its shape have been analysed. When one wants to study the dynamics of the system, the momentum and the energy must be evaluated. From the basic principles of the Lagrangian theory, the momentum can be determined as

$$\mathcal{P}_s = \frac{\partial L}{\partial v_S} \quad (5.26)$$

Carrying out explicitly the partial derivative of the Lagrangian  $L = \int_{-\infty}^{\infty} \mathcal{L}$  (with the Lagrangian density  $\mathcal{L}$  given in (5.17)) with respect to the soliton velocity leads to

$$\mathcal{P}_s = \int_{-\infty}^{\infty} dx \left[ -\kappa(a)a^2 \frac{\partial \theta}{\partial x} + 2v_S Q |\Phi|^2 \left( \frac{\partial \theta}{\partial x} \right)^2 + 2v_S (Q - 2R |\Phi_{\infty}|^2 a^2) |\Phi_{\infty}|^2 \left( \frac{\partial a}{\partial x} \right)^2 \right]$$

The energy is instead defined as

$$\mathcal{E}_s = v_S \mathcal{P}_s - \mathcal{L}, \quad (5.27)$$

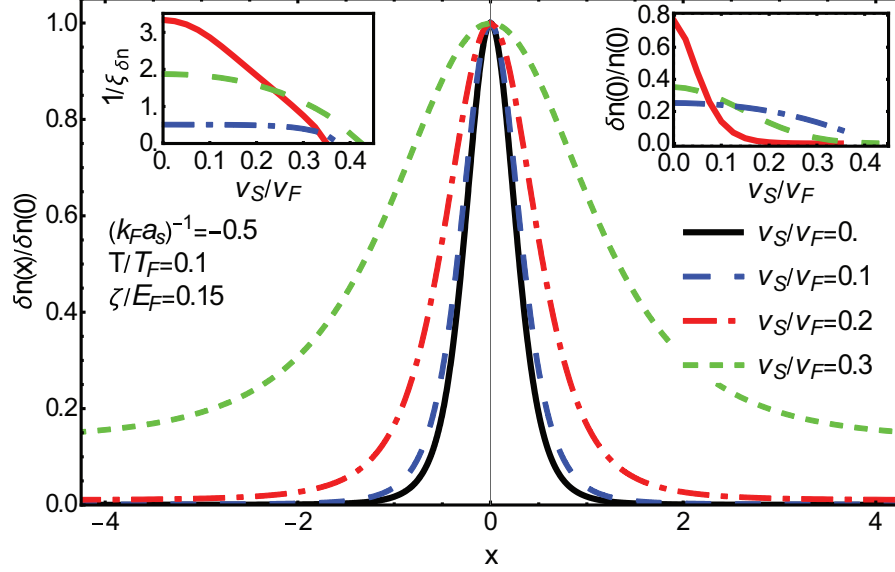


Figure 5.8: Excess component density at  $T = 0.1T_F$ ,  $\zeta = 0.15$  on the BEC side of the resonance  $(k_F a_s)^{-1} = 0.5$  for different values of the soliton velocity. The left [right] insets show the behaviour of the ratio  $\delta n(0)/n(0)$  [inverse width  $(\xi_{\delta n})^{-1}$  of the excess component distribution] in the BCS (blue dot-dashed line), unitarity (green dashed line) and BEC (red line) regimes as a function of the soliton velocity. The position  $x$  and widths  $\xi_n$  are given in units of  $k_F^{-1}$ , the imbalance parameter  $\zeta$  is in units of  $E_F$  and the velocities are in units of  $v_F$ .

corresponding to the explicit expression

$$\begin{aligned} \mathcal{E}_s = \int_{-\infty}^{\infty} dx \left[ v_S^2 Q |\Phi|^2 \left( \frac{\partial \theta}{\partial x} \right)^2 + v_S^2 (Q - 2R |\Phi_\infty|^2 a^2) |\Phi_\infty|^2 \left( \frac{\partial a}{\partial x} \right)^2 + \right. \\ \left. + [\Omega_s(a) - \Omega_s(a_\infty)] + \frac{1}{2} \tilde{\rho}_{qp}(a) \left( \frac{\partial a}{\partial x} \right)^2 + \frac{1}{2} \tilde{\rho}_{sf}(a) \left( \frac{\partial \theta}{\partial x} \right)^2 \right] \end{aligned} \quad (5.28)$$

In [70] it was analytically proven that, within the special version of the effective field theory excluding terms with higher-than-first order time derivatives (i.e. in the case with  $Q = R = 0$ ), a soliton obeys the energy-momentum relation of classic Hamiltonian dynamics

$$\frac{\partial \mathcal{E}_S}{\partial \mathcal{P}_S} = v_S, \quad (5.29)$$

i.e. the soliton behaves as if it were a classic particle. The same relation was later on verified also in the case of a Fermi superfluid with population imbalance [3]. When considering the most general form of the action (2.118) (with second order time derivatives), the relation between energy and momentum could in principle be affected by the presence of additional

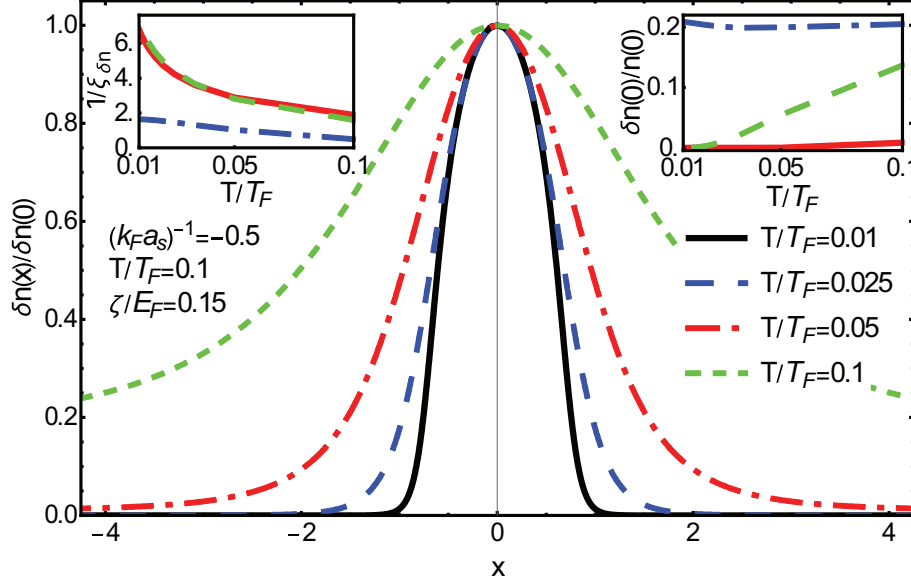


Figure 5.9: Excess component density at  $\zeta = 0.15$ ,  $v_S = 0.4$  on the BCS side of the resonance  $(k_F a_s)^{-1} = -0.5$  for different values of the temperature. The left [right] insets show the behaviour of the ratio  $\delta n(0)/n(0)$  [inverse width  $(\xi_{\delta n})^{-1}$  of the excess component distribution] in the BCS (blue dot-dashed line), unitarity (green dashed line) and BEC (red line) regimes as a function of the temperature. The position  $x$  and widths  $\xi_n$  are given in units of  $k_F^{-1}$ , the imbalance parameter  $\zeta$  is in units of  $E_F$  and the velocities are in units of  $v_F$ .

terms proportional to the EFT coefficients  $Q$  and  $R$ . To demonstrate that equation (5.29) still holds we are going to use the results of [70] and study how the additional terms affect the analytic procedure. It is therefore convenient to separate momentum and energy into the component coming from the simplified theory and the additional terms, i.e.

$$\begin{aligned} \mathcal{P}_s &= \mathcal{P}_s^{(0)} + \mathcal{P}_s^{(1)} = \\ &= \mathcal{P}_s^{(0)} + 2v_S \int_{-\infty}^{\infty} dx \left[ Q|\Phi|^2 \left( \frac{\partial \theta}{\partial x} \right)^2 + (Q - 2R|\Phi_\infty|^2 a^2) |\Phi_\infty|^2 \left( \frac{\partial a}{\partial x} \right)^2 \right] \end{aligned} \quad (5.30)$$

$$\begin{aligned} \mathcal{E}_s &= \mathcal{E}_s^{(0)} + \mathcal{E}_s^{(1)} = \\ &= \mathcal{E}_s^{(0)} + v_S^2 \int_{-\infty}^{\infty} dx \left[ Q|\Phi|^2 \left( \frac{\partial \theta}{\partial x} \right)^2 + (Q - 2R|\Phi_\infty|^2 a^2) |\Phi_\infty|^2 \left( \frac{\partial a}{\partial x} \right)^2 \right] \end{aligned} \quad (5.31)$$

Relation (5.29) is more easily proven by rewriting

$$\frac{\partial \mathcal{E}_s}{\partial \mathcal{P}_s} = \left( \frac{\partial \mathcal{E}_s}{\partial v_S} \right) \left( \frac{\partial \mathcal{P}_s}{\partial v_S} \right)^{-1} = \left( \frac{\partial (\mathcal{E}_s^{(0)} + \mathcal{E}_s^{(1)})}{\partial v_S} \right) \left( \frac{\partial (\mathcal{P}_s^{(0)} + \mathcal{P}_s^{(1)})}{\partial v_S} \right)^{-1}$$

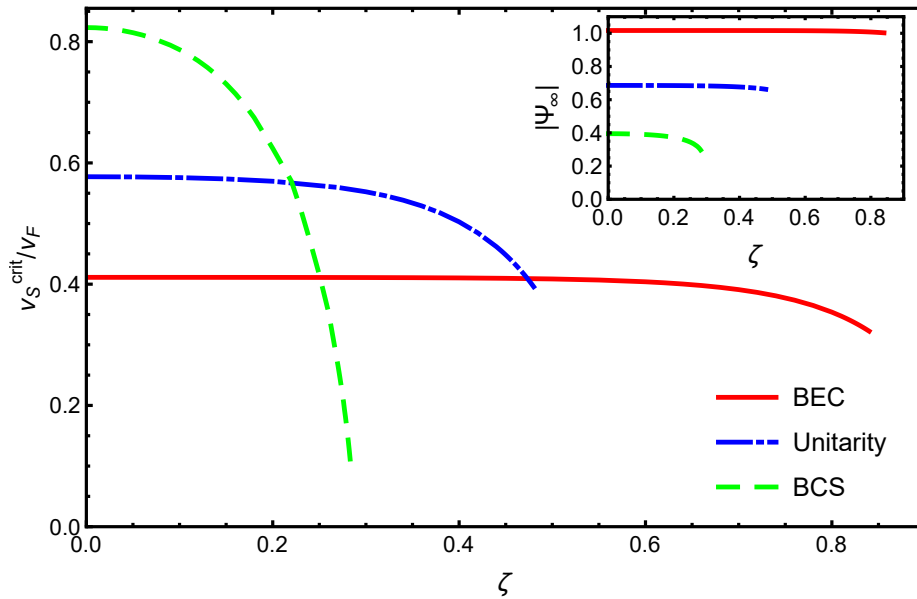


Figure 5.10: (Color online) Critical velocity of the soliton as a function of the imbalance at  $T = 0.1T_F$  across the BEC-BCS crossover. The inset shows the corresponding behaviour of  $|\Phi_\infty|$ . The imbalance parameter  $\zeta$  is given in units of  $E_F$ , the velocities in units of  $v_F$  and  $|\Phi_\infty|$  in units of  $E_F$ .

The equality

$$\frac{\partial \mathcal{E}_S^{(0)}}{\partial \mathcal{P}_S^{(0)}} = v_S$$

has been demonstrated in detail in ref. [70]. The missing piece needed to confirm the validity of (5.29) in the most general case is the verification that

$$\frac{\partial \mathcal{E}_S^{(1)}}{\partial \mathcal{P}_S^{(1)}} = v_S.$$

This last passage is trivial: from (5.30) and (5.31) it is clear that  $\mathcal{P}_s^{(1)}$  and  $\mathcal{E}_s^{(1)}$  have the same expression with the exception of the prefactor in front of the space integral, which is  $2v_S$  for  $\mathcal{P}_s^{(1)}$  and  $v_S^2$  for  $\mathcal{E}_s^{(1)}$ . The derivative with respect to the soliton velocity acts only on the prefactors and gives 2 and  $2v_S$  respectively, thus proving that equality (5.3.2) holds and, as a consequence, that the general relation (5.29) is true.

The soliton's motion can then be therefore treated as the motion of a classical particle moving with velocity  $v_S$  and an effective mass  $M_S$  which can be defined in terms of the soliton momentum  $\mathcal{P}_S$  (5.27) or of the soliton energy  $\mathcal{E}_S$  (5.28) as in [97], i.e.

$$M_S \equiv \frac{\partial \mathcal{P}_S}{\partial v_S} \equiv \frac{1}{v_S} \frac{\partial \mathcal{E}_S}{\partial v_S}. \quad (5.32)$$

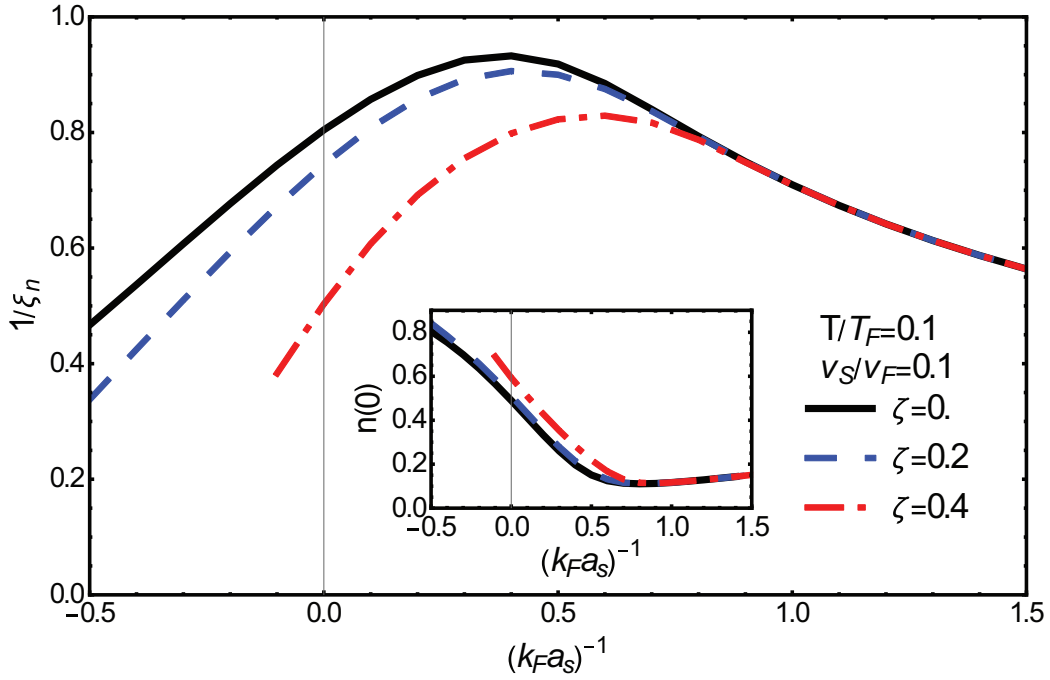


Figure 5.11: Inverse width of the soliton, calculated as the width at half height of the density profile, across the BEC-BCS crossover. The inset shows the corresponding behaviour  $n(0)$ : the density at the soliton center. All the data sets are calculated at  $T = 0.1T_F$  and  $v_S = 0.1v_F$ : the full black lines correspond to  $\zeta = 0$ , the blue dashed lines to  $\zeta = 0.2$  and the red dot-dashed lines to  $\zeta = 0.4$ .

The effective mass is a negative quantity because it must have the same sign as the soliton's physical mass that is defined as the missing mass of the particles that would fit into the soliton dip if the system were uniform. Figure 5.14 depicts the behaviour of the absolute value of the effective mass calculated at  $v_S = 0$  across the BEC-BCS crossover for different values of the temperature. The effect of temperature is small both in the BCS and far BEC limit, while it is sizable in the interval of values of the interaction parameter ranging roughly between 0 and 1. For the lowest temperature configuration considered, i.e.  $T/T_F = 0.01$  a sharp peak centered around  $(k_F a_s)^{-1} = 0.5$  appears. At higher temperatures this peak is smoothed out and  $|M_S|$  monotonically increases as the interaction changes from the BCS side towards the BEC side of the Feshbach resonance. Also population imbalance has a non trivial effect on the behaviour of  $M_S$ : figure 5.15 shows the dependence of the absolute value of the effective mass on the interaction parameter  $(k_F a_s)^{-1}$  for various values of  $\zeta$ . In the BCS regime  $|M_S|$  decreases with increasing  $\zeta$  consistently with what we observed in relation to the filling of the soliton by unpaired particles. In the opposite limit, for high positive values of  $(k_F a_s)^{-1}$  instead the effective mass is not affected by imbalance: this is due to the fact that in the deep BEC regime the background value of the order parameter is not affected by a non-zero  $\zeta$ . As was the case for temperature dependence, the unitary region shows the most interesting features. In the immediate vicinity of  $(k_F a_s)^{-1} = 0$  in

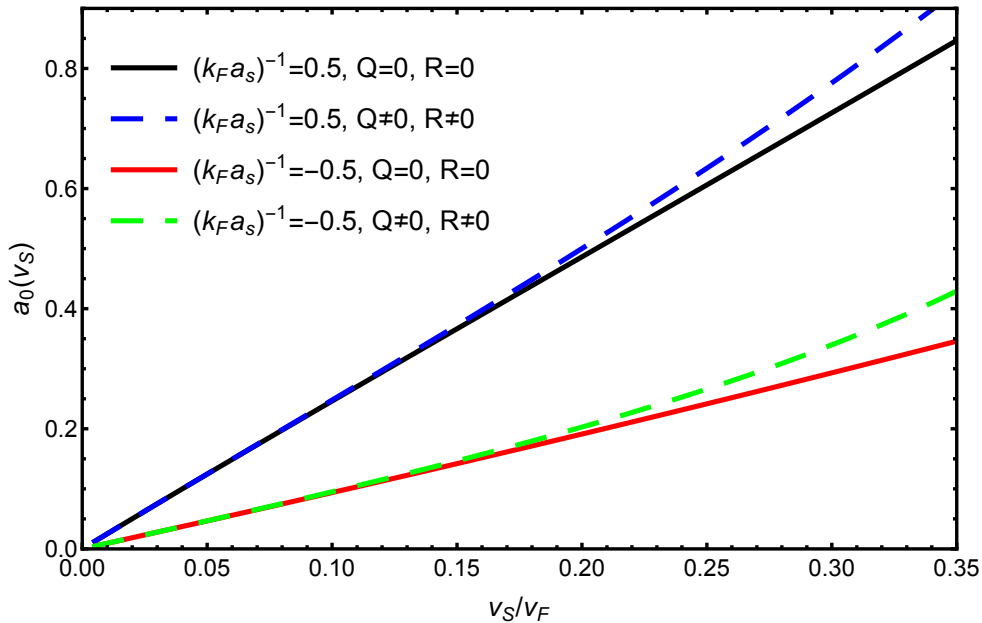


Figure 5.12: Value of the amplitude modulation coefficient  $a(x)$  of the order parameter calculated at the soliton center,  $a_0$ , at temperature  $T = 0.01T_F$ , in the near BEC regime  $(k_F a_s)^{-1} = 0.5$  as a function of the soliton velocity  $v_s$ . The full lines show the results in the simplified case without the inclusion of higher-than-first order time derivatives respectively in the BEC (black line) and BCS (red line) regime. Correspondingly the dashed lines show the effect of the inclusion of the terms proportional to  $Q$  and  $R$ , again in the BEC (blue line) and BCS (green line) regime.

fact, a higher value of  $|M_s|$  is observed for high values of the imbalance ( $\zeta = 0.4$ ), whereas in all other regions  $|M_s|$  is largest for the balanced system (full black line).

It is important to remark that a discrepancy is found between the predictions of the present EFT and the results of Bogoliubov-de Gennes simulations [125, 126, 142]. The absolute value of the effective mass according to the EFT treatment is substantially lower than the one expected by the BdG theory. Another evidence in favor of a high value of  $|M_s|$  is the experimental observation by Yefsah *et al.* [127] relative to solitonic vortices that observed an increase of the ratio between the effective mass and the physical mass as the interaction strength changes from the BEC to the BCS regime. The most probable source of this discrepancy can be identified in the fact that the physics of Andreev bound states is not captured by the effective field theory derived in the present work. Andreev bound states are a typically fermionic phenomenon, which is expected to give sizable contributions to the dynamics of the system especially in the BCS regime: due to the bosonic nature of the EFT, a straightforward inclusion of such effects in the theoretical description is difficult.

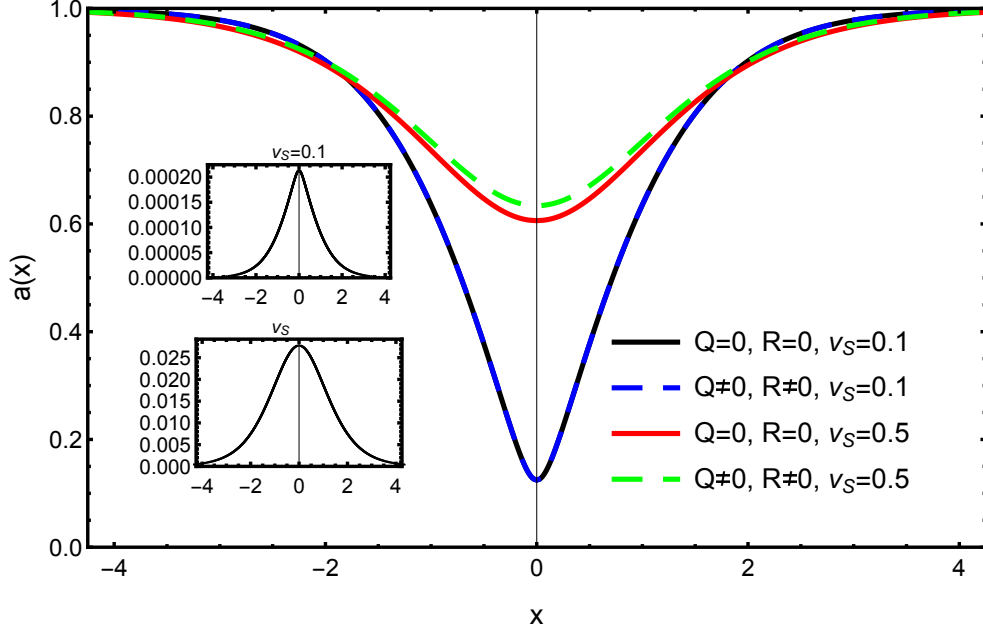


Figure 5.13: Order parameter amplitude profiles at  $T = 0.01T_F$ , on the BEC side of the resonance  $(k_F a_s)^{-1} = 0.5$  for different values of the soliton velocity. The insets show the absolute difference between the profiles calculated with or without the corrections due to the presence of the terms with second order imaginary-time derivatives.

## 5.4 Perturbative treatment

The study carried out in this section is based on the perturbation of stationary soliton solutions which are obtained from the analytic expressions for the phase and amplitude profiles of the order parameter derived in Section 5.2. As discussed before, these expressions provide a good description of the physical system in the quasi-1D configuration corresponding to a highly elongated shape of the atomic cloud, or, in the 3D uniform configuration. While the first case does not allow for the inclusion of transverse perturbations because of the reduced dimensionality, the second does, and moreover the recent realization of box-like optical traps [141] provides the possibility to reproduce this setup in experiment.

Throughout this analysis we will focus on stationary solitons (with  $v_s = 0$ ), therefore, as remarked in Section 5.3, we can neglect the terms of the EFT action (2.118) and consider the simplified Euclidean-time action functional given by

$$S_{EFT}(\beta) = \int_0^\beta d\tau \int d\mathbf{r} \left[ \frac{D}{2} \left( \bar{\Phi} \frac{\partial \Phi}{\partial \tau} - \frac{\partial \bar{\Phi}}{\partial \tau} \Phi \right) + \mathcal{H} \right], \quad (5.33)$$

where the Hamiltonian  $\mathcal{H}$  has the same form as in (5.4). The simplified and regularised version of the real-time Lagrangian density (5.6) is

$$\mathcal{L} = i \frac{D}{2} \left( \bar{\Phi} \frac{\partial \Phi}{\partial t} - \frac{\partial \bar{\Phi}}{\partial t} \Phi \right) - (\mathcal{H} - \Omega_s(\Phi_\infty)). \quad (5.34)$$

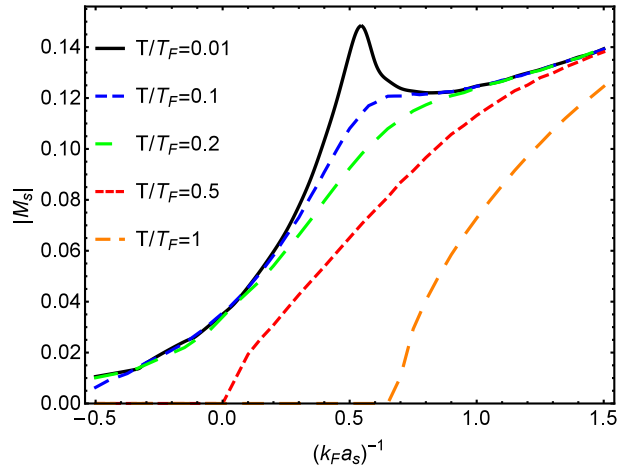


Figure 5.14: (Color online) Absolute value of the effective mass of the soliton as a function of the interaction parameter  $(k_F a_s)^{-1}$  for different values of the temperature without imbalance ( $\zeta = 0$ ). The mass is given in units of  $2m$ .

As mentioned above, the subtraction of the term  $\Omega_s(\Phi_\infty)$  means that in the present treatment we consider the energy difference with respect to the value of the thermodynamic potential for the uniform system.

From the effective field Lagrangian, the simplified ( $v_S = 0$ ) equation of motion for the pair field  $\Phi$  of the Fermi superfluid can be obtained, reading

$$i\tilde{D}(|\Phi|^2)\frac{\partial\Phi}{\partial t} = -\frac{C}{2m}\nabla_r^2\Phi + \left(A(|\Phi|^2) + \frac{E}{m}\nabla_r^2|\Phi|^2\right)\Phi. \quad (5.35)$$

The solution of this equation in the quasi-1D configuration was discussed at length in the previous sections of the thesis.

In order for the snake instability to develop a perturbation representing a small oscillation in the direction perpendicular to the propagation direction of the soliton must be added. Therefore to describe the deformation of the soliton plane that leads to its decay, a transverse perturbation is added to the stationary 1D solution  $\Phi_s$  in the following way [143]

$$\Phi(x, z, t) = \Phi_s(x - v_s t) + \Phi_p(x - v_s t, z, t), \quad (5.36)$$

where the perturbation  $\Phi_p(x - v_s t, z, t)$  is assumed to be small. The space- and time-dependence of the perturbation is assumed to have the form  $x - v_s t$ , meaning that it propagates in the  $x$  direction with velocity  $v_s$  in the same way as the soliton does. The perturbation is further assumed to consist of a combination of plane wave components propagating in opposite directions along the  $z$  axis:

$$\Phi_p(x - v_s t, z, t) = \phi_1(x - v_s t)e^{i(kz - \Omega t)} + \phi_2^*(x - v_s t)e^{-i(kz - \Omega^* t)} \quad (5.37)$$

The next step then is to insert this perturbed solution into the equation of motion (5.35) and to perform an expansion around the stationary solution up to first order in  $\Phi_p$ . From

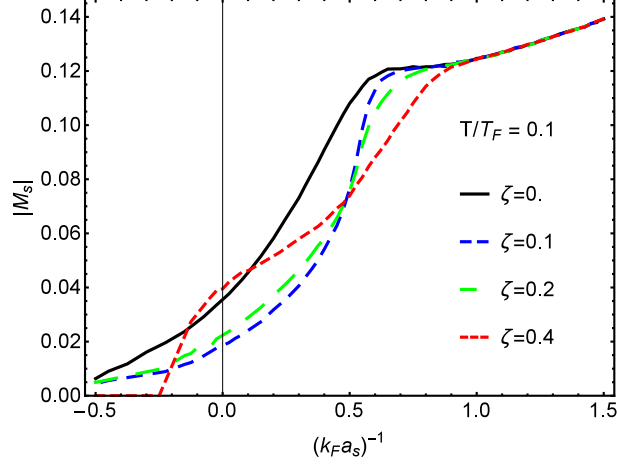


Figure 5.15: (Color online) Absolute value of the effective mass of the soliton as a function of the interaction parameter  $(k_F a_s)^{-1}$  at temperature  $T = 0.1 T_F$  for different values of the imbalance chemical potential (given in units of  $E_F$ ). The mass is given in units of  $2m$ .

previous considerations, we know that the coefficients  $C$  and  $E$  can be kept constant and equal to their value in the uniform system case. On the other hand, the dependence of both  $\tilde{D}$  and  $A$  on the order parameter has to be fully taken into account. A Taylor expansion of these two coefficients up to first order around the stationary solution leads to

$$\tilde{D}(|\Phi|^2) = \tilde{D}(|\Phi_s|^2) + \frac{\partial \tilde{D}(|\Phi_s|^2)}{\partial |\Phi_s|^2} [(\Phi_s^* \phi_1 + \Phi_s \phi_2^*) e^{i(kz - \Omega t)} + (\Phi_s \phi_1^* + \Phi_s^* \phi_2) e^{-i(kz - \Omega t)}] + \dots \quad (5.38)$$

$$A(|\Phi|^2) = A(|\Phi_s|^2) + \frac{\partial A(|\Phi_s|^2)}{\partial |\Phi_s|^2} [(\Phi_s^* \phi_1 + \Phi_s \phi_2^*) e^{i(kz - \Omega t)} + (\Phi_s \phi_1^* + \Phi_s^* \phi_2) e^{-i(kz - \Omega t)}] + \dots \quad (5.39)$$

After inserting (5.38) and (5.39) into the equation of motion and expanding the temporal and spatial derivatives, the terms of order zero in the perturbation can be collected, leading to

$$i\tilde{D}(|\Phi_s|^2) \frac{\partial \Phi_s}{\partial t} = -\frac{C}{2m} \nabla_{\mathbf{r}}^2 \Phi_s + \left( A(|\Phi_s|^2) + \frac{E}{m} \nabla_{\mathbf{r}}^2 |\Phi_s|^2 \right) \Phi_s \quad (5.40)$$

which is, as expected, just the equation of motion for the stationary solution. From the selection of the terms that are linear in the perturbation, two coupled differential equations are obtained for the perturbation amplitudes  $\phi_1$  and  $\phi_2$ :

$$\alpha_1 \frac{\partial^2 \phi_1}{\partial x^2} - \alpha_2 \frac{\partial \phi_1}{\partial x} + \alpha_3(\Omega) \phi_1 - \alpha_4 \frac{\partial^2 \phi_2}{\partial x^2} - \alpha_5 \frac{\partial \phi_2}{\partial x} - \alpha_6 \phi_2 = 0 \quad (5.41)$$

$$\alpha_1 \frac{\partial^2 \phi_2}{\partial x^2} - \alpha_2^* \frac{\partial \phi_2}{\partial x} + \alpha_3^*(-\Omega) \phi_2 - \alpha_4^* \frac{\partial^2 \phi_1}{\partial x^2} - \alpha_5^* \frac{\partial \phi_1}{\partial x} - \alpha_6^* \phi_1 = 0 \quad (5.42)$$

where the coefficients  $\alpha_j$ ,  $j = 1, 2, 3, 4, 5, 6$  are defined as

$$\alpha_1 = \frac{C}{2m} - \frac{E}{m} |\Phi_s|^2 \quad (5.43)$$

$$\alpha_2 = iv_s \tilde{D}_s + 2 \frac{E}{m} \Phi_s \frac{\partial \Phi_s^*}{\partial x} \quad (5.44)$$

$$\begin{aligned} \alpha_3 = \Omega \tilde{D}_s - \frac{C}{2m} k^2 - \partial_s (|\Phi_s|^2 A_s) - iv_s \partial_s \tilde{D}_s \frac{\partial \Phi_s}{\partial x} \Phi_s^* + \\ - \frac{E}{m} \frac{\partial^2 |\Phi_s|^2}{\partial x^2} - \frac{E}{m} \Phi_s \frac{\partial^2 \Phi_s^*}{\partial x^2} + \frac{E}{m} |\Phi_s|^2 k^2 \end{aligned} \quad (5.45)$$

$$\alpha_4 = \frac{E}{m} \Phi_s^2 \frac{\partial^2 \phi_2}{\partial x^2} \quad (5.46)$$

$$\alpha_5 = 2 \frac{E}{m} \Phi_s \frac{\partial \Phi_s}{\partial x} \frac{\partial \phi_2}{\partial x} \quad (5.47)$$

$$\alpha_6 = \partial_s A_s \Phi_s^2 + iv_s \partial_s \tilde{D}_s \frac{\partial \Phi_s}{\partial x} \Phi_s + \frac{E}{m} \Phi_s \frac{\partial^2 \Phi_s}{\partial x^2} - \frac{E}{m} \Phi_s^2 k^2 \quad (5.48)$$

For the sake of notational aesthetics, in the last set of expressions we introduced the notations

$$\begin{aligned} A(|\Phi_s|^2) = A_s, \quad \frac{\partial A}{\partial |\Phi_s|^2} = \partial_s A, \\ \tilde{D}(|\Phi_s|^2) = \tilde{D}_s, \quad \frac{\partial \tilde{D}}{\partial |\Phi_s|^2} = \partial_s \tilde{D}. \end{aligned}$$

## 5.5 Results for the snake instability

From the system of coupled differential equations (5.41) and (5.42) one can obtain information about the perturbation's frequency spectrum  $\Omega(k)$ . In particular, the soliton solution will be unstable for every wavevector  $k$  that corresponds to an imaginary value of the frequency. Therefore, the first goal of the present section is to analyze the imaginary part of the spectrum  $\Omega(k)$  and obtain a description of the growth rate of the instability in different interaction regimes across the BEC-BCS crossover. To do this, the system of equations is approached as an eigenvalue problem of the form

$$\begin{pmatrix} W_{11} & W_{12} \\ W_{21} & W_{22} \end{pmatrix} \begin{pmatrix} \phi_1 \\ \phi_2 \end{pmatrix} = \Omega \begin{pmatrix} \phi_1 \\ \phi_2 \end{pmatrix} \quad (5.49)$$

and is solved numerically for the case of a stationary soliton ( $v_S = 0$ ) [144]. A large space grid is used to discretize the positions, and the space derivatives are approximated by finite central differences: for example the first derivative of a generic function  $f$  calculated at the position  $x_i$  corresponding to the  $i^{\text{th}}$  grid point, is given by

$$f'(x_i) = \frac{f(x_{i+1}) - f(x_{i-1}))}{2\delta x},$$

where  $\delta x$  represents the grid spacing.

Figure 5.16 shows the results for the imaginary part of the eigenvalues  $\Omega(k)$  at  $T = 0.01T_F$  and for different values of the interaction parameter  $(k_F a_s)^{-1}$ .<sup>2</sup> It is clear that the snake instability is a long-wavelength phenomenon that only exists up to a maximum wavenumber  $k_c$  since the imaginary part of the frequency  $\Omega$  is zero for  $k > k_c$ . The full red line interpolates between the values of  $\text{Im}[\Omega(k)]$  calculated in  $k = k_c/\sqrt{2}$ . As predicted by Muryshev *et al.* in the case of Bose Einstein condensates [129], this line nicely connects the maxima of the dispersion relations for different  $(k_F a_s)^{-1}$  across the entire BEC-BCS crossover.

Fig.5.17 and Fig.5.18 compare the results for  $(k_F a_s)^{-1} = 0$  and  $(k_F a_s)^{-1} = 0.2$  with the

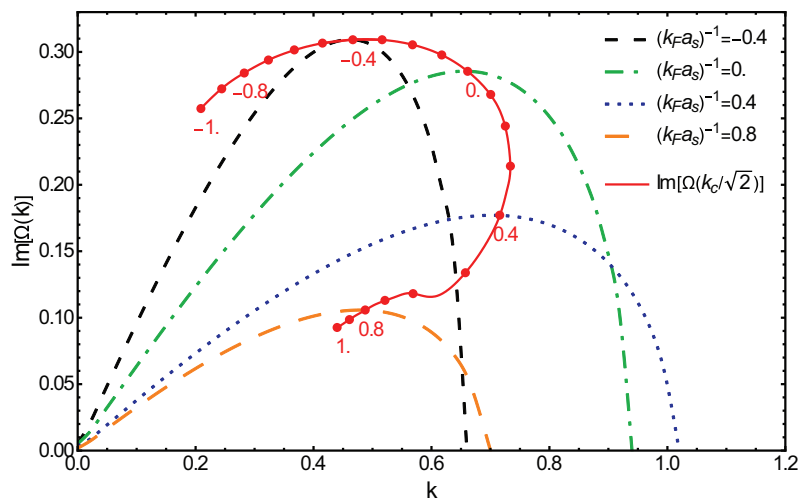


Figure 5.16: Dispersion relations for the snake instability for different interaction strengths across the BEC-BCS crossover, i.e. on the BCS side of the resonance at  $(k_F a_s)^{-1} = -0.4$  (black dashed line), at unitarity  $(k_F a_s)^{-1} = 0$  (green dot-dashed line), in the near-BCS regime  $(k_F a_s)^{-1} = 0.4$  (blue dotted line) and further towards the BEC limit at  $(k_F a_s)^{-1} = 0.8$  (orange wide-dashed line). The full red line connects the values of  $\text{Im}[\Omega(k)]$  calculated in  $k = k_c/\sqrt{2}$  for different values of  $(k_F a_s)^{-1}$ . The markers correspond to values of  $(k_F a_s)^{-1}$  ranging from  $-1$  to  $1$  in steps of  $0.1$ .

corresponding spectra that were calculated in Ref. [138]. There, the authors made use of three different approaches to analyze the spectra of the snake instability: a hydrodynamic approximation, the random-phase approximation (RPA) and the solution of the time-dependent Bogoliubov-de Gennes (TDBdG) equations. As far as the width of the band of unstable wavelengths goes, the latter method shows the best agreement with the EFT results. The RPA results on the other hand show a sharp decrease of  $\text{Im}[\Omega]$ , which might

<sup>2</sup>The choice of  $T = 0.01T_F$  is motivated by the requirement of an extremely low temperature coming from the fact that the perturbation theory adopted in the present treatment is technically valid just at  $T = 0$ : the study of the actual  $T = 0$  case can cause problems in the numerical implementation, but the behaviour at low enough temperatures appears to be hardly distinguishable from the real  $T = 0$  situation.

be caused by the necessary use of an energy cutoff in this type of calculations, an issue that does not occur in the presently used EFT. Another consequence of this cutoff is that the RPA method fails to find any imaginary frequency at all for  $(k_F a_s)^{-1} > 0.2$ . The hydrodynamic approximation, that describes a linear relation between  $\Omega$  and  $k$ , is only expected to hold near  $k = 0$ , where it indeed agrees quite well with the initial slope of the EFT results.

The existence of a minimum wavenumber  $k_c$  for which  $\text{Im}(\Omega)$  becomes zero implies that

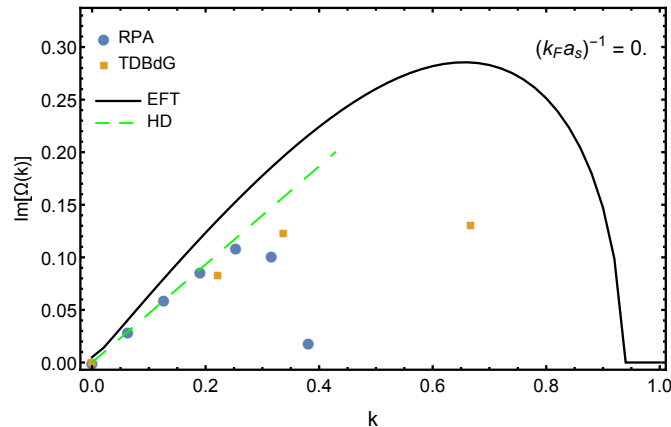


Figure 5.17: Dispersion relations for the snake instability at unitarity for  $(k_F a_s)^{-1} = 0$ . The full black line represents the EFT prediction and it is compared to the results of hydrodynamic approximation (green dashed line), of the RPA (blue circles), and of the time dependent Bogoliubov-de Gennes simulations (orange squares) [138]

there exists a minimal transverse length the ultracold gas must have in order for the soliton to decay. If the transverse width is smaller than this minimal value, the soliton is expected to be stable as the wavelength of the perturbation cannot fit the system width. A good estimate for this critical length is given by the inverse of  $k_c$ . In figure 5.19 this quantity is compared to the RPA and TDBdG results of [138] as well as to the data from [139] relative to a treatment based on the coarse-grained BdG equation introduced by Simonucci and Strinati [99]. Numerical factors have been introduced after a cross-comparison between Refs. [129, 138, 139] in order to overcome the difference in the definitions of the healing lengths<sup>3</sup>. The values calculated in the framework of the EFT (black line) appear to be in good agreement with the results of the time-dependent Bogoliubov-de Gennes equations (blue circles with error bars) across the whole range of available data. Moreover it seems that the present EFT is the approach that better captures the fact that the characteristic length of the system changes from the healing length in the BEC regime (purple dot-dot-dashed line) to the correlation length in the BCS regime (green dashed line). In the far

<sup>3</sup>In [139] the quantity  $r_0$  is defined as  $r_0 = (\pi/\sqrt{-2\lambda}) \xi$ . Therefore the data plotted in Fig. 5.19, i.e.  $r_0/(\sqrt{2\pi})$  describe a “corrected healing length” accounting for the modulation effect due to the variation of the (bound) ground state eigenvalue  $\lambda$  across the BEC-BCS crossover. The factor  $1/\sqrt{2}$  comes instead from a difference in the definition of  $\xi$  with respect to [129]

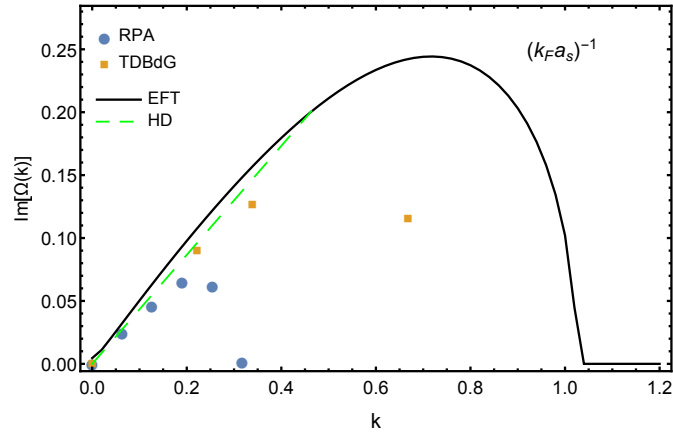


Figure 5.18: Dispersion relations for the snake instability in the near BEC regime for  $(k_F a_s)^{-1} = 0.2$ . The full black line represents the EFT prediction and it is compared to the results of hydrodynamic approximation (green dashed line), of the RPA (blue circles), and of the time dependent Bogoliubov-de Gennes simulations (orange squares) [138]

BEC limit the EFT results are in excellent agreement with both the data from [139] (red dot-dashed line) and with the healing length obtained from the standard Gross-Pitaevskii treatment. The influence of temperature on the characteristic length are examined in 5.20: while on the BEC side of the crossover temperature has no effect, on the BCS side at higher temperatures the critical transverse width of the system is enhanced.

In Figure 5.21 the effect of spin imbalance on the critical transverse size is examined. It appears that the presence of unpaired particles stabilises the soliton: the value of  $k_c$  at a fixed interaction strength decreases when increasing the imbalance parameter  $\zeta$ , meaning that for a given width of the atomic cloud a soliton in an imbalanced setup can be stable while one in a balanced system is unstable. This can be qualitatively explained in terms of the observation that in an imbalanced configuration the soliton core is an energetically favorable place to accommodate the unpaired particles [3]. Because of this the system may favor the soliton configuration over the vortex one since the former offers more space to store the excess component particles. To conclude it is important to remark that this last observation is consistent with the discussion about the effects of temperature (Fig.5.20) since, similarly to imbalance, an increase in temperature also enhances the number of unpaired particles in the system in the BCS regime.

## 5.6 Discussion and conclusions

In the previous sections an extensive description of the properties of dark solitons in a Fermi superfluid was carried out in the framework of the effective field theory presented in [1, 70] and derived in detail in Chapter 2 of this thesis. The first part of the chapter was dedicated to the study of the soliton solutions of the equation of motion for the Lagrangian (5.6) in terms of the amplitude and phase of the order parameter  $\Phi$ . The effect of

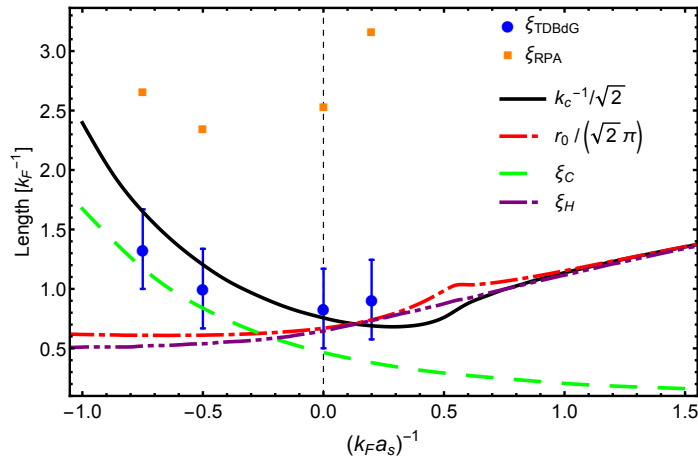


Figure 5.19: The EFT prediction for the minimum transverse dimension necessary for observing soliton decay through the snake instability (full black line) is compared to the results of the RPA (orange squares), of the time dependent Bogoliubov-de Gennes simulations (blue circles) [138], and of the calculations by Muñoz Mateo and Brand [139] (red dot-dashed line) based on the coarse-grained BdG theory [99]. In addition the BCS coherence length  $\xi_C$  (green dashed line) and BEC healing length  $\xi_H$  (purple dot-dot-dashed line) are shown. The numerical factors are introduced to overcome differences in the definitions of the healing lengths between Refs. [129, 138, 139] as discussed in [4].

temperature and population imbalance were analysed across the BEC-BCS crossover. The fact that in the building of the EFT no hypothesis is made requiring the pair field to be small, in principle extends the range of validity of this theory with respect to the widely employed Ginzburg-Landau and BdG approaches enabling us to consider also the effect of temperature on the system. From the discussion of Section 3.4 it emerged that, while the calculations relative to the BEC regime are valid for all temperatures in the range from 0 to  $T_c$ , at unitarity and on the BCS side of the resonance this is true just for temperatures close to the critical one.

Based on analytic expressions for the amplitude and phase spatial profiles, the density and the density of the excess-spin component were obtained in the LDA approximation using for the bulk value of the order parameter the mean field results. By systematically analyzing the density profiles we have observed how increasing the imbalance (and consequently decreasing the number of particles available for pairing) results in a filling of the soliton core that thus proves to be a convenient place where the unpaired particles can be stored. This translates into a decrease of the modulus of the effective mass of the soliton with increasing imbalance. However, in the crossover region in the vicinity of the unitarity regime we observe that the effect of the imbalance on  $M_s$  is reversed. A discrepancy was observed between the EFT predictions concerning the effective mass across the BEC-BCS crossover and those reported in other papers all based on the solution of the time-dependent Bogoliubov-de Gennes equations [125, 126, 142] at zero temperature.

Keeping in mind the experimental setup employed in the investigation of solitons in ul-

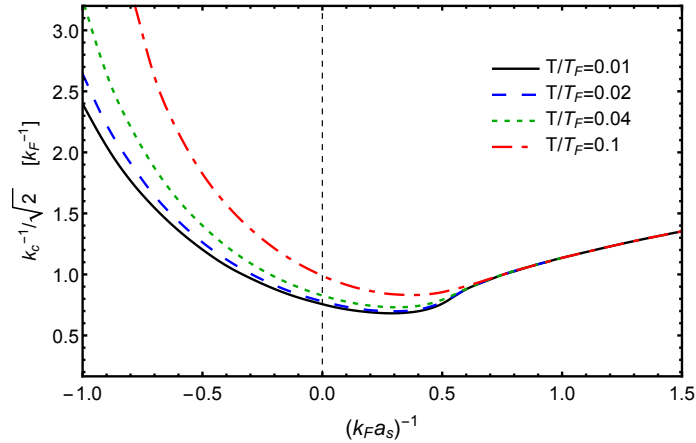


Figure 5.20: Minimum size of the atomic cloud  $k_c^{-1}/\sqrt{2}$  for the occurrence of the snake instability across the BEC-BCS crossover for different temperatures, i.e.  $T = 0.01T_F$  (full black line),  $T = 0.02T_F$  (blue dashed line),  $T = 0.04T_F$  (green dotted line) and  $\zeta = 0.1$  (red dot-dashed line).

tracold gases a substantial part of our results was presented as a function of the soliton velocity  $v_S$  in order to facilitate a direct comparison with future experimental results.

Motivated by the theoretical predictions and experimental observations of the decay of dark solitons through the snake instability mechanism, in the second part of the chapter this phenomenon was studied as a function of interaction strength and population imbalance. The distortion of the depletion plane characteristic of the onset of the snake instability is treated by adding a transverse perturbation in the form (5.37) to the stable solution  $\Phi_s$  of the equations of motion for the *quasi*-1D configuration described in Section 5.2. The numerical solution of the coupled system of nonlinear differential equations describing the perturbation amplitude provides the spectra of the instability. The dispersion  $\Omega(k)$  is examined in different interaction regimes and the BEC prediction [129] for the position of the maxima of  $\text{Im}[\Omega(k)]$  is verified and extended to the BCS-side of the resonance. The minimal transverse size for the soliton decay is qualitatively estimated as  $k_c^{-1}$ ,  $k_c$  being the maximal wave number for which unstable modes exist. The results obtained show a good quantitative agreement with those of the coarse-grained BdG theory [139] in the BEC-regime and the available numerical results of the TDBdG calculations [138] across the crossover. Moreover the EFT results seem to correctly characterise the change in the relevant length scale, from the condensate healing length in the BEC limit to the correlation length in the BCS regime.

At a later stage in Section 5.5 the effects of spin-imbalance and temperature on the stability of the soliton are discussed. The maximum transverse size that the atomic cloud can have in order for the soliton to be stable is shown to increase in the presence of spin-imbalance or at higher temperatures. This could in principle offer a way to stabilise the soliton configuration in experiments without being forced to reduce the transverse size of the trap. The analysis carried out in the present work is based on the perturbation of

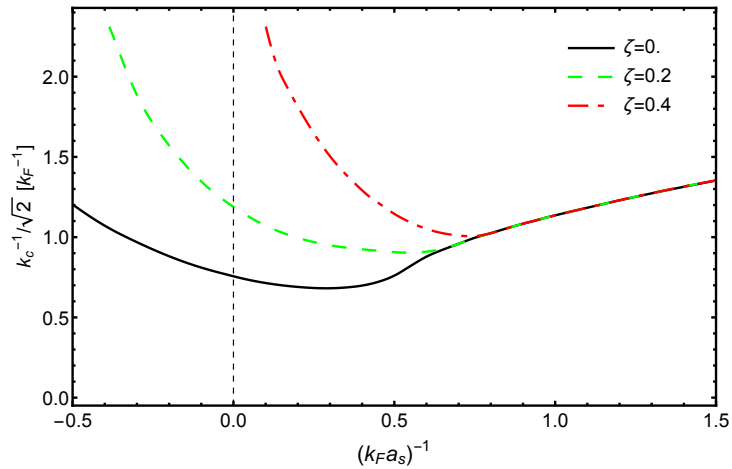


Figure 5.21: Minimum transverse size of the atomic cloud  $k_c^{-1}/\sqrt{2}$  for the occurrence of the snake instability across the BEC-BCS crossover for different values of the imbalance parameter  $\zeta$ , i.e.  $\zeta = 0$  (full black line),  $\zeta = 0.2$  (green dashed line) and  $\zeta = 0.4$  (red dot-dashed line). The lines for  $\zeta \neq 0$  do not cover the entire interaction domain due to the fact that in the presence of imbalance the superfluid state does not exist across the whole BEC-BCS crossover.

stable solitons solutions derived in Section 5.2 and published in [3, 70] which were obtained under the hypothesis of a uniform system. While most experiments concerning ultracold quantum gases employ harmonic traps to confine the atomic cloud, recently box-like optical traps that well approximate a uniform configuration were developed [141]: such setups can provide the opportunity of directly testing the predictions of this work in experiment.

# Chapter 6

## Conclusions and outlook

In this thesis an effective field theory suitable to describe the superfluid phase of a system of ultracold Fermi atoms in terms of the pairing order parameter was developed.

Starting from the weak requirement of having an order parameter that varies slowly in both time and space, in Chapter 2 the mathematical derivation of the EFT in the framework of the path integral formalism was carried out in full detail. The result is an effective field action that includes terms with space and time derivatives up to second order of the superfluid order parameter  $\Phi$ . Thanks to the form of the gradient expansion of  $\Phi$  exploited in order to enforce the requirement of slow variations, the different terms can be calculated separately. In Section 2.7 the final expression for the effective action  $S_{EFT}$  was given, along with the definitions of the EFT coefficients, which formally still depend on  $\Phi$ .

In Chapter 3 the first simple applications of the EFT were reviewed. In Section 3.1 the spectrum of the collective excitations of the superfluid was calculated starting from a quadratic expansion of the EFT action in terms of the beyond mean-field fluctuations of the order parameter. In the long-wavelength limit the dispersion relation for the Bogoliubov modes is determined by a linear term plus a cubic correction, with prefactors that can be determined in terms of the EFT coefficients: the dependence of the latter on  $\Phi$  permits to describe how the spectrum changes in function of the interaction. The prefactor of the linear term is interpreted as the sound velocity  $c_S$ , and a comparison between the EFT predictions and those by Salasnich *et al.* [71] shows a very good agreement across the entire BEC-BCS crossover. The same level of agreement was not found when the coefficient  $\lambda$  of the cubic correction was compared to the results of Kurkjian *et al.* [74]: while in the BEC limit the predictions coincide, a discrepancy arises and becomes more and more relevant when going towards the BCS side of the resonance. In particular the EFT version of  $\lambda$  remains positive across the entire interaction regime, while the one of [74] crosses zero around unitarity and becomes negative in the BCS regime.

In Section 3.2 the fluctuation correction to the total density were calculated using a hybrid EFT-NSR approach. The transition temperature  $T_c$  was calculated and the results compared to the implementations of the NSR scheme by Perali *et al.* [84] and by Sá de Melo *et al.* [46] finding an overall good agreement. In the BCS limit the mean-field prediction

was correctly retrieved.

Section 3.3 is dedicated to the calculation of correlation functions starting from the EFT action. To do so a generating functional method was derived that enables to calculate correlation functions of all orders. This method was then applied to the calculation of the condensate fraction and of the pair coherence length at the mean-field level. The pair coherence length serves as an estimate of the size of the Cooper pairs and, in Section 3.4, this quantity was employed to test whether the requirement of slow variations of the order parameter that lies at the basis of the EFT is fulfilled in different interaction regimes. This test yielded an indirect estimate of the region of validity for the predictions of the theory. In particular it was demonstrated that the EFT provides very good results in the BEC regime at all temperatures below  $T_c$  but, when going towards the BCS side of the resonance the reliability of the predictions at low temperatures decreases. In the BCS limit the EFT still remains valid close to  $T_c$  similar to the Ginzburg-Landau treatment.

In Subsection 3.5.1 it was demonstrated that, in the BEC limit at  $T = 0$ , the EFT equation of motion becomes equivalent to the Gross-Pitaevskii equation for bosonic particles of mass  $M = 2m$  that interact through a contact potential with an effective boson-boson scattering length equal to twice the fermion-fermion one. Comparing the EFT coefficients to those of the time-dependent Ginzburg-Landau theory developed by Sá de Melo and coworkers [46], in Subsection 3.5.2, a very good agreement is found for all of the coefficients, with the only exception of the coefficient  $D$  of the first order time derivative. The EFT coefficient  $D$  is real in all interaction regimes, while its TDGL counterpart has an imaginary part that becomes more and more important as the interaction is tuned towards the BCS regime. This imaginary part accounts for a damped dynamics of the order parameter which is not captured by the present effective field theory.

In Chapter 4 a system composed by a single impurity atom interacting with the collective excitations of a fermionic superfluid was studied by mapping the problem on the Fröhlich Hamiltonian which, in recent years, has been widely used to study the similar BEC polaron problem. The validity of the parallel between the present problem and the BEC polaron one is in principle limited to the extreme BEC side of the Feshbach resonance. Thanks to the fact that the EFT can describe the interaction dependence of the spectrum of the collective excitations of the superfluid (that play the role of the phonons in the standard condensed matter version of the polaron problem), this similitude is extended to a wider region of the BEC-BCS crossover. The (generally small) corrections to the polaronic coupling constant and effective mass are estimated for different values of the strength of the fermion-fermion and of the boson-impurity interaction.

In Chapter 5 various aspects of dark solitons in Fermi superfluids were investigated. The first part of the chapter focuses on the properties of stable dark solitons in a quasi-1D configuration. The predictions obtained are well-suited for comparison with the results of experiments that employ an elongated trap which enables the soliton to move almost freely in one direction while being tightly confined in the transverse plane. The behaviour of the width and depth of the soliton was described in detail in different interaction regimes across

the BEC-BCS crossover, and different conditions of temperature, imbalance and soliton velocity were considered. The main result of this part of the chapter is the conclusion that the soliton core is an energetically convenient place where the unpaired particles (which may be present in the system because of finite temperature and/or nonzero population imbalance) can be accommodated. Also some dynamical properties of the soliton, such as its effective mass, were examined. A discrepancy was found between the EFT predictions for this quantity and the corresponding results obtained within the Bogoliubov-de Gennes treatment. The soliton effective mass in the BCS regime appears to be underestimated in the EFT approach: the source of the discrepancy may be that the bosonic nature of the EFT cannot capture the contribution to this quantity due to the presence of Andreev bound states in the soliton core, which is expected to become more and more relevant as the BCS limit is approached.

The second part of the chapter is dedicated to the study of the snake instability mechanism responsible for the decay of dark solitons into one (or more) vortex-like excitations. The stable soliton solution was modified with the addition of a transverse perturbation in the form of a combination of plane waves and the spectrum of the instability was obtained by linearising the equation of motion in the perturbation amplitudes and solving the corresponding eigenvalue problem for the frequency. The prediction by Muryshev *et al.* [129] about the position of the maximum of the dispersion relation for the unstable mode, made in the context of Bose-Einstein condensate, is confirmed and extended to the whole BEC-BCS crossover. Moreover a good qualitative agreement was detected in the comparison of the dispersion curves with the data obtained from time-dependent Bogoliubov-de Gennes calculations in [138]. The quantity that represents the main focus of this part of the chapter is the maximum transverse size that the atomic cloud can have in order for the soliton to be stable. The snake instability is a long-wavelength phenomenon: this means that above a critical value of the momentum  $k_c$  no unstable modes are detected. The inverse of the critical momentum, i.e.  $k_c^{-1}$ , can therefore be used as an estimate of the critical transverse size of the system. The dependence of  $k_c^{-1}$  on the fermion-fermion interaction was studied and the results were compared to the ones from the TDBdG treatment [138] and of the coarse-grained version of the BdG equation [139]: the EFT results agree with the predictions of both these methods on the BEC side of the resonance. Moreover the EFT data seem to be the only ones that correctly capture the change in the relevant length scale from the healing length in the BEC regime to the pair coherence length in the BCS regime.

In the final part of the chapter the effect of imbalance on the critical transverse size was examined. We find that, in the BCS regime, the value of  $k_c^{-1}$  for a given interaction strength is larger for an imbalanced system than for a balanced situation. This consideration, together with the similar observation made in regard to the finite-temperature case, represents another indication that the soliton core is a favorable place where the unpaired particles can be stored. In fact a soliton offers more space that can be used for this purpose than a vortex (which would be the product of the soliton's decay through the snake instability). Moreover it offers a possible direct method for stabilising solitons in experiment through imbalance, without having to reduce the dimensionality of the system.

In this thesis we have given an overview of only a part of the research about Fermi superfluids that has been carried out in the framework of the effective field theory derived in Chapter 2. The EFT has been employed also in the study of two-component fermionic systems [1] and of vortex configurations [145,146]. Moreover a study about soliton collisions is currently ongoing: the inelasticity of the collisions, the spatial displacement of the solitons after the collision, and the collective waves that originate from the collisions are being systematically analysed.

Other directions of further study concern the precise identification of the causes, and the solution, of some of the discrepancies between the predictions of the EFT and of other approaches found in literature. As highlighted in the course of the present work disagreeing results are most often found when considering the BCS regime, where the fermionic nature of the system strongly affects the physics. However it is not yet clear whether an elegant and direct way to incorporate fermionic corrections to the intrinsically bosonic EFT can be implemented.

The EFT description opens the way to many applications. With respect to other models, such as the Bogoliubov-de Gennes theory, that are computationally demanding even when a single vortex or soliton is considered, the current treatment has the advantage of requiring much less computational time and memory. Thus, in the future it will be possible to study the behaviour of the system when it contains many vortices or solitons. Moreover, this theory allows for an easy extension to multi-component systems, which enables us to investigate whether new phenomena – that do not occur in individual superfluids – can instead occur in multi-component mixtures.

# References

- [1] S. N. Klimin, J. Tempere, G. Lombardi, and J. T. Devreese, “Finite temperature effective field theory and two-band superfluidity in Fermi gases,” *Eur. Phys. J. B*, vol. 88, no. 5, 2015.
- [2] G. Lombardi and J. Tempere, “Polaronic effects of an impurity in a Fermi superfluid away from the BEC limit,” *arXiv:1604.00776 [cond-mat.quant-gas]*, Apr 2016.
- [3] G. Lombardi, W. Van Alphen, S. N. Klimin, and J. Tempere, “Soliton-core filling in superfluid Fermi gases with spin imbalance,” *Phys. Rev. A*, vol. 93, p. 013614, Jan 2016.
- [4] G. Lombardi, W. Van Alphen, S. N. Klimin, and J. Tempere, “Snake instability of dark solitons across the BEC-BCS crossover: an effective field theory perspective,” *arXiv:1612.07558 [cond-mat.quant-gas]*, Dec 2016.
- [5] B.-B. Huang and S.-L. Wan, “Polaron in Bose-Einstein-condensation system,” *Chin. Phys. Lett.*, vol. 26, p. 080302, 2009.
- [6] A. Novikov and M. Ovchinnikov, “A diagrammatic calculation of the energy spectrum of quantum impurity in degenerate Bose-Einstein condensate,” *Journal of Physics A: Mathematical and Theoretical*, vol. 42, no. 13, p. 135301, 2009.
- [7] D. K. K. Lee and J. M. F. Gunn, “Polarons and Bose decondensation: A self-trapping approach,” *Phys. Rev. B*, vol. 46, pp. 301–307, Jul 1992.
- [8] F. M. Cucchietti and E. Timmermans, “Strong-coupling polarons in dilute gas Bose-Einstein condensates,” *Phys. Rev. Lett.*, vol. 96, p. 210401, Jun 2006.
- [9] R. M. Kalas and D. Blume, “Interaction-induced localization of an impurity in a trapped Bose-Einstein condensate,” *Phys. Rev. A*, vol. 73, p. 043608, Apr 2006.
- [10] K. Sacha and E. Timmermans, “Self-localized impurities embedded in a one-dimensional Bose-Einstein condensate and their quantum fluctuations,” *Phys. Rev. A*, vol. 73, p. 063604, Jun 2006.
- [11] D. C. Roberts and S. Rica, “Impurity crystal in a Bose-Einstein condensate,” *Phys. Rev. Lett.*, vol. 102, p. 025301, Jan 2009.

- 
- [12] J. Tempere, W. Casteels, M. K. Oberthaler, S. Knoop, E. Timmermans, and J. T. Devreese, “Feynman path-integral treatment of the BEC-impurity polaron,” *Phys. Rev. B*, vol. 80, p. 184504, Nov 2009.
- [13] F. Grusdt, Y. E. Shchadilova, A. N. Rubtsov, and E. Demler, “Fröhlich polaron model: application to impurity-BEC problem,” *Sci. Rep.*, vol. 5, p. 12124, July 2015.
- [14] L. A. Peña Ardila and S. Giorgini, “Impurity in a Bose-Einstein condensate: Study of the attractive and repulsive branch using quantum Monte Carlo methods,” *Phys. Rev. A*, vol. 92, p. 033612, Sep 2015.
- [15] S. N. Bose, “Plancks gesetz und lichtquantenhypothese,” *Zeitschrift für Physik*, vol. 26, no. 1, pp. 178–181, 1924.
- [16] A. Einstein, “Quantentheorie des einatomigen idealen gases,” *Sitzungsberichte der Preussischen Akademie der Wissenschaften*, vol. 1, pp. 3–14, 1925.
- [17] M. H. Anderson, J. R. Ensher, M. R. Matthews, C. E. Wieman, and E. A. Cornell, “Observation of Bose-Einstein condensation in a dilute atomic vapor,” *Science*, vol. 269, no. 5221, pp. 198–201, 1995.
- [18] K. B. Davis, M. O. Mewes, M. R. Andrews, N. J. van Druten, D. S. Durfee, D. M. Kurn, and W. Ketterle, “Bose-Einstein condensation in a gas of sodium atoms,” *Phys. Rev. Lett.*, vol. 75, pp. 3969–3973, Nov 1995.
- [19] C. C. Bradley, C. A. Sackett, J. J. Tollett, and R. G. Hulet, “Evidence of Bose-Einstein condensation in an atomic gas with attractive interactions,” *Phys. Rev. Lett.*, vol. 75, pp. 1687–1690, Aug 1995.
- [20] C. Pethick and H. Smith, *Bose-Einstein Condensation in Dilute Gases*. Cambridge University Press, 2002.
- [21] L. Pitaevskii and S. Stringari, *Bose-Einstein Condensation*. International Series of Monographs on Physics, Clarendon Press, 2003.
- [22] W. Ketterle, D. S. Durfee, and D. M. Stamper-Kurn, *Making, Probing and Understanding Bose-Einstein condensates*, pp. 67–176. IOS Press, Amsterdam, 1999.
- [23] W. Ketterle and M. Zwierlein, “Making, probing and understanding ultracold Fermi gases,” *Rivista del nuovo cimento*, vol. 31, pp. 247–422, 2008.
- [24] W. D. Phillips and H. Metcalf, “Laser deceleration of an atomic beam,” *Phys. Rev. Lett.*, vol. 48, pp. 596–599, Mar 1982.
- [25] S. Chu, L. Hollberg, J. E. Bjorkholm, A. Cable, and A. Ashkin, “Three-dimensional viscous confinement and cooling of atoms by resonance radiation pressure,” *Phys. Rev. Lett.*, vol. 55, pp. 48–51, Jul 1985.

- 
- [26] A. Aspect, E. Arimondo, R. Kaiser, N. Vansteenkiste, and C. Cohen-Tannoudji, “Laser cooling below the one-photon recoil energy by velocity-selective coherent population trapping,” *Phys. Rev. Lett.*, vol. 61, pp. 826–829, Aug 1988.
- [27] C. J. Myatt, E. A. Burt, R. W. Ghrist, E. A. Cornell, and C. E. Wieman, “Production of two overlapping Bose-Einstein condensates by sympathetic cooling,” *Phys. Rev. Lett.*, vol. 78, pp. 586–589, Jan 1997.
- [28] L. D. Landau, “Über die Bewegung der Elektronen in Kristallgitter,” *Phys. Z. Sowjetunion*, vol. 3, p. 644–645, 1933.
- [29] T. D. Lee, F. E. Low, and D. Pines, “The motion of slow electrons in a polar crystal,” *Phys. Rev.*, vol. 90, pp. 297–302, Apr 1953.
- [30] H. Fröhlich, “Electrons in lattice fields,” *Advances in Physics*, vol. 3, no. 11, pp. 325–361, 1954.
- [31] L. Landau and S. I. Pekar, “Effective mass of a polaron,” *Zh. Eksp. Teor. Fiz.*, vol. 18, p. 419, 1948.
- [32] V. Popov, “Theory of a Bose Gas Produced by Bound States of Fermi Particles,” *Sov. Phys. JETP*, vol. 23.
- [33] K. L. D. and A. N. Kozlov, “Collective Properties of Excitons in Semiconductors,” *Sov. Phys. JETP*, vol. 27.
- [34] D. M. Eagles, “Possible pairing without superconductivity at low carrier concentrations in bulk and thin-film superconducting semiconductors,” *Phys. Rev.*, vol. 186, pp. 456–463, Oct 1969.
- [35] A. J. Leggett, *Diatomic molecules and Cooper pairs*, pp. 13–27. Berlin, Heidelberg: Springer Berlin Heidelberg, 1980.
- [36] B. DeMarco and D. S. Jin, “Onset of Fermi degeneracy in a trapped atomic gas,” *Science*, vol. 285, no. 5434, pp. 1703–1706, 1999.
- [37] C. A. Regal and D. S. Jin, “Measurement of positive and negative scattering lengths in a Fermi gas of atoms,” *Phys. Rev. Lett.*, vol. 90, p. 230404, Jun 2003.
- [38] S. Jochim, M. Bartenstein, A. Altmeyer, G. Hendl, S. Riedl, C. Chin, J. Hecker Denschlag, and R. Grimm, “Bose-Einstein condensation of molecules,” *Science*, vol. 302, no. 5653, pp. 2101–2103, 2003.
- [39] M. Greiner, C. A. Regal, and D. S. Jin, “Emergence of a molecular Bose-Einstein condensate from a Fermi gas,” *Nature*, vol. 426, pp. 537–540, 2003.

- 
- [40] M. W. Zwierlein, C. A. Stan, C. H. Schunck, S. M. F. Raupach, S. Gupta, Z. Hadzibabic, and W. Ketterle, "Observation of Bose-Einstein condensation of molecules," *Phys. Rev. Lett.*, vol. 91, p. 250401, Dec 2003.
- [41] M. Bartenstein, A. Altmeyer, S. Riedl, S. Jochim, C. Chin, J. H. Denschlag, and R. Grimm, "Crossover from a molecular Bose-Einstein condensate to a degenerate Fermi gas," *Phys. Rev. Lett.*, vol. 92, p. 120401, Mar 2004.
- [42] M. W. Zwierlein, J. R. Abo-Shaeer, A. Schirotzek, C. H. Schunck, and W. Ketterle, "Vortices and superfluidity in a strongly interacting Fermi gas," *Nature*, vol. 435, pp. 1047–1051, 2003.
- [43] M. W. Zwierlein, C. A. Stan, C. H. Schunck, S. M. F. Raupach, A. J. Kerman, and W. Ketterle, "Condensation of pairs of fermionic atoms near a Feshbach resonance," *Phys. Rev. Lett.*, vol. 92, p. 120403, Mar 2004.
- [44] C. A. Regal, M. Greiner, and D. S. Jin, "Observation of resonance condensation of fermionic atom pairs," *Phys. Rev. Lett.*, vol. 92, p. 040403, Jan 2004.
- [45] P. Nozières and S. Schmitt-Rink, "Bose condensation in an attractive fermion gas: From weak to strong coupling superconductivity," *Journal of Low Temperature Physics*, vol. 59, no. 3, pp. 195–211, 1985.
- [46] C. A. R. Sá de Melo, M. Randeria, and J. R. Engelbrecht, "Crossover from BCS to Bose superconductivity: Transition temperature and time-dependent Ginzburg-Landau theory," *Phys. Rev. Lett.*, vol. 71, pp. 3202–3205, Nov 1993.
- [47] C. A. R. Sá de Melo, "When fermions become bosons: Pairing in ultracold gases," *Physics Today*, vol. 61, no. 10, pp. 45–51, 2008.
- [48] A. M. Clogston, "Upper limit for the critical field in hard superconductors," *Phys. Rev. Lett.*, vol. 9, pp. 266–267, Sep 1962.
- [49] B. S. Chandrasekhar, "A note on the maximum critical field of high-field superconductors," *Applied Physics Letters*, vol. 1, no. 1, 1962.
- [50] J. P. A. Devreese, *De Fulde-Ferrell-Larkin-Ovchinnikov toestand in een Fermi gas met spin-onevenwicht*. PhD thesis, Universiteit Antwerpen, May 2013.
- [51] M. W. Zwierlein, A. Schirotzek, C. H. Schunck, and W. Ketterle, "Fermionic superfluidity with imbalanced spin populations," *Science*, vol. 311, no. 5760, pp. 492–496, 2006.
- [52] G. B. Partridge, W. Li, R. I. Kamar, Y.-a. Liao, and R. G. Hulet, "Pairing and phase separation in a polarized Fermi gas," *Science*, vol. 311, no. 5760, pp. 503–505, 2006.

- 
- [53] P. Fulde and R. A. Ferrell, “Superconductivity in a strong spin-exchange field,” *Phys. Rev.*, vol. 135, pp. A550–A563, Aug 1964.
- [54] A. I. Larkin and Y. N. Ovchinnikov, “Nonuniform state of superconductors,” *Sov. Phys. JETP*, vol. 20, p. 762, 1965.
- [55] E. P. Gross, “Structure of a quantized vortex in boson systems,” *Il Nuovo Cimento (1955-1965)*, vol. 20, no. 3, pp. 454–477, 1961.
- [56] L. Pitaevskii, “Vortex lines in an imperfect Bose gas,” *Sov. Phys. JETP*, vol. 13, no. 2, pp. 451–454, 1961.
- [57] G. B. Hess and W. M. Fairbank, “Measurements of angular momentum in superfluid helium,” *Phys. Rev. Lett.*, vol. 19, pp. 216–218, Jul 1967.
- [58] V. L. Ginzburg and L. D. Landau, “On the Theory of superconductivity,” *Zh. Eksp. Teor. Fiz.*, vol. 20, pp. 1064–1082, 1950.
- [59] A. Abrikosov, “The magnetic properties of superconducting alloys,” *Journal of Physics and Chemistry of Solids*, vol. 2, no. 3, pp. 199 – 208, 1957.
- [60] M. Tinkham, *Introduction to Superconductivity: Second Edition*. Dover Books on Physics, Dover Publications, 2004.
- [61] L. P. Gor’kov, “Microscopic derivation of the Ginzburg-Landau equations in the theory of superconductivity,” *Sov. Phys. JETP*, vol. 36(9), pp. 1364–1367, 1959.
- [62] M. Machida and T. Koyama, “Time-dependent Ginzburg-Landau theory for atomic Fermi gases near the BCS-BEC crossover,” *Phys. Rev. A*, vol. 74, p. 033603, Sep 2006.
- [63] L. Salasnich, N. Manini, and F. Toigo, “Macroscopic periodic tunneling of Fermi atoms in the BCS-BEC crossover,” *Phys. Rev. A*, vol. 77, p. 043609, Apr 2008.
- [64] K. Huang, Z.-Q. Yu, and L. Yin, “Ginzburg-Landau theory of a trapped Fermi gas with a BEC-BCS crossover,” *Phys. Rev. A*, vol. 79, p. 053602, May 2009.
- [65] S. Chen and B. Guo, “Classical solutions of time-dependent Ginzburg-Landau theory for atomic Fermi gases near the BCS-BEC crossover,” *Journal of Differential Equations*, vol. 251, no. 6, pp. 1415 – 1427, 2011.
- [66] S. Klimin, J. Tempere, and J. Devreese, “Extension of the Ginzburg-Landau approach for ultracold Fermi gases below a critical temperature,” *Physica C: Superconductivity*, vol. 503, pp. 136 – 139, 2014.
- [67] R. P. Feynman, “Space-time approach to non-relativistic quantum mechanics,” *Rev. Mod. Phys.*, vol. 20, pp. 367–387, Apr 1948.

- 
- [68] H. T. C. Stoof, D. B. M. Dickerscheid, and K. Gubbels, *Ultracold Quantum Fields*. Theoretical and Mathematical Physics, Springer Netherlands, 2009.
- [69] J. Tempere and J. P. Devreese, *Path-integral description of Cooper pairing*. New York, USA: Intech open publishing, 2012.
- [70] S. N. Klimin, J. Tempere, and J. T. Devreese, “Finite-temperature effective field theory for dark solitons in superfluid Fermi gases,” *Phys. Rev. A*, vol. 90, p. 053613, Nov 2014.
- [71] L. Salasnich, P. A. Marchetti, and F. Toigo, “Superfluidity, sound velocity, and quasicondensation in the two-dimensional BCS-BEC crossover,” *Phys. Rev. A*, vol. 88, p. 053612, Nov 2013.
- [72] Marini, M., Pistolesi, F., and Strinati, G. C., “Evolution from BCS superconductivity to Bose condensation: analytic results for the crossover in three dimensions,” *Eur. Phys. J. B*, vol. 1, no. 2, pp. 151–159, 1998.
- [73] G. Bighin, L. Salasnich, P. A. Marchetti, and F. Toigo, “Beliaev damping of the Goldstone mode in atomic Fermi superfluids,” *Phys. Rev. A*, vol. 92, p. 023638, Aug 2015.
- [74] H. Kurkjian, Y. Castin, and A. Sinatra, “Concavity of the collective excitation branch of a Fermi gas in the BEC-BCS crossover,” *Phys. Rev. A*, vol. 93, p. 013623, Jan 2016.
- [75] H. Hu, X.-J. Liu, and P. D. Drummond, “Universal thermodynamics of strongly interacting Fermi gases,” *EPL (Europhysics Letters)*, vol. 74, no. 4, p. 574, 2006.
- [76] H. Hu, P. D. Drummond, and X.-J. Liu, “Equation of state of a superfluid Fermi gas in the BCS-BEC crossover,” *EPL (Europhysics Letters)*, vol. 3, p. 469, 2007.
- [77] R. B. Diener, R. Sensarma, and M. Randeria, “Quantum fluctuations in the superfluid state of the BCS-BEC crossover,” *Phys. Rev. A*, vol. 77, p. 023626, Feb 2008.
- [78] R. B. Diener and M. Randeria, “BCS-BEC crossover with unequal-mass fermions,” *Phys. Rev. A*, vol. 81, p. 033608, Mar 2010.
- [79] J. Keeling, P. R. Eastham, M. H. Szymanska, and P. B. Littlewood, “BCS-BEC crossover in a system of microcavity polaritons,” *Phys. Rev. B*, vol. 72, p. 115320, Sep 2005.
- [80] N. Lerch, L. Bartosch, and P. Kopietz, “Absence of fermionic quasiparticles in the superfluid state of the attractive Fermi gas,” *Phys. Rev. Lett.*, vol. 100, p. 050403, Feb 2008.

- 
- [81] S. N. Klimin, J. Tempere, and J. T. Devreese, “Pseudogap and preformed pairs in the imbalanced Fermi gas in two dimensions,” *New Journal of Physics*, vol. 14, no. 10, p. 103044, 2012.
- [82] N. Andrenacci, P. Pieri, and G. C. Strinati, “Evolution from BCS superconductivity to Bose-Einstein condensation: Current correlation function in the broken-symmetry phase,” *Phys. Rev. B*, vol. 68, p. 144507, Oct 2003.
- [83] P. Pieri and G. C. Strinati, “Popov approximation for composite bosons in the BCS-BEC crossover,” *Phys. Rev. B*, vol. 71, p. 094520, Mar 2005.
- [84] A. Perali, P. Pieri, L. Pisani, and G. C. Strinati, “BCS-BEC crossover at finite temperature for superfluid trapped Fermi atoms,” *Phys. Rev. Lett.*, vol. 92, p. 220404, Jun 2004.
- [85] P. Pieri, L. Pisani, and G. C. Strinati, “Comparison between a diagrammatic theory for the BCS-BEC crossover and quantum Monte Carlo results,” *Phys. Rev. B*, vol. 72, p. 012506, Jul 2005.
- [86] Y. Ohashi and A. Griffin, “Superfluidity and collective modes in a uniform gas of Fermi atoms with a Feshbach resonance,” *Phys. Rev. A*, vol. 67, p. 063612, Jun 2003.
- [87] E. Taylor, A. Griffin, N. Fukushima, and Y. Ohashi, “Pairing fluctuations and the superfluid density through the BCS-BEC crossover,” *Phys. Rev. A*, vol. 74, p. 063626, Dec 2006.
- [88] N. Fukushima, Y. Ohashi, E. Taylor, and A. Griffin, “Superfluid density and condensate fraction in the BCS-BEC crossover regime at finite temperatures,” *Phys. Rev. A*, vol. 75, p. 033609, Mar 2007.
- [89] K. Levin, Q. Chen, C.-C. Chien, and Y. He, “Comparison of different pairing fluctuation approaches to BCS-BEC crossover,” *Annals of Physics*, vol. 325, no. 2, pp. 233 – 264, 2010.
- [90] M. Y. Kagan, *Modern trends in Superconductivity and Superfluidity*. Lecture Notes in Physics 874, Springer Netherlands, 1 ed., 2013.
- [91] A. Fetter and J. Walecka, *Quantum theory of many-particle systems*. International series in pure and applied physics, McGraw-Hill, 1971.
- [92] L. Salasnich, N. Manini, and A. Parola, “Condensate fraction of a Fermi gas in the BCS-BEC crossover,” *Phys. Rev. A*, vol. 72, p. 023621, Aug 2005.
- [93] F. Palestini and G. C. Strinati, “Temperature dependence of the pair coherence and healing lengths for a fermionic superfluid throughout the BCS-BEC crossover,” *Phys. Rev. B*, vol. 89, p. 224508, Jun 2014.

- [94] F. Pistolesi and G. C. Strinati, “Evolution from BCS superconductivity to Bose condensation: Role of the parameter  $k_F\xi$ ,” *Phys. Rev. B*, vol. 49, pp. 6356–6359, Mar 1994.
- [95] A. Leggett, *Quantum Liquids: Bose Condensation and Cooper Pairing in Condensed-matter Systems*. Oxford graduate texts in mathematics, OUP Oxford, 2006.
- [96] V. V. Konotop and L. Pitaevskii, “Landau dynamics of a grey soliton in a trapped condensate,” *Phys. Rev. Lett.*, vol. 93, p. 240403, Dec 2004.
- [97] D. J. Frantzeskakis, “Dark solitons in atomic Bose-Einstein condensates: from theory to experiments,” *Journal of Physics A: Mathematical and Theoretical*, vol. 43, no. 21, p. 213001, 2010.
- [98] A. J. Heeger, S. Kivelson, J. R. Schrieffer, and W. P. Su, “Solitons in conducting polymers,” *Rev. Mod. Phys.*, vol. 60, pp. 781–850, Jul 1988.
- [99] S. Simonucci and G. C. Strinati, “Equation for the superfluid gap obtained by coarse graining the Bogoliubov-de Gennes equations throughout the BCS-BEC crossover,” *Phys. Rev. B*, vol. 89, p. 054511, Feb 2014.
- [100] L. Pitaevskii and S. Stringari, *Bose-Einstein Condensation and Superfluidity*. International series of monographs on physics, Oxford University Press, 2016.
- [101] S. Simonucci, P. Pieri, and G. C. Strinati, “Temperature dependence of a vortex in a superfluid fermi gas,” *Phys. Rev. B*, vol. 87, p. 214507, Jun 2013.
- [102] A. S. Alexandrov and J. T. Devreese, *Advances in Polaron Physics*, vol. 159 of *Springer Series in Solid-State Sciences*. Springer-Verlag Berlin Heidelberg, 2010.
- [103] N. N. Bogoliubov and S. V. Tyablikov, “An approximate method of finding the lowest energy levels of electrons in metals,” *Zh. Eksper. Teor. Fiz.*, vol. 19, p. 256, 1949.
- [104] N. V. Prokof’ev and B. V. Svistunov, “Polaron problem by diagrammatic quantum Monte Carlo,” *Phys. Rev. Lett.*, vol. 81, pp. 2514–2517, Sep 1998.
- [105] M. Hohmann, F. Kindermann, B. Ganger, T. Lausch, D. Mayer, F. Schmidt, and A. Widera, “Neutral impurities in a Bose-Einstein condensate for simulation of the frohlich-polaron,” *EPJ Quantum Technology*, vol. 2, no. 1, p. 23, 2015.
- [106] M.-G. Hu, M. J. Van de Graaff, D. Kedar, J. P. Corson, E. A. Cornell, and D. S. Jin, “Bose polarons in the strongly interacting regime,” *Phys. Rev. Lett.*, vol. 117, p. 055301, Jul 2016.
- [107] N. B. Jørgensen, L. Wacker, K. T. Skalmstang, M. M. Parish, J. Levinsen, R. S. Christensen, G. M. Bruun, and J. J. Arlt, “Observation of attractive and repulsive polarons in a Bose-Einstein condensate,” *Phys. Rev. Lett.*, vol. 117, p. 055302, Jul 2016.

- 
- [108] N. Prokof'ev and B. Svistunov, "Fermi-polaron problem: Diagrammatic Monte Carlo method for divergent sign-alternating series," *Phys. Rev. B*, vol. 77, p. 020408, Jan 2008.
- [109] M. Punk, P. T. Dumitrescu, and W. Zwerger, "Polaron-to-molecule transition in a strongly imbalanced Fermi gas," *Phys. Rev. A*, vol. 80, p. 053605, Nov 2009.
- [110] C. J. M. Mathy, M. M. Parish, and D. A. Huse, "Trimers, molecules, and polarons in mass-imbalanced atomic Fermi gases," *Phys. Rev. Lett.*, vol. 106, p. 166404, Apr 2011.
- [111] P. Massignan, "Polarons and dressed molecules near narrow Feshbach resonances," *EPL (Europhysics Letters)*, vol. 98, no. 1, p. 10012, 2012.
- [112] A. Schirotzek, C.-H. Wu, A. Sommer, and M. W. Zwierlein, "Observation of Fermi polarons in a tunable Fermi liquid of ultracold atoms," *Phys. Rev. Lett.*, vol. 102, p. 230402, Jun 2009.
- [113] F. Chevy and C. Mora, "Ultra-cold polarized Fermi gases," *Reports on Progress in Physics*, vol. 73, no. 11, p. 112401, 2010.
- [114] Y. Nishida, "Polaronic atom-trimer continuity in three-component fermi gases," *Phys. Rev. Lett.*, vol. 114, p. 115302, Mar 2015.
- [115] S. Shadkhoo and R. Bruinsma, "Impurities in Bose-Einstein condensates: From polaron to soliton," *Phys. Rev. Lett.*, vol. 115, p. 135305, Sep 2015.
- [116] D. S. Petrov, C. Salomon, and G. V. Shlyapnikov, "Diatomic molecules in ultracold fermi gases-novel composite bosons," *Journal of Physics B: Atomic, Molecular and Optical Physics*, vol. 38, no. 9, p. S645, 2005.
- [117] L. Salasnich and G. Bighin, "Scattering length of composite bosons in the three-dimensional BCS-BEC crossover," *Phys. Rev. A*, vol. 91, p. 033610, Mar 2015.
- [118] C. W. Litton, K. J. Button, J. Waldman, D. R. Cohn, and B. Lax, "Verification of polaron cyclotron-resonance theory and determination of the coupling constant in  $n - \text{CdTe}$ ," *Phys. Rev. B*, vol. 13, pp. 5392–5396, Jun 1976.
- [119] J. Denschlag, J. E. Simsarian, D. L. Feder, C. W. Clark, L. A. Collins, J. Cubizolles, L. Deng, E. W. Hagley, K. Helmerson, W. P. Reinhardt, S. L. Rolston, B. I. Schneider, and W. D. Phillips, "Generating solitons by phase engineering of a Bose-Einstein condensate," *Science*, vol. 287, no. 5450, pp. 97–101, 2000.
- [120] S. Burger, K. Bongs, S. Dettmer, W. Ertmer, K. Sengstock, A. Sanpera, G. V. Shlyapnikov, and M. Lewenstein, "Dark solitons in Bose-Einstein condensates," *Phys. Rev. Lett.*, vol. 83, pp. 5198–5201, Dec 1999.

- [121] B. P. Anderson, P. C. Haljan, C. A. Regal, D. L. Feder, L. A. Collins, C. W. Clark, and E. A. Cornell, “Watching dark solitons decay into vortex rings in a Bose-Einstein condensate,” *Phys. Rev. Lett.*, vol. 86, pp. 2926–2929, Apr 2001.
- [122] C. Becker, S. Stellmer, P. Soltan-Panahi, S. Dörscher, M. Baumert, E.-M. Richter, J. Kronjäger, K. Bongs, and K. Sengstock, “Oscillations and interactions of dark and dark-bright solitons in Bose-Einstein condensates,” *Nature*, vol. 4, p. 496, 2008.
- [123] M. Antezza, F. Dalfovo, L. P. Pitaevskii, and S. Stringari, “Dark solitons in a superfluid Fermi gas,” *Phys. Rev. A*, vol. 76, p. 043610, Oct 2007.
- [124] A. Spuntarelli, P. Pieri, and G. Strinati, “Solution of the Bogoliubov-de Gennes equations at zero temperature throughout the BCS-BEC crossover: Josephson and related effects,” *Physics Reports*, vol. 488, no. 4, pp. 111 – 167, 2010.
- [125] R. Liao and J. Brand, “Traveling dark solitons in superfluid Fermi gases,” *Phys. Rev. A*, vol. 83, p. 041604, Apr 2011.
- [126] R. G. Scott, F. Dalfovo, L. P. Pitaevskii, and S. Stringari, “Dynamics of dark solitons in a trapped superfluid Fermi gas,” *Phys. Rev. Lett.*, vol. 106, p. 185301, May 2011.
- [127] T. Yefsah, A. T. Sommer, M. J. H. Ku, L. W. Cheuk, W. Ji, W. S. Bakr, and M. W. Zwierlein, “Heavy solitons in a fermionic superfluid,” *Nature*, vol. 499, p. 426, 2013.
- [128] M. J. H. Ku, W. Ji, B. Mukherjee, E. Guardado-Sanchez, L. W. Cheuk, T. Yefsah, and M. W. Zwierlein, “Motion of a solitonic vortex in the BEC-BCS crossover,” *Phys. Rev. Lett.*, vol. 113, p. 065301, Aug 2014.
- [129] A. E. Muryshev, H. B. van Linden van den Heuvell, and G. V. Shlyapnikov, “Stability of standing matter waves in a trap,” *Phys. Rev. A*, vol. 60, pp. R2665–R2668, Oct 1999.
- [130] D. L. Feder, M. S. Pindzola, L. A. Collins, B. I. Schneider, and C. W. Clark, “Dark-soliton states of Bose-Einstein condensates in anisotropic traps,” *Phys. Rev. A*, vol. 62, p. 053606, Oct 2000.
- [131] J. Brand and W. P. Reinhardt, “Solitonic vortices and the fundamental modes of the “snake instability”: Possibility of observation in the gaseous Bose-Einstein condensate,” *Phys. Rev. A*, vol. 65, p. 043612, Apr 2002.
- [132] V. E. Zakharov and A. M. Rubenchik, “Instability of waveguides and solitons in nonlinear media,” *Sov. Phys. JETP*, vol. 38, pp. 494–500, March 1974.
- [133] M. Ma, R. Carretero-González, P. G. Kevrekidis, D. J. Frantzeskakis, and B. A. Malomed, “Controlling the transverse instability of dark solitons and nucleation of vortices by a potential barrier,” *Phys. Rev. A*, vol. 82, p. 023621, Aug 2010.

- 
- [134] S. Adhikari, “Stable, mobile, dark-in-bright, dipolar bose-einstein-condensate solitons,” *Phys. Rev. A*, vol. 89, p. 043615, Apr 2014.
- [135] S. Adhikari, “Stable and mobile two-dimensional dipolar ring-dark-in-bright bose-einstein condensate soliton,” *Laser Phys. Lett.*, vol. 13, p. 035502, Feb 2016.
- [136] N. Meyer, H. Proud, M. Perea-Ortiz, C. O’Neale, M. Baumert, M. Holynski, J. Kronjäger, G. Barontini, and K. Bongs, “Observation of Stable Jones-Roberts Solitons in Bose-Einstein Condensates,” *arXiv:1609.08504 [cond-mat.quant-gas]*, Sep 2016.
- [137] S. Donadello, S. Serafini, M. Tylutki, L. P. Pitaevskii, F. Dalfovo, G. Lamporesi, and G. Ferrari, “Observation of solitonic vortices in Bose-Einstein condensates,” *Phys. Rev. Lett.*, vol. 113, p. 065302, Aug 2014.
- [138] A. Cetoli, J. Brand, R. G. Scott, F. Dalfovo, and L. P. Pitaevskii, “Snake instability of dark solitons in fermionic superfluids,” *Phys. Rev. A*, vol. 88, p. 043639, Oct 2013.
- [139] A. Muñoz Mateo and J. Brand, “Chladni solitons and the onset of the snaking instability for dark solitons in confined superfluids,” *Phys. Rev. Lett.*, vol. 113, p. 255302, Dec 2014.
- [140] M. J. H. Ku, B. Mukherjee, T. Yefsah, and M. W. Zwierlein, “Cascade of solitonic excitations in a superfluid Fermi gas: From planar solitons to vortex rings and lines,” *Phys. Rev. Lett.*, vol. 116, p. 045304, Jan 2016.
- [141] A. L. Gaunt, T. F. Schmidutz, I. Gotlibovych, R. P. Smith, and Z. Hadzibabic, “Bose-Einstein condensation of atoms in a uniform potential,” *Phys. Rev. Lett.*, vol. 110, p. 200406, May 2013.
- [142] R. Liao and J. Brand, “Erratum: Traveling dark solitons in superfluid Fermi gases [Phys. Rev. A **83**, 041604(R) (2011)],” *Phys. Rev. A*, vol. 87, p. 059901(E), May 2013.
- [143] E. A. Kuznetsov and S. K. Turitsyn, “Instability and collapse of solitons in media with a defocusing nonlinearity,” *Sov. Phys. JETP*, vol. 67, p. 1583, Aug 1988.
- [144] J. T. Cole and Z. H. Musslimani, “Spectral transverse instabilities and soliton dynamics in the higher-order multidimensional nonlinear Schrödinger equation,” *Physica D: Nonlinear Phenomena*, vol. 313, pp. 26 – 36, 2015.
- [145] N. Verhelst, S. Klimin, and J. Tempere, “Verification of an analytic fit for the vortex core profile in superfluid Fermi gases,” *Physica C: Superconductivity and its Applications*, vol. 533, pp. 96 – 100, 2017. Ninth international conference on Vortex Matter in nanostructured Superconductors.
- [146] S. N. Klimin, J. Tempere, N. Verhelst, and M. V. Milošević, “Finite-temperature vortices in a rotating Fermi gas,” *Phys. Rev. A*, vol. 94, p. 023620, Aug 2016.



# List of publications by the author

## EFT-related publications

S. N. Klimin, J. Tempere, G. Lombardi, J. T. Devreese, “*Finite temperature effective field theory and two-band superfluidity in Fermi gases*”, European Physical Journal B **88**, 122 (2015)

G. Lombardi, W. Van Alphen, S. N. Klimin, J. Tempere, “*Soliton core filling in superfluid Fermi gases with spin-imbalance*”, Physical Review A **93**, 013614 (2016)

## EFT-related submitted material

G. Lombardi, J. Tempere, “*Polaronic effects of an impurity in a Fermi superfluid away from the BEC limit*”, arXiv: 1604.00776 [cond-mat.quant-gas] (2016)

G. Lombardi, W. Van Alphen, S. N. Klimin, J. Tempere, “*Snake instability of dark solitons across the BEC-BCS crossover: an effective field theory perspective*”, arXiv: 1612.07558 [cond-mat.quant-gas] (2016)

## Other publications

A. Ambrosetti, G. Lombardi, L. Salasnich, P. Silvestrelli, F. Toigo, “*Polarization of a quasi-two-dimensional repulsive Fermi gas with Rashba spin-orbit coupling: A variational study*”, Physical Review A **90**, 043614 (2014)



# Acknowledgements

Although a single name is written next to the entry "Author:" on the title-page of this dissertation, this work has been made possible by the contribution of a number of people.

First I would like to thank my supervisor prof. Jacques Tempere for all the precious advice he gave me, for his ability to find simple explanations to complicated concepts and for the wonderful environment that he managed to create in the TQC research group. When I was looking for a PhD position around Europe I couldn't have dreamed of carrying out my research activity in a more stimulating, rewarding and, at the same time, relaxed context. Also my co-supervisor dr. Sergei Klimin deserves a sincere acknowledgement for the huge amount of work notes that he put to my disposal, as well as for teaching me that, no matter how well I write a numerical code, his version will always be faster. I gratefully thank all the other TQC members that shared this four years with me: a particular mention goes to my long-term office mates Nick "the Elder", Jeroen, and Mathias, and to Nick "the Younger", Wout, and Wouter for contributing to the building of that magnificent piece of architecture that is the "Carrasco pyramid".

A special acknowledgement goes to the professors that followed me during the years at the University of Padova, particularly prof. Toigo and prof. Vitturi, who introduced me to the realm of scientific research supervising my Master's and Bachelor's thesis respectively. I also thank prof. Salasnich for the useful discussions, and for giving me the possibility to go back to the physics department in Padova and give a talk in the same room where I had followed so many classes.

My colleagues during the University years, Alessandro, Fabrizio, Francesco, Marta, and all the others, deserve the thank you that was missing – alongside the entire Acknowledgments section – from my Master thesis.

During the time I have been living in Antwerp I have met many people which, in one way or another, have given their contribution to this thesis. First and foremost I thank my Italian company: Giovanni, for countless volleyball games and his wonderful cuisine; the two Stefanos, for surviving a couple of Dutch courses together and many nice evenings; and Valentina, for many afternoons spent looking for vinyls in the most maze-like record stores in town. Also I would like to thank Agata, Laura, Maciek, Marija, Serena and Ute with whom I have shared Dutch classes and/or movies and/or concerts and, this for sure,

a couple of Belgian beers.

I cannot thank enough my family – my mum, my dad, my brother, and my sister-in-law – for the love and the constant unconditioned support that they gave me throughout my life. Also my uncles and aunties, and my awesome cousins deserve the greatest credit.

My long-terms friends from my hometown – Marco, Marta, and Stefano – as well as my flat-mates in Padova – Andrea, Damiano, Enrico, and Stefano – also deserve that great thank you that I owed them since my Master’s thesis.

Finally an immense thank you goes to Marta: her loving support and joyful smile accompanied me through the final stretch of my PhD giving me a inestimable boost in confidence and in happiness.